GABAergic regulation of proliferation in the postnatal spinal cord

Lauryn Emma New

Submitted in accordance with the requirements of the degree of

Doctor of Philosophy

The University of Leeds

School of Biomedical Sciences

January 2019

The candidate confirms that the work submitted is her own and that appropriate credit has been given where reference has been made to the work of others.

Acknowledgements

Firstly, I would like to express great thanks to my supervisors Sue and Jim Deuchars for all of their knowledge, guidance, and enthusiasm, which has been invaluable to me during my PhD. I am eternally grateful for the endless encouragement and support you have provided me these past 4 years, and the understanding, patience, and belief in my abilities that you have shown when my body has sometimes conspired against me. Thank you for always letting me explore my ideas and fuelling my passion for neuroscience. A special thanks must also go to my postdoctoral supervisor, Beatrice Filippi, for her patience as I slowly figured out how to postdoc and finish writing a thesis at the same time!

I would also like to thank the entire Deuchars' lab past and present for all of their advice and support, especially when I was complaining for the one millionth time that something hadn't worked, or that I had too many cells to count. Cat, Jess, Claudia, Pierce, Aaron, Nazlah, Nurha, Norah, Brenda, Christian, Lucy, Varinder, and Bianca: thank you for keeping me going. I must also thank the numerous project students who have helped unburden me from some of the long hours of cell counting, particularly Jon, Jacelyn, and Kate.

Without my friends and family all of this would have been so much harder. Thank you to my Mam for always being there for a long whinge on the phone, my dad for letting me talk his ear off about my project whenever I'm home, and my Nanna for always knowing when to send a silly message to cheer me up. Thanks also to Lucy the cat for always letting me hug you when I feel stressed, even though you'd rather be biting me!

Finally, I cannot express enough thanks to Nick for always being there and believing in me during my PhD. I really can't write how grateful I am for all of the things you have done to support me in this small space here, just know that you are the best and I love you.

Abstract

Ependymal cells (ECs) of the central canal (CC) are a quiescent population of neural stem cells (NSCs) present in the intact spinal cord. Normally dormant ECs are activated by injury; exhibiting increased proliferation, migration, and differentiation. Astrocytes and oligodendrocytes also generate new progeny in the intact and injured postnatal spinal cord. Understanding how the microenvironment of the spinal cord modulates proliferation and differentiation is essential if we are to consider harnessing endogenous mechanisms such as these to aid spinal cord repair. This project aims to investigate the role that the neurotransmitter GABA may play in modulating proliferation and differentiation in the adult spinal cord.

Alterations in the levels of ambient γ-aminobutyric acid (GABA) in the spinal cord in vigabatrin- treated or GAD67-GFP mice resulted in either a decrease or an increase in the number of proliferating EdU^+ cells in the white matter (WM), grey matter (GM), and CC compared to control, respectively. In the postnatal spinal cord there appears to be an inverse relationship between GABAergic signalling and the number of proliferating cells. Potentiation of GABAaR by the central benzodiazepine (BZ) recognition site (CBR) ligands etifoxine and midazolam also increased the number of EdU^+ cells compared to vehicle. The endogenous CBR site ligand diazepam binding inhibitor (DBI) was found to be expressed in the spinal cord, with robust expression in ECs, suggesting the presence of an intrinsic mechanism which modulates the basal inhibitory GABAergic tone to restrict proliferation. Indeed, animals with alteration in ligand binding at the CBR site as a result of either flumazenil treatment, Ro15-4513 treatment, or G2F77I mutation possessed greater numbers of EdU^+ cells compared to control animals. Flumazenil treatment also increased proliferation after lysophosphatidylcholine (LPC) -induced demyelination in the dorsal column. The effect of GABAergic modulation upon differentiation was varied, and its contribution to differentiation of specific cell types in the spinal cord was unclear.

This study shows that GABA both positively and negatively influences proliferation in the postnatal spinal cord and that endogenous ligands such as DBI may be instrumental in the restrictive nature of GABA. Work presented here provides a basis for further study into how modulation of GABAaR by endogenous ligands such as DBI may also influence spinal cord self-regeneration and recovery.

Table of contents

List of figures

List of tables

Abbreviations

aEC – activated ependymal cell

ANOVA – analysis of variance

BBM - breast to brain metastases

BrdU – 5-bromo-2'-deoxyuridine

BZ – benzodiazepine

Ca^{2+} - calcium ion

CBR – central benzodiazepine receptor site

CC – central canal

CD24 – cluster of differentiation 24

Cl^- - chloride ion

CNS – central nervous system

CSF – cerebrospinal fluid

CSFcC- cerebrospinal fluid contacting cell

CSPG – chondroitin sulphate proteoglycans

DAPI – 4', 6-diamidino-2-phenylindole

DBI – diazepam binding inhibitor

DCX – doublecortin

DiI - 1,1'dioctadecyl6,6'di(4sulphopentyl) 3,3,3',3'tetramethylindocarbocyanin

dpi – days post injection

EC – ependymal cell

EdU – 5-ethynyl-2'-deoxyuridine

ETX – etifoxine

FoxJ1 – forkhead-box J1

GABA – γ-ammino butyric acid

GABAaR – GABA A receptor

GABA-T – GABA-transaminase

GAD – glutamic acid decarboxylase

GAD65 – glutamic acid decarboxylase 65

GAD67- glutamic acid decarboxylase 67

GCL – granule cell layer

GFAP – glial fibrillary acid protein

GFP – green fluorescent protein

GM – grey matter

HuC/D – neurone specific RNA binding protein

IML – interomediolateral cell column

IMM – interomediomedial cell column

IP – intraperitoneal

KCC2 – potassium chloride transporter 2

LPC – lysophosphatidylcholine

MBP – myelin basic protein

MDZ – midazolam

MGE – medial ganglion eminence

MN – Motor neurone

MOA – mechanism of action

MS – multiple sclerosis

NAM – negative allosteric modulator

NeuN – neuronal nuclei

Ngn2 – Neurogenin-2

NKCC1 – potassium chloride transporter 1

NSC- neural stem cell

OLC – oligodendrocyte lineage cell

OPC – oligodendrocyte progenitor cell

PAM – positive allosteric modulator

PBR – peripheral benzodiazepine receptor

PBS – phosphate buffered saline

PBST – phosphate buffered saline with 0.1% triton

PFA – paraformaldehyde

PSA-NCAM – polysialylated neural cell adhesion molecule

SCI – spinal cord injury

SEM – standard error of the mean

SGZ – subgranular zone

Sox2 – Sex determining region Y-Box 2

SPN – sympathetic preganglionic neurone

SPN – sympathetic preganglionic neurone

SVZ – subventricular zone

TSPO – translocator protein

Tuj - Beta III tubulin

WM – white matter

Chapter 1 – General introduction

1.1 The spinal cord

The central nervous system (CNS) is comprised of the brain and the spinal cord. The spinal cord is essential for the connection of brain and body, allowing signal transmission to the sensory cortex by ascending sensory afferents and providing a path for descending signals to effector organs from the motor cortex. The spinal cord also acts as a centre for the integration and coordination of complex neuronal circuits involved in sensory, autonomic, and motor functions. The central pattern generator, the neural network comprised of spinal motor neurones (MNs) involved in rhythmic movement, is also housed in the spinal cord. Furthermore, independent control of reflex action also arises from the spinal cord.

The spinal cord begins at the brainstem, where it extends from the caudal medulla oblongata, passes through the foramen magnum at the base of the skull, and continues through the vertebral column, eventually terminating at the first lumbar vertebrae as the filum terminale. The cauda equina, a bundle of lumbar and sacral nerves and nerve rootlets, occupies the lumbar cistern surrounding the filum terminale. The spinal cord is split into 4 segments; cervical, thoracic, lumbar, and sacral, where exiting spinal nerves are named for the segment from which they originate.

Spinal nerves contain mixed sensory and motor nerve fibres which arise from the dorsal and ventral root, respectively (figure 1.1). Sensory primary afferents enter the spinal cord via the dorsal root and synapse onto spinal neurones within the dorsal horn GM, their cell bodies are located within dorsal root ganglia. Axons from both motor neurones and sympathetic preganglionic neurones exit via ventral roots. Cell bodies of motor neurones and sympathetic

preganglionic neurones are primarily located in the ventral horn GM and intermediolateral nucleus (IML), respectively.

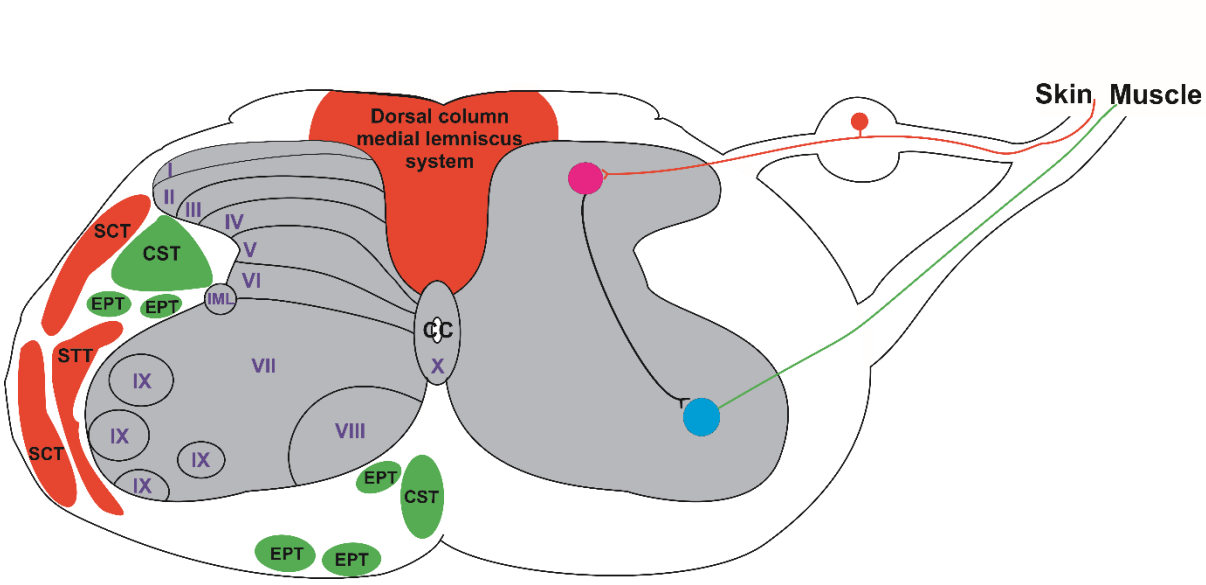

Figure 1.1 The spinal cord is a highly organised structure

Schematic of the spinal cord in the transverse plane depicting the GM laminae (**DH**: dorsal horn, **VH**: ventral horn), WM ascending and descending tracts, and ventral and dorsal rootlets. Ascending tracts are coloured in red and include: **SCT**: spinocerebellar tract, **STT**: spinothalamic tract, and the dorsal column medial lemniscus system. Descending tracts are coloured in green and include **CST**: corticospinal tract and **EPT**: extrapyramidal tract.

Neuronal cell bodies are housed within the central GM of the spinal cord which is cytoarchitectonically divided into defined anatomical layers or laminae (Rexed, 1952; Rexed, 1954). The 10 laminae (I-X) can be broadly divided into: the sensory dorsal horn (I-VI), the intermediate grey (lamina VII), and the ventral horn (VIII-IX). Lamina X surrounds the spinal cord CC a cerebrospinal fluid (CSF) filled space which extends longitudinally through the rostrocaudal extent of the spinal cord. The GM contains sites of termination of primary afferent neurones and descending neurones, interneurones, and cells from ascending tracts which project to the brain. The GM is surrounded by the WM. WM comprises the myelinated and unmyelinated axons which form the ascending and descending spinal tracts that relay

signals to and from the brain and between spinal segments. Ascending tracts relay sensory information and include the dorsal columns, spinothalamic, and spinocerebellar tracts which are found in the dorsal, lateral, and ventral columns. Conversely, descending tracts, including the corticospinal, corticobulbar, and extrapyramidal tracts relay motor information and are present in the lateral and ventral columns (figure 1.1).

1.2 Spinal cord injury

Axonal fibre tracts within the spinal cord are essential for communication between the spinal cord and the brain in order to coordinate sensory input and motor output. Spinal cord injury (SCI) disrupts these crucial pathways, leading to sensorimotor deficits below the lesion site which result in variable degrees of loss of movement and sensation. Each year, around the world, between 250,000 and 500,000 experience significant trauma which results in SCI (https://www.who.int/news-room/fact-sheets/detail/spinal-cord-injury). A patient's experience of SCI, including the degree of physical impairment, costs associated with care, and life expectancy, is directly related to injury severity and the spinal level affected (Hawryluk *et al*., 2008). Higher level and/or more complete spinal injuries are associated with greater functional impairments, poorer prognoses, and a greater cost to society by healthcare, whereas lower level and/or incomplete injuries are generally associated with a more favourable clinical outcome (McDonough, Ashley and Martínez-Cerdeño, 2012).

1.2.1 Mechanisms of spinal cord injury

The neuropathology of SCI begins when the spinal cord is lacerated or macerated by a sharp penetrating force, or is contused or compressed by high energy mechanical blunt trauma (Silva *et al*., 2014). This initial primary neurological insult leads to a cascade of secondary injury events which result in further tissue damage and cellular degeneration in the WM and GM which persist over a period of minutes to weeks after the initial insult (McDonough, Ashley and Martínez-Cerdeño, 2012; Faulkner *et al*., 2004). These include vascular changes (Figley *et al*., 2014; Tator and Koyanagi, 1997), oxidative neuronal cell

death by free radial formation (Toborek *et al*., 1999), intense local inflammation and release of inflammatory cytokines (Stammers *et al*., 2012), glutamate excitotoxicity (Park, E. *et al*., 2004; Mazzone *et al*., 2013) and disruption of ionic balance of K^+, Na^+, and Ca^{2+} (Silva *et al*., 2014; Stys and Lopachin, 1998). The culmination of these primary and secondary injury processes results in the death of significant numbers of neurones, oligodendrocytes, microglia, and astrocytes. The death of oligodendrocytes continues for many weeks following injury, causing wide-spread demyelination in spared axons which prevents efficient signal propagation in remaining axons, and leaves them vulnerable to further degeneration (Crowe *et al*., 1997; Meletis *et al*., 2008; Silva *et al*., 2014). Finally, there is a chronic phase of injury which leads to neurological impairment in both antero- and retrograde directions, including the brain (Silva *et al*., 2014; Cramer *et al*., 2005; Yiu and He, 2006).

1.2.2 New avenues and challenges in spinal cord repair

Unlike the rest of the body, the CNS shows poor regenerative capabilities, and until recently, reconstruction of damaged neural circuits following SCI was thought to be hopeless. As yet, there is no effective cure for SCI (Harvey, 2016).

One of the major barriers to axonal regeneration following SCI is the presence of an inhibitory environment at the lesion site (Cregg *et al*., 2014). Following injury there is a period of reactive gliosis in which astrocytes proliferate and swell in size, exhibiting higher expression levels of GFAP, vimentin, and nestin (Cregg *et al*., 2014). These hypertrophic astrocytes undergo major restructuring and extend long filamentous processes which entangle to form a mesh-like layer that acts as a physical barrier to regenerating axons of descending and ascending tracts (Wanner *et al*., 2013; Menet *et al*., 2003). The dense glial scar has also been shown to synthesise and deposit inhibitory chondroitin sulphate proteoglycans (CSPGs) which further limit axonal regeneration (Jones *et al*., 2003; McKeon *et al*., 1991; Tang *et al*., 2003).

Conversely, other studies, which genetically abrogate mechanisms involved in reactive gliosis and glial scar formation, have shown that seclusion of the lesion site limits tissue damage, restricts inflammation, and preserves function in the subacute phase of SCI (Faulkner *et al*., 2004; Sabelstrom *et al*., 2013; Sofroniew, 2015; Renault-Mihara *et al*., 2017; Okada, S. *et al*., 2006). Animals with defective glial scar formation exhibit enhanced demyelination, increased neuronal loss, poor lesion sealing and cavitation, and greater motor impairment compared to injury matched controls (Okada, S. *et al*., 2006; Faulkner *et al*., 2004; Sabelstrom *et al*., 2013; Herrmann *et al*., 2008). More recently, the glial scar has also been shown to support, rather than hinder, axon outgrowth, even in the chronic phase of SCI (Anderson, M.A. *et al*., 2016).

Whilst the exact contribution of the glial scar to regenerative failure following SCI remains to be determined, it is clear that spontaneous recovery is limited and current therapeutic options are lacking. However, replacement of the damaged cells and introduction of scar 'bridging' cells by cell transplantation has emerged as a potential strategy to promote repair following SCI. Such interventions have already shown efficacy at both the pre-clinical and clinical level (Mackay-Sim and St John, 2011; Saberi *et al*., 2011) and have therefore garnered interest as a possible new approach for the treatment of SCI.

1.2.3 Cell transplantation for neural regeneration

Numerous cell types have been assessed for their capacity to treat SCI by transplantation (Chhabra and Sarda, 2017; Nakamura and Okano, 2013). Embryonic stem cells (ESCs) were the first population studied for their regenerative potential. ESCs can differentiate into neuronal cell types both *in vitro* and *in vivo* (Okada, Y. *et al*., 2008). However, owing to the tumorigenic potential of transplantation of undifferentiated ESCs much work has focused on the effects of ESC-derived neural stem cells (NSCs) or neural stem/progenitor cells (NSPCs) transplantation following SCI. Transplantation of NS(P)Cs derived from foetal spinal cord tissue into injured spinal cord results in successful graft survival, differentiation of

transplanted cells, and graft connectivity by host-graft integration (Bregman *et al*., 1993; Bonner *et al*., 2011). Improved functional recovery has also been reported in animal models of SCI following transplantation of rat foetal spinal cord-derived NSPCs (Ogawa *et al*., 2002), mouse foetal striatum-derived NSPCs (Okada, S. *et al*., 2005; Abematsu *et al*., 2010), and human foetal brain-derived NSPCs (Iwanami *et al*., 2005; Cummings *et al*., 2005). Intraspinal grafting of human foetal spinal cord tissue is also feasible and safe in humans (Wirth *et al*., 2001).

Transplanted foetal NSPC grafts clearly possess the capacity to differentiate, promote axon growth, and myelinate the injured cord, leading to improved functional recovery, however ethical concerns regarding the source of these cells remain (Rosenfeld *et al*., 2008). Furthermore, there are also concerns regarding the possibility of immunological rejection and the effects that immunosuppression would have on the health of patients with SCI. Induced pluripotent stem cells (iPSCs), which are generated by reprogramming adult somatic cells to a pluripotent state (Takahashi *et al*., 2007), may help to circumvent these issues. Clinical iPSC-based therapy for SCI would allow skin cells taken from a patient with SCI to be reprogrammed into autologous iPSCs, followed by further differentiation into NSCS, for implantation into the lesion site of the patient (Lee-Kubli and Lu, 2015). Preclinical studies have shown that these iPSC-derived NSCs survive, proliferate and differentiate following implantation and give rise to extensive axon growth throughout both the WM and GM (Lu *et al*., 2014). Lu *et al*., (2014) report that the majority of grafted cells (71.2%) differentiated into $NeuN^+$ mature neurones which extended axons reaching as far rostrally as the olfactory bulb and as far caudally as the lumbar spinal cord (Lu *et al*., 2014). Implantation of iPSC-derived NSCs however did not result in functional improvement in tests of forelimb function. There was an absence of neurofilament expression in graft-derived axons and myelination by host oligodendrocytes was not observed, suggesting that neural conduction may not have been repaired despite evidence of host axonal regeneration (Lu *et al*., 2014).

Disappointing results from functional studies following implantation of iPSC-derived NSC grafts are overshadowed by concerns about the safety of iPSC-derived cell grafts. Several studies have found that iPSCs exhibit tumorigenicity even if all undifferentiated cells are purged from the population (Nori *et al*., 2011; Lee, A.S. *et al*., 2013). Therefore, despite promising results relating to the differentiation and integration of iPSC-derived NSCs in SCI, such concerns seriously limit the consideration of iPSC-derived grafts for clinical use at this current time. Despite early optimism in NSC grafts, novel therapeutic avenues to replace lost and damaged cells following SCI are still absent.

1.2.4 Potential for repair by endogenous NSCs

The mammalian spinal cord lacks the remarkable self-regenerative capability which is seen following SCI in lower vertebrates such as the eel (Dervan and Roberts, 2003), lamprey (Zhang, G. *et al*., 2014), axolotl (Thygesen *et al*., 2016), and zebrafish (Reimer *et al*., 2008), which permits functional recovery in these organisms. This is in direct opposition to the mammalian spinal cord which shows little evidence of self-repair following SCI (McDonough, A. *et al*., 2013; Barnabe-Heider *et al*., 2010; Meletis *et al*., 2008; Mothe and Tator, 2005). However, the mammalian spinal cord exhibits an injury-induced proliferative response, much like that seen in lower vertebrates (Johansson *et al*., 1999; Barnabe-Heider *et al*., 2010; Meletis *et al*., 2008; Lytle and Wrathall, 2007; Mothe and Tator, 2005; Lacroix *et al*., 2014). The majority of new cells following injury differentiate into scar forming astrocytes which occupy the lesion core rather than reparative neurones or remyelinating oligodendrocytes (Barnabe-Heider *et al*., 2010; Meletis *et al*., 2008). The gliogenic environment of the injured mammalian spinal cord may therefore contribute to its poor recovery.

It has been suggested that injury-induced proliferation is due to activation of dormant NSC properties in resident spinal cord cells which are relatively quiescent under normal conditions (Hamilton, L.K. *et al*., 2009). Investigation into the proliferative capacity of the spinal cord, how these NSC-like populations behave in the intact cord, including the signals which

modulate their proliferation and differentiation is essential if we are the harness any endogenous proliferating cells for repair in conditions such as SCI. One of the major barriers to repair following SCI is the development of an inhibitory environment, including the glial scar, which prevents adequate neuroaxonal recovery for significant sensorimotor improvement. Understanding how niche signalling in the spinal cord restrains proliferation and differentiation in the intact cord, where cells only exhibit self-renewal for population maintenance, will also help elucidate signalling pathways which may be involved in the inhibitory environment seen after SCI.

1.3 Proliferation and neurogenesis in the adult CNS

For 100 years a central dogma existed in neuroscience which postulated that the vast majority of neural cells were established during embryonic development and that after birth no new cells were added to the CNS. The advent of tritiated thymidine autoradiography to label proliferating cells allowed Altman and colleagues to show for the first time that new neurones were indeed generated in the adult brain (Altman and Das, 1965). Following this, continuing advances in the field such as *in vivo* thymidine analogue labelling of proliferating cells, cell-type-specific immunohistochemical markers, retroviral tracing, and genetic fate mapping studies have established that pools of NSCs and NSPCs exist within specific niches of the adult CNS. *In vitro* generation of neurospheres from specific regions of the adult brain and spinal cord has given evidence for the existence of cells within these specialised niches which possess the fundamental hallmarks of NSCs; self-renewal and multipotency of progeny. NSC behaviour within the postnatal CNS has been evidenced many times in many different species (reviewed by (Ma *et al*., 2009)), including humans (Eriksson *et al*., 1998; Spalding *et al*., 2013; Dromard *et al*., 2008) and generates excitement and optimism in the field about the possibility of a new therapeutic avenue for CNS repair.

1.3.1 What is a neural stem cell?

Stem cells are notoriously difficult to define and identify, often encompassing a heterogenous population of cells, with regional diversity, within a specialised niche, as is often seen in somatic stem cell populations (Goritz and Frisen, 2012; Bonaguidi *et al*., 2011). These difficulties also apply to NSCs and are compounded by the fact that there is no single molecular marker to unambiguously identify NSCs *in situ* as they express a wide range of markers which are also expressed by other neural cell types.

In general, NSCs are defined as cells which possess both self-renewal capacity and multipotency within the CNS; that is the ability to generate newly proliferated progeny which are capable of differentiation into mature neural lineage cells, either neurones, astrocytes, or oligodendrocytes. NSC possess 2 patterns of division, either asymmetric; involving the generation of another NSC and a progenitor which differentiates into another neural cell type, or symmetric; involving the generation of 2 NSCs or 2 progenitor cells (Egger *et al*., 2010) (figure 1.2). The balance of asymmetric vs symmetric division is an important mechanism which allows control over the stem cell population and prevents proliferative exhaustion of the stem cell pool (Urban *et al*., 2016).

In the CNS, cells with self-renewal capacity and multipotency are found in the subventricular zone (SVZ) of the lateral ventricle and the subgranular zone (SGZ) of the dentate gyrus (Kempermann, G. and Gage, 1999; Lim and Alvarez-Buylla, 2016). It is debated however whether NSCs must be tripotent, and therefore generate neurones, astrocytes, and oligodendrocytes, in order to be classified as a ‘true’ NSC. Indeed, recent studies using genetic fate mapping and clonal lineage tracing of SVZ and SGZ NSCs has called the tri-lineage potential of well-established NSCs into question. Recent work shows that type B radial-glia like cells of the SVZ population generate only neurones and astrocytes (Calzolari *et al*., 2015; Ortega *et al*., 2013). Furthermore, it also appears that SGZ NSCs only produce neurones and astrocytes (Bonaguidi *et al*., 2011). It has long been argued that ECs are not

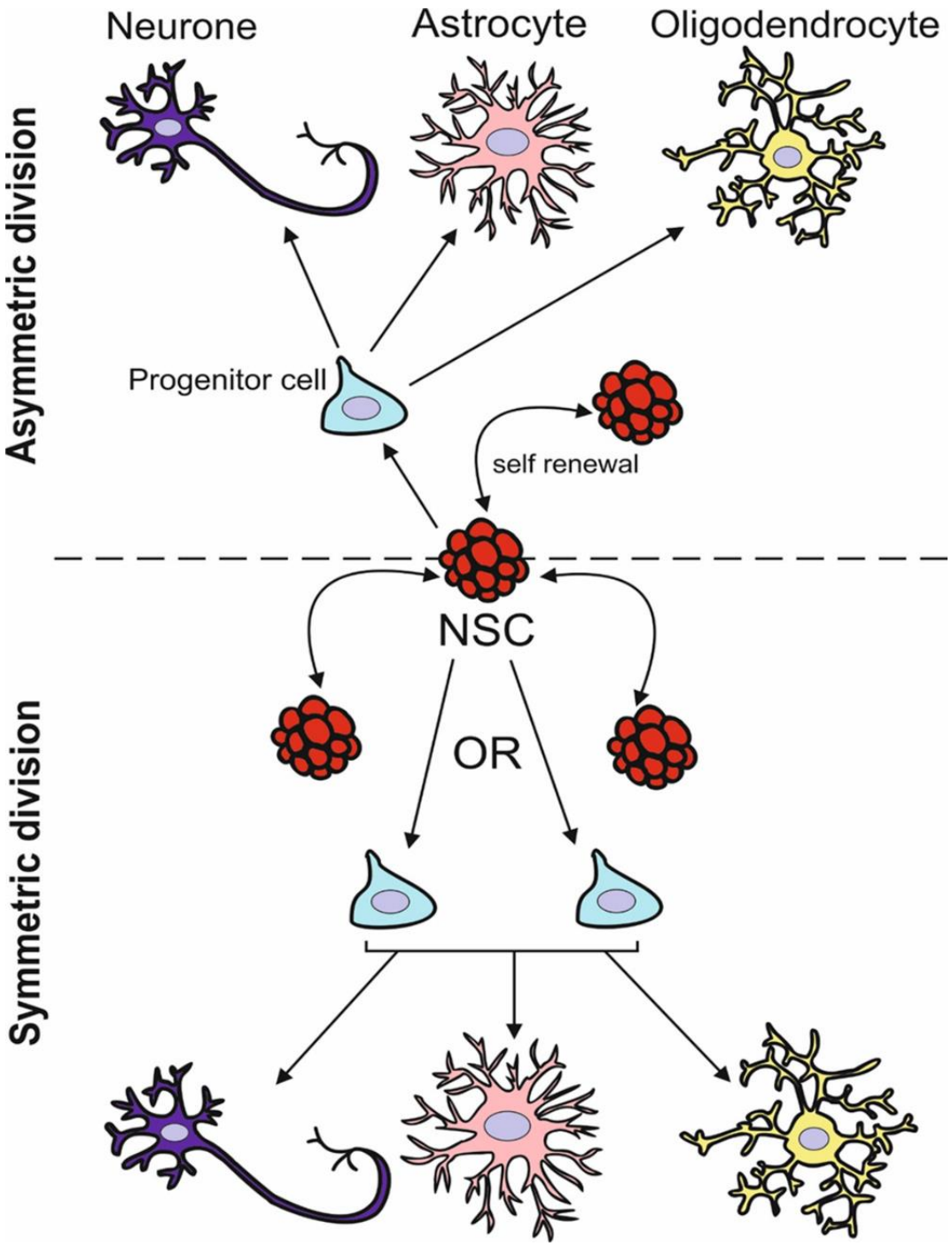

Figure 1.2 NSCs exhibit either asymmetric or symmetric division

NSCs in the true sense as they are not tripotent and only generate astrocytes and oligodendrocytes for tissue repair after SCI (Barnabe-Heider *et al*., 2010). Mature neurones are rarely generated from EC progeny (Barnabe-Heider *et al*., 2010). However, if we were to use this definition for all NSCs then the long established SVZ and SGZ NSCs would also fail to fit this categorisation.

These findings highlight the need for a standardised NSC definition in regards to how these stem cells behave in order to prevent ambiguity when attempting to identify possible novel latent NSC populations such as spinal cord ECs.

1.3.2 Neurogenic niches in the adult brain

There are 2 areas within the postnatal mammalian brain where NSCs reside, proliferate, and differentiate in a specialised neurogenic niche environment; the SVZ of the lateral ventricle and the SGZ of the hippocampal DG.

Radial glia-like NSCs of the SVZ, also known as type B cells, reside within the subependymal layer and extend a basal process towards a blood vessel, and an apical process through the ependymal layer and towards the ventricular space (Mirzadeh *et al*., 2008) (figure 1.3). Upon activation, type B cells divide asymmetrically, giving rise to another type B cell and a transit amplifying cell/type C cell. Transit amplifying cells then enter the cell cycle and proliferate themselves before maturing and generating neuroblasts/type A cells (Doetsch *et al*., 1999a; Doetsch *et al*., 1997) (figure 1.3). Neuroblasts migrate tangentially along astrocyte-ensheathed chains within the rostral migratory stream towards the olfactory bulb (Sun, W. *et al*., 2010). Once within the olfactory bulb, neuroblasts differentiate into mature interneurons and integrate into the olfactory bulb network (Doetsch and Alvarez-Buylla, 1996; Doetsch *et al*., 1999a; Doetsch *et al*., 1997; Lois and Alvarez-Buylla, 1994; Lois and Alvarez-Buylla, 1993; Belluzzi *et al*., 2003; Carleton *et al*., 2003)

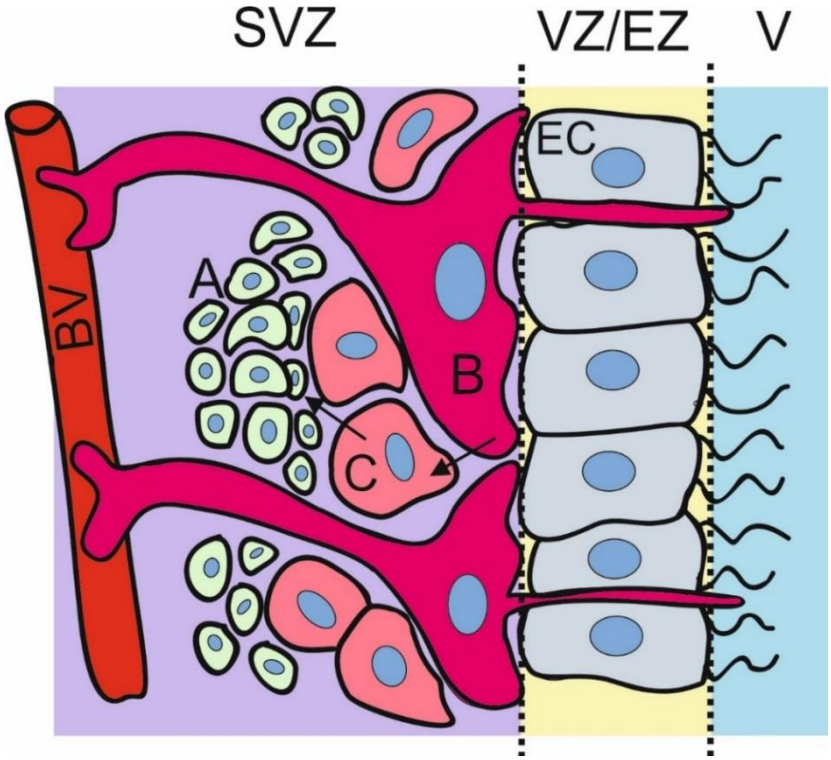

Figure 1.3 The SVZ is a neurogenic niche

Schematic of the SVZ depicting the arrangement of NSC/type B cells (B), transit amplifying cells (B), and neuroblasts (A) within the niche. **SVZ**: subventricular zone, **VZ/EZ**: ventricular zone/ependymal zone, **V**: ventricular space**, BV**: blood vessel

In the DG SGZ radial glia-like NSCs, known as type 1 cells do not migrate as far as SVZ NSCs to reach, and integrate into, their target location/network (figure 1.4). Type 1 cells of the SGZ generate immediate progenitor cells which undergo limited rounds of proliferation before generating neuroblasts (Seri *et al*., 2001). These neuroblasts eventually migrate tangentially along the SGZ before migrating radially into the granule cell layer of the DG where they differentiate into granule neurones (Sun, G.J. *et al*., 2013) (figure 1.4). In addition to new neurones, these NSCs of the SVZ and SGZ can also give rise to oligodendrocytes and astrocytes (Ortega *et al*., 2013; Bonaguidi *et al*., 2011 Lois and Alvarez-Buylla, 1993).

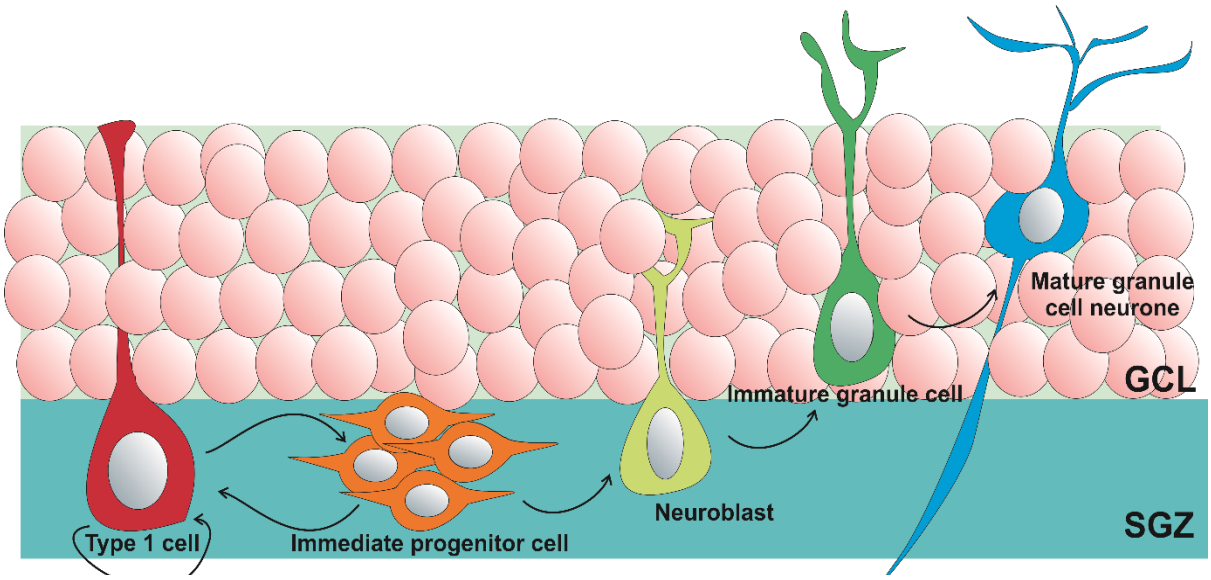

Figure 1.4 Neurogenesis in the SGZ provides new granule cells in the hippocampus

Schematic depicting the proliferation of NSCs (type 1 cells) in the SGZ of the hippocampal DG and their maturation along the neural lineage to become mature granule cell neurones in the granule cell layer (GCL) of the hippocampus

1.4 Proliferation in the adult spinal cord

The SVZ and SGZ are often stated to be the only postnatal neurogenic niches of the CNS, however, results from both *in vitro* neurosphere culture assays and *in vivo* genetic lineage tracing studies show that the postnatal spinal cord also contains proliferative cells which may be NSCs.

Proliferating cells are frequently found in the GM and WM of the rat spinal cord (Horner *et al*., 2000). 0.6-0.7% of $NG2^+$ glial cells in the adult spinal cord incorporate BrdU over a 4-week period, illustrating the presence of a slowly dividing glial population in the adult spinal cord parenchyma (Horner *et al*., 2000). More stringent analysis, using genetic fate mapping of oligodendrocyte, astrocyte, and ependymal progenitors has shown that oligodendrocyte, astrocyte, and ependymal progeny make up more than 90% of the $BrdU^+$ proliferative cell population in the intact adult spinal cord (Barnabe-Heider *et al*., 2010). Oligodendrocyte lineage cells (OLCs) are the most numerous of the proliferating populations, making up more

than 80% of $BrdU^+$ cells. In the intact cord oligodendrocyte progenitor cells (OPCs) both self-renew and generate an increasing number of mature oligodendrocytes over time. Ependymal and astrocytes instead proliferate by self-renewal to maintain their population size (Barnabe-Heider *et al*., 2010; Meletis *et al*., 2008).

Due to the proliferation of $NG2^+$ glial cells within the spinal cord WM and GM, the identity of spinal cord NSCs has been difficult to establish and their existence remains controversial, however there is evidence that NSC potential within the spinal cord resides within the ECs which line the spinal cord CC (Mothe and Tator, 2005; Sabourin *et al*., 2009).

1.4.1 The spinal cord neurogenic niche

The cells surrounding the CC are a heterogeneous population of cells, including ECs, cerebrospinal fluid contacting cells (CSFcCs), and radial-glial like ECs (figure 1.5) (Hugnot and Franzen, 2011). ECs are FoxJ1-expressing ciliated cells which possess short basal processes and are primarily located at the lateral domains of the CC (figure 1.5), these cells are discussed in detail below (section 1.1.4). Radial-glial like ECs are mainly concentrated at the dorsal and ventral poles of the CC (figure 1.5). Radial-glial like ECs also are unique in their expression of the intermediate filament protein nestin (Hamilton, L.K. *et al*., 2009; Sabourin *et al*., 2009). CSFcCs are sporadically distributed around the CC and make contact with the lumen by a thick dendritic process which is terminated by a large bulb (figure 1.5). Although the exact function of CSFcCs remains elusive, these cells express immunohistochemical (IHC) markers of immature neurones including PSA-NCAM and synthesize GABA (Roberts *et al*., 1995; Stoeckel *et al*., 2003; Reali *et al*., 2011). CSFcCs are therefore anatomically well situated to influence the activity of cells within the CC neurogenic niche.

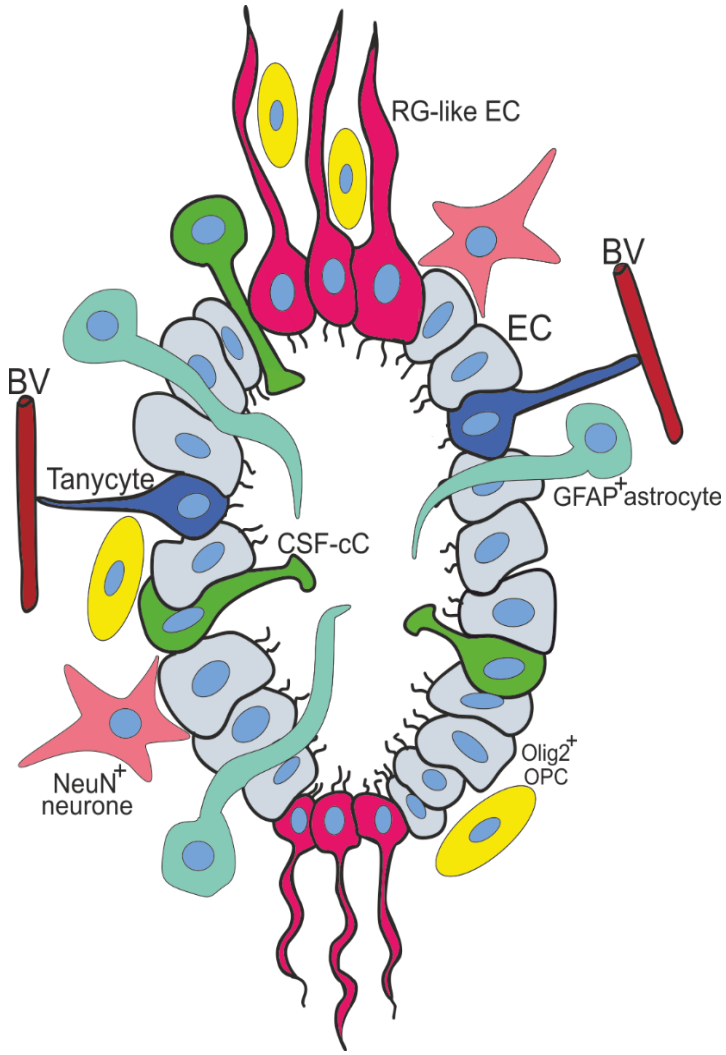

Figure 1.5 The spinal cord CC is a heterogenous population of cells

Schematic depicting the arrangement of cells around the CC of the spinal cord, illustrating that the CC is lined by CC which are interspersed with other cell types including radial glia and CSFcCs. **RG-like EC**: radial glia-like EC **GFAP$^+$**: glial fibrillary protein$^+$, **NeuN$^+$**: Neuronal nuclei$^+$, **OPC**: oligodendrocyte progenitor cell, **BV**: blood vessel

1.5 Spinal cord ependymal cells

ECs are often cited as NSC-like population of the adult spinal cord (Meletis *et al*., 2008; Hamilton, L.K. *et al*., 2009; Panayiotou and Malas, 2013). ECs are ciliated cells which line the ventricular neuraxis of the brain and the spinal cord CC. ECs are embryonically derived from radial glial cells (Spassky *et al*., 2005), therefore sharing a common developmental

origin with the NSCs of the SVZ and SGZ (Kriegstein and Alvarez-Buylla, 2009). ECs first appear at embryonic day 15.5 and surround the CC by birth (P0) (Li, X. *et al*., 2016).

Ultrastructural analysis has posited the existence of 3 distinct morphological signatures of CC ECs (Bruni and Reddy, 1987; Meletis *et al*., 2008). Cells displaying a typical bicilated cuboidal EC morphology are most common (Alfaro-Cervello *et al*., 2012). These cells have motile cilia which are essential for the propulsion of CSF (Alfaro-Cervello *et al*., 2012) (figure 1.5). A smaller subset of ECs, often referred to as radial ECs, reside at the dorsal and ventral poles of the CC and extend long processes along the dorsoventral axis toward the pial surface of the spinal cord (Alfaro-Cervello *et al*., 2012; Meletis *et al*., 2008). The existence of another EC-subtype known as tanycytes, characterised by a single cilium and a long basal process which terminates on the basal lamina of blood vessels or neurones (Bruni and Reddy, 1987; Hugnot and Franzen, 2011), is debated. Some authors identify tanycyte-like cells to exist only at the dorsal and ventral regions of the central canal (Mothe and Tator, 2005; Hamilton, L.K. *et al*., 2009). Others however, suggest that tanycytes are also present within the lateral walls of the CC alongside cuboidal and radial ependymal cells. Analysis by electron microscopy (EM) has shown that the CC is composed of ECs with radial processes which reside in dorsal, ventral, and lateral aspects of the CC (Meletis *et al*., 2008; Alfaro-Cervello *et al*., 2012) (figure 1.5).

ECs are also present lining the lateral ventricle wall where they are in close apposition to the neurogenic SVZ (Mirzadeh *et al*., 2008) (figure 1.2). However, these are functionally distinct from the ECs of the spinal cord and do not constitute the NSC population of the SVZ (Doetsch *et al*., 1999a; Alfaro-Cervello *et al*., 2012; Shah *et al*., 2018). In the SVZ, ECs separate the NSCs/type B cells from the lateral ventricle and aid the flow of CSF by beating their motile cilia (Bond *et al*., 2015). SVZ ECs also cluster to form a pinwheel architecture where NSCs are found in the centre of ependymal rosettes (Mirzadeh *et al*., 2008).

SVZ ECs provide support to the NSCs by secreting the pro-neurogenic factor Noggin, an inhibitor of bone morphogenic protein signalling, which induces NSC activation (Lim *et al*., 2000). Therefore, although ECs are not the NSC population of the SVZ, as they may be within the spinal cord, they are essential for the maintenance and functioning of the SVZ neurogenic niche. From here, unless stated, EC refers to ECs within the spinal cord, and not the SVZ.

1.6 Evidence that ECs are NSCs in the adult cord

There is much debate as to whether postnatal spinal cord ECs are indeed NSCs, whether they exhibit the properties of NSCs *in vivo* or whether their NSC properties are merely an *in vitro* artefact. In addition, there is further debate concerning whether these cells are simply latent NSCs which are not active in normal homeostatic or intact conditions.

1.6.1 ECs share express markers common to other NSC populations

There is significant heterogeneity between NSC molecular markers, many of these markers are also found to be expressed in mature astrocytes in addition to NSCs (McDonough, Ashley and Martínez-Cerdeño, 2012), therefore complicating the identification of NSCs within the adult spinal cord.

Despite such complications, ECs within the spinal cord have repeatedly been shown to possess many IHC markers associated with NSCs including nestin (Frisen *et al*., 1995; Meletis *et al*., 2008), sex determining region Y-box 2 (Sox2) (Hamilton, L.K. *et al*., 2009; Corns *et al*., 2015), and vimentin (Hamilton, L.K. *et al*., 2009). An extensive literature search carried out by Pfenninger *et al*., (2010) revealed that adult ECs also express many genes which are known to play a role in cell division, cell cycle regulation, and telomere stability (Pfenninger *et al*., 2011).

Table 1.1 Immunohistochemical markers of NSCs are shared by spinal cord CC ependymal cells and NSCs of the neurogenic niches of the brain, the SGZ and SVZ

Marker	ECs	SVZ NSCs	SGZ NSCs
Sox2	+	+	+
Nestin	+ (dorsal and ventral poles)	+	+
Vimentin	+	+	+
CD133/Prominin	+	+	
GFAP	+	+	+
Notch1 receptor	+	+	
BLBP	+	+	+
Musashi1	+	+	+
PSA-NCAM	+	+	+
Mash1	-	+	+
CD24	+	+	+
Ki67	+	+	+
EdU/BrdU	+	+	+
CB1	+	+	+

Furthermore, NSC markers present within ECs are often also expressed by NSCs of the known neurogenic niches of the SVZ and SGZ (Hamilton, L.K. *et al*., 2009) (table 1.1). Some of these markers, such as polysialylated neural cell adhesion molecule (PSA-NCAM), S100 calcium binding protein (S100β), cluster of differentiation 24 (CD24), are often associated with progenitor cells rather than NSCs (Zhang, J. and Jiao, 2015). Such markers may also be expressed when the cell begins to differentiate toward a more mature state such as a migrating neuroblast, as is the case within the SVZ.

As with NSCs in other niches, ECs undergo proliferation within the intact adult spinal cord, as evidenced by their positive staining for the proliferative markers Ki67, EdU, and BrdU (Hamilton, L.K. *et al*., 2009). Detection of Ki67 labels cells undergoing proliferation as the Ki67 nuclear protein is present during all active phases of the cell cycle (G(1), S, G(2), and mitosis) but is absent from resting cells in G0 (Ping Yuan *et al*., 2015; Sobecki *et al*., 2017). The thymidine analogues EdU and BrdU label cells in S-phase and therefore highlight a smaller fraction of cells undergoing proliferation (Salic and Mitchison, 2008). Despite such technical differences, both methods have shown that ECs in the intact cord are mitotically active (Corns *et al*., 2015; Namiki and Tator, 1999; Meletis *et al*., 2008).

Whilst ECs do show expression of many molecular markers associated with NSCs, they do not express mammalian achaete scute homolog 1 (Mash1). Mash1 is associated with neurogenic SVZ progenitors (Yamamoto *et al*., 2001a) and is thought to be important for neural differentiation (Tomita *et al*., 1996). This may explain why when ECs do proliferate and differentiate, they preferentially become astrocytes or oligodendrocytes, rather than neurones (Meletis *et al*., 2008; Barnabe-Heider *et al*., 2010). ECs may therefore be considered to be latent NSCs due to their *in vitro* stem cell potential and NSC molecular signature common to NSCs of both the SVZ and SGZ.

1.6.2 ECs generate neurospheres

As early as the 1990s cell culture protocols which allow for the culture of free-floating cell aggregates, known as neurospheres, have provided *in vitro* evidence of cell populations with self-renewal and multi-lineage neural differentiation potential within the CNS (Weiss *et al*., 1996). Neurosphere forming cells which generate new clones during serial passaging and possess the ability to differentiate into other neural cell types are classified as NSCs. The ability to generate neurospheres is a hallmark feature of both SVZ and SGZ derived NSCs (Weiss *et al*., 1996; Guo *et al*., 2012).

Neurosphere forming cells have also been reported to be present throughout the spinal cord (Sabelstrom *et al*., 2014), including the CC (Johansson *et al*., 1999; Martens, D.J. *et al*., 2002), and the medial and lateral areas of the cord (Yamamoto *et al*., 2001b; Yoo and Wrathall, 2007). However, only neurospheres derived from ECs from the CC have been found to self-renew after several passages. These cells are also multipotent, differentiating into oligodendrocytes, and astrocytes, in culture (Meletis *et al*., 2008). High intrinsic NSC potential of EC is present from postnatal day 10 and appears to reduce with age (Li, X. *et al*., 2016). No neurosphere-initiating activity has been seen in non-EC fractions of the cord (Johansson *et al*., 1999; Martens, D.J. *et al*., 2002; Mothe and Tator, 2005; Barnabe-Heider *et al*., 2010), indicating that NSC potential in the adult cord resides at the ependyma and is present from early postnatal life.

1.6.3 Lineage tracing experiments show EC generate clones and mature progeny

Genetic fate mapping using tamoxifen-dependent Cre-recombination under the control of EC specific promotors including FoxJ1 and Nestin has been used to further examine and confirm NSC properties of ECs in both the intact and injured cord (Meletis *et al*., 2008; Barnabe-Heider *et al*., 2010). Meletis *et al*., (2008) illustrate that Nestin-CreER and FoxJ-CreER transgenes are expressed in identical EC populations lining the CC. Following culture

in neurosphere forming conditions it was found that ~76% of neurospheres from Nestin-CreER and ~85% of FoxJ1-CreER neurospheres had undergone tamoxifen dependent recombination, and were therefore derived from recombined ECs. Neurospheres generated from the Nestin-CreER and FoxJ1-CreER populations could be passaged up to eight times to give rise to new neurospheres, indicating self-renewal capacity. Furthermore, analysis of differentiation potential showed that 100% of the neurosphere clones were multipotent and could generate neurones, astrocytes, and oligodendrocytes. Barnabe-Heider *et al*., (2010) also showed that almost all neurospheres originate from ECs in both injured and uninjured conditions.

Cell turnover and EC proliferation in the intact adult spinal cord is limited and it appears that in the intact cord ECs undergo self-renewal only (Barnabe-Heider *et al*., 2010; Meletis *et al*., 2008; Mothe and Tator, 2005; Horner *et al*., 2000; Johansson *et al*., 1999). It is for this reason that existence of NSCs in the spinal cord has been contested. BrdU labelling has shown that ECs constitute ~4.8% of proliferating cells in the intact mouse spinal cord (Johansson *et al*., 1999; Barnabe-Heider *et al*., 2010). BrdU labelled ECs were commonly found in pairs, indicating that mitotic events most likely resulted in self-renewal, rather than generation of a cell which migrated away from the EC layer (Meletis *et al*., 2008). This finding suggests that ECs undergo mitosis in the intact spinal cord for the purpose of self-renewal and maintainence of EC population numbers. This finding was confirmed by Barnabe-Heider *et al*., (2010) who showed that the number of recombined cells from the FoxJ1-CreER line did not change significantly 4 months post tamoxifen administration. The phenotype of FoxJ1-CreER recombined cells remained the same at 4 months post tamoxifen as that seen at 5 days post tamoxifen, indicating that in the intact cord ECs do not produce differentiated progeny (Barnabe-Heider *et al*., 2010).

1.6.4 Quiescent ECs are activated following injury

Whilst ECs are limited in their proliferation and differentiation in the intact cord, following SCI ECs markedly increase their proliferation, by approximately 50-fold (Johansson *et al*., 1999), and generate glial-differentiated progeny which contribute to the glial scar (Barnabe-Heider *et al*., 2010; Sabelstrom *et al*., 2013). Following injury, ECs downregulate EC specific makers such as Sox2, Sox3, and FoxJ1, migrate toward the lesion site, and differentiate toward an astrocytic phenotype. ECs then generate the largest new population of glial cells in the injured cord, where 39% of new astrocytes are derived from ECs (Barnabe-Heider *et al*., 2010). SCI also increases the *in vitro* NSC potential of ECs, resulting in more numerous and faster growing neurospheres (Barnabe-Heider *et al*., 2010). Furthermore, TUNEL staining has shown that whilst SCI results in death of significant numbers of neurones, astrocytes, and oligodendrocytes, the EC population does not undergo apoptosis after SCI. This finding indicates the importance of this population of dormant NSCs which can be activated when required for tissue repair or cellular repopulation (Mothe and Tator, 2005).

The age of ECs contributes to their NSC and reactive potential following injury, where lesion size and severity impacts juvenile (P21) EC behaviour (Li, X. *et al*., 2016). Juvenile ECs do not appear to be recruited following a mild dorsal funiculi transection in the same way they are in adult (4 month) mice. Adult ECs migrate toward the lesion core in both mild injuries and also more severe dorsal hemisection injuries. However, it appears that in juvenile mice, ECs seal the lesion more efficiently without EC migration en masse, as shown by smaller lesion cores in P21 mice compared to adults following mild SCI. It is only when subjected to more severe injuries, that lesions in juvenile animals are comparable to those seen adults. Furthermore, when ECs are prevented from entering the cell cycle and proliferating following severe SCI, using FoxJ1-CreER-rasless mice (Sabelstrom *et al*., 2013), juvenile mice continue to seal lesions as 50% of adult mice exhibit ineffective lesion sealing. These results suggest that in juvenile mice other glial cells, such as astrocytes and microglia, appear to

have appropriate lesion sealing properties, and that ECs are a reservoir for repair in adulthood when other glial populations are no longer as efficient at tissue repair.

Cells which appear to be capable of self-renewal and multipotency following injury but are latent or quiescent NSCs in homeostatic conditions, such as spinal cord ECs, are therefore likely to be overlooked when considering NSC populations of the CNS. For example, Coskun *et al* (2008) provide evidence that a subpopulation of $CD133^+$ ECs within the ependyma close to the SVZ neurogenic nice are not 100% postmitotic as previously thought, and possess the characteristics of *bona fide* NSCs (Coskun *et al*., 2008). These $CD133^+$ ECs exhibit *in vitro* NSC properties and colabel with the proliferative marker Ki67. $CD133^+$ ECs appear quiescent under normal conditions, dividing infrequently, similarly to ECs of the spinal cord. However, upon ablation of fast dividing type B NSCs of the SVZ, by intracereboroventricular (ICV) injection of Cytosine-β-D-arabinofuranoside (AraC), $CD133^+$ ECs proliferate rapidly and contribute to the differentiation and migration of new neurones along the rostral migratory stream toward the olfactory bulb (Coskun *et al*., 2008).

Coskun *et al*., (2008) therefore argue that $CD133^+$ ECs are a quiescent population of NSCs, which reside in the SVZ ependyma, but do not contribute to SVZ neurogliogenesis to the same extent as other NSC populations such as the type B cells which are already active in this location (Coskun *et al*., 2008). It is only upon chemical ablation by AraC treatment that ECs are activated, leave quiescence, and realise their NSC potential to replace the normally fast dividing NSC population. This may also be the case in the spinal cord, where the proliferation and differentiation of ECs is markedly upregulated in injury situations to replace lost cells.

Work has shown that it is not only SCI which activates the proliferation of ECs. Danilov *et al*., 2006 show that following induction of experimental autoimmune encephalitis (EAE) in rats, a model of multiple sclerosis (MS), ECs labelled by injection of the lipophilic tracer DiI not only proliferated, but their progeny could also be seen migrating toward areas of

neuroinflammation (Danilov *et al*., 2006). DiI labelled EC progeny were also colabelled with the neuronal markers NeuN and Tuj1 (Danilov *et al*., 2006). These results would suggest that following EAE ECs are capable of proliferating, migrating toward the neuroinflammatory lesions, and differentiating into cells with neuronal morphology, to aid repair following autoimmune induced demyelination. This study relies upon specific labelling of EC by DiI injections. However, it is possible that nearby oligodendrocytes or astrocytes may have also been labelled by ventricular DiI injection and contribute to the effects seen in response to EAE.

1.6.5 Transplantation of ECs to other neurogenic niches

Cell transplantation studies allow us to determine whether NSC-candidate cells, such as ECs, possess *in vivo* NSC behaviour when removed from their niche, clonally expanded, and placed into their original neurogenic niche (homotopic transplantation) or into a different niche (heterotopic transplantation). For example, it has been shown that when cultured adult hippocampal progenitors, which remain mostly uncommitted in culture, are homotopically grafted into the hippocampus they migrate into the neuronal layers of the DG, undergo maturation, and express the neuronal markers NeuN and calbindin, as expected for adult hippocampal progenitors (Suhonen *et al*., 1996). However, this study also showed that when these cells were grafted into a heterotopic location, the rostral migratory stream adjacent to the neurogenic SVZ, cells migrated along the rostral migratory stream and into the granule and glomerular cell layers of the olfactory bulb. By 8 weeks post-graft, adult hippocampal progenitors which migrated to the olfactory bulb expressed tyrosine hydroxylase, calbindin, and NeuN. These results show that following heterotopic transplantation to the rostral migratory steam adult hippocampal progenitors behave similarly to endogenous SVZ progenitors, suggesting that regional cues can confer regional specific developmental behaviour to progenitors of heterotopic origin (Suhonen *et al*., 1996).

Transplantation of NSC candidate cells into well-known neurogenic niches has provided *in vivo* demonstration of NSC potential. Coskun *et al*., 2008 show that $CD133^+$ ECs, which line the lateral ventricle and have *in vitro* NSC potential, proliferate and exhibit multipotency when transplanted into the neurogliogenic environment of the adjacent SVZ via injection into the lateral ventricle.

Similarly, heterotopic transplantation of ECs provides us with strong evidence that ECs are NSCs which are trapped in the restrictive signalling environment of the intact spinal cord, which therefore limits NSC behaviour. Shihabuddin (2000) showed that when transplanted into the neurogenic niche of the hippocampus, fibroblast growth factor responsive clonally expanded cultures of cells originating from cervical or thoracic spinal cord migrate and integrate into the neuronal layers of the DG. By six weeks post transplantation, many of the cells originally from the spinal cord exhibited morphologies characteristic of native hippocampal granule cells, including a large rounded nucleus, an ovoid cell body, and polarised branching dendritic processes (Shihabuddin *et al*., 2000).

$BrdU^+$ transplanted cells preferentially expressed molecular markers of hippocampal neurones, with 47.5±3.7% expressing NeuN and 43.7±3.7% expressing the DG granule cell layer specific marker calbindin. Heterotopically transplanted spinal cord cells also exhibited multipotency, 2.8±0.6% of $BrdU^+$ cells expressed GFAP, 21.5±5.7% expressed NG2, and 2.8% expressed the mature oligodendrocyte marker RiP. $BrdU^+$ cells within grafts also possessed synaptophysin immunoreactive (IR) elements on their surface, indicating that spinal cord cell grafts had integrated into the local hippocampal GCL network by receiving synaptic contacts (Shihabuddin *et al*., 2000). Proliferating cells of the spinal cord usually become oligodendrocytes in intact cord, and astrocytes in injured cord, indicating a strong gliogenic drive within the spinal cord. However, when transplanted into the neurogenic environment of the hippocampus, these cells respond to the intrinsic cues of the environment and behave similarly to native hippocampal NSCs and progenitors.

Ultimately, work by Shihabuddin *et al*., (2000) shows that ECs are NSCs, however their local environment does not possess the intrinsic cues to permit NSC behaviour as is seen when these cells are relocated to the hippocampus. Therefore, rather than completely lacking NSCs, the spinal cord lacks the correct environment and intrinsic cues which permit NSC behaviour.

1.6.6 Transplantation of cells to the restrictive spinal cord environment

Work by Braz *et al*., (2012) however suggests that the spinal cord environment may not be as restrictive as previously imagined. Using heterotopic transplantation of embryonic cortical interneurone precursors, originating from the medial ganglion eminence (MGE), into the dorsal horn of the adult spinal cord, MGE transplants survive, retain cortical interneurone features, and integrate into host spinal cord circuitry. The majority of the MGE-derived precursors transplanted into the spinal cord expressed markers of distinct subpopulations of cortical GABAergic neurones including GABA, neuropeptide Y, parvalbumin, and somatostatin, and so recapitulate the heterogeneity of native cortical GABAergic neurones (Braz *et al*., 2012).

MGE grafts also developed into mature neurones and exhibited firing patterns similar to endogenous cortical and spinal inhibitory GABAergic interneurone populations (Etlin *et al*., 2016). Furthermore, the successful integration of MGE grafts into the spinal cord, which established new inhibitory dorsal horn circuits in the host, overcame mechanical hypersensitivity and hyperalgesia induced by a nerve injury model of neuropathic pain (Etlin *et al*., 2016; Llewellyn-Smith *et al*., 2018).

Whilst these results may suggest that the spinal cord environment is not as restrictive as it may seem, they may instead indicate the rigidity of the differentiation programme intrinsically ascribed to MGE-derived cortical progenitors. MGE precursors appear to possess a strict differentiation programme which allows the cells to maintain their neurochemical phenotype irrespective of the restrictive environment they find themselves in. The results may have

been different if undifferentiated hippocampal NSCs were instead introduced into the cord. Furthermore, it is also possible that the transplantation of MGE cells by injection causes a 'stab-like' injury which results in afferent sprouting to repair damage to existing spinal neurones of the dorsal horn (Braz *et al*., 2012; Etlin *et al*., 2016; Llewellyn-Smith *et al*., 2018). Results such as these highlight the need to understand the niche signals which control cell proliferative behaviour in the spinal cord.

1.6.7 Transplantation of ECs into the injured spinal cord

Transplantation of healthy donor spinal cord derived NSC/NSPCs cells into an injured spinal cord has also provided evidence of NSC capabilities within the spinal cord. Transplanted spinal cord derived NSC/NSPCs are able to differentiate and slightly improve functional motor recovery following SCI in rats (Hofstetter *et al*., 2005). However, animals also develop allodynia and hypersensitivity as a result of aberrant axonal sprouting and infiltration of new CGRP-IR sensory fibres into superficial and deep layers of the dorsal horn (Hofstetter *et al*., 2005). Grafted cells also exhibit poor survival (Hou *et al*., 2018) and failure to differentiate *in vivo* (Li, J. and Lepski, 2013). In addition, the overwhelming gliogenic environment of the spinal cord seems to result in predominant differentiation of grafts into cells of the astrocytic lineage which then further contribute to the already problematic glial scar (Hofstetter *et al*., 2005).

Most studies investigating SC derived NSC grafts to aid in SCI repair use dissociated tissue from the entire spinal cord. Moreno-Manzano (2009) illustrate that functional recovery can be improved in a rat model of SCI if ECs are isolated and used for transplantation, rather than undifferentiated neurospheres generated from the entire spinal cord. In particular, activated ECs (aECs), taken from an injured rat spinal cord, provide more successful grafts for transplantation than their healthy counterparts. As a result of the environmental changes which result following SCI, it appears aECs are already primed to proliferate and

differentiate, and also show greater self-renewal potential, for optimal reparative outcomes (Moreno-Manzano *et al*., 2009).

Furthermore, aECs can either be transplanted undifferentiated into the cord, and are alone successful in motor repair, or can be subjected to a differentiation programme *in vitro* prior to transplantation. Following directed differentiation, aECs were able to generate OPCs and functional motor neurones which were then transplanted into the injured cord, further contributing to functional recovery. There is a greater yield of OPCs and motor neurones following directed differentiation of aECs when compared to ECs isolated from healthy intact donor cords, 87% vs. 21% for OPCs and 45% vs 12% for motor neurones (Moreno-Manzano *et al*., 2009).

SCI rats which received grafts of either aEC or OPCs exhibited significant motor recovery compared to animals that received healthy donor EC grafts, including consistent plantar stepping, weight bearing capacity, and improved coordination 1-month post transplantation (Moreno-Manzano *et al*., 2009). These results therefore illustrate improved hindlimb coordination in animals following post SCI transplantation of aECs.

In conclusion, rats receiving grafts of aECs had greater regenerative capacity and smaller cavities following SCI, leading to greater functional repair. These results show that EC do possess the crucial NSC properties of self-renewal and differentiation, but appear dormant until switched on following injury, and if ECs with these enhanced properties are grafted into another injured SC environment, then they can have greater functional outcomes than healthy ECs.

Hoffstetter *et al*., (2005) showed that whilst grafts improve functional recovery, their utility is limited by aberrant axonal sprouting induced allodynia. In order to overcome this, NSCs were transduced with the transcription factor Neurogenin-2 (Ngn2) prior to transplantation. Ngn2 modulates the fate of engrafted NSCs, suppressing astroglial differentiation. Animals which received Ngn2-NSC grafts rather than naïve NSCs showed increased levels of

myelination and WM volume at the injury centre which positively correlated with recovery of hindpaw locomotor and sensory function without the development of allodynia (Hofstetter *et al*., 2005). These results indicate that overcoming the gliogenic environment of the spinal cord, by suppression of astroglial differentiation of grafts, is essential for successful reparative behaviour of the spinal cord stem cells, the ECs.

In conclusion for this section, results from transplantation studies provide strong evidence for NSC properties of ECs. Studies using transplantation of ECs have provided clear evidence that ECs possess NSC properties and that when in their local environment of the spinal cord, their NSC abilities remain dormant, unless activated by environmental changes such as injury (Barnabe-Heider *et al*., 2010; Meletis *et al*., 2008), or placed into a permissive environment such as the hippocampus (Shihabuddin *et al*., 2000).

1.7 Neurotransmitters as niche signals which restrict proliferation in the spinal cord

If ECs are indeed *bona fide* NSCs but only exhibit NSC behaviour in certain conditions and environments, then we must consider which niche signals may be present in the spinal cord which maintains their dormancy under normal conditions. It is clear that the local environment and its intrinsic signalling pathways play a large part in determining NSC behaviour (Massirer *et al*., 2011). Niche signalling within the CC ependymal layer may therefore exist to keep the cells in a quiescent state, although what exactly constitutes these restrictive signals remains unclear.

Neurotransmitters are known to be an important aspect of the neurogenic niche microenvironment, controlling the delicate balance between quiescence, proliferation, and differentiation (Ma *et al*., 2004; Jansson and Akerman, 2014; Trujillo *et al*., 2009; Catavero *et al*., 2018). For example, acetylcholine is known to be an important regulator of proliferation, differentiation, and new born neurone survival in other postnatal neurogenic niches (Corns *et*

al., 2015). Cholinergic inputs enhance NSC proliferation within the SVZ (Paez-Gonzalez *et al*., 2014; Asrican *et al*., 2016), indicating that cholinergic neurotransmission may be essential for postnatal neurogenesis and modulation of proliferation in other neurogenic niches such as that of the spinal cord CC. Indeed, recent work has shown how acetylcholine is an important regulator of EC proliferation in both physiological and simulated pathological situations (Corns *et al*., 2015).

Cholinergic structures have been found in close apposition to ECs within the CC and are therefore well situated to influence and modulate the proliferative capacity of cells within the CC (Corns *et al*., 2015; Gotts *et al*., 2016). Corns *et al*., (2015) illustrate that treatment with the α7*nAchR modulator PNU 120596 significantly increased the number of newly proliferated Sox2/CD24/Na^+K^+ATPase $\alpha1^+$ ECs within the CC in *in vivo* intact mature animals and also in *in vitro* organotypic spinal cord slice culture, a method which resembles an injurious situation (Fernandez-Zafra *et al*., 2017). Furthermore, treatment with the antagonist MLA in naïve organotypic spinal cord slices reduced the level of EC proliferation, suggesting that endogenous activation of α7*nAchRs contributes to baseline levels of EC proliferation (Corns *et al*., 2015). The numbers of proliferative cells in the WM and GM were also influenced by modulation of α7*nAchRs, indicating the widespread effects of cholinergic enhancement upon proliferation within the spinal cord (Corns *et al*., 2015).

These results illustrate that acetylcholine may therefore be an important signal within the CC neurogenic niche for the control of postnatal proliferation of ECs. Such results also demonstrate the role that neurotransmitters may play in controlling proliferation in the adult spinal cord. The classic inhibitory neurotransmitter γ-aminobutyric acid (GABA) is another possibly important player in the control of proliferation and maintenance of EC quiescence within the postnatal spinal cord (Corns *et al*., 2013; Catavero *et al*., 2018).

1.8 GABA

GABA is produced in the CNS in a closed loop system known as the GABA shunt. First, α - ketoglutarate, produced during the Kreb's cycle, is converted into glutamate by glutamate dehydrogenase. Glutamic acid decarboxylase (GAD) catalyses the decarboxylation of glutamate to produce GABA. GABA is then packaged into vesicles and released from the synaptic terminal into the cleft following action potential-induced depolarisation of the neurone. The action of GABA is terminated by GABA reuptake into presynaptic neurones and surrounding glia cells by GABA transporters such as GABA transporter 1 (Soudijn and van Wijngaarden, 2000) (figure 1.6). Reuptake into neurones is around 4- to 5-fold greater than in astrocytes (Salat and Kulig, 2011).

Following reuptake, GABA transaminase, present in mitochondria of glial cells and neurones (Schousboe *et al*., 1973; Jeon *et al*., 2000), breaks down GABA in neurones and glia to form succinic semialdehyde which re-enters the citric acid cycle for the production of α - ketoglutarate to eventually form GABA by resynthesis in neurones. Glial cells however lack GAD expression and so in glia GABA is converted to glutamine which is transferred back to the neurone. Glutamine is then converted to glutamate by glutamate synthase which re-enters the GABA shunt (Ben-Menachem, 2011) (figure 1.6)

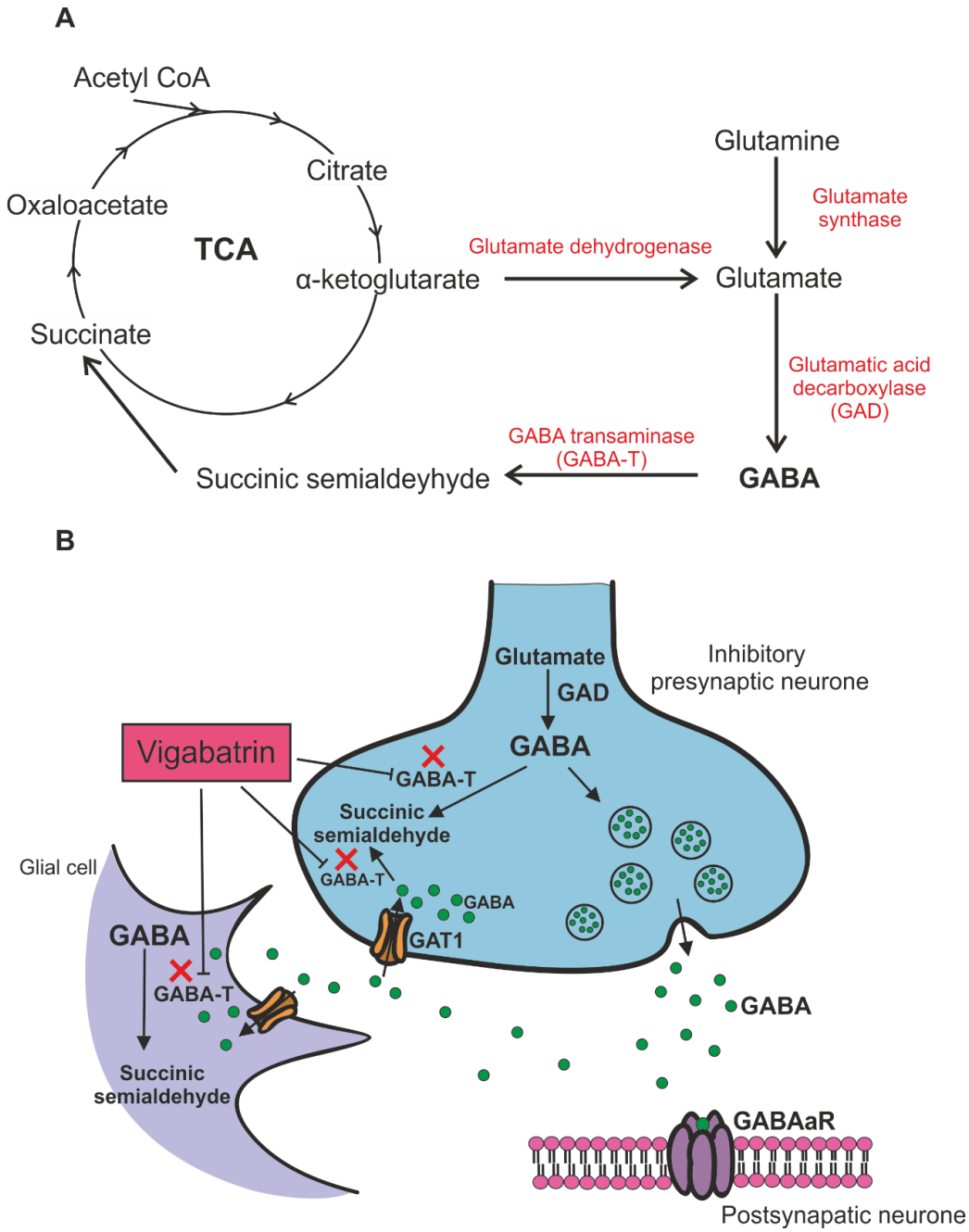

Figure 1.6 Schematic depicting GABA synthesis and neurotransmission

GABA is produced in a closed loop system (A) where, following action potential arrival at the presynaptic neurone, it is released and binds to GABAaRs on the postsynaptic membrane (B). The action of GABA is terminated by GABA-transaminase mediated catabolism. Vigabatrin inhibits GABA-transaminase to increase GABA availability (B) **GABA-T**: GABA-transaminase **GAT1**: GABA transporter 1 (Adapted from Ben-Menachem, E., 2011).

GABA signalling is known to have important roles in pre- and postnatal neural development through effects upon embryonic stem cells (Varju *et al*., 2001; Wang, D.D. and Kriegstein, 2009). GABA has also been shown to modulate proliferation, differentiation, and migration of adult NSCs and neural progenitor cells of the SVZ and the SGZ in postnatal CNS (Catavero *et al*., 2018). These cells express functional GABAaRs in addition to the enzymes required to synthesise GABA, GAD65 and GAD67 (Nguyen *et al*., 2003; Wang, D.D. *et al*., 2003; Fernando *et al*., 2011). Depolarisation of proliferating progenitors by GABAergic signalling results in a cascade of events which combines activity and development of new neurones by activation of differentiating signals in the NSCs. Work suggests that it is GABA, and its activity at GABAaRs, which holds the key to 'excitation-neurogliogenesis coupling' in the adult brain (Song, J. *et al*., 2012; Deisseroth, K. and Malenka, R. C., 2005; Ge *et al*., 2007).

1.8.1 GABAaR subunit composition and allosteric modulators

GABAaRs are heteropentameric protein complexes which form ligand-gated ionotropic receptors arranged around a central channel pore which is permeable to Cl- (Bormann *et al*., 1987). GABAaRs are part of the evolutionarily conserved cys-loop superfamily of ligand gated ion channels and are widely expressed throughout the CNS, within multiple cell types, and with considerable subunit heterogeneity (Sigel, E. and Steinmann, 2012). A repertoire of 19 different subunits have been identified so far in mammals, divided into 8 different subunit classes based on sequence homology, these include α (1-6), β (1-3), γ (1-3), δ, ε, ρ (1-3), θ, and π (Hevers and Luddens, 1998; D'Hulst *et al*., 2009; Sieghart, W. and Sperk, 2002). Whilst the vast array of subunit isoforms suggests an infinite number of possible subunit-isoform combinations, in reality limited numbers of these combinations have been shown to exist *in vivo* (McKernan and Whiting, 1996). Each subunit possesses a large extracellular N-terminal domain and a C-terminal domain. The extracellular N-terminal domains are believed to implicated in receptor assembly and the formation of agonist and allosteric modulatory binding sides (Xu, M. and Akabas, 1996; Uchida *et al*., 1997). The C-terminal domain

possesses four transmembrane spanning segments, designated TM1-4, which are connected by short loops. The ion-conducting channel pore is lined by the TM2 domains of the five subunits (Xu, M. and Akabas, 1996; Goren *et al*., 2004).

The majority of native GABAaRs in the CNS are comprised of α-, β-, and γ- subunits and those with 2 α1s, 2 β2, and 1 γ2 subunits are most abundant (Olsen and Sieghart, 2008; McKernan and Whiting, 1996) (figure 1.7). These isoforms are frequently located at the synapse, where they mediate transient phasic synaptic GABAergic transmission (Farrant and Nusser, 2005; Belelli *et al*., 2009). Thus, they are responsible for 'classic' neurotransmission for the communication between pre- and postsynaptic neurones.

In some neurones however there also exists a level of GABA-mediated tonic inhibition which is conferred by extrasynaptic GABAaRs. These extrasynaptic GABAaRs are activated by GABA spill-over from the synaptic cleft following vesicular GABA release from the presynaptic neurone (Otis *et al*., 1991; Salin and Prince, 1996a; Salin and Prince, 1996b). Extrasynaptic GABAaRs are often formed from more 'uncommon' subunits such as α4, α5, α6, and δ subunits (Belelli *et al*., 2009; Wang, L. *et al*., 2008). This leads to their unique sensitivity to some ligands such as ethanol (Santhakumar *et al*., 2007) and insensitivity to benzodiazepines (BZs), for example, extrasynaptic α4, α6, and δ expressing GABAaRs are insensitive to BZs (Belelli *et al*., 2009). GABAaR subunit composition therefore confers specific ligand binding properties and behaviour and responses of GABAaRs.

Pentameric assembly and receptor subunit heterogeneity of GABAaRs results in the formation of various ligand binding sites at the extracellular- or transmembrane domain of certain subunits at the interface between subunits (Sieghart, Werner, 2015). Ligand binding at these sites modulates the activity of the GABAaR. αβγ GABAaRs have two agonist binding sites, where GABA binds (Wagner and Czajkowski, 2001; Baumann *et al*., 2003), and another for the binding site for BZ-like allosteric modulators (Sigel, E. and Buhr, 1997; Sigel, Erwin and P. Luscher, 2011). GABA binding to these sites induces opening of the

channel pore which then allows flow of Cl- ions down their electrochemical gradient. Entry of Cl- leads to hyperpolarisation of the cell membrane in most cells, although there are some exceptions where GABA causes depolarisation (Spitzer, 2010).

There are five main modulatory mechanisms at GABAaR, these include; positive allosteric modulation (PAM) e.g. BZs, negative allosteric modulation (NAM)/inverse agonists e.g. DBI, agonists at the GABA binding site e.g. muscimol, antagonists at the GABA binding site e.g. bicuculline, and pore/channel blockers e.g. picrotoxin. GABAaRs were therefore initially characterised based upon the presence of their 3 major drug binding sites. 2 of these binding sites are located in the extracellular domain and include the GABA binding site at β-subunits, and the BZ/central BZ recognition (CBR) site at the interface between and y2 subunits. The third GABAaR defining ligand binding site is specific for the channel blocker picrotoxin and is located within the transmembrane domain of the channel ionic pore (Ticku *et al*., 1978) (figure 1.7).

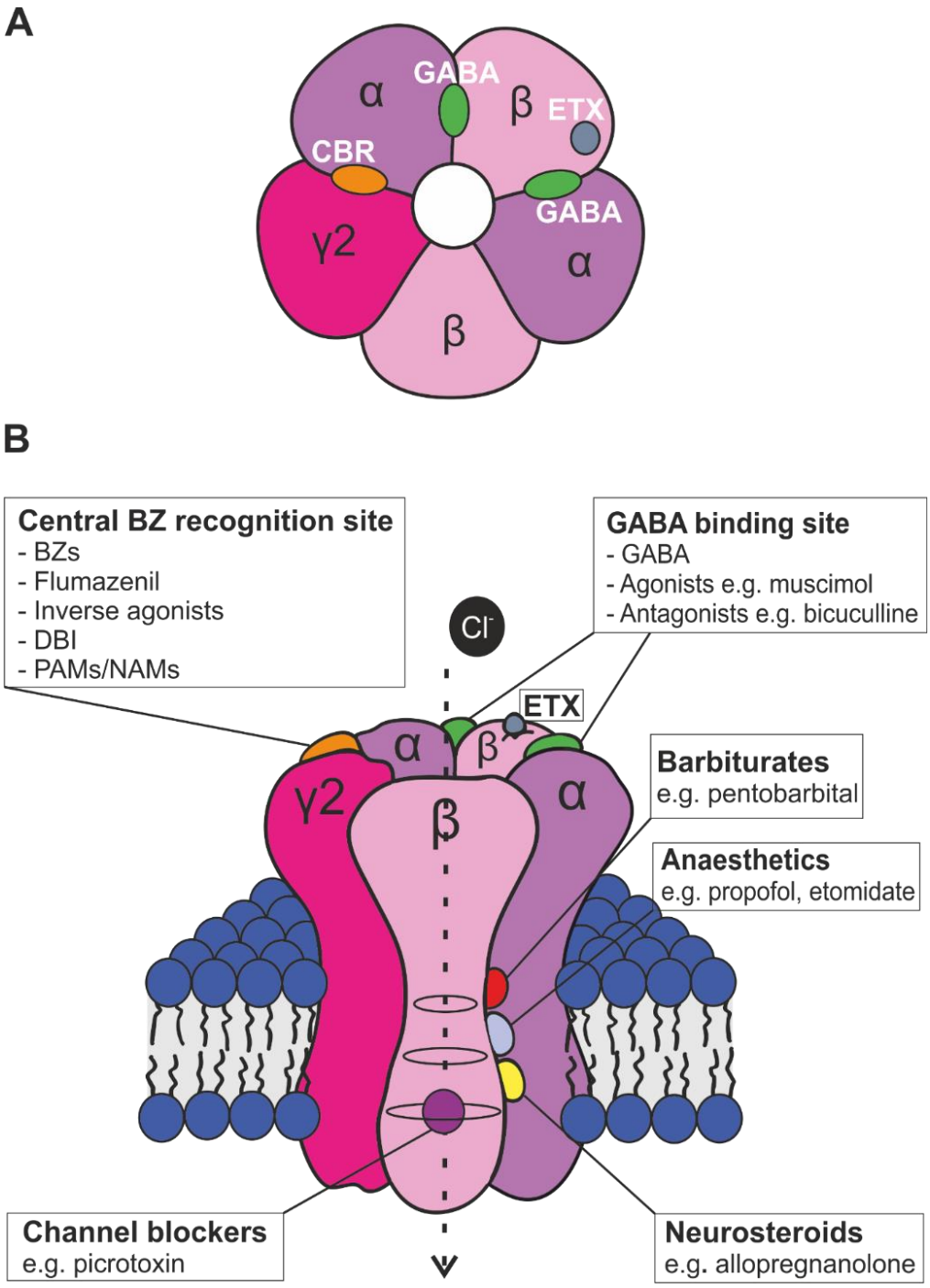

Figure 1.7 The GABAaR receptor is a pentameric ion channel with binding sites for common neuromodulatory pharmacological agents located at subunit interfaces

A: Schematic showing a top down view of the pentameric assembly of the GABAaR and the location of binding sites for GABA, ETX, and the CBR site. **B**: Schematic detailing the intracellular, extracellular, and transmembrane binding sites for common GABAaR modulators

1.8.1.1 Extracellular binding domains of GABAaRs

Firstly, located between the extracellular sites of β/α interfaces are the orthosteric GABA sites. It is at this site where GABA and various agonists and antagonists such as muscimol and bicuculline bind (Smith, G.B. and Olsen, 1995) (figure 1.6). At the interface between the α and γ2 subunits, at the extracellular domain, exist the allosteric BZ/CBR sites, where PAMs such as BZs (e.g. diazepam) bind and potentiate GABAaR activity (Squires and Braestrup, 1977; Olsen, 2018). The long sought-after endogenous ligand of the GABAaR CBR site diazepam binding inhibitor (DBI) acts as a NAM of GABAaR by binding to this site (Dumitru *et al*., 2017; Slobodyansky *et al*., 1989). Drugs of the β-carboline family, such as DMCM, also bind to the CBR site, whereupon they also act as NAMs (Hanson and Czajkowski, 2008). Furthermore, inverse agonists and competitive antagonists of the BZ site, such as Ro15-4513 and Ro15-1788 (flumazenil), also bind specifically to CBR (Votey *et al*., 1991; Buck, K.J. and Harris, 1990).

1.8.1.2 Transmembrane domains of GABAaRs

GABAaR subunit interfaces have also been shown to possess specific binding sites within the receptor transmembrane domain. Specific transmembrane domain subunit interface binding sites include binding sites for barbiturates, located at α^+/β- and γ^+/β- subunit interfaces (Thompson *et al*., 1996), and anaesthetics, such as etomidate, propofol, at β^+/α-subunit interfaces (Chiara *et al*., 2013; Li, G.D. *et al*., 2006) (figure 1.7).

Neurosteroids, such as allopregnanolone (AlloP) also bind within the transmembrane domain of GABAaR, where they act as either PAMs or NAMs, depending upon their specific molecular composition and subunit composition of the GABAaR it binds to (Wang, Mingde, 2011).

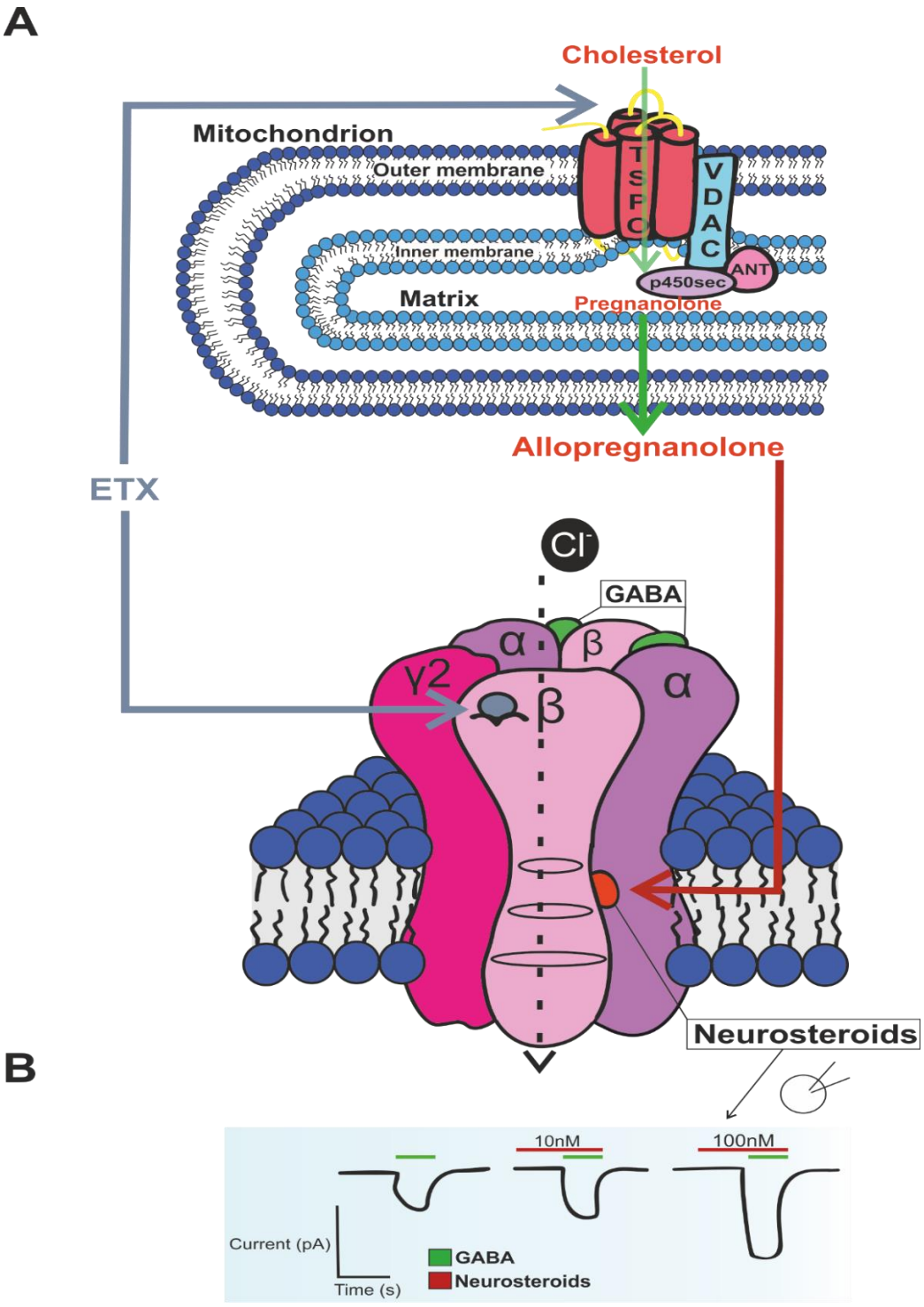

Figure 1.8 Mixed modulators of GABAaR and TSPO such as ETX influence GABAergic signalling by both PAM activity at GABAaR and neurosteroidogenesis

A: Schematic illutrating the dual effects of ETX at TSPO and GABAaR. **B**: Schematic depicting the synergistic affects of mixed modulators which potentiate GABAergic signaling by direct PAM of GABAaR and by production of neurosteroids

The 18kDa mitochondrial translocator protein TSPO, previously known as PBR, for which the GABAaR ligands BZs and DBI are also ligands, is implicated in the synthesis of such neurosteroids which can modulate GABAergic signalling (Ante and Ljiljana, 2016) (figure 1.9).

Some GABAaR-CBR site ligands can therefore have additive effects upon GABAergic transmission, by either direct binding to CBR or by influencing neurosteroid synthesis. The recent discovery that the CBR specific NAM of GABA, DBI, influences proliferation and differentiation of NSCs within the brain (Dumitru *et al*., 2017; Alfonso *et al*., 2012), and is linked to neurogenic effects of enriched environment, has generated new interest in the CBR site of GABAaR, and its endogenous ligands.

1.8.1.3 Endozepines and the CBR site

Co-immunoprecipitation with GABAaR subunit isoform specific antibodies and application of such antibodies for *in-situ* hybridisation, showed that seventy five percent of GABAaRs have a classical high affinity BZ binding site/CBR site, located extracellularly at the α and γ2 subunit interface (figure 1.7) (Wisden and Stephens, 1999; Sigel, E. and Buhr, 1997; Ernst *et al*., 2003). The predominant GABAaR CBR site is most commonly composed of an α1 subunit isoform which forms a binding pocket with the interface of a neighbouring γ2. Following binding to the CBR site, there is a conformational change in the GABAaR which increases the affinity of at least one GABA/agonist site resulting in increased GABA-mediated currents and increased GABA affinity (Tallman and Gallager, 1985; Serfozo and Cash, 1992; Lavoie and Twyman, 1996).

Binding at α1 containing CBR sites produces sedation and muscle relaxation, whereas CBR sites with α2 or α3 subunits with γ2 results in the anxiolytic and anticonvulsant effects of BZs. Extrasynaptic GABAaRs however can also express α5 which is responsible for amnestic effects of some BZs, and also mediates the amnestic effects of ethanol when α5 is expressed alongside δ subunits (Nutt *et al*., 2007). Within the α subunit of α1, 2, 3, and 5

isoforms, there exists a histidine residue (H101, H101, H126 and H105, respectively) which possesses a high affinity for BZs. However, α4 and α6 isoforms contain an arginine residue instead and therefore do not have affinity for BZs (Kelly *et al*., 2002).

The γ2 subunit is essential for the formation and function of the CBR site (Gunther *et al*., 1995). Peak sensitivity of GABAaR CBR sites requires γ2 expression as decreased sensitivity to BZs is seen when either γ1 or γ3 are expressed (Hadingham *et al*., 1995; Ymer *et al*., 1990). The γ2 subunit is also required for the synaptic postsynaptic membrane clustering, and therefore function, of GABAaRs (Schweizer *et al*., 2003; Essrich *et al*., 1998).

Global knockout (KO) of the γ2 subunit results in mice which lack the CBR site of GABAaR and are insensitive to the hypnotic effects of diazepam (Gunther *et al*., 1995). Homozygous γ2 KOs appear normal at birth, however they show retarded growth, sensorimotor dysfunction, and a drastically reduced lifespan (Gunther *et al*., 1995). Previous studies have shown that reduced lifespan in homozygous γ2 KO is likely due to impaired postsynaptic receptor clustering and loss of GABAaR function in mature neurones (Gunther *et al*., 1995; Essrich *et al*., 1998; Schweizer *et al*., 2003). The deleterious effects of γ2 subunit/CBR site KO also possibly suggests the importance and necessity of postnatal GABAaR regulation by an endogenous ligand at the CBR site.

Heterozygous γ2 knockdown (KD) mice have also been generated where γ2 expression is, on average, 35% of normal levels (Crestani *et al*., 1999; Chandra *et al*., 2005). These mice are viable, develop well, and have normal lifespans, however they exhibit enhanced anxiety-like behaviours and have significantly decreased binding of the CBR ligand Ro15-4513. This is expected as CBR is located at the interface of select alpha and γ2 subunits of GABAaR, where the deficiency of the γ2 abolishes binding of CBR specific ligands (Chandra *et al*., 2005; Gunther *et al*., 1995). However, γ2 KD mice have unaltered behavioural responses to BZ GABAergic modulators such diazepam or midazolam. These results suggest that unlike global γ2 KO mice, which exhibit 6% CBR site binding, and are therefore insensitive to the

behavioural effects of BZs, those with heterozygous γ2 KD retain some CBR site binding. Chandra *et al*., (2005) suggest that perhaps the remaining 20-40% of BZ binding in these mice is sufficient to induce the hypnotic effects of diazepam and midazolam. Alternatively, the significant inter-animal differences in γ2 KD efficiency, which ranged from 10-95% of normal levels, may have masked any change in behavioural responses to these drugs (Chandra *et al*., 2005).

1.9 Effects of GABA and GABAaR signalling in other neurogenic niches

PSA-NCAM$^+$ cells persist in several regions of the adult brain and are particularly enriched in areas involved in postnatal neurogenesis such as the SVZ and SGZ (Nguyen *et al*., 2003). Proliferation of purified cultured PSA-NCAM$^+$ progenitor cells, as assessed by BrdU incorporation, is reduced following treatment with GABA itself and the GABAaR agonist muscimol. This effect however is not seen upon treatment with the GABAbR agonist baclofen, indicating the GABAaR mediated effect upon proliferation of PSA-NCAM$^+$ neural progenitor cultures. TUNEL staining illustrates that the GABA/muscimol induced reduction in the percentage of PSA-NCAM$^+$ cells which incorporate BrdU is not due to increased cell death mediated by GABAaR activation, and is instead a GABAaR mediated reduction in cell proliferation (Nguyen *et al*., 2003). These results indicate the role GABAergic signalling plays in modulating proliferation in neurogenic niches of the brain. In addition, GABAergic signalling via GABAaR also induces differentiation of neural progenitors within the SGZ (Tozuka *et al*., 2005) and modulates the speed of neuroblast migration through the rostral migratory stream (Bolteus and Bordey, 2004).

1.9.1 Effects of GABA on NSCs in the SVZ

Contrary to the hyperpolarising effects normally induced by GABA binding to GABAaR, GABA depolarises SVZ neural progenitors (Wang, D.D. *et al*., 2003). In addition, application of the GABAaR antagonist, bicuculline, to organotypic cerebral slices containing SVZ results

in an increase in proliferating cells, as assessed by BrdU incorporation (Liu, X. *et al*., 2005). GABA also has roles in promoting differentiation of NSCs and progenitors (Tozuka *et al*., 2005). Furthermore, migratory speed of neuroblasts from the SVZ to the olfactory bulb is controlled by the release of GABA from astrocytes which line the rostral migratory stream (Bolteus and Bordey, 2004). In the SGZ niche, GABA, spilled over from nearby terminals of parvalbumin$^+$ interneurones regulates proliferation and differentiation of both NSCs and young neurones/neuroblasts by tonic and synaptic activation of GABAaRs, respectively (Song, J. *et al*., 2012; Ge *et al*., 2007; Song, Juan *et al*., 2013).

Less is known however about how GABA may influence NSC niche behaviour by regulating quiescence and activation of NSCs through the regulation of cell cycle kinetics. A large majority of NSCs within a given niche remain in a dormant state (Morizur *et al*., 2018), which is thought to be due to the influence of a GABA mediated paracrine stop signal released from neighbouring neuroblasts within the niche. GABA then activates GABAaR in NSCs and limits their progression through the cell cycle (Fernando *et al*., 2011). It is well established that GABA released from neuroblasts within the SVZ exerts inhibitory control over astrocyte-like GFAP$^+$ NSCs via action on GABAaR, and disinhibition of this process by treatment with bicuculline results in increased proliferation of transit amplifying cells and NSCs (Liu, X. *et al*., 2005).

Antimitotic agents and ionisation radiation induces death of neuroblasts, removing the source of inhibitory GABA, which results in NSC proliferation and subsequent recovery of SVZ populations (Daynac *et al*., 2013; Doetsch *et al*., 1999b; Morshead *et al*., 1994). For example, following irradiation of the SVZ to selectively ablate fast dividing progenitors, the numbers of proliferating Mash1$^+$ transit amplifying cells and DCX$^+$ neuroblasts were reduced by 90%. However, GFAP$^+$ cells, likely NSCs with slow cell-cycle kinetics and turnover, remained unchanged (Daynac *et al*., 2013). Furthermore, whilst qRT-PCR analysis showed maintenance of NSC markers GLAST and TLX were maintained 24-48 hours post-irradiation, markers for transit amplifying cells, such as Mash1, Sox2 and Nestin, and

neuroblasts, DCX, were significantly reduced. Treatment with BrdU following irradiation confirmed that $GFAP^+$ quiescent NSCs are resistant to irradiation and increase their population size by approximately 6-fold to repopulate the niche following depletion of other cells within the SVZ. $DCX/BrdU^+$ cells were later found in the olfactory bulb, indicating that surviving NSCs are capable of producing functional migrating neuroblasts (Daynac *et al*., 2013).

Daynac *et al*., (2013) also illustrate that 24 hours following GABAaR inhibition by bicuculline treatment the population of NSCs in intact SVZ increases 6.4-fold, suggesting GABAaR antagonist treatment allows cell cycle entry of quiescent NSCs to increase the population of activated, actively cycling, and proliferating NSCs. GABA-secreting neuroblasts die shortly after irradiation, therefore removing the source of GABA which prevents NSC proliferation. It is likely that through the loss of the GABA mediated stop signal in this way, quiescent NSCs are able to enter the cell cycle, increase their proliferation by 6-fold and repopulate the niche. This was confirmed by treatment with the GABAaR agonist muscimol, where muscimol delayed activation and proliferation of surviving quiescent NSCs which also delayed recovery of SVZ neurogenesis until 96 hours post-irradiation. Activated NSCs and transit amplifying cells were below basal levels following irradiation in muscimol treated mice. In addition, very few active cycling cells were found scattered in the SVZ compared to untreated irradiated animals. Conversely, bicuculline improved recovery of the niche at 7 days post irradiation where recovery was associated with a higher level of cycling cells in both quiescent and activated NSC populations. These results show that GABA maintains NSCs in a quiescent state under physiological conditions, however following loss of GABAergic signalling following irradiation-induced neuroblast death, quiescent NSCs can be reactivated to exit dormancy/quiescence, and this is particularly critical in times of niche population depletion.

1.10 Effects of GABA on spinal cord NSCs

Whilst some of the effects of GABA on the NSC niches of the hippocampus and SVZ may remain elusive and need to be fully explored, even less is known about how GABA may play a part in influencing NSCs in the spinal cord. ECs consistently respond with a robust depolarisation following GABA application in patch clamp experiments (Corns *et al*., 2013). Depolarisation of ECs by GABA was determined to be mediated in part by GABAaR as these responses were significantly smaller upon co-application of the GABAaR antagonists bicuculline and gabazine which decreased the size of the depolarisation to GABA by 38 ± 10% and 37 ± 11%, respectively. The remainder of the GABAergic response in ECs was not found to be mediated by either GABA transporters, tested using nipecotic acid or guvacaine to block transporters, or GABAbR activation since baclofen activates GABABRs (Corns *et al*., 2013). Therefore, exactly what mediates the bicuculline-resistant component of the GABAergic response in ECs remains to be determined. However, it is evident that ECs are able to respond to local GABA release, where their response is similar to progenitor cells within the neurogenic niches of the brain (Liu, X. *et al*., 2005).

Endogenous GABA is likely to influence ECs through release of GABA from the GABAergic terminals that synapse with ECs (Kaduri *et al*., 1987; Magoul *et al*., 1987). These terminals may arise from local GABAergic interneurons of lamina X (Gotts *et al*., 2016), or from neighbouring cells present within the highly heterogenous CC cytoarchitecuture (Hugnot and Franzen, 2011). GABAergic terminals have been found in close apposition in CSFcCs (McLaughlin *et al*., 1975) and this possibility may extend to ECs.

Glutamate decarboxylase 67-green fluorescent protein (GAD67-GFP) mice, which have expression of GFP in all cells expressing the enzyme responsible for the formation of GABA by glutamate decarboxylation, GAD67, allow identification of GABA synthesising cells in the CNS (Tamamaki *et al*., 2003). GAD67-GFP mice show robust expression of GFP in CSFcCs of the CC, indicating the presence of GABA synthesising machinery in these cells

(Tamamaki *et al*., 2003). Furthermore, CSFcCs are located in the subependymal layer in close apposition to ECs (Corns *et al*., 2015). It has been suggested that CSFcCs may constitute a neurosecretory system which influence CSF composition as CSFcCs exhibit of dense granular and clear synaptic vesicles in the CSFcC terminal bulb (unpublished observation, Deuchars' lab) (Vigh *et al*., 1983a; Vigh *et al*., 1977). These vesicles may contain GABA as VGAT-IR has also been observed in CSF-contacting end-bulbs (Conte *et al*., 2009). Furthermore, immunohistochemistry (IHC) for both synaptophysin and synaptic vesicle protein 2 has shown that these molecules, which are critical for vesicle exocytosis (Edelmann *et al*., 1995; Chang and Sudhof, 2009), are present in CSFcCs (Stoeckel *et al*., 2003), suggesting that CSFcCs may be able to release GABA or other peptides into the CSF from these terminal projections.

These GABAergic cells are therefore well situated to influence EC behaviour by paracrine activation whereby secreted GABA would keep ECs in a quiescent state, similar to the mechanism in which GABA released by neuroblasts inhibits proliferation of SVZ NSCs (Liu, X. *et al*., 2005).

CSFcCs also receive functional GABAergic contacts and exhibit functional GABAaRs (Reali *et al*., 2011; Marichal, Nicolás *et al*., 2009). CSFcCs in the turtle spinal cord depolarise in response to GABA, due to the predominance of NKCC1 expression over KCC2, leading to an excitatory response to GABA and an increase in intracellular Ca^{2+} (Reali *et al*., 2011). A situation may therefore exist depolarisation of CSFcCs at the CC, causing them to release GABA, which then acts on CSFcCs and also ECs to restrict proliferation within the CC niche. However, whether these processes occur in the mammalian spinal cord remain to be seen.

Oligodendrocyte progeny make up the majority of newly proliferated cells in the intact postnatal spinal cord (Barnabe-Heider *et al*., 2010) and are also likely to be affected by changes in GABAergic signalling in the spinal cord. In the brain OPCs receive synaptic contacts from GABAergic interneurones (Lin and Bergles, 2004) and endogenous GABA

release has been shown to modulate the differentiation of OPCs (Zonouzi *et al*., 2015). A decrease in GABAaR mediated signalling following hypoxia has been shown to increase OPC proliferation but delay myelination (Zanouzi *et al*., 2015). Conversely, endogenous GABA release, acting on GABAaRs, greatly reduced the number of oligodendrocytes and reduced the amount of myelin present in organotypic cortical slices (Hamilton, L.K. *et al*., 2009). GABAergic signalling has also been implicated in the migration of OPCs (Tong, X.P. *et al*., 2009). Such results illustrate that the effects of the basal inhibitory GABAergic tone upon proliferation and differentiation of oligodendrocytes must also be considered in the adult spinal cord.

1.10.1 Could changes in GABA explain changes in EC behaviour and their activation following injury?

Following injury, ECs increase their proliferation by up to 50-fold (Johansson *et al*., 1999). Could the process of activating dormant NSCs to replace lost cells which seen in the SVZ following irradiation also be occurring in the spinal cord and therefore explain the change in EC behaviour following injury? It is only when there is an injury, where 50% of the glial population is lost in the first 2 days following insult (Grossman *et al*., 2001; Lytle and Wrathall, 2007; Rabchevsky *et al*., 2007), that normally quiescent ECs become activated NSCs, increase their proliferation by ~3x, are able to differentiate into glial cells and migrate toward the lesion site (Barnabe-Heider *et al*., 2010; Meletis *et al*., 2008). ECs may therefore remain quiescent under normal conditions, but retain NSC properties and appearance, as they serve as an emergency repair mechanism that can be activated in times of oligodendrocyte and astrocyte population depletion, as occurs in injury.

Alternatively, if CSFcCs do secrete GABA which acts on ECs to induce dormancy, could injury result in changes in the CSFcCs which removes the GABA-mediated proliferative brake so ECs realise their NSC potential? If so, this would be similar to the effects seen in the SVZ following the ablation of GABA secreting neuroblast (Daynac *et al*., 2013; Morshead

et al., 1994). One could hypothesise that such changes could include cell death of CSFcCs, migration of CSFcCs away from the CC and ECs, or changes in the level of GABA synthesised or released by the cells, all of which might then allow ECs to proliferate, differentiate, and migrate toward areas of damage as the GABAergic signal which acts to maintain EC dormancy has been removed by the injury process. For example, reduced GABA levels have been found in the brains of patients with relapsing-remitting MS and have been linked to greater levels of disability, motor- and cognitive impairment (Cao *et al*., 2018; Cawley *et al*., 2015). Such results suggest that changes in GABAergic signalling may influence proliferation and differentiation in response to CNS pathologies such as MS.

This possibility however is purely speculation at this point in time, as no studies have yet investigated the effects of injury on the activity of CSFcCs and how this would affect NSC behaviour of ECs. Despite this, there is a wealth of evidence which shows that there is a change in the GABAergic system of the spinal cord following SCI (Zhang, A.L. *et al*., 1994; Gwak, Young S. and Hulsebosch, 2011; Meisner *et al*., 2010). Following SCI there is a reduction in the number of GABAergic interneurones, leading to hypofunction in the basal GABAergic tone of the spinal cord which is a key factor in the development of central neuropathic pain, allodynia, and hyperalgesia (Gwak, Young S. and Hulsebosch, 2011; Gwak, Y. S. *et al*., 2006; Drew *et al*., 2004). Loss of inhibitory GABAergic tone following injury may also result in activation of EC NSC capabilities, indicating that these cells are indeed kept dormant by GABAergic signalling in the intact cord.

1.11 Diazepam binding inhibitor

Whilst it is clear that GABA has a role in controlling NSC cell cycle entry, and therefore quiescence, the exact mechanism of this and how GABAaR itself is modulated has remained elusive until recently. Work from Alfonso *et al*., 2012 and Dimutru *et al*., 2017 suggests NAM of GABAergic neurotransmission via the endogenous ligand DBI delicately balances quiescence vs. proliferation by regulating cell cycle exit of NSCs (Alfonso *et al*., 2012;

Dumitru *et al*., 2017). These studies suggest that DBI provides a mechanism by which GABA can be modulated differentially in distinct cell types of the neurogenic niche, and attempts to explain how GABA can simultaneously increase the number of new neural cells whilst also maintaining NSC quiescence in the CNS.

DBI is an endogenous 10kDa peptide, also known as endozepine or acyl-CoA binding protein. DBI was first characterised upon isolation from rat brain in 1983 by Guidotti *et al* by examining the ability of the peptide to bind to and displace radio labelled diazepam from $GABA_AR$ (Guidotti *et al*., 1983; Alho *et al*., 1985). DBI binds to the extracellular domain between α and γ2 subunits of $GABA_AR$ which forms the CBR site (see section 1.7.1.1). DBI also binds to the peripheral-type BZ receptor (PBR) within the mitochondrial membrane, more recently renamed translocator protein (18 KDa) (TSPO) (Papadopoulos *et al*., 1991; Papadopoulos *et al*., 2006). DBI is broken down within astrocytes to form its two main processing products; octadecaneuropeptide (ODN) and triakontatetraneuropeptide (TTN) (Alho *et al*., 1990). ODN and TTN are secreted by astrocytes (Christian *et al*., 2013; Loomis et al., 2013; Loomis et al., 2010), and bind preferentially to CBR and TSPO, respectively, as confirmed by pharmacological study of these receptors with their specific antagonists flumazenil and PK-11195 (Slobodyansky *et al*., 1989).

1.11.1 Expression of DBI in the adult CNS

High levels of DBI mRNA have been reported in the cerebellum, hypothalamus, amygdala, the reticular thalamic nucleus, ependyma of third ventricle, and the area postrema (Alho *et al*., 1990; Alho *et al*., 1985; Alho *et al*., 1991; Tong, Y. *et al*., 1991; Costa, E. and Guidotti, 1991).

Astroglial cells have extremely high concentrations of DBI protein and DBI mRNA, and have also been shown to express the DBI gene (Costa, E. and Guidotti, 1991; Alho *et al*., 1994).. Thus, DBI appears to be preferentially located in glial cell populations such as hypothalamic glial cells, and Bergmann glia of the cerebellum (Tong, Y. *et al*., 1991). Similarly, it has also

been suggested that the strong *in situ* labelling found in the area postrema may be due to labelling of its prolific glial network (Roth and Yamamoto, 1968). Cultured rat astroglial cells also contain and release substantial amounts of DBI-related peptides (Gandolfo *et al*., 2000), suggesting that DBI processing products may regulate glial cell activity, in addition to affecting other cells in the vicinity. *In situ* hybridisation and IHC have also shown the expression of DBI within ependymal and subependymal populations of the third ventricle (Tong, Y. *et al*., 1991; Dumitru *et al*., 2017).

IHC shows that DBI and DBI-related peptides appear to be highly to moderately concentrated in several key areas of the brain including, the cytoplasm of astroglial cells in the cerebellum and dentate gyrus, the ventricular ECs, tanycytes of the 3rd ventricle, and the choroid plexus (Alfonso *et al*., 2012; Dumitru *et al*., 2017; Yanase *et al*., 2002). It is possible that DBI is highly expressed throughout the ventricular system as expression of TSPO in ECs lining these areas may be involved in the modulation of the formation of CSF. Binding of the TSPO specific ligand Ro 5-4864 decreases CSF formation by 48% (Williams *et al*., 1990). DBI immunoreactivity has also been reported within NSCs of the hippocampus (Nochi *et al*., 2013; Dumitru *et al*., 2017). The presence and expression of DBI within NSCs appears to decrease in association with progression of cellular differentiation (Nochi *et al*., 2013).

In areas of the brain thought to express DBI, *in situ* hybridisation signal to DBI antisense has been shown to be absent from neurons (Tong, Y. *et al*., 1991; Ferrero *et al*., 1984). More recent studies however have shown that DBI is indeed expressed within neurones, with reports of DBI expression within neurones of the retricular thalamic nucleus (Christian *et al*., 2013). The gene expression nervous system atlas (GENSAT) project at Rockefeller University has also reported that DBI is expressed within neurones of the hypothalamus, thalamus, cerebellum, and hippocampus.

DBI and DBI-like peptides are also present within human brain and CSF (Ferrero *et al*., 1986a). Furthermore, DBI immunoreactivity within the human brain parallels that of the

GABAergic system, showing the strong link between DBI and CBR (Ferrero *et al*., 1986a; Ferrarese *et al*., 1989).

1.11.2 Expression of TSPO in the adult CNS

The GABAaR CBR site ligands BZs and DBI also bind at 'peripheral type' BZ receptor/ translocator protein, TSPO, discovered in 1970s (Squires and Braestrup, 1977; Gavish *et al*., 1999; Alho *et al*., 1988b). These peripheral binding sites were originally thought to be specifically expressed in mitochondria of peripherally located steroidogenic tissues such as Leydig cells and adrenal glands (Papadopoulos, 1993; Gavish *et al*., 1999). However, whilst TSPO expression is particularly enriched in steroidogenic tissues by up to 50-fold (Gavish *et al*., 1999) later work unveiled that PBR was ubiquitously expressed throughout the mammalian body, including the CNS.

Autoradiography using the TSPO ligand 3[H]PK11195 has shown that TSPO is expressed within the olfactory bulb (Anholt *et al*., 1984; Bolger *et al*., 1984), the ventricular ependyma and choroid plexus (Benavides *et al*., 1983; Bénavidès *et al*., 1984), and the cerebellum (Anholt *et al*., 1984). In the healthy CNS, TSPO is expressed at a low level within glial cells, particularly within microglia and astrocytes (Gavish *et al*., 1999; Cosenza-Nashat *et al*., 2009; Notter *et al*., 2018). Unlike DBI, low levels of TSPO have also been reported to be present in neurones (Notter *et al*., 2018; Wang, H.J. *et al*., 2012). In the SVZ neurogenic niche TSPO immunoreactivity (IR) is found in $Nestin^+$ and $GFAP^+$ NSPCs of the SVZ ependyma and rostral migratory stream. TSPO-IR is also observed throughout the entire hippocampal region, with concentrated expression in the $Nestin^+$ and $GFAP^+$ NSPCs of the neurogenic SGZ (Betlazar *et al*., 2018).

TSPO is located at the outer mitochondrial membrane and is mainly present at contact sites between the outer mitochondrial membrane and the inner mitochondrial membrane (McEnery *et al*., 1992). TSPO has been suggested to be an integral part of an 800kDa complex located at the outer mitochondrial membrane which is involved in cholesterol

transport to the inner mitochondrial membrane for steroid biosynthesis. The complex includes TSPO, a voltage dependent anion channel, cytochrome p450, the ATPase family AAA domain-containing protein 3A, and optic atrophy type 1 proteins (Rone *et al*., 2012) (figure 1.8). Following transport of cholesterol to the inner mitochondrial membrane by TSPO, the first and rate-limiting step of steroid synthesis, cholesterol is converted to pregnenolone, the first steroid, by the enzyme cytochrome p450 side chain cleavage.

P450 side chain cleavage transcripts are also expressed in the brain, although estimated to be 0.01% of that measured in the adrenal gland. Only a small subpopulation of cells in the brain are capable of *de novo* neurosteroidogenesis (Mellon and Deschepper, 1993). P450 side chain cleavage expression is reported to be localised in the cortex, basal ganglia, hippocampus, olfactory bulb, hypothalamus, thalamus, and cerebellum (Compagnone *et al*., 1995; Mellon and Deschepper, 1993). Binding at TSPO may therefore induce neurosteroidogenesis, and since these ligands have also act as modulators of GABAaR, DBI may have amplified effects on GABAergic signalling by its effects on both GABAaR and its role in the production of neurosteroids which also bind to GABAaR (Tokuda, Kazuhiro *et al*., 2010). There may also exist a situation in which DBI and GABAergic neurosteroids exhibit opposing effects at GABAaR and instead act to balance one another.

1.11.3 Effects of DBI on quiescence and NSC proliferation and differentiation

DBI is robustly expressed in the neurogenic niches of the brain, the SVZ of the lateral ventricle and the SGZ of the hippocampus in both juvenile and adult mice (Alfonso *et al*., 2012; Dumitru *et al*., 2017). Expression appears to be limited to similar populations of cells within these 2 areas. For example, in the SVZ, strong DBI immunoreactivity is detected in astrocyte-like $GFAP^+$/$Nestin^+$ NSCs, and in $Mash1^+$ fast dividing transit amplifying progenitors, but not in DCX^+ neuroblasts (Alfonso *et al*., 2012). Similarly, within the SGZ, DBI expression is limited to $Nestin^+$/$Sox2^+$ NSCs, Nestin-/$Sox2^+$ early amplifying neural progenitors, $Mash1^+$/$Tbr2^+$ late neural progenitors, but absent/barely detectable in most

DCX^+ neuroblasts (Dumitru *et al*., 2017). These results suggest that DBI is expressed during early neurogenesis and therefore may be important in regulating these processes. DBI also appears to be expressed in $Nestin^+/Sox2^+$ tanycytes lining the recently identified neurogenic niche at the 3rd ventricle. Furthermore, DBI has also been detected in $GFAP^+/Sox2^+$ RG-like NSCs and $Sox2^+$ amplifying neural progenitors in the hippocampal SGZ of a 1-year old rhesus monkey, indicating that DBI may regulate such behaviours beyond that of rodents (Dumitru *et al*., 2017).

Loss/gain of function experiments were carried out in both studies in order to determine the action of DBI upon neurogenic niche behaviour *in vivo*. Whilst Alfonso *et al*., 2013 use targeted lenti- or retro-virus to induce DBI loss- or gain of function, Dumitru *et al*., 2017 utilise several methods to manipulate DBI levels *in vivo*. Methods used by Dumitru *et al*., 2017 include an inducible genetic system to selectively delete DBI in NSCs following tamoxifen administration, a combination of a genetic model and viral injections that allows tracing of labelled stem cells and their progeny, and finally intracranial lentiviral injections in the SGZ of WT mice.

Using these various methods, targeted KD of DBI expression in $Nestin^+$ NSCs resulted in an overall decrease in proliferation in SVZ and SGZ. In the SVZ, KD of DBI expression in NSC also resulted in a decrease in $BrdU^+/NeuN^+$ cells in the olfactory bulb, indicating that DBI is essential for the proliferation of the new neuronal population migrating to the olfactory bulb from the SVZ. Whilst KD resulted in fewer new neurones, the proportion of new $BrdU^+$ cells reaching the olfactory bulb was greater following DBI KD, suggesting a greater migratory capacity of new cells following DBI KD as fewer cells were present in the rostral migratory stream compared to the olfactory bulb. Using a similar viral mediated strategy to induce DBI KD in NSCs and their progeny in the SGZ, Dumitru *et al*., 2017, showed DBI KD in the hippocampus has similar results to those seen in the SVZ, where the proportion of proliferating $Ki67^+$ NSCs, amplifying neural progenitors, and neuroblasts decreased, but the

number of new neurones increased. These results provide further support to the notion that DBI regulates the progenitor pool in postnatal neurogenesis.

Targeted DBI overexpression (OE) gain-of-function experiments in SVZ and SGZ NSCs and their progeny resulted in increased proliferation of SVZ progenitors and an increase of NSCs, astrocytes, and neuroblasts. Concurrently, DBI OE decreased numbers of young neurones in the SGZ. DBI OE therefore results in expansion of the progenitor pools of the SVZ and SGZ, demonstrating the role of DBI in balancing preservation of the progenitor pool and the production of new neurones in these niches. Furthermore, DBI OE also affected the level of migration from SVZ, through rostral migratory stream, to the olfactory bulb. DBI OE resulted in more cells remaining in the rostral migratory stream at 7dpi compared to control cells without DBI OE. This was not the result of an increase in cell death of migrating cells. A likely explanation is that similarly to DBI KD, DBI OE results in changes to the cell cycle where overexpressing progenitors remain in division for longer than their control counterparts and therefore more time is required for these cells to differentiate to neuroblasts, migrate through the rostral migratory stream, and eventually incorporate into olfactory bulb. This hypothesis is in line with the finding that DBI OE results in a larger $Mash1^{+}$ progenitor population in the SVZ.

1.11.4 The effects of DBI are dependent on GABAaR CBR site binding

Alfonso *et al*., 2013 and Dumitru *et al*., 2017 confirm that the effects of DBI KD/OE are dependent upon the NAM action of DBI binding to the CBR site on GABAaR. DBI OE in neurosphere cultures from SVZ resulted in increased proliferation of spheres (Alfonso *et al*., 2012). However, introduction of flumazenil, an inverse agonist at CBR which removes DBI from its binding site on GABAaR, prevented DBI OE mediated changes in proliferation. This result indicates that DBI relies on its binding to CBR to mediate its proliferative effects in NSCs. Furthermore, the shorter fragment of full length DBI protein, ODN, which binds specifically to CBR, was also able to reduce GABA mediated currents in outside out patches

of isolated transit amplifying progenitors from the SVZ. Together these results confirm that DBI acts to inhibit GABA currents in SVZ progenitors and so attenuates GABA induced quiescence of NSCs.

These findings were mirrored in the SGZ niche, whereby GABAergic mediated responses in NSCs were partially inhibited by ODN. Specificity of ODN binding to CBR to induce NAM of GABAaR induced currents was confirmed using γ2F77I mutant mice. Γ2F77I mutant mice possess a phenylalanine (F) to isoleucine (I) substitution at position 77 in the γ2 subunit and as a result are unable to bind BZs, and similar compounds such as DBI, at the CBR site with the same affinity as WT animals (Buhr and Sigel, 1997; Cope *et al*., 2004). The γ2 subunit is extremely important in the formation of CBR in GABAaR as of CBR in GABAaR as γ2 KO results in a loss of 94% of all BZ binding sites (Gunther *et al*., 1995). CBR deficient mice show retarded growth, sensorimotor dysfunction, and a drastically reduced lifespan (Gunther *et al*., 1995). These results indicate the importance of postnatal GABAaR regulation by an endogenous ligand at CBR, such as DBI/ODN. Without usual CBR function in γ2F77I mutant mice ODN-mediated decreases in GABA induced currents are absent. Moreover, the DBI OE-mediated increase in the number of $Sox2^+$ NSCs within the SGZ was absent in γ2F77I mice, further indicating that DBI/ODN modulates the stem cell niche by NAM of GABAaR by specific binding to CBR (Dumitru *et al*., 2017).

Modulation of GABAaR by DBI also appears to be essential for the proneural effects of enriched environment upon the hippocampus (Dumitru *et al*., 2017). It is well established that animals given access to enriched environment, such as the inclusion of running wheels in their home cage, over standard housing show increased levels of neurogenesis in the brain (van Praag *et al*., 2000; van Praag *et al*., 2005). Interestingly, a similar finding has also been seen in the spinal cord, where increased physical activity in rats via free access to a running wheel, which results in a significant 2.6-fold increase in $BrdU^+$ proliferating ECs (Cizkova *et al*., 2009).

As expected, Dumitru *et al*., (2017) show that control animals in an enriched environment possess increased numbers of DCX^+ immature neurones over WT littermates placed in standard housing. However, DBI KD prevented the increase in DCX^+ cells seen in enriched environment compared to standard housing, illustrating the way in which modulation of GABAaR by DBI couples activity and neurogenesis in the hippocampus. DBI modulation of GABAaR allows GABA seemingly opposing effects in different cell types, whereby GABA signalling can both increase the survival and development of new neurones whilst keeping NSCs quiescent.

1.11.5 DBI and pathological proliferation

High levels of DBI and GABAaR expression have been found in astrocytomas, neurocytomas, and human gliomas (Alho *et al*., 1995, Labrakakis *et al*., 1999, Young and Bordey, 2010). During patch clamp experiments using glioma cells, Labrakakis *et al*., (1998) illustrated that GABA triggered depolarisation in the majority of cells which resulted in an increase in intracellular Ca^{2+} concentration, likely through activation of voltage gated Ca^{2+} channels present within the tumour membrane. Changes in intracellular Ca^{2+} are a known downstream signalling effector for the transduction of GABA-mediated effects on proliferation (Young, S.Z. *et al*., 2010). Activation of GABAaR by diazepam in a human glioma cell line inhibited proliferation (Chen, J. *et al*., 2013), indicating that similar to NSCs, GABA is a negative regulator of proliferation in glioma cells. GABA therefore appears to regulate proliferation in the CNS at both a physiological and a pathological level, however the effects of GABA upon proliferation within the intact spinal cord remain to be determined.

1.12 Hypotheses and aims

It has been argued that the SVZ and SGZ are not the only neurogenic niches present within the adult CNS. There is mounting evidence that NSCs are present in the adult spinal cord and exist within a specialised niche surrounding the CC. This has led to optimism in the field of SCI research as these cells may constitute an endogenous pool of proliferative cells which

could be used for tissue repair. However, if endogenous NSC-derived repair is ever to become a reality, we must first understand the signals which modulate proliferative behaviour within the postnatal spinal cord.

GABA is an important negative regulator of proliferation in other neurogenic niches. ECs at the CC respond to GABA and neighbouring GABAergic CSFcCs are a possible source of ambient GABA in the CC niche which may induce quiescence within the intact spinal cord. It is hypothesised that GABA will negatively affect proliferation in the intact postnatal spinal cord, and that the negative influence of GABAergic signalling in the spinal cord is modulated by endogenous ligand binding to the CBR site of GABAaR.

Work described here therefore attempts to investigate the possibility that GABA is involved in keeping ECs and other neural progenitors in a dormant state, as the signal which controls the proliferation of these cells in the adult spinal cord is not yet known. Ultimately such work will also provide clues as to why the spinal cord shows poor regenerative capabilities in mammals, and whether modulation of such signalling events lead to greater therapeutic outcomes.

The aims of this study are to: -

1. Use both transgenic and pharmacological methods to determine whether modulating GABAergic signalling influences proliferation of cell populations at the CC and within both the WM and GM of the postnatal spinal cord
2. Determine the fate of proliferating cells in response to GABAergic modulation
3. Examine the expression of the GABAaR modulator and CBR site ligand DBI in the adult spinal cord
4. Examine the expression of TSPO in the intact spinal cord in order to consider whether neurosteroids may also be a likely GABAergic modulator in the control of proliferation and differentiation

5. Examine the effects of TSPO and GABAaR mixed modulators upon basal levels of proliferation alongside the effects of TSPO or GABAaR specific ligands
6. Use both transgenic and pharmacological interventions to determine whether perturbation of GABAaR modulation by endogenous CBR site ligands such as DBI is a plausible mechanism for the low levels of proliferation in the intact cord
7. Investigate whether the GABAaR CBR site antagonist increases proliferation of OPCs in response to a demyelinating lesion

Chapter 2 – General methods

2.1 Animals

All experiments were carried out under the UK Animals (Scientific Procedures) Act 1986 and in line ethical standards set out by the University of Leeds Ethical Review Committee. Every effort was made to minimise the number of animals used and their suffering. Animals were housed in groups, given ad libitum access to food and water, and experienced a 12 hour light-dark cycle (lights on 06.30– 18.30).

Five strains of adult mice (4-8 weeks) were used in these experiments. C57BL/6 mice, nestin-GFP mice and GAD67-GFP knock-in mice were bred in-house at the University of Leeds. When in-house supply failed to meet demand adult C57BL/6 mice were sourced from Charles River Laboratories. Two other transgenic mouse lines were also used, γ2F77I mice and TSPO global K/O mice, their tissue was a kind gift of collaborators in Germany and the USA, respectively. These are discussed in further detail below.

2.1.1 GAD67-GFP mice

GAD67-GFP mice (Tamamaki *et al*., 2003) were originally sourced from Yuchio Yanagawa, leading to the establishment of successful GAD67-GFP breeding trios in-house, consisting of one GAD67-GFP male paired with two C57BL/6 females. GAD67-GFP mice harbour enhanced GFP cDNA between the GAD67 5' flanking region and the GAD67 codon start of the GAD67 promotor (Tamamaki *et al*., 2003). Productive breeding results in heterozygous GAD67-GFP ($GAD67^{+/-}$) pups, with GAD67 haplodeficiency due to GFP knock in, as $GAD67^{-/-}$ is lethal at birth due to cleft palate development (Asada, H. *et al*., 1997). At 2-3 days of age mice are genotyped by GFP visualisation under an ultraviolet light, as at this age fluorescence can be visualised through the thin bones of the skull.

GAD67-GFP mice are seizure free and phenotypically normal in terms of growth and reproductive behaviour despite showing a reduction in brain GABA content, as measured by high performance liquid chromatography (HPLC) (Tamamaki *et al*., 2003). The use of

GAD67-GFP knock-in mice allowed us to not only visualise GABA producing GAD67-GFP positive cells, such as CSF-cCs, but also provided an invaluable tool to examine how reductions in ambient GABA may affect cellular proliferation and differentiation in the spinal cord.

2.1.2 Nestin-GFP mice

In addition to GAD67-GFP transgenic mice adult nestin-GFP mice (Yamaguchi *et al*., 2000) were used for visualisation of the ependymal cell layer. A productive in-house breeding colony was set up similarly to the GAD67-GFP colony.

Nestin is expressed in radial glia and nestin-GFP mice have been previously used to analyse neurogenic events in SGZ and SVZ (Abla and Sanai, 2013; Murdoch and Roskams, 2008; Mignone *et al*., 2004). Nestin has also been shown to be expressed in ECs in both health and disease (Alfaro-Cervello *et al*., 2012; Dromard *et al*., 2008; Xu, R. *et al*., 2008; Matsumura *et al*., 2010; Cawsey *et al*., 2015; Cizkova *et al*., 2009; Namiki and Tator, 1999). Therefore nestin-GFP mice were used in these experiments as a means to label the EC layer of the CC.

2.1.3 γ2F77I mice

Adult (~8-12 weeks) transgenic (C57/Bl6, γ2F77I/F77I) γ2F77I mice, with the point mutation F77I in the Gabrg2 gene were examined for changes in proliferation and differentiation within the intact spinal cord compared to WT animals. Spinal cord tissue from these animals was a kind gift of Dr I. Dumitru (Prof. H. Monyer's Lab, DKFZ, Heidelberg, Germany).

Binding of BZs to GABAaR occurs at the interface between α and γ2 subunits (Sigel, E., 2002; Ernst *et al*., 2003). γ2F77I mice possess a phenylalanine (F) to isoleucine point mutation (I) at position 77 in the Gabrg2 gene which alters the affinity and specificity of the drug binding site within the γ2 subunit (Buhr and Sigel, 1997; Cope *et al*., 2004). γ2F77I mice breed normally and behave similarly to control C57BL/6 mice when examined with a range of behavioural observational tests (Cope *et al*., 2004). GABAaRs within these mice

however, show altered responses various CBR ligands including, but not limited to, zolpidem (Cope *et al*., 2004), zopiclone, diazepam, and flumazenil (Ramerstorfer *et al*., 2010). The endogenous protein DBI also binds to GABAaR at the α and γ2 subunits, modulating GABAergic signalling through CBR (Bormann, 1991; Alfonso *et al*., 2012) (Bormann *et al*., 1985, Alfonso *et al*., 2012).

These mice were therefore chosen to examine any changes in the level of proliferation within the spinal cord as a result of transgenic manipulation of the CBR site within GABAaR, which may affect binding of endogenous GABAaR modulators, such as DBI and its smaller peptide derivatives ODN and TTN.

2.1.4 TSPO KO mice

Transgenic global TSPO K/O mice were also examined for changes in proliferation and differentiation within the spinal cord compared to control C57/Bl6 mice. Tissue from these animals was a kind gift of Dr O. Chechneva (Dr W. Deng's lab, UC Davis, Sacramento, California, USA).

The endogenous protein DBI binds and has cellular effects at 2 locations, the CBR site located within GABAaRs (Bormann, 1991; Alfonso *et al*., 2012; Dumitru *et al*., 2017), and also at the glial TSPO receptor, located at the outer mitochondrial membrane (Papadopoulos *et al*., 1991; Veenman and Gavish, 2012). Whilst DBI is able to bind to TSPO, it is the smaller neuropeptide fragment of DBI TTN which is seen to preferentially bind with high affinity to the TSPO receptor, as confirmed by pharmacological study of these receptors using the specific ligand PK11185 (Alfonso *et al*., 2012; Slobodyansky *et al*., 1989). Whilst the specific primary function of TSPO is still debated, TSPO has been shown to be involved in many mitochondrial-based functions including steroidogenesis, ion transport, and cell proliferation (Gavish *et al*., 1999).

The TSPO specific ligand TTN increases intracellular [Ca^{2+}] (Gandolfo *et al*., 2001) and stimulates proliferation in cultured rat astrocytes (Gandolfo *et al*., 2000). This pro-

proliferative effect was determined to be due to TTN binding at TSPO as these effects were abolished by PK11195 but not by the CBR specific antagonist flumazenil (Gandolfo *et al*., 2000). Furthermore, increased levels of TSPO expression have been found in high-grade gliomas (Roncaroli *et al*., 2016). These results suggest that TSPO may also influence postnatal proliferation within the CNS, and therefore global TSPO KO mice were used to investigate this possibility.

Detailed information on the numbers of animals used in different experimental conditions can be found in table 2.1

Table 2.1 Numbers and types of animals used in each experiment

Experiment	Strain	Number used
Day vs. Night	C57BL/6	6
Day vs. Night	GAD67-GFP	6
WT vs. GAD in light hours	C57BL/6 and GAD67-GFP	3 of each strain
WT vs. GAD in dark hours	C57BL/6 and GAD67-GFP	3 of each strain
HPLC to determine GABA content	C57BL/6 and GAD67-GFP	3 of each strain
VGB vs. Vehicle	C57BL/6	6
IHC analysis of DBI expression	C57BL/6, GAD67-GFP, nestin-GFP	3 of each strain
IHC analysis of TSPO expression	C57BL/6, GAD67-GFP, nestin-GFP	3 of each strain
TSPO expression in MNs and SPNs	C57BL/6 and GAD67-GFP	3 of each strain
IHC analysis of TSPO and DBI in injury	Nestin-GFP	3
ETX vs. Vehicle	C57BL/6 and GAD67-GFP	3 of each strain

MDZ vs. Vehicle	C57BL/6	6
Flumazenil vs. Vehicle	C57BL/6	6
Ro15-4513 vs. Vehicle	C57BL/6	6
G2F77I vs WT	G2F77I and C57BL/6	3 of each strain
TSPOKO vs TSPOflox	TSPOKO and TSPOflox	3 of each strain
Intact animal for LPC studies	C57BL/6	3
Intraspinal saline injection $^{+}$ flumazenil	C57BL/6	3
LPC injection $^{+}$ vehicle	C57BL/6	3
LPC injection $^{+}$ flumazenil	C57BL/6	3

2.2 *In vivo* studies

In vivo studies were carried out to determine if there were changes in the levels of proliferation and differentiation within the spinal cord in various experimental conditions. *In vivo* experiments played an integral role in the investigation of GABAergic influences over proliferative behaviour.

Experiments were carried out for 5 days, unless stated otherwise. Animals received intraperitoneal (I.P) injections of EdU $^{+}$/- a pharmacological agent or vehicle daily until the end of the experiment. Animals were sacrificed on day 5 to allow processing of CNS tissue for immunofluorescent analysis.

Injections were given at the same time of day to maintain uniformity across all *in vivo* studies. Although first experiments begun with administration of EdU and pharmacological agents during daytime/light hours, injections in subsequent studies were later given during the evening in the dark hours of the animal unit, between 19.00 and 21.00, when animals would be awake and most active. Numbers are proliferating cells are known to increase in established neurogenic regions, such as the SVZ, during periods of activity (Kempermann, Gerd *et al*., 2010; van Praag *et al*., 2005). It is possible that treating animals during periods of wakefulness and activity may allow for labelling of more proliferating cells. Labelling a greater population of proliferating cells can then be useful when using drugs which result in a decrease in the numbers of EdU labelled cells.

A timeline to show the general injection paradigm for experiments investigating proliferation and differentiation within the spinal cord is detailed below (figure 2.1).

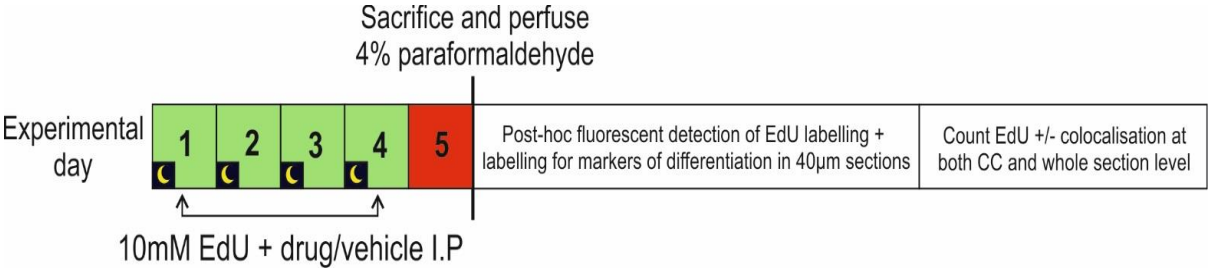

Figure 2.1 Animals received 4 days of EdU I.P before tissue analysis

Timeline showing the timings of experiments investigating the number and fate of proliferative cells in the adult spinal cord in drug vs. vehicle treated animals

2.2.1 *In vivo* administration of 5-ethynl-2'-deoxyuridine for the detection of proliferating cells

In order to label newly proliferated cells for later visualisation using immunofluorescence, animals received daily 100µl I.P injections of 5-ethynyl-2'-deoxyuridine (EdU) (Carbosynth, product number: NE08701). EdU was made up in distilled water to give a final concentration of 10mM and stored at -20ºC in 1 ml foil wrapped eppendorfs until needed.

Interest in using proliferation assays to investigate cellular turnover and neurogenesis in the CNS has existed since the 1960s when early pioneers of the field such as Smart and Leblond, (1961) and Altman and Das (1965) utilised the incorporation of tritiated thymidine into diving cells and its detection by autoradiography. Such studies were the first to illustrate that not only do we find dividing glial cells throughout the postnatal parenchyma (Smart and Leblond, 1961), but these cells, born in the SVZ, migrate and mature into postnatally born neurones within the olfactory bulb (Altman and Das, 1965; Altman, 1969).

Later development of the thymidine analogue 5-bromo-2'-deoxyuridine (BrdU), which incorporates into DNA during the S-phase and is later detected by IHC, has been invaluable for the quantification of newly divided cells, and has further opened up the study of neurogenesis (Seki and Arai, 1993; Kuhn *et al*., 1996; Corotto *et al*., 1993; van Praag *et al*., 2000). Proliferation assays using BrdU incorporation have long been considered the 'gold-standard' for the detection of newly proliferated cells (Zeng *et al*., 2010; Wojtowicz and Kee, 2006). Whilst BrdU staining is more convenient than tritiated thymidine autoradiography, and can be carried out alongside other cell type markers to determine cell fate, significant drawbacks still remain. Detection of BrdU requires a harsh DNA denaturation step to allow

the anti-BrdU antibody access to the incorporated BrdU residues and can result in the destruction of many cellular antibody epitopes (Buck, S.B. *et al*., 2008). Recently however, a novel technique, which instead employs the thymidine analogue EdU for the detection of DNA synthesis, has allowed for the circumvention of such problems associated with using BrdU.

EdU is readily incorporated into cellular DNA during DNA replication (Salic and Mitchison, 2008). Detection of the incorporated nucleoside is achieved by a copper catalysed [3^{+}2] cycloaddition reaction ('click' chemistry) of the ethynyl group of EdU with a small biotin-azide group followed by a biotin-fluorescent streptavidin conjugation step for later analysis by fluorescent microscopy (Salic and Mitchison, 2008; Buck, S.B. *et al*., 2008; Chehrehasa *et al*., 2009; Zeng *et al*., 2010; Corns *et al*., 2015). The protocol for the detection of EdU uses small reaction components (~0.6kDa) which easily diffuse into, and have easier access to, the incorporated EdU within the double stranded DNA compared to the larger macromolecules of BrdU detection protocols i.e. anti-BrdU antibodies (150kDa), therefore bypassing the need for harsh denaturation steps and possible loss of tissue structure and antigenicity (Salic and Mitchison, 2008; Buck, S.B. *et al*., 2008; Chehrehasa *et al*., 2009).

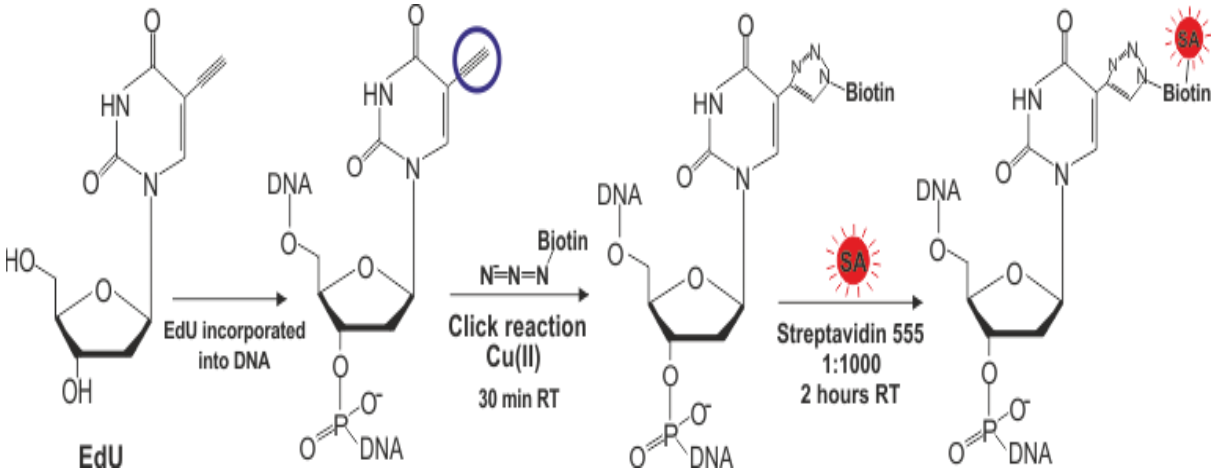

Figure 2.2 EdU is incorporated into DNA and can be detected by copper catalysed click chemistry and a fluorescent azide

EdU has been shown to be successful in labelling proliferating cells in the prenatal and postnatal mouse brain (Salic and Mitchison, 2008; Chehrehasa *et al*., 2009; Corns *et al*., 2015). Furthermore, studies by Zeng *et al*., 2010 showed that when injected with 200 mg/kg EdU and an equimolar dose of BrdU (243.5 mg/kg) there was no significant difference between the number of EdU-positive cells and BrdU-positive cells in the adult hippocampus. In addition, almost all (over 95%) of EdU-positive and BrdU-positive cells were colocalised in the dentate gyrus, demonstrating that EdU and BrdU label the same cells in this neurogenic niche with similar efficiency (Zeng *et al*., 2010). EdU therefore has been validated as a useful means to study cellular proliferation and differentiation in relation to neurogenesis.

2.3 *In vivo* administration of GABAergic modulators

In addition to EdU treatment, some animals were also treated daily with various GABAergic modulators (table 2.2). All drugs were given I.P at a volume of 100µl. *In vivo* experiments were always carried out alongside a control group which received 100µl of vehicle I.P rather than drug (table 2.2)

Table 2.2 Details of all drugs used in *in vivo* experiments

Drug name	Supplier	Dose (mg/kg)	Vehicle	MOA
Vigabatrin	Tocris	200	Saline	GABA-T inhibitor
Etifoxine	Sigma	50	1% TWEEN-80 saline	GABAaR PAM and TSPO agonist
Midazolam	Tocris	0.3	Saline	GABAaR PAM and TSPO agonist
PK11195	Tocris	3	4% DMSO/0.8% TWEEN-80 saline	TSPO specific ligand
Flumazenil	Tocris	5	0.1% TWEEN-80 saline	CBR site antagonist
Ro15-4513	Tocris	3	4%TWEEN-80/3% DMSO saline	CBR site inverse agonist

2.3.1 Use of transgenic animals to assess changes in baseline proliferation

Transgenic mice including GAD67-GFP mice (Tamamaki *et al*., 2003), γ2F77I mutant mice (Buhr and Sigel, 1997; Cope *et al*., 2004), and TSPO global KO mice (Wang, H. *et al*., 2016) were used alongside control C57BL/6 mice to investigate changes in proliferation and differentiation following changes in CNS GABA content, CBR binding affinity, and TSPO expression, respectively. These are discussed in further detail in the chapters 3 and 5.

In experiments where transgenic animals were used as the experimental group vs C57BL/6 mice as the control, EdU was introduced in the same manner and time frame as previously described for other *in vivo* experiments investigating proliferation (section 2.2.2). Briefly, animals received nightly 100ul injections of 10mM EdU for 4 days and were perfused on the 5^{th} day.

2.3.2 Preparation of tissue for immunohistochemistry

At the end of each experimental period animals were terminally anaesthetised by I.P injection of pentobarbitone sodium 20% w/v (60 mg/kg) (Pentoject, Animalcare, UK). Pedal and corneal withdrawal reflexes were tested until absent to ensure that the animal was suitably anaesthetised. The chest cavity was opened at the xiphoid process using blunt ended scissors, the diaphragm was perforated, and cuts were made along the lateral edges of the chest wall up to the clavicle. The ribcage was reflected back to expose the heart and lungs. Care was taken so as not to accidentally damage the liver and compromise the quality of the perfusion by premature disruption of the circulation. A cannula was inserted into the left ventricle and an opening was made in the right atrium to allow transcardial perfusion of 50 ml 0.1M phosphate buffer (PB), followed by 200 ml of 4% paraformaldehyde (PFA) in 0.1M PB, to effectively flush the circulation and fix the tissue.

Once fixed, an incision was made along the midline of the back. Soft tissue was scraped away using a scalpel to reveal the vertebrae before the spinal cord and brain were removed using coarse forceps and small spring scissors (World Precision Instruments, catalogue #

654558). Harvested tissue was postfixed overnight in 4% PFA at 4ºC. Following postfixation, fine forceps (World Precision Instruments, catalogue # 500235) were used to remove the meninges. Spinal cords and brains were then placed in 0.1M phosphate buffered saline (PBS) supplemented with 0.1% sodium azide, to prevent bacterial growth, and kept at 4ºC until use. Tissue from the thoracolumbar region was sectioned transversely at 40µm on a vibrating microtome (Leica, VT1000S, Microsystems, UK). Sections were placed in PBS in a 24 well plate, with a maximum of 8 sections per well, ready for later fluorescent labelling of EdU and other cellular markers of differentiation.

2.3.3 Detection of proliferating cells using EdU

EdU detection was performed before any fluorescence IHC. Use of $Cu(II)SO_4$ as a catalyst during the click reaction creates copper ions which may negatively affect the outcome of fluorescent secondary antibody detection as copper has been shown to be a fluorescence quencher (Choi, Y.-A. *et al*., 2015; Rahimi *et al*., 2008).

Unless otherwise stated, all steps were carried out at room temperature whilst placed on an orbital shaking platform to gently agitate the sections and prevent sections sticking together.

For the fluorescent detection of EdU incorporation into DNA; tissue sections were permeabilised by washing in 0.2% PBS-triton (PBST) for 30 minutes, followed by 2 x 10 minute washes in Tris buffer (pH 7.6) before a 30 minute light protected incubation in 320 µl distilled water, 25 µl Tris buffer (2 M), 50 µl $Cu(II)SO_4$ (10mM), 5 µl biotinylated azide (Kerafast, Boston MA,1mM, catalogue # FCC371), and 100 µl of ascorbic acid (0.5 M). Ascorbic acid must be added last to start the reaction by the reduction of $Cu(II)$ SO_4 to Cu(I), where Cu(I) ions catalyse the $[3^{+}2]$ cycloaddition reaction used to detect the incorporation of EdU in DNA of newly born cells.

Sections were washed a further two times in Tris buffer (pH 7.6) before being incubated for 2 hours in Streptavidin $Alexa^{555}$ (Invitrogen, catalogue # S-32355) diluted 1:1000 in PBS, to allow fluorescent detection of azide binding to EdU present in DNA of newly born cells.

Finally; sections were washed in PBS and checked for evidence of positive staining before undergoing fluorescence IHC.

2.3.4 Overview of immunohistochemical method and rationale

IHC allows visualisation of cells or proteins of interest by utilising the principle that antibodies will bind specifically to an antigen of interest. A primary antibody can be raised against an antigen of interest by immunisation of a host animal, e.g. a rabbit, with the antigen. The animal will then produce antibodies to the antigen which can be extracted, purified, and used in biological research. Antibodies raised in this way are generally polyclonal, meaning that they recognise and bind to multiple different epitopes within the protein. Monoclonal antibodies, which instead bind to one epitope, can also be generated against a protein of interest using cell lines. A secondary antibody, raised against the species the primary antibody is raised in, with a fluorescent tag for visualisation is then used for the detection of the primary antibody.

2.3.5 Immunohistochemistry protocol

IHC was usually carried out on sections that had previously undergone staining to reveal the incorporation of EdU into DNA to examine changes in proliferation and differentiation (chapters 3, 5, and 6). Other sections however were used purely for IHC analysis and characterisation of the expression of certain antibodies, such as DBI and TSPO, within the adult spinal cord (chapter 4). However, whether the sections underwent EdU detection or not, the methods for the staining of other antibodies are the same and are discussed below.

Sections in 24 well plates were washed three times in PBS for a total of 30 minutes. Following this, sections were placed in 300ul of primary antibody solution diluted to optimal working concentrations (table 2.3). Unless otherwise stated, primary antibodies were made up in 0.1% PBST to aid tissue permeabilisation. For the localisation of some antigens, such as CD24 and TSPO, membranes needed to remain intact for successful staining and visualisation to occur. In these cases, triton was omitted from the staining protocol and

sections instead received a 30 minute wash in 0.1% TWEEN-20 PBS before incubation in primary antibody. Sections were left in primary antibodies overnight at 4ºC on an orbital shaker.

Table 2.3 Primary antibodies used to determine cell fate acquisition of EdU$^+$ cells

Antigen	Species	Dilution	Supplier and cat. #
CD24-FITC	Mouse	1 in 500 (TWEEN)	BD Pharmingen 564664
DBI	Rabbit	1 in 2000	Frontier Institute B_2571690
GFAP	Mouse	1 in 100	Neuromab 73-240
HuC/D	Rabbit	1 in 1000	Proteintech 130321AP
Iba1	Rabbit	1 in 1000	Wako 019-19741
MBP	Chicken	1 in 250	Abcam 134018
Nestin	Rat	1:1000	BD Pharmingen 556309
NeuN	Mouse	1 in 1000	Millipore MAB377
ODN	Rabbit	1:250	Gift of M.C.Tonon
PanQKI	Mouse	1 in 100	Neuromab 73-168
S100β	Rabbit	1 in 1000	Abcam ab52642
Sox2	Goat	1 in 500	Santa Cruz sc17320
TSPO/PBR	Goat	1 in 100 (TWEEN)	Abcam ab118913
Tuj/B-tubulin III	Rabbit	1 in 1000	Proteintech 10068-1-AP

After primary antibody incubation, sections were washed three times in PBS for a total of 30 minutes in order to remove any unbound primary antibody. Antigens were visualised by a 2-

hour incubation at room temperature with the appropriate Alexa-Fluor-conjugated secondary antibody (table 2.4). Sections were protected from light during secondary antibody incubation in order to prevent bleaching of the fluorescent probes which would affect later antigen visualisation.

For some antibodies visualisation of primary antibodies using an Alexa fluorophore-conjugated secondary antibody was not sufficient. In these cases, sections were incubated for 2 hours with a species specific biotinylated secondary antibody (1:200). The biotinylated antibody was washed from the sections by 3 x 10-minute washes in PBS. Following this, an Alexa fluorophore-conjugated streptavidin step was used to visualise areas of antibody-biotin binding and allow visualisation.

Table 2.4 Table of all secondary antibodies used

Secondary antibody	Dilution	Supplier and cat. #
Donkey anti-Goat IgG Alexa Fluor 555	1 in 1000	Invitrogen A-21432
Donkey anti-Mouse IgG Alexa Fluor 555	1 in 1000	Invitrogen A-31570
Donkey anti-Rabbit IgG Alexa Fluor 555	1 in 1000	Invitrogen A-31572
Donkey anti-Goat IgG Alexa Fluor 488	1 in 1000	Invitrogen A-11055
Donkey anti-Mouse IgG Alexa Fluor 488	1 in 1000	Invitrogen A-21202
Donkey anti-Rabbit IgG Alexa Fluor 488	1 in 1000	Invitrogen, A-21206
Donkey anti-Sheep IgG Alexa Fluor 488	1 in 1000	Invitrogen A-11015
Goat anti-Chicken IgG Alexa Fluor 488	1 in 1000	Invitrogen A-11039

Following incubation with secondary antibodies, sections were washed another 3 times in PBS for a total of 30 minutes, before being mounted on glass slides using a fine paintbrush. Slides were allowed to air dry before adding vectashield or vectashield plus 4',6-diamidino-2-phenylindole (DAPI) (Vector Laboratories, Burlingame, CA) to sections and covering with a glass coverslip and sealing with nail polish.

When counting EdU positive cells to determine levels of proliferation, streptavidin autofluorescence can sometimes produce 'false positive' non-specific staining in some areas which could be mistaken for EdU positive cells. Therefore, sections which had undergone double labelling for EdU plus markers of differentiation were always mounted in vectashield plus DAPI. DAPI binds to DNA within cells and fluoresces blue and is used to prevent inclusion of autofluorescent spots in later cell counts.

2.3.6 Cell counting

Cell counts, including colocalisation of EdU and specific cellular markers, were performed manually using a Nikon E600 microscope equipped with epifluorescence at custom settings at x40 magnification. The number of EdU^+ cells, in addition to EdU^+ cells which were also immunopositive for specific cellular markers detailed above, were counted in the WM, GM, and the CC region of every 3rd 40µm section. The total number of EdU^+ cells given is the sum of these 3 regions. Cells were mapped onto a digital spinal cord template representing the lumbar level and later counted using a digital tally counter. In order to determine that no cell had been counted twice and that no cell had been missed, the top of the section was first visualised in the Z-plane and the focus was then gradually moved through this plane. This method was used in order to focus on each cell present to give a reliable count in each plane of focus. The percentage of total EdU^+ cells which colocalised with markers of differentiation were also determined for each section. The raw number of EdU^+/differentiation $marker^+$ cells were also examined.

2.3.7 Statistical analysis

Data were collated in Microsoft Excel and later analysed using GraphPad Prism 7 software (GraphPad Software, California, USA). Cell counts are given as mean number of EdU^+ cells per 40µm section where *n*=number of sections counted in each condition and *N*= number of animals included in each experimental group. Data are presented as means ± SE and for statistical analysis. Student's t-tests and one-way ANOVA with post-hoc Tukey's testing for multiple comparisons were carried out to determine significant differences in the levels of proliferation between the two groups, including any changes in the percentage of colocalisation between EdU^+ cells and specific cellular markers. Data were considered significant when $p < 0.05$ (denoted by *); $p < 0.05$ (denoted by **), $p < 0.005$) (denoted by ***); or $p < 0.001$ (denoted by ****).

2.3.8 Image capture and analysis

Sections of particular interest were checked for colocalisation using a Zeiss LSM880 upright confocal laser scanning microscope with Airyscan equipped with argon and He-Ne lasers and 40x and 63x Fluor oil objective. Using Carl Zeiss Zen software (Zeiss microscopy, Germany) 3x2 tile scans were acquired when it was necessary to view the entire spinal cord section. Images were also acquired, processed, and exported using ZEN software. CorelDRAWx6 graphics suit was used for image manipulation, including correction of brightness, contrast, and intensity, and production of figures. Figures are presented as single plane confocal images.

2.4 Intraspinal injections for focal demyelination in the spinal cord

Lysophosphatidylcholine (LPC), also known as lysolethicin, is a detergent derived from egg yolk, which can be injected directly into either the brain or spinal cord to induce focal demyelination at the site of injection (Keough *et al*., 2015). The focal lesions induced by LPC provide a good model to investigate the changes in cell proliferation and

oligodendrocyte differentiation following CBR manipulation in a model of WM injury, and so have been utilised here for such purposes.

2.4.1 Preparation of tools and equipment for surgery and injection

Prior to surgery all tools were sterilised in an autoclave. Surgical tools and materials required included: 2 pairs of Dumont #55 fine forceps (World Precision Instruments, catalogue # 500235), 2 pairs of crocodile teeth forceps, 1 pair of haemostat locking clamps, small pair of spring scissors, scalpel handle, sterile #10 scalpel blades (Swann Morton), surgical tissue retractors, 1 ml glass syringe (Thermo Fisher), sterile 23-gauge needles, vicryl absorbable sutures (W9015, Ethicon), black braided silk non-dissolvable sutures with 16mm curved needle (W2502, Ethicon), battery-operated high temperature cautery (Bovie medical, Change-A-Tip cautery, catalogue number: DEL1)

Glass electrodes for injecting solution, either sterile saline or 1% LPC, were pulled using a Sutter P27 micropipette puller (Sutter Instruments, USA), from thick walled borosilicate glass capillaries. A CMA 4004 syringe pump (Harvard apparatus) was used to deliver precise 1 µl microinjections of either 1% LPC or saline at a flow rate of 0.5 µl over 10 minutes followed by a pulse of a further a 0.5 µl. The A 1 ml glass syringe, primed with sterile saline, was fitted to the microdialysis pump, and plastic tubing, also filled with sterile saline, was used to connect the syringe to the injecting glass capillary. The glass capillary for injecting was secured to a probe holder on the stereotactic frame (Stoelting Co., Illinois, USA) where the animal was situated following spinal cord exposure.

2.4.2 Preparation of animals for surgery and injection

Adult (6-8 weeks) male C57BL/6 mice were used throughout these experiments.

Prior to surgery mice were weighed to calculate the appropriate dose of anaesthetic and to record baseline measurements for the maintenance of postsurgical recovery records. Mice were then anaesthetised with an I.P injection of ketamine (75 mg/kg, Ketavet, Zoetis) and medetomidine (1 mg/kg, Domitor, Pfizer). It was planned that the animal would be under

anaesthesia for approximately 1 hour. The animal was determined to be properly anaesthetised when it no longer exhibited pedal withdrawal reflexes upon pinching of the foot.

Using electric clippers, a 2-3cm patch of hair was removed from the dorsal surface of the animal below the rib cage and care was taken to remove all shaved hair from the preoperative area and the animal's skin. Protective lubricant (Lacri-Lube) was added to the eyes to prevent drying of the cornea during surgery.

2.4.3 Surgery to expose the spinal cord for injection

Throughout surgery, all procedures were carried out whilst the animal was placed on a heated table at 37ºC in order to maintain body temperature. Using a surgical microscope at lowest magnification a #10 scalpel blade was used to cut through the dorsal skin and into the underlying superficial layers of muscle covering the spinal column. The 2-3cm cut must be made rostral to the ending of the rib cage, a landmark which should be palpated and identified before incising the dorsal surface. Once the first opening had been made, retractors were then used to open the surgical field further. In order to gain access to the vertebral column, fine forceps were used for blunt dissection of the overlying paraspinal musculature.

Once the spinal column was visible, a dorsal laminectomy was not necessary as natural intervertebral foramen exist between the vertebrae at this lower thoracic-upper lumbar region. Surgery aimed to expose an intervertebral space for needle insertion and LPC/saline injection (figure 2.3). The spinal cord was visualised between the intervertebral spaces and was seen to be covered in a thick shiny layer of visible dura. A prominent blood vessel can be seen running rostral to caudal through the approximate midline of the spinal cord at this point.

For successful injection the thick outer dura mater and underlying pia mater must be removed from the spinal cord surface, as remaining meningeal tissue can prevent smooth

insertion of the injecting glass electrode. If this occurs the electrode instead compresses the cord, likely resulting in greater injury, elevated inflammatory cascades, and higher levels of proliferation. To remove the meninges a curved 23-gauge needle was gently scraped laterally across the surface of the cord until the dura was cleared. Following removal of the rostral/caudal blood vessel at the midline can be seen with greater clarity.

Once the dura had been cleared, and any leaking CSF which had been cleared using a cotton bud, a handheld battery-operated high temperature cautery was then used to remove the pia mater. The handheld cautery was heated and slowly advanced toward the exposed cord, the cautery tip was briefly touched to the cord surface to remove the pia. Following the successful removal of the pia, intraspinal insertion of the glass microelectrode and injection of solution was able to take place.

2.4.4 Intraspinal injections of lysophosphatidylcholine

Once the spinal cord was exposed and the pia fully removed, the animal was transferred to a stereotactic frame (Harvard Apparatus). To secure the animals head the teeth were placed in a toothbar and light pressure was applied at the bridge of the nose. A rolled section of gauze was placed underneath the animal to accentuate curvature of the spine and aid visibility during intraspinal injection.

The glass microelectrode was viewed with the surgical microscope and the tip was broken back using fine forceps before being attached to the probe holder on the z-direction stereotactic arm. Depending upon whether animals were assigned to the experimental group, and therefore received LPC injection (*N*=8), or the control group, which received saline (*N*=4), LPC or saline was drawn up into the electrode ready for injection. An air bubble separated the priming sterile saline solution and the injecting solution. Prior to placement of the electrode tip at the injection site solution was ejected from the electrode to ensure that the tip was not blocked.

Following loading of the injection apparatus the probe holder was lowered toward the injection site until the tip of the electrode was just visible when viewing the intervertebral space with the surgical microscope. The microscope was repositioned so that both the tip of the electrode and the spinal cord were in focus and small movements, using the micromanipulator controls of the Z-direction stereotactic arm, were carried out until the tip of the electrode was visible at the midline of the spinal cord surface. Once visible at the surface the electrode tip was moved laterally to displace the large rostral-caudal blood vessel and induce a lateral trajectory of the injection away from the midline.

Using the graded measurements of the Z-direction stereotactic arm a baseline position measurement was calculated. The micromanipulator was then used to make a swift downwards movement to pierce the tissue and achieve a depth of 300 μm for injection into the dorsal horn. A schematic of the processes involved in injection up to this point are detailed in figure 2.3 below.

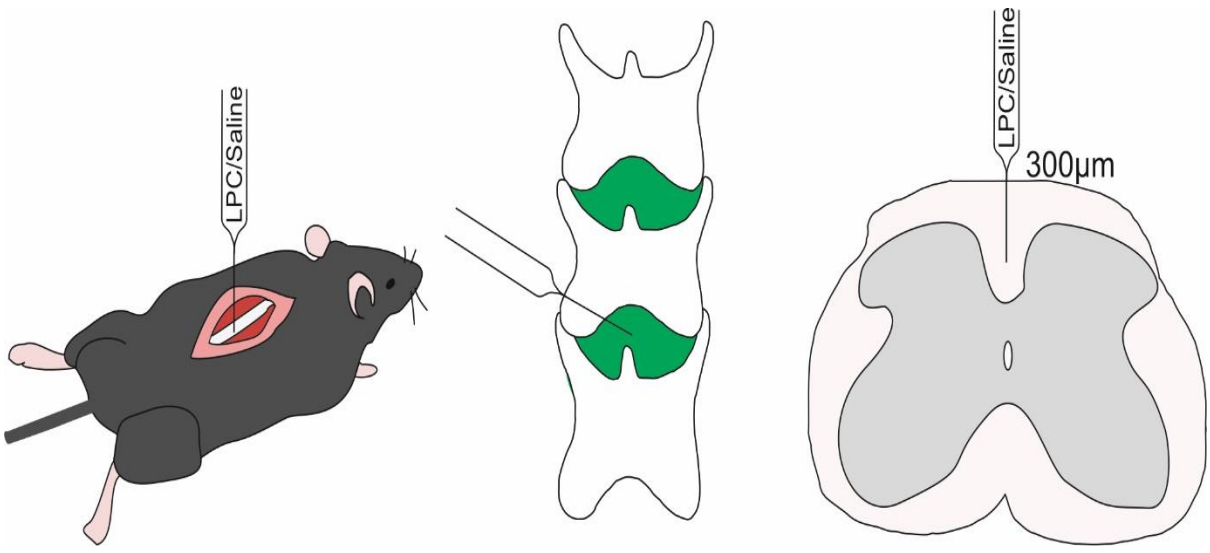

Figure 2.3: LPC or saline was directly injected into the dorsal columns *in vivo* through the intervertebral space

A CMA 4004 infusion pump was used to deliver precise 1 µl microinjections of either 1% LPC or saline at a flow rate of 0.5 µl over 10 minutes, followed by a pulse of a further a 0.5 µl. Once the infusion was complete the capillary was left *in situ* for 2 minutes to prevent backflow upon removal of the capillary.

Upon completion of LPC or saline infusion the electrode was slowly withdrawn from the spinal cord and discarded. The underlying muscle and adipose tissue overlaying the spinal column were brought together with a simple interrupted suture using vicryl absorbable sutures (Ethicon, W9015). Black braided silk non-dissolvable sutures with 16mm curved needle (Ethicon, W2502) were used to close the skin and antibacterial wound powder (Battles, 2273) was applied to the site of the incision to prevent infection.

2.4.5 Postoperative care of animals

Immediately following surgery animals received a subcutaneous injection of the α2 adrenergic receptor antagonist atipamezole (1 mg/kg, 0.2 ml per 20 g weight, Antisedan Pfizer) for the reversal of the sedative and muscle relaxant effects of medetomidine. Animals also received I.P injection of buprenorphine (Vetergesic, 0.3 ml/mg solution given at 0.1 mg/kg) for postoperative analgesia. The duration of the effect of buprenorphine has been documented to be between 3 and 5 hours in mice (Tubbs *et al*. 2011, Gades *et al*., 2000). Therefore, mice were checked periodically for signs of postoperative pain by cage side behaviour observations e.g. presence of hunching, isolation, and non-explorative behaviour, and by assessing facial expressions using the mouse grimace scale. Further doses of buprenorphine were given accordingly (I.P). Any animals which appeared to be suffering/in pain beyond the moderate procedure severity, as defined in the Home Office project license, during any of the periodic welfare checks were euthanised by schedule 1 methods; exposure to rising concentration of CO_2 followed by dislocation of the neck. These methods will be referred to as ‘Sch1’ from now on.

During immediate recovery following surgery, animals were placed in a heated recovery chamber and were observed until fully ambulatory. Whilst surgery involves direct injection into the spinal cord WM and, possible corticospinal tract disruption, animals are capable of walking, self-voiding, -drinking, and -feeding after they recover from anaesthesia. Animals were placed back into home cages with cage mates following recovery from anaesthesia.

Although animals are capable of self-feeding and drinking soaked diet was given for the first few days post-surgery to aid food and water intake. To further assess postoperative recovery animals were weighed daily and compared to their baseline weights taken before surgery.

2.4.6 *In vivo* injection paradigm for introduction of drugs and EdU

Following intraspinal injections, animals were further split into 3 experimental groups and randomised to each arm. Group 1 received 1% LPC intraspinal injection followed EdU and 5 mg/kg flumazenil nightly on days 5-8 post surgery. Group 2 received 1% LPC intraspinal injection followed by EdU and saline nightly on days 5-8 post surgery. Group 3 received saline intraspinal injection followed by EdU and flumazenil on days 5-8 post surgery. EdU and flumazenil were given at day 5 (figure 2.4) in an attempt to avoid labelling the immediate post-injury proliferative peak which is likely due to tissue disruption by injection rather than LPC-induced demyelination. The rationale behind the time points used in these experiments are discussed in further detail in chapter 6.

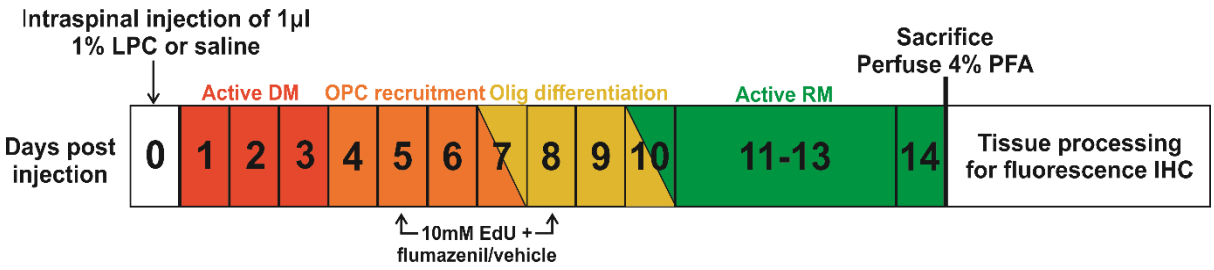

Figure 2.4 Timeline of experimental paradigm

Diagram of the experimental timeline showing the time following intraspinal injection of LPC or saline, the effects of LPC, and the period in which animals were treated with EdU alongside flumazenil or saline. The diagram also shows the length of the experiment and details timing of sacrifice, perfusion, and tissue processing for IHC

2.4.7 Processing of tissue for EdU and immunohistochemistry

After 14 days post- LPC or saline intraspinal infusion, animals were terminally anaesthetised by I.P injection of sodium pentobarbital 20% w/v (60 mg/kg) (Pentoject, Animal care, UK). A transcardial perfusion was performed as described previously in this chapter, section 2.2.4. Following perfusion fixation spinal cords were harvested and post-fixed in 4% PFA at 4ºC for 4-18 hours as described in section 2.2.5.

Intraspinal LPC/saline injection sites were situated at approximately mid-lumbar level and were determined by the presence of a slight pinprick sized bruise on the cord surface which made the area appear irregular and distinct from the rest of the tissue. Injection sites were isolated from each spinal cord to give a ~3mm tissue block which were sectioned and analysed as detailed below.

Tissue was sectioned at 40 µm on a vibrating microtome and processed for post-hoc detection of newly proliferated EdU^+ cells as previously described (section 2.2.5). Following this, sections were incubated in primary antibodies overnight and detected the following day by a 2-4 hour incubation in a species appropriate Alexa fluorophore conjugated secondary antibody (section 2.2.7). Analysis of oligodendrocyte differentiation and remyelination was

most important following LPC-induced demyelination, therefore staining for PanQKI (table 2.3) was carried out alongside EdU detection.

Following incubation with secondary antibodies, sections were washed 3 x10 minutes in PBS and mounted on glass slides using a fine paintbrush. Sections were allowed to air dry before adding vectashield or vectashield plus 4',6-diamidino-2-phenylindole (DAPI) (Vector Laboratories, Burlingame, CA), covering with a glass coverslip, and sealing with nail polish.

2.4.8 Analysis of spinal cord sections following LPC induced demyelination or saline infusion

Following tissue processing, sections from the injection sites of each animal (*n*=12 *N*=9) were imaged using a Zeiss LSM880 upright confocal laser scanning microscope with Airyscan equipped with argon and He-Ne lasers. ZEN software (Carl Zeiss, Germany) was used to acquire z-plane tile scan stacks of entire spinal cord sections imaging Alexa-Fluor555 and Alexa-Fluor488, to capture EdU and markers of differentiation, from the entire injection site. The following settings were used to achieve this: zoom 0.6, averaging 1, speed 9, tile 2x2 or 3x2 depending on whether the section was located at the upper or lower lumbar level, gain 500-700, digital offset 0, pinhole 1AU, and a manual set centre of focus so that number of sections for z-stack was ~ 60-70 with 1 µm increments between sections. Processing in ZEN was used to stitch tiles together before exporting the final images for analysis in ImageJ.

Confocal images were processed to generate maximum intensity projections of z-stacks in order to count the total number of EdU^+ cells and EdU/$PanQKI^+$ cells in the z-plane. These images were exported as .tif files and counted using the cell counter plugin in Fiji. Counts of EdU^+ and EdU/$PanQKI^+$ cells in the WM and GM were determined and collated in Microsoft Excel and analysed using GraphPad Prism 7 as previously described (2.2.9).

Sections were also imaged using the Axio Scan.Z1 slide scanner microscope for high throughput collection of tiles and z-stacks of sections taken from the injection site of all experimental groups. These images were counted and analysed as described above.

Chapter 3 – Endogenous GABA inhibits proliferation in the postnatal spinal cord

3.1 Introduction and rationale

Endogenous neurogenic niche signalling is known to regulate the cellular output of the neurogenic niches within the brain (Wang, D.D. *et al*., 2003; Nguyen *et al*., 2003; Alfonso *et al*., 2012; Daynac *et al*., 2013; Morizur *et al*., 2018), balancing proliferation and differentiation of NSCs by matching niche output to population demand in their end targets i.e. olfactory bulb or granule cell layer. Similarly, previous work from our lab has shown that modulation of cholinergic neurotransmission modulates proliferation and differentiation in the adult spinal cord (Corns *et al*., 2015).

However, it is currently unclear whether other well documented signals which are known to affect other proliferative niches, such as GABA, affect proliferation and differentiation within the spinal cord. Determining the signals which regulate EC behaviour is important if we are to consider whether these cells may be modulated and transformed for *in vivo* repair in conditions such as MS, SCI, and in situations of 'excessive proliferation' such as CNS cancers.

The role of GABA in niche maintenance and as a master regulator of proliferation is covered in detail in section 1.8. Briefly, in the SVZ and SGZ, GABA is a strong negative regulator of proliferation (Bolteus and Bordey, 2004; Catavero *et al*., 2018; Nguyen *et al*., 2003; Ge *et al*., 2007), restricting NSCs to dormancy, by regulation of cell cycle exit, until required (Fernando *et al*., 2011; Daynac *et al*., 2013). GABA however is also involved in the differentiation and migration of NSCs and immature neural cells (Bolteus and Bordey, 2004; Tozuka *et al*., 2005). GABA in these areas is secreted by nearby neuroblasts or parvalbumin^{+} interneurones and forms a paracrine feedback loop for maintenance of niche size and output. GABA has also been implicated in embryonic development and tumour cell proliferation (Blanchart *et al*., 2016; Young, S.Z. and Bordey, 2009), indicating that GABA is a ubiquitous signal in the control of cellular proliferation in many pre- and postnatal neuronal and non-neuronal tissues.

ECs represent a population of latent stem cells within the adult spinal cord (Hamilton, L.K. *et al*., 2009; Panayiotou and Malas, 2013; Barnabe-Heider *et al*., 2010). Much like NSCs within the brain, ECs surrounding the spinal cord CC respond to applications of GABA with a robust depolarisation (Corns *et al*., 2013). Furthermore, as ECs possess similarities to other neurogenic niches, where GABA has been implicated in the control of proliferation vs. differentiation, it is possible that GABA may play a similar role within the spinal cord. GABA is known to suppress proliferation in other regions and EC turnover and proliferation is extremely slow compared to other cell types in the cord, suggesting that EC dormancy may be influenced by GABA in the spinal cord. Preliminary studies in our lab have shown that increasing ambient GABA by vigabatrin (VGB) treatment results in a significant decrease in the level of post-injury proliferation (figure 3.2). However, the effects of GABA upon proliferation in the intact adult spinal cord have not yet been fully investigated.

Work discussed here investigates the effects of increasing CNS GABA content by both transgenic and pharmacological means, with the aim of determining whether or not EC proliferation, and proliferation of other cell types in the spinal cord, is influenced by changes in GABAergic neurotransmission.

3.1.1 Using GAD67-GFP mice to assess proliferation in response to changes in GABA

GAD is the main enzyme responsible for the production of GABA and is expressed in 2 main isoforms; GAD65 and GAD67. GAD67 is thought to be more important during development than GAD65, as GAD65 heterozygous knockout mice have similar CNS GABA levels to WT mice at birth. However, GABA mRNA and protein were reduced to approximately one half of the level of WT littermates in the brain of GAD67 heterozygote knockouts (Asada, H. *et al*., 1997). These differences continued into adulthood, suggesting that in these animals GAD65 does not compensate for the loss of GAD67 to normalise GABA levels in adulthood (Asada, Hideo *et al*., 1996; Asada, H. *et al*., 1997).

In order to investigate the expression and distribution of GABAergic neurones many researchers have attempted to induce ectopic green fluorescent protein (eGFP) expression in GABAergic neurones (Oliva *et al*., 2000; Huang, J. *et al*., 2006). However, in these studies, cDNA encoding for eGFP was inserted randomly into the mouse genome, leading to variations in the accuracy of GFP expression in GABAergic neurones (Tamamaki *et al*., 2003). Tamamaki *et al*., (2003) circumvent these issues and induce robust and specific expression of GFP in GABAergic neurones by targeted insertion of cDNA encoding eGFP into the locus encoding GAD67 with homologous recombination (Tamamaki *et al*., 2003).

GAD67-GFP mice harbour enhanced GFP cDNA between the GAD67 5' flanking region and the GAD67 codon start of the GAD67 promotor, a location chosen to ensure accuracy of GFP expression within GABAergic neurones (Tamamaki *et al*., 2003). The first step involved in GAD67-GFP transgene production involves the use of homologous recombination of ES cells where a loxP-flanked PGK-neo cassette was used as a positive selection marker for screening homologous recombinant ES cells. GAD67-GFP mice therefore retain the eGFP cDNA and the loxP-flanked PGK-neo cassette in the GAD67 locus. The loxP flanked PGK-neo cassette may have unexpected effects upon GFP expression and so was removed by crossing GAD67-GFP mice containing the PKG-neo cassette with CAG cre-transgenic mice on a C57Bl/6 background, resulting in excision of the floxed PKG-neo cassette in the 'final' animals. These animals were referred to as GAD67-GFP (**Δ**neo) mice, and these were the particular strain bred and housed in our animal facility. These animals will be referred to as GAD67-GFP mice from here on. A schematic of the WT and recombinant alleles of the GAD67-GFP mice are detailed in figure 3.1. Figure 3.1B is a representative image taken from a sagittal section of adult GAD67-GFP spinal cord illustrating the GFP expression in GABAergic CSFcCs lining the CC (arrow).

Productive breeding results in heterozygous GAD67-GFP ($GAD67^{+/-}$) pups, with GAD67 haplodeficiency due to GFP knock in, as $GAD67^{-/-}$ is lethal at birth due to cleft palate development (Asada, H. *et al*., 1997). GAD67-GFP mice are heterozygotes and therefore

express one WT allele and one modified GFP containing allele of GAD67 (figure 3.1A). At 2-3 days of age mice are genotyped by GFP visualisation under an ultraviolet light, as at this age fluorescence can be visualised through the thin bones of the skull. GAD67-GFP mice are seizure free and phenotypically normal in terms of growth and reproductive behaviour despite showing a reduction in brain GABA content, as measured by high performance liquid chromatography (Tamamaki *et al*., 2003). There are no abnormalities in the brains of GAD67-GFP animals when examined at a macroscopic level.

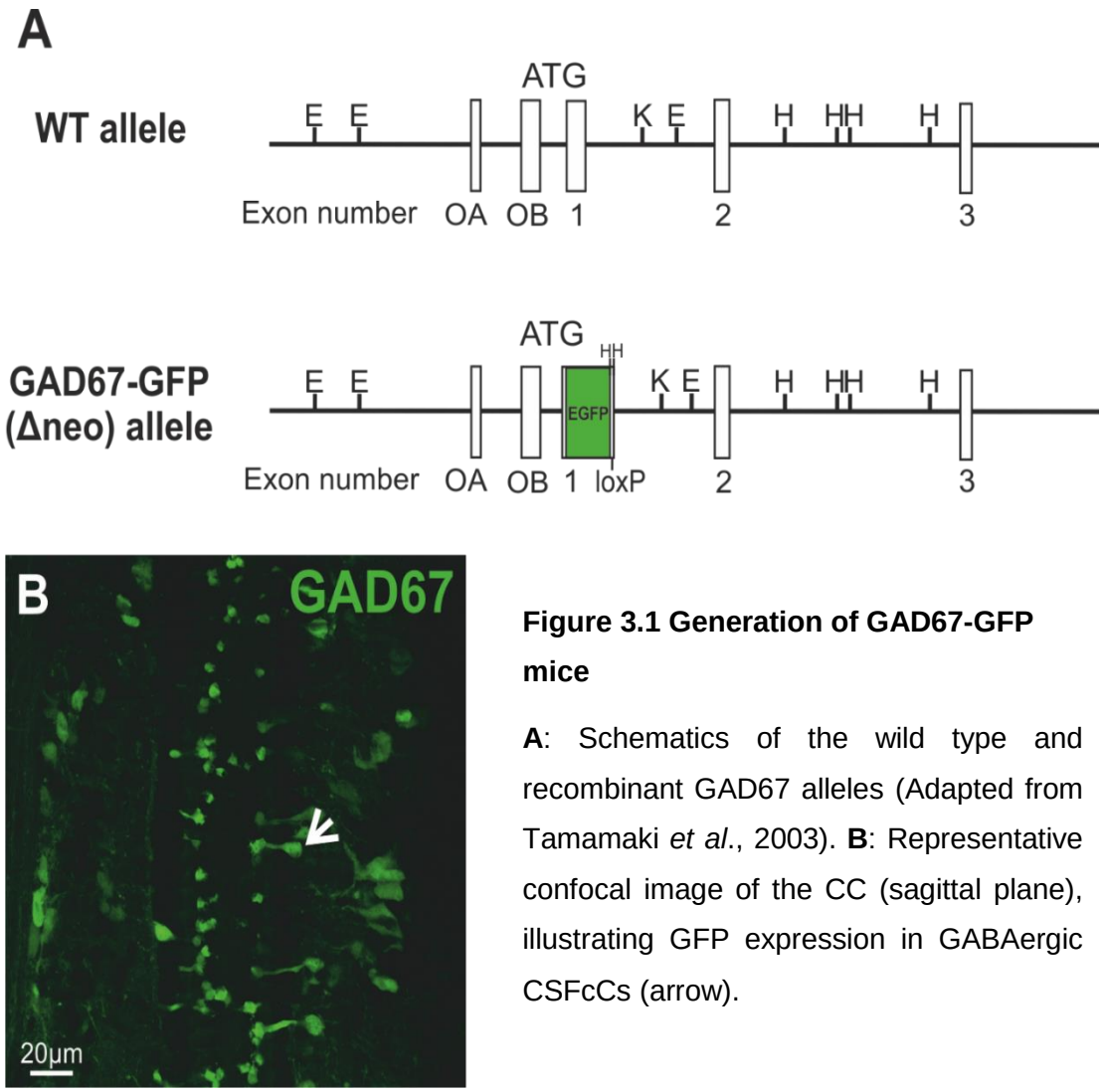

Figure 3.1 Generation of GAD67-GFP mice

A: Schematics of the wild type and recombinant GAD67 alleles (Adapted from Tamamaki *et al*., 2003). **B**: Representative confocal image of the CC (sagittal plane), illustrating GFP expression in GABAergic CSFcCs (arrow).

The use of GAD67-GFP knock-in mice allowed us to not only visualise GABA producing GAD67-GFP positive cells, such as CSFcCs, but also provided an invaluable tool to examine how reductions in ambient GABA may affect cellular proliferation and differentiation in the

spinal cord. Preliminary work from our lab has shown that GAD67-GFP mice have differences in the number of $Ki67^+$ cells at the CC compared to WT animals, therefore further investigation of this phenomenon using *in vivo* markers of proliferation, such as EdU, was necessary.

3.1.2 Increasing GABAergic neurotransmission by vigabatrin treatment

GAD67-GFP transgenic mice provide a model *in vivo* situation in which CNS GABA content may be reduced, thereby affecting proliferation, without the use of pharmacological agents. However, there are many licensed drugs available which influence GABAergic neurotransmission. Treatment with drugs that influence GABAergic proliferation, alongside EdU administration, provides a useful tool to investigate the effects of GABA, or rather influencing GABA levels, upon proliferation in the spinal cord.

VGB (vinyl-γ-aminobutyric acid) is an antiepileptic which acts specifically to prevent GABA catabolism by irreversible suicide inhibition of GABA transaminase (Mumford and Dam, 1989; Jung *et al*., 1977). The concentration of GABA present in synaptic vesicles, and therefore available for synaptic transmission, is dependent upon the equilibrium between GABA synthesis and degradation. Inhibition of GABA transaminase by VGB therefore results in an increase in GABA levels in the brain (Gram *et al*., 1988; Löscher *et al*., 1989) and an increase in the availability of GABA within the synaptic cleft, resulting in enhanced GABAergic neurotransmission (Jung *et al*., 1977; Sarhan *et al*., 1979; Ben-Menachem, 2011). VGB induced GABA transaminase reduction in activity resulted in a 5-fold increase in brain GABA 4 hours after a single 1500 mg/kg injection in mice. VGB has rapid plasma pharmacokinetics, however the increase in GABA persists much longer, where GABA transaminase activity remains low for as long as 5 days after VGB administration, suggesting that VGB has a long biologic half-life. Similar results have also been observed in humans, where GABA remains elevated in the CSF for more than 1 week following a single 50 mg/kg dose (Menachem *et al*., 1988).

Others have suggested that VGB may also inhibit GABA uptake into astrocytes (Leach *et al*., 1996), stimulate GABA release (Ben-Menachem, 2011), and influence glutamate/glutamine cycling between neurones and glial cells (Yang and Shen, 2009)(figure 1.6). Whilst these results are yet to be replicated, all of these aforementioned mechanisms would invariably lead to an increase in ambient GABA available for neurotransmission, hence the effectiveness of VGB as an antiepileptic medication (Ben-Menachem, 2011).

GAD67-GFP animals have been shown to have alterations in their baseline GABA levels (Tamamaki *et al*., 2003), in addition to more proliferative $Ki67^{+}$ cells at the CC compared to WT animals (unpublished observation, Deuchars' lab). VGB was chosen as it has a similar effect to GFP insertion to GAD67 allele; altering the level of ambient GABA available for neurotransmission (Tamamaki *et al*., 2003; Yang and Shen, 2009). VGB therefore allows investigation of the effects of pharmacological modulation of GABA availability upon proliferation without influencing GABAaR directly.

It was hypothesised that as VGB increases GABA levels it may decrease proliferation, whereas lower GABA levels in GAD67-GFP animals may result in more proliferation. Therefore, examining these experimental conditions together will provide evidence of whether modulation of GABA in the adult spinal cord can induce bidirectional changes in proliferation i.e. both increases and decreases in proliferation.

Preliminary data from our lab have shown that modulating GABAergic neurotransmission by VGB treatment has an effect upon post-injury proliferation following stab injury to the dorsal WM. Whilst injury to the spinal cord results in a significant increase in EC proliferation at the CC (13.3 ± 2.4 EdU^{+} cells at the CC in injured animals vs. 3.6 ± 1.4 cells in intact animals, $p < 0.005$, student's t-test, $N=3$ $n=36$ figure 3.2A,B,D), VGB treatment, dramatically reduces EC proliferation to near intact/uninjured levels (6 ± 0.8 EdU^{+} cells at the CC, $p < 0.005$, student's t-test, figure 3.2C-D). These results illustrate that GABA is a powerful controller of

proliferation in the spinal cord, so much so that following injury it is able to dampen the increased proliferative response when GABA levels are increased by VGB.

.

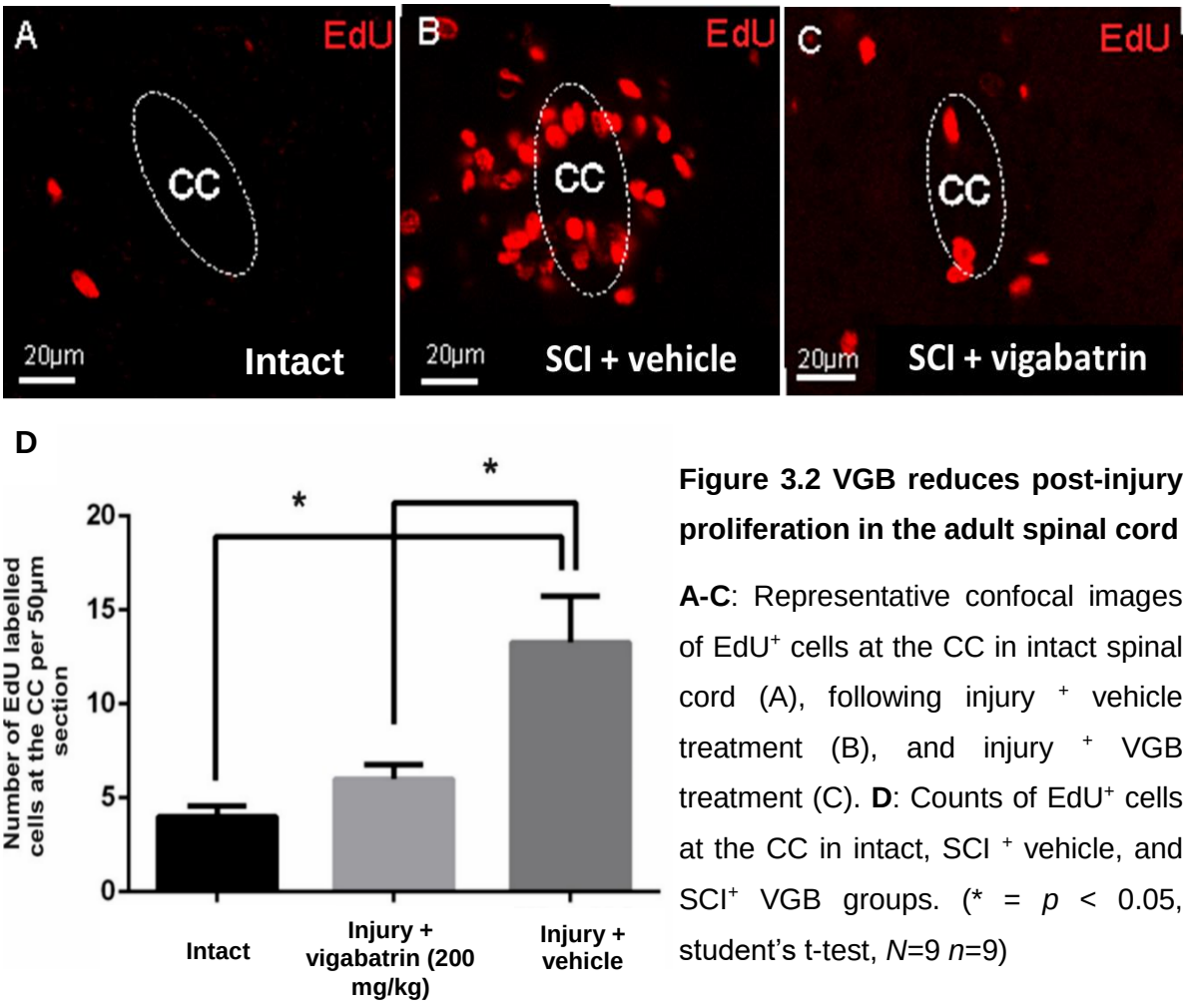

Figure 3.2 VGB reduces post-injury proliferation in the adult spinal cord

A-C: Representative confocal images of EdU$^+$ cells at the CC in intact spinal cord (A), following injury $^+$ vehicle treatment (B), and injury $^+$ VGB treatment (C). **D**: Counts of EdU$^+$ cells at the CC in intact, SCI $^+$ vehicle, and SCI$^+$ VGB groups. (* = $p < 0.05$, student's t-test, N=9 n=9)

Investigating how changes in GABA availability may impact baseline proliferation is essential to further understand the role that GABA may play in postnatal spinal cord proliferation. Much work has investigated the possibility of reactivation of endogenous NSCs in the spinal cord for repair, however more work must be carried out to identify regulatory factors that control EC proliferative behaviour if this possibility is to ever become a reality.

3.1.3 The importance of considering natural behaviours in experimental animals

Experiments carried out in research are usually are usually performed during the normal daytime working hours of the experimenter, however during this time nocturnal mice are normally asleep/inactive. Unless animals undergo light-dark cycle reversal, experiments in the day are carried out at the 'wrong physiological time' for rodents. In order to assess proliferation within the spinal cord during the normal waking hours for mice, experiments were carried out in the evening rather than the day. This was especially pertinent as research has shown that proliferation at the CC is influenced by physical activity (Cizkova *et al*., 2009).

3.2 Aims and objectives

The aim of studies in this chapter is to determine whether GABA has an effect upon proliferation and differentiation within the adult spinal cord, as GABA is known to be particularly important in regulating these processes in other neurogenic niches.

This chapter employs EdU labelling to investigate proliferation *in vivo* following manipulation of GABAergic signalling in both GAD67-GFP transgenic mice and VGB treated animals.

Baseline proliferation in the intact spinal cord is particularly low, therefore studies described here also aim to determine whether a greater proliferative population is apparent following EdU administration during periods of wakefulness.

3.3 Methods

3.3.1 Animals

To determine the effects of waking activity (*N*=6), reduced ambient GABA in GAD67-GFP (*N*=6), and vigabatrin treatment (*N*=3) upon on spinal cord proliferation adult wild-type C57Bl/6 mice (~4-8 weeks) of either sex were used in line with the UK animals (Scientific

Procedures) Act 1986 and ethical standards set out by the University of Leeds Ethical Review Committee. Every effort was made to minimise the number of animals used and their suffering. Animals were given ad libitum access to food and water and were housed in a 12-hour light dark cycle.

In addition to adult WT C57Bl/6 mice, adult (~8-12 weeks) transgenic GAD67-GFP knock-in mice (*N*=12) were also used in order to investigate changes in spinal cord proliferation following genetic manipulation of pathways involved in the production of the neurotransmitter GABA.

Adult C57Bl/6 (*N*=3) and GAD67-GFP (*N*=3) mice (~4-6 weeks) were also used for analysis of GABA levels in the brain and spinal cord by HPLC.

3.3.2 *In vivo* drug and EdU administration

Animals, both C57Bl/6 and GAD67-GFP, received a nightly 0.1 ml injection of the thymidine EdU as described previously (section 2.2). Animals receiving EdU in the light hours were injected between 10:00 and 11:00, whereas animals receiving EdU in the dark hours were injected between 20:00 and 21:00. When examining the effects of vigabatrin upon proliferation, animals also received either 0.1 ml vigabatrin (200 mg/kg) (*N*=3) or 0.1% TWEEN-80 containing saline (*N*=3) I.P each evening.

3.3.3 Tissue preparation, EdU detection, and immunohistochemistry

Tissue from the spinal cord of animals treated with EdU and vigabatrin or vehicle was prepared for the detection of EdU and IHC for other cellular markers as previously described (section 2.2). 40µm sections from the thoracolumbar region underwent Cu^{2+} catalysed click chemistry for the detection of EdU^{+} cells. Following EdU localisation, sections were incubated with primary antibodies in order to determine the identity of EdU^{+} cells. Immunofluorescence was performed with antibodies against NeuN, for mature neurones, (mouse, 1:1000, Millipore, Watford, UK), Sox2, for undifferentiated stem-progenitor cells, (goat, 1:1000, Santa Cruz), PanQKI, for oligodendrocytes, (mouse, 1:100, UC Davis/NIH

Neuromab Facility, Davis, CA), S100B, for astrocytes, (rabbit, 1:750, Abcam, Cambridge, UK), and Iba1, for microglia (rabbit, 1:1000, Wako, Japan). Antibodies were detected using appropriate Alexa488 conjugated secondary antibodies (section 2.2.7).

3.3.4 Cell counts, image capture, and statistical analysis of data

Cell counts and image capture including colocalisation of EdU and specific cellular markers, were performed as described previously in sections 2.2.8 and 2.2.9

Data was collated and analysed as described in section 2.2.10. EdU^+ cell counts are given as mean number of EdU^+ cells per 40µm section ± SE. Data were considered significant when $p < 0.05$ (denoted by *); $p < 0.05$ (denoted by **), $p < 0.005$) (denoted by ***); or $p < 0.001$ (denoted by ****).

3.3.5 Using HPLC to measure ambient GABA levels in the spinal cord and brain of WT and GAD67-GFP mice

Using HPLC, Tamamaki *et al*., (2003) show that GAD67-GFP mice have lower levels of ambient GABA in the brain as a result of genetic manipulation of GAD67 expression, where one allele of GAD67 is replaced by GFP to allow for expression, and therefore detection, of GFP in GABAergic cells in the CNS (Tamamaki *et al*., 2003). GABA levels were not examined in the adult spinal cord however, and manipulations in the expression of GAD67 by introduction of GFP, may result in changes in the level of ambient GABA available in the spinal cord of adult mice. Brain and spinal cord samples for HPLC were taken from adult C57Bl/6 (*N*=3) and GAD67-GFP (*N*=3) mice perfused with PB as described earlier (section 2.2.4). Brains and spinal cords were dissected as previously described and kept in PB on ice for ~10 minutes before HPLC.

HPLC of these samples from C57Bl/6 and GAD67-GFP mice was kindly carried out by Ellen Tedford of Dr Glenn McConkey's lab (Faculty of Biological Sciences, University of Leeds, UK), due to their expertise in the method.

Briefly, brain and spinal cord tissue were homogenised by sonication with 0.1M perchloric acid (PCA) to extract amino acids and precipitate proteins (Fisher *et al*., 2001). GABA standards were made using 5mM GABA in methanol:water (80:20 w/v). The solution was filtered through a 0.22 µm membrane filter. Amino acids in the samples were derivatised with o-phthaldialdehyde. The determination of GABA concentration in brain and spinal cord samples was carried out by HPLC with a UV spectrophotometric detector at 360nm.

HPLC analysis was performed with a Dionex HPLC system consisting of a P580 Pump (Dionex, USA) and Ultimate 3000 Autosampler Column Compartment with a C18 Acclaim 150 column and an ESA Coulochem III cell. The mobile phase contained 57mM anhydrous citric acid (Fisher Scientific, UK), 43mM sodium acetate (Dionex, USA buffer containing 0.1mM EDTA (Sigma, USA), 1mM sodium octanesulphonate monohydrate, and 10% methanol. The pH was adjusted to 4. The mobile phase was delivered at a flow rate of 0.8 ml/min, and the column temperature was set at 40ºC. GABA standards were dissolved in 0.1M PCA for chromatography. The concentration of compounds was determined and analysed using Chromeleon software. Statistical analysis of replicants and differences between WT and GAD brain and spinal cord were carried out using GraphPad Prism 7.

3.4 Results

3.4.1 Proliferation is greater in both WT and GAD67-GFP mice when EdU is given in dark hours compared to light hours

In adult WT mice the number of newly proliferated EdU^+ cells, is significantly greater ($p < 0.0001$, students t-test) in mice treated with EdU during waking hours, between 19:00 and 21:00, compared to animals injected with EdU during daylight hours (10:00-11:00).

When comparing the total number of EdU^+ cells in mice given EdU during dark hours vs. mice given EdU during light hours, those which were administered EdU during the dark hours had significantly more EdU^+ cells than animals treated with EdU during the day (71.6 ±

2.7 cells vs. 13.2 ± 1.9 cells, $p < 0.0001$, student's t-test, N=3 n=12, figure 3.3A). Furthermore, when counting EdU^+ cells specifically within the EC layer surrounding the CC, EdU administration in the dark/waking hours resulted in more newly proliferated EdU^+ cells at the CC compared to the numbers of EdU^+ cells at the CC in animals which received EdU during the light/sleeping hours (2.4 ± 0.2 cells vs. 0.3 ± 0.1 cells, respectively, $p < 0.0001$, student's t-test, N=3 n=12, figure 3.3Ai).

When conducting the same experiment in GAD67-GFP mice it was found that there were significantly more total EdU^+ cells in animals given EdU at night compared to those given EdU during the day (70.9 ± 1.7 cells vs. 30.2 ± 2.9 cells, $p < 0.0001$, student's t-test, N=3 n=12, figure 3.3B). However, there were no significant differences in the numbers of EdU^+ cells specifically located at the CC in animals given EdU during the evening compared to animals given EdU during the day (3.4 ± 0.4 vs. 3.8 ± 0.3, n.s, student's t-test, N=3 n=12, figure 3.3Bi)

These findings confirm the hypothesis that animals treated with EdU during their period of wakefulness and activity would exhibit higher baseline levels of proliferation compared to animals treated with EdU during their sleeping hours of the day/light phase

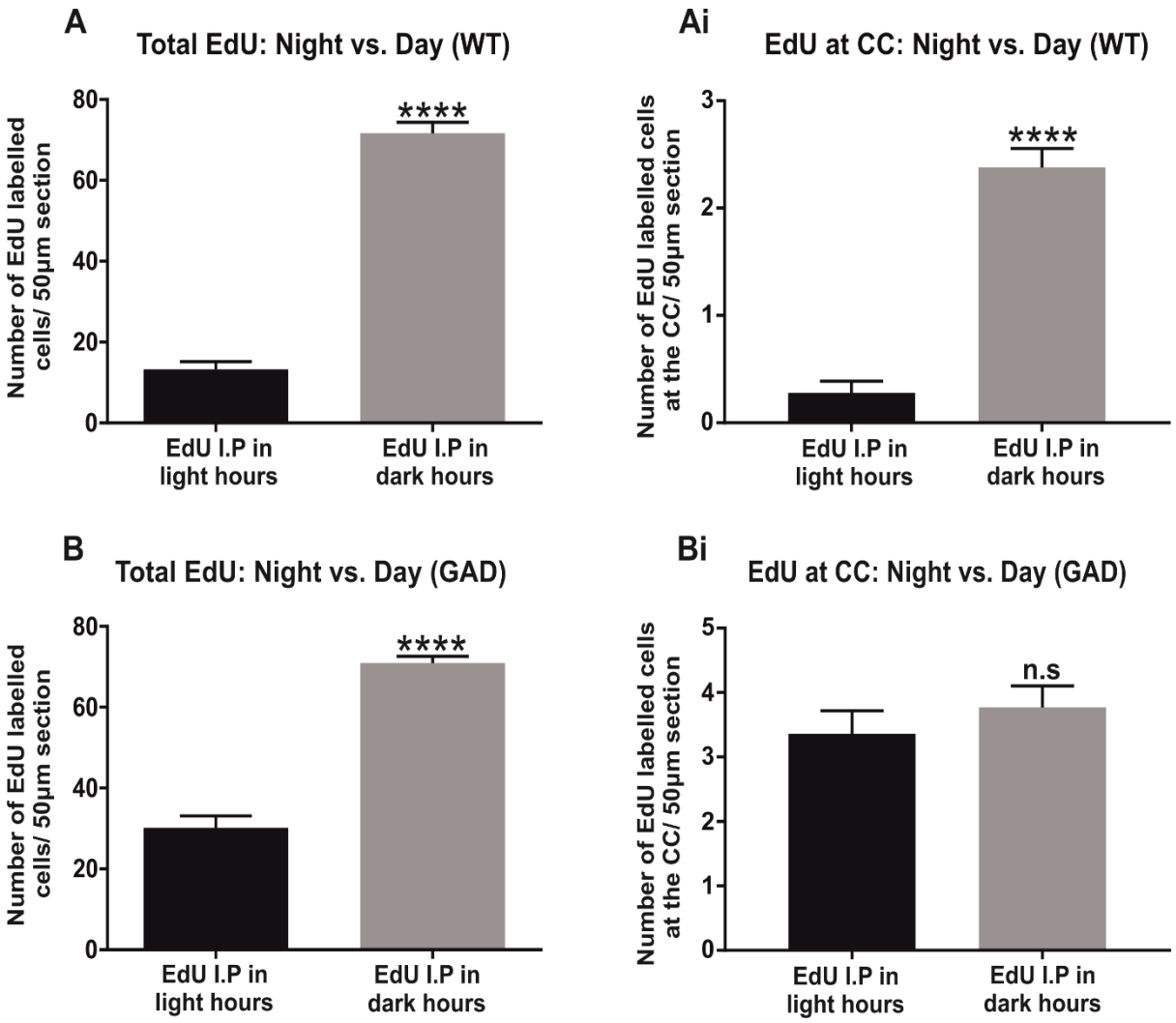

Figure 3.3 Administration of EdU during the evening results in more EdU-labelled cells in the spinal cord compared to animals given EdU I.P during the day

A-Ai: Effects of EdU administration in either light hours or dark hours upon the number of proliferative cells in the spinal cord of WT mice, including cell counts of EdU^+ cells specifically located at the CC compared to vehicle treatment. **B-Bi**: Effects EdU administration in either light hours or dark hours in GAG67-GFP mice upon the number of EdU^+ cells in the WM and GM and CC compared to vehicle treatment (n.s = $p > 0.05$, ****= $p < 0.0001$, student's t-test, *N*=3 *n*=12) Light hours = EdU given between 10:00 and 11:00. Dark hours = EdU given between 20:00 and 21:00.

3.4.2 GAD67-GFP animals have greater numbers of newly proliferated EdU$^+$ cells in the adult spinal cord compared to C57Bl/6 mice

Baseline spinal cord proliferation in GAD67-GFP animals was compared to that of WT C57Bl/6 mice in order to investigate whether these animals had changes in their proliferative capacity as a result of transgenic manipulation of the GAD67 gene.

Following EdU administration over 5 days in both the light-phase and dark-phase of the 12:12 light-dark cycle, it was determined that GAD67-GFP animals exhibited greater levels of baseline proliferation compared to WTs (figure 3.4).

Experiments carried out during the day/light-phase showed that GAD67-GFP animals had significantly greater numbers of total EdU$^+$ cells (31.1 ± 2.8 vs.13.2 ± 2.8, respectively, $p <$ 0.0001, student's t-test, N=3 n=12) and EdU$^+$ cells localised at the CC (3.4 ± 0.4 vs. 0.27 ± 0.1, respectively, $p <$ 0.0001, student's t-test, N=3 n=12) compared to WT animals (figure 3.4A-Ai).

Similarly, when EdU was administered to GAD67-GFP and WT mice during the evening/dark-phase there were significantly more EdU$^+$ cells at the CC of GAD67-GFPs compared to WT animals (3.8 ± 0.3 vs. 2.6 ± 0.3, respectively, $p <$ 0.001, student's t-test, N=3 n=12. figure 3.4Bi). However, the total number of EdU$^+$ cells were similar between WT and GAD67-GFP animals when EdU was administered during the evening when the animals were awake (76.3 ± 4.1 vs. 70.9 ± 1.7, respectively, $p >$ 0.05, n.s, student's t-test, N=3 n=12. figure 3.4B). This is in contrast to findings observed when EdU I.P is given during the day, and at the CC at both day and night, where GAD67-GFPs exhibit significantly greater levels of baseline proliferation compared to WTs.

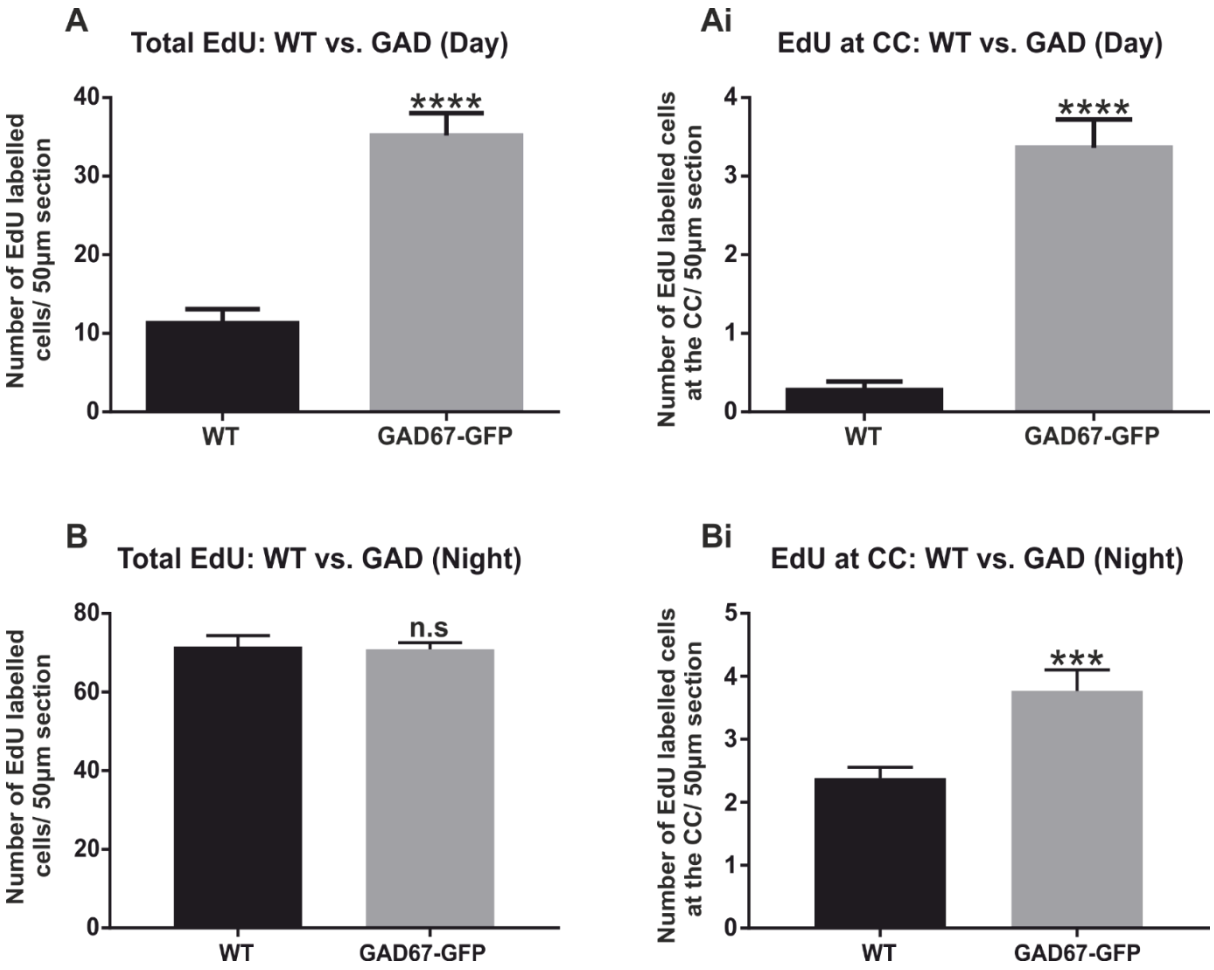

Figure 3.4 Spinal cord proliferation is significantly greater in GAD67-GFP animals

A-Ai: Cell counts of EdU$^+$ cells in the spinal cord of both WT and GAD67-GFP mice following 4 days of EdU administration during light hours **B-Bi**: Cell counts of EdU$^+$ cells in the spinal cord of both WT and GAD67-GFP mice following 4 days of administration of EdU during the dark hours (**** = $p < 0.0001$, *** $p < 0.001$, n.s = $p > 0.05$, student's t-test, N=3 n= 12)

These findings therefore illustrate that GAD67-GFP animals have differences in their baseline levels of proliferation compared to WTs where GAD67-GFPs exhibit significantly greater levels of baseline proliferation compared to WTs.

3.4.3 GAD67-GFP mice have lower levels of ambient GABA in the brain and spinal cord

HPLC was used to determine whether GAD67-GFP mice had differences in their CNS GABA content compared to WT C57BL/6 mice. If so, these results may explain differences in baseline proliferation between these 2 strains.

GABA content was significantly reduced in both the brain and spinal cord samples from GAD67-GFP animals compared to WT mice ($p < 0.05$, students t-test, N=3, figure 3.5). Brains of GAD67-GFP mice had on average 65% less GABA than WT brains, whereas spinal cords had 71% less GABA than WTs. Glutamine content was also measured by HPLC in the brain and spinal cord of GAD67-GFP mice, however whilst results showed a trend toward a decrease in glutamine in GADs, these results were not statistically significant ($p > 0.05$).

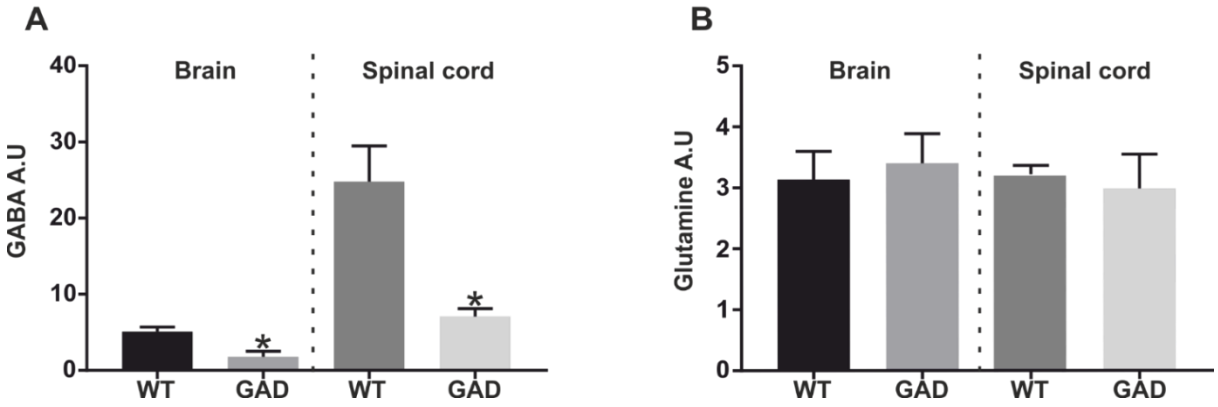

Figure 3.5 CNS GABA content is significantly reduced in GAD67-GFP mice with no change in glutamine levels

A: GABA content of brain and spinal cord from adult WT and GAD67-GFP mice measured by HPLC **B**: Brain and spinal cord glutamine content in adult WT and GAD67-GFP mice measured by HPLC analysis (* = $p < 0.05$, student's t-test, N=3)

3.4.4 VGB significantly reduces proliferation in the spinal cord compared to vehicle treatment

Animals treated with VGB, and therefore greater levels of ambient GABA, had significantly fewer EdU$^+$ cells in total compared to animals treated with vehicle (42.82 ± 1.95 vs. 56.16 ± 2.47, respectively $p < 0.0001$, student's t-test, N=3 n=15, figure 3.6A). VGB treated animals exhibited a 24% decrease in proliferation compared to vehicle treated animals. These differences were not confined to one specific parenchymal region as VGB treated animals exhibited significantly less proliferation in both the WM and GM (26.02 ± 1.45 vs. 32.21 ± 2.24, p <0.01, and 16.42 ± 0.91 vs. 20.97 ± 0.89, p <0.001, for WM and GM, respectively, student's t-test, N=3 n=15 figure 3.6A) compared to vehicle treated littermates. Furthermore, in VGB treated animals there were significantly fewer EdU$^+$ cells present at the CC compared to vehicle (0.68 ± 0.13 vs. 1.8 ± 0.2, respectively, $p < 0.0001$, student's t-test, N=3 n=15, figure 3.6Ai). VGB treated animals possessed 62% fewer cells at the CC compared to vehicle treated animals. In conclusion, together these results show that increasing ambient

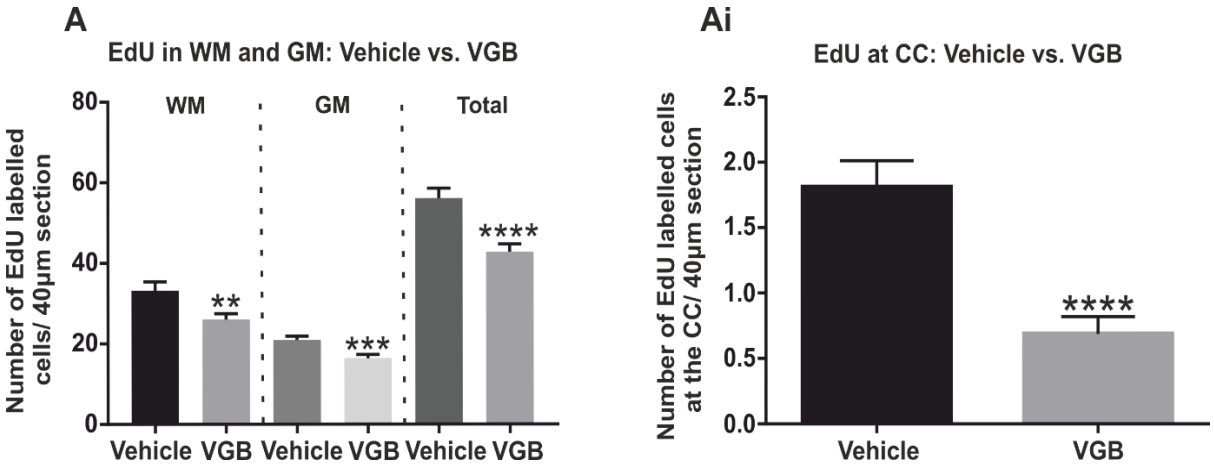

Figure 3.6 VGB significantly reduces proliferation in the intact adult spinal cord

A: Effects of VGB upon the number of total EdU$^+$ cells in the spinal cord compared to vehicle treatment. The numbers of EdU$^+$ cells specific to the WM and GM are also shown. **Ai**: Numbers of EdU$^+$ cells located at the CC in VGB and vehicle treated animals (** = $p < 0.01$, *** = $p < 0.001$, **** = $p < 0.0001$, student's t-test, N=3 n=15)

GABA by VGB treatment results in a significant reduction in proliferation compared to vehicle treated animals.

3.4.5 PanQKI$^+$ oligodendrocytes and Sox2$^+$ NSCs represent the largest population of proliferating cells in the spinal cord

Immunohistochemical markers of specific cell types were used to determine the fate of newly proliferated cells by analysis of frequency of colocalisation with EdU$^+$ cells. EdU$^+$ cells regularly colocalised with undifferentiated Sox2$^+$ cells and PanQKI OPCs and oligodendrocytes. EdU also colocalised with some S100b$^+$, and Iba1$^+$ astrocytes and microglia. Colocalisation of EdU with Sox2, PanQKI, S100b, and Iba1 was found in both the WM and GM (figure 3.7). Colocalisation of EdU$^+$ cells and NeuN was never seen in any sections from animals in either condition, therefore NeuN has been omitted from data examining changes in percentage colocalisation of EdU and other cellular markers as values were always 0. To examine colocalisation, the number of EdU$^+$ cells which also showed immunoreactivity (IR) for the marker in question was divided by the total number of EdU$^+$ cells in the section to give percentage colocalisation to compare to other markers.

Colocalisation of EdU$^+$ and Sox2$^+$ cells occurred in the WM and GM, however EdU$^+$ cells at the CC were exclusively immunopositive for either Sox2 and S100b (figure 3.8A and 3.8B). Colocalisation of ECs was not seen with any other markers due to expression pattern of ECs i.e. ECs do not express PanQKI or Iba1. Percentage of EdU$^+$ cells at the CC that were also Sox2-IR in vehicle animals was 2.77 ± 2.77 %, whereas this increased to 11.11 ± 7.34% in VGB treated animals. S100b$^+$ cells were colocalised with 20.3 ± 11.7% of EdU$^+$ cells at the CC of vehicle treated animals, but this was reduced to 5.56 ± 5.56% of CC EdU$^+$ cells in VGB treated animals. This occurred despite the fact that the average numbers of EdU$^+$ cells at the CC were similar in sections counted with S100b immunolabelling (< 1, 0.33 cells, *n*= 9, *N*=3).

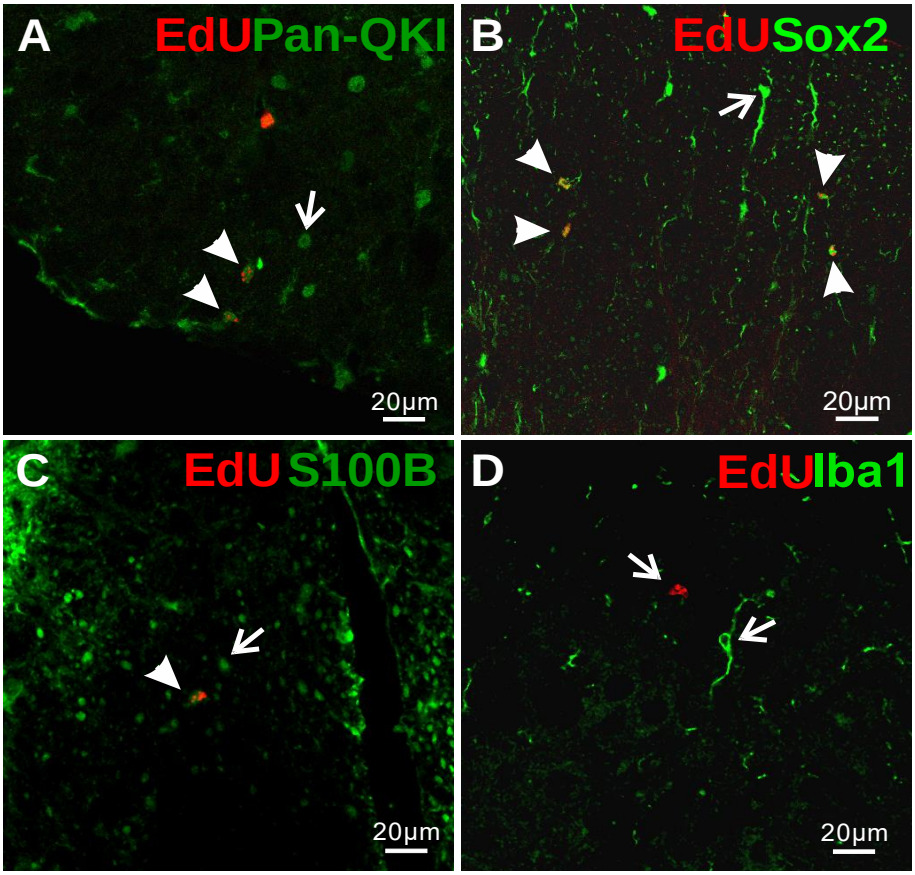

Figure 3.7 EdU⁺ cells colocalise with other specific cell-type markers

A-C: Representative confocal images illustrating the presence of EdU/PanQKI+ (A), EdU/Sox2+ (B), and EdU/S100β+ (C) cells in the intact postnatal spinal cord **D**: Representative confocal image illustrating the presence of Iba1+ microglia in the WM. Non-colocalised cells are labelled with open arrows. Closed arrows denote colocalised cells

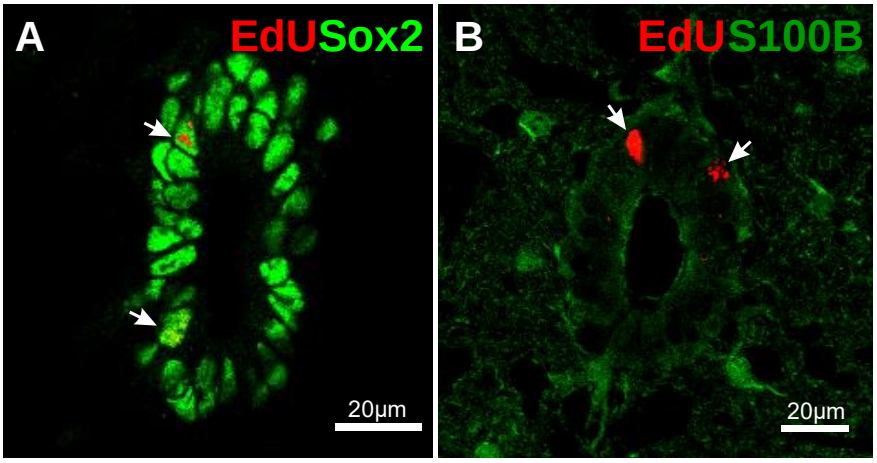

Figure 3.8 EdU⁺ cells at the CC are frequently Sox2-IR and S100β-IR

A-B: Representative confocal images showing that EdU+ cells colocalise with the NSC marker Sox2 (A, arrows) and the EC marker S100β at the CC (B, arrows) of the intact spinal cord

In the spinal cord WM and GM of both vehicle and VGB treated animals, EdU^+ cells were most frequently Sox2-IR and PanQKI-IR, illustrating that undifferentiated NSCs and cells of the oligodendrocyte lineage represent the highest proliferating populations within the spinal cord of these animals (figure 3.9). The percentages of total EdU^+ cells which were PanQKI-IR or Sox2-IR were significantly greater than the percentage of total EdU^+ cells which were either S100b-IR or Iba1-IR (Figure 3.9). This was the case for both vehicle and VGB treated animals, indicating that $Sox2^+$ and $PanQKI^+$ cells remained the greatest contributors to proliferation independent of experimental condition.

The percentage colocalisation of Sox2/EdU^+ in the GM of vehicle treated animals was significantly smaller than the percentage colocalisation of PanQKI/EdU^+ cells in the GM of vehicle treated animals (23.24 ± 5.32% vs. 40.72 ± 4.98%, respectively, $p < 0.05$, one-way ANOVA, N=3 n=9, figure 3.9A) suggesting that the GM has more proliferation of $PanQKI^+$ OLCs than new $Sox2^+$ cells. There were no other significant differences between the percentage colocalisation of EdU/PanQKI or EdU/Sox2 in any other conditions of spinal cord region.

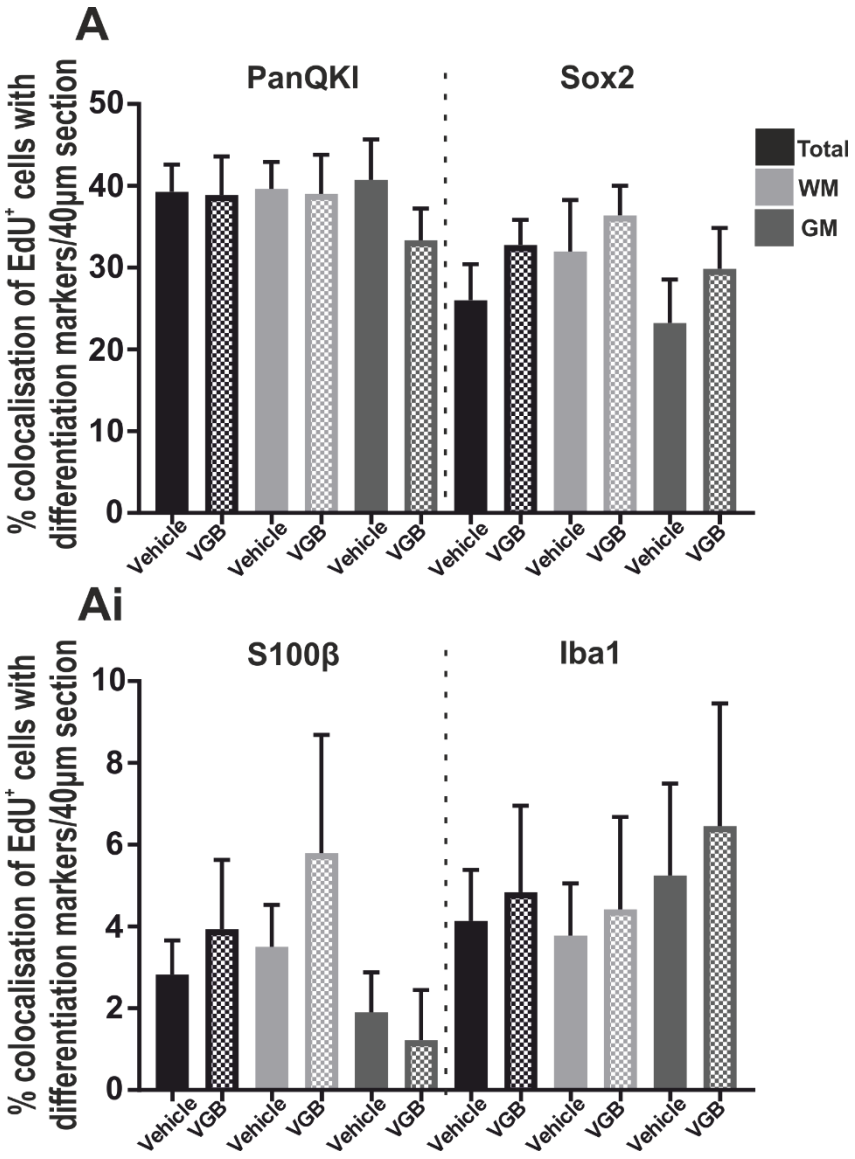

Figure 3.9 Sox2 and PanQKI represent the largest population of proliferating cells in the intact spinal cord. These populations remained unchanged by VGB treatment

A-Ai: Average percentages of EdU^+ cells which were also either $PanQKI^+$, $Sox2^+$, S100 β^+, or $Iba1^+$ in both the WM and GM in each experimental condition (solid bars: vehicle treated animals and hatched bars: VGB treated animals

3.4.6 Increasing ambient GABA levels by VGB does not change amount of differentiation or % fate acquisition of new cells compared to vehicle treatment

Whilst PanQKI and Sox2 represent the highest proliferating population of cells in the spinal cord of vehicle and VGB treated animals, as they have the greatest percentage colocalisation with EdU across any of the conditions and markers, there were no significant differences in the frequency of EdU colocalisation with any of the markers examined in vehicle and VGB treated animals (figure 3.9).

Therefore, whilst treatment with VGB resulted in a significant reduction in both overall proliferation (figure 3.6A) and EC proliferation at the CC (figure 3.6Ai), VGB did not significantly change the percentage of EdU^+ cells which colocalised with either PanQKI, Sox2, S100β, or Iba1. That is to say VGB treatment did not affect differentiation of these newly proliferated cells as their colocalisation with PanQKI, Sox2, S100β, and Iba1 was similar in vehicle treated animals.

Whilst, the percentage of $Sox2/EdU^+$ cells showed a trend toward an increase following VGB treatment, this was not statistically significant ($p > 0.05$).

3.5 Discussion

This chapter provides evidence that proliferation within the adult spinal cord can be modulated by GABA, either by a reduction in CNS GABA content by transgenic manipulation of GAD67 expression or by pharmacological inhibition of GABA catabolism. Whilst previous work from our lab has shown that ECs exhibit GABAergic responses (Corns *et al*., 2013), results discussed here are the first to show that proliferation in the postnatal spinal cord WM and GM can be modulated by changes in the level of ambient GABA available for neurotransmission. EC proliferation is also affected by changes in GABA availability. Much work suggests that ECs are latent NSCs (Barnabe-Heider *et al*., 2010, Meletis *et al*., *2008)*.

The effects of GABA upon proliferation of ECs seen here is similar to the way in which GABA influences proliferation of SVZ and SGZ NSCs, suggesting that ECs are regulated by the similar niche signalling mechanisms as NSCs of other niches. Furthermore, work discussed here illustrates that experiments investigating proliferation in the adult spinal cord should be carried out during times in which animals are awake and active, particularly when reductions in proliferation are hypothesised.

3.5.1 Effects of the sleep/wake cycle on baseline levels of spinal cord proliferation

Whilst cells with NSC properties have been isolated from the spinal cord, baseline levels of proliferation in the healthy adult spinal cord are particularly low when compared to cell turnover in both the SVZ and SGZ, where proliferation continues well into adulthood (Barnabe-Heider *et al*., 2010; Meletis *et al*., 2008; Bond *et al*., 2015). Determining reductions in proliferation in the spinal cord, as a result of pharmacological manipulation of GABA, may therefore prove difficult.

Animals used in these experiments were housed in standard conditions with 24-hour *ad libitum* access to food and water in a constant temperature- and humidity-controlled environment. Temperature fluctuations and availability of food and water are variables which are known to confine animals to temporal niches which govern their day-night sleep-wake cycle (Asher and Sassone-Corsi, 2015). Light/dark cycles also influence rodent behaviour, where mice will exhibit a 23.73- hour circadian rhythm if left in constant darkness. Mice are nocturnal and therefore exhibit waking behaviour during the evening hours. A study of the transcriptome of 12 different mouse organs found that 43% of protein encoding genes display circadian rhythms in transcription (Zhang, R. *et al*., 2014), further highlighting the importance of considering how external factors such as sleep/wake and day/night cycles influence physiology. Animals used in these studies experience a 12:12 dark-light cycle,

between 06:00 and 18:00, and are therefore awake, most active, and exhibiting more 'natural' behaviour, in the dark hours between 18:00 and 06:00.

It was therefore hypothesised that cell proliferation may be higher in the spinal cord in the evening when mice would be naturally awake and active during lights off, between 19:00 and 21:00. These experiments confirmed this hypothesis and showed WT animals treated with EdU in the evening had significantly more proliferation than animals given EdU during the day. This was also the case for the total number of EdU^+ cells in GAD67-GFP mice.

3.5.1.1 Nocturnal activity results in more EdU labelling

It is well established that exercise increases proliferation and neurogenesis in both the SGZ and SVZ (van Praag *et al*., 2005; Kempermann, Gerd *et al*., 2010). However, enhanced physical activity has also been shown to increase EC proliferation in the thoracic spinal cord, with a 2.1-2.6-fold increase in the $BrdU^+$ EC population following use of a running wheel (Cizkova *et al*., 2009; Krityakiarana *et al*., 2010). Preliminary findings from our lab have also shown that mice with access to a running wheel have more $Ki67^+$ cells at the CC (Deuchars' lab, unpublished observation). Furthermore, following SCI, exercise has also been shown to increase EC proliferation and differentiation of EC progeny into neural precursors, oligodendrocytes, and astrocytes, leading to improvements in both functional recovery and autonomous micturition following SCI (Foret *et al*., 2010 2007 2007; Kulbatski *et al*., 2007). Foret *et al*., (2010) report a positive correlation between behavioural locomotor scores and the number of nestin expressing cells around the CC, indicating that increased EC proliferation in the exercise group contributed to improved recovery. It is possible that in these situations, proliferation of ECs leads to beneficial outcomes by the increased production of neurotrophic factors which aid tissue repair (Cusimano *et al*., 2018 2008, Cusimano *et al*., 2018 2008, Cusimano *et al*., 2018).

Exercise has not only been linked to increased EC proliferation in the spinal cord but has also been shown to enhance oligodendrogenesis in the intact adult spinal cord

(Krityakiarana *et al*., 2010). In exercising animals, the expression levels of the immature oligodendrocyte marker NG2 was 124% of that of sedentary animals. Expression of CNPase, which is present in both immature and mature oligodendrocyte cell bodies, processes, and in the myelin sheath, was also significantly increased in thoracic segments following exercise (Krityakiarana *et al*., 2010).

Therefore, a simple explanation for the increased number of EdU^+ cells in animals injected with EdU during the evening is that as mice are nocturnal animals, increased activity during the time when EdU is present and incorporating into dividing cells, results in the labelling of more cells. Natural increases in activity by being awake will lead to more EdU^+ cells compared to animals that are given EdU during daytime inactivity.

Previous work has shown that exercise increases EC proliferation (Krityakiarana *et al*., 2010 2010 2010; Cizkova *et al*., 2009). Significantly more EdU^+ cells are found at the CC in the evening group, and this is in agreement with the hypothesis that evening EdU administration during increased activity results in the increases in EC proliferation described here. In the parenchyma oligodendrocytes are the most abundant cell type contributing proliferation in the intact cord (Barnabe-Heider *et al*., 2010), which also exhibit exercise-induced increases in proliferation (Krityakiarana *et al*., 2010). It is possible that the increases in the total EdU labelled cells in evening treated animals, which include EdU counts from WM and GM, are a result of increased OLC proliferation. This possibility needs to be confirmed using IHC for oligodendrocytes alongside EdU labelling of new cells.

In order to investigate whether these increases in proliferation following evening EdU vs. daytime EdU are indeed due to increased activity the same experiment could be carried out alongside automated home cage analysis of animal cage activity. This would help determine whether a correlation exists between the level of evening waking activity and the number of EdU^+ cells in the spinal cord, as has been illustrated previously using more intense physical activity/exercise paradigms.

3.5.1.2 Exposure to light at night exerts widespread effects upon physiology

Many have advised of the issues involved in working with rodents during human working hours outside of the physiologically relevant period of the animal itself. Such arguments advocate for light/dark cycle reversal in experimental animals so experiments are more ethologically relevant and may yield more reliable data. However, whilst this may be the case, and indeed results discussed here provide evidence for differences in results between day and night, there are still problems associated with disruption of light/dark and sleep/wake cycles by exposing animals to light at night (LAN) for experimental purposes. Exposure to light during the dark phase appears to negatively affect molecular circadian rhythms and physiology (Fonken *et al*., 2013). These include inflammatory responses in mice (Fonken *et al*., 2013) and is also associated with elevated body mass and changes in metabolism (Fonken *et al*., 2013 2015 2015; Gnocchi *et al*., 2015). Exposure to light and internal desynchronization by experimental jet lag has also been shown to cause deficits in learning and memory with parallel reductions in hippocampal proliferation and neurogenesis (Iggena *et al*., 2017 2010 2010; Gibson, Erin M. *et al*., 2010; Yagita *et al*., 2010). Therefore, even in light/dark cycle reversed animals, exposure to light during the dark phase may continue to cause experimental and reproducibility issues.

Nocturnal light exposure suppresses melatonin production and secretion (Russart and Nelson, 2018). Melatonin has been shown to augment hippocampal neurogenesis and reverse the effects of experimental jet lag on hippocampal proliferation and differentiation (Iggena *et al*., 2017). These findings suggest that LAN exposure and circadian dysrhythmia have widespread effects upon physiology which extend to CNS proliferative niches, likely in part mediated by light-induced suppression of nocturnal melatonin. Dosing animals with EdU at night requires brief exposure (~10-20 minutes of the animals to white light, which may affect circadian rhythmicity and melatonin production, therefore resulting in changes in proliferation in the cord, as is seen in night treated animals. Administration of EdU in drinking

water or subcutaneous implantation of EdU-containing osmotic minipumps, which are designed to dispense EdU at night, could be used to investigate this possibility further.

3.5.1.3 Circadian rhythms govern fluctuations in cell proliferation

Circadian rhythms are endogenous oscillations in gene expression and physiology. These oscillations are generated by transcriptional-translational feedback loops in individual cells where core clock genes Period (Per1 and 2), Cryptochrome (Cry1 and 2), and Bmal1 are rhythmically activated throughout the day (Ko and Takahashi, 2006). Cell proliferation follows similar oscillatory behaviours as a result of the circadian rhythmic control of these genes in proliferative cells (Dickmeis and Foulkes, 2011). Hippocampal cells also exhibit rhythmic clock gene expression (Bouchard-Cannon *et al*., 2013) and exhibit rhythmic patterns of differentiation *in vitro* (Malik *et al*., 2015). Expression of key clock components such as Bmal, Per, and Cry have been implicated in the mechanism controlling cell cycle entry and exit of quiescent neural progenitors (Bouchard-Cannon *et al*., 2013). Disruption of the molecular clock leads to aberrant proliferation in the SGZ (Bouchard-Cannon *et al*., 2013). Bmal KO has reduces neuronal differentiation of neurospheres generated from the dentate gyrus (Malik *et al*., 2015), and survival of newborn neurones *in vivo* (Rakai *et al*., 2014). Neurosphere cultures from Cry KO mice also exhibit decreased proliferation and secondary neurosphere generation (Malik *et al*., 2015).

It therefore appears that proliferation of NSCs is also influenced by the circadian clock and may explain the increase in spinal cord proliferation at night. However, whether these processes are also occurring in the spinal cord remain to be seen. Whilst circadian rhythms in clock gene expression are usually absent in embryonic- and multi-potent somatic stem cells, they do appear in more differentiated tissues (Malik *et al*., 2015). Whether ECs and other neural progenitors of the spinal cord express these components, and can therefore be influenced by the circadian clock, is currently unknown.

In conclusion, whatever the reason for a greater number of EdU^+ cells in the spinal cords of animals treated with EdU during the dark phase, these results inform a new method of working when examining adult spinal cord proliferation. Therefore, later experiments looking at the effects of various GABAergic modulators upon proliferation and differentiation in the spinal cord, discussed in chapter 5, were all carried out in the dark phase.

3.5.2 GABA influences proliferation in the postnatal spinal cord

In both the SVZ and SGZ, GABA secreted from nearby neuroblasts induces a paracrine negative feedback loop which suppresses proliferation and restricts NSCs to quiescence (Nguyen *et al*., 2003; Daynac *et al*., 2013). In these neurogenic areas of the brain, GABAergic signalling also influences differentiation, migration, and integration of neural progenitors to their target network/location (Ge *et al*., 2007; Nguyen *et al*., 2003; Tozuka *et al*., 2005; Deisseroth, Karl and Malenka, Robert C., 2005; Wang, D.D. *et al*., 2003). Moreover, endogenous modulation of GABA by DBI regulates niche output by controlling balance of NSC population or the population of new born neurones via dampening of the GABAergic 'brake' (Alfonso *et al*., 2012, Dumitru *et al*., 2017). These mechanisms, and how they may be relevant to spinal cord proliferation, are discussed in detail in chapter 5.

Results described here, which show that the level of ambient GABA and the level of spinal cord proliferation are inversely proportional to one another, are in agreement with the effects of GABA in the proliferative niches of the brain. Increased proliferation in GAD67-GFP mice is likely due to their reduced CNS GABA content, whereas significant increases in GABA availability by VGB, results in a reduction in spinal cord proliferation. These results suggest that GABA may also control proliferation in the adult spinal cord in a similar way to that of the brain by suppressing proliferation. These effects were seen in the WM and GM, in addition to the CC. Although ECs have NSC properties they are relatively quiescent cells, proliferating rarely for self-renewal purposes, could an excess of GABA in the CC niche be one of the reasons for this?

3.5.2.1 Could neighbouring CSFcCs release GABA and inhibit EC proliferation in a paracrine fashion?

Neighbouring CSFcCs are GABAergic cells which possess the machinery for GABA synthesis and secretion (Corns *et al*., 2015; Roberts *et al*., 1995), and therefore may provide the source of GABA to restrict proliferation, similarly to the role neuroblasts play in the SVZ (Liu, X. *et al*., 2005)li(Nguyen *et al*., 2003; Wang, D.D. *et al*., 2003; Daynac *et al*., 2013). Selective killing of CSFcCs, perhaps by PKD2L1 targeted mutations, followed by EdU administration to label proliferating ECs may help determine whether these GABAergic paracrine feedback loops also occur in the spinal cord to keep ECs dormant. For example, in the SVZ, radiation induced death of fast dividing GABAergic progenitors results in activation of dormant NSCs previously restricted by GABAergic signalling (Daynac *et al*., 2013). Is this occurring in a less intense fashion in GAD67-GFPs where CSFcCs produce less GABA, and so the spinal cord is slightly released from GABA suppression? Additionally, is GABA something that changes following injury and could this explain why we see differences in NSC behaviour of ECs following this? Or rather do ECs overcome GABAergic signalling, perhaps by upregulating DBI expression, to switch on their multipotent proliferative NSC behaviour to replace depleted populations lost to cell death following tissue injury? These are pertinent research questions which still need to be addressed if we are to ever fully understand the role GABA plays in spinal cord proliferation and differentiation in both the intact and injured spinal cord.

3.5.2.2 Does the way in which VGB changes GABA metabolism affect energy availability for proliferation?

VGB has a well-defined mechanism of action whereby irreversible selective suicide inhibition of GABA transaminase results in an increase in synaptic GABA availability, and therefore enhanced GABAergic neurotransmission (Ben-Menachem, 2011; Jung *et al*., 1977; Sarhan *et al*., 1979). 50 mg/kg VGB increases GABA levels by 200-300% in human cerebrospinal fluid and CNS tissues (Ben-Menachem *et al*., 1993), illustrating the powerful effect VGB has on CNS GABA levels. Preliminary data from our lab has also hinted at the power of VGB in increasing GABA and the resultant effects this has in decreasing reactive post-injury proliferation (figure 1.2). Results described here show that VGB also reduces proliferation in the intact spinal cord.

There are very few other studies which have directly investigated the effects of VGB upon neurogenesis or proliferation within the CNS. However, VGBs increase epithelial cell proliferation, leading to gingival overgrowth, a common adverse drug reaction associated with VGB treatment (Mesa *et al*., 2003), suggesting that VGB influences proliferation in many other cell types.

In the brain, GABAergic signalling regulates NG2-cell development *in vivo* (Zonouzi *et al*., 2015). In young mice (P5-11) VGB decreases NG2- cell proliferation and increases the number of mature oligodendrocytes compared to vehicle injected mice (Zonouzi *et al*., 2015). Furthermore, in a mouse model of tuberous sclerosis complex, a condition involving disinhibition of the mTOR pathway which causes excessive cell growth and tumour formation, VGB significantly reduces tuberous sclerosis complex-induced over-proliferation of $GFAP^+$ astrocytes (Zhang, B. *et al*., 2013). These results were linked to a 40% reduction in the mTOR pathway in the neocortex and hippocampus of VGB treated mice. VGB also significantly reduced mTOR signalling in WT mice, suggesting that VGB may reduce

proliferation by effects upon both GABAergic signalling but also by inhibiting mTOR, a key signalling pathway involved in cell growth and proliferation (Zhang, B. *et al*., 2013).

In a study examining breast to brain cancer metastases (BBMs), upregulation of all GABA receptor mRNA isoforms was found in cultured cells from $HER2^+$ BBMs. BBM cells also over-expressed GABA transaminase and GAD67 (Neman *et al*., 2014). Furthermore, following exogenous GABA treatment, BBM cells increased their proliferation in a dose dependent manner. Whilst this may seem counterintuitive to the effects of GABA upon proliferation which have been previously described, Neman *et al*., (2014) show that the effects of GABA upon proliferation of BBM cells was not due to GABAergic signalling as cultures treated with muscimol showed no change in proliferation relative to non-treated cells. Instead, it appears that BBM cells metabolise GABA as an energy source for proliferation by metabolising GABA to increase NADH levels by 47%. BBMs have increased GABA transaminase expression relative to primary breast cancer cells. GABA transaminase inhibition by VGB treatment abolished the increased tumour cell proliferation in BBMs, and attenuated the exogenous GABA induced increase in NADH levels, suggesting that in BBMs GABA increases proliferation independent of GABAergic neurotransmission and instead provides a source of energy that BBM cells can use to fuel proliferation via the GABA shunt.

In conclusion results described here are in agreement with other papers which show that VGB reduces proliferation of neural cells. However, whether this effect is solely related to the VGB induced increases in GABAergic neurotransmission is unknown as other studies suggest that VGB may mediate its effects by alternative mechanisms such as mTOR signalling and changing how the cell produces and utilises energy for proliferation.

3.5.3 Identity of newly proliferated cells remains the same in VGB treated animals

NSC-like ECs represent less than 5% of the proliferative population (Johansson *et al*., 1999), astrocytes contribute <1%, and OLCs make up more than 80% of $BrdU^+$ newly proliferated

cells in the intact adult spinal cord (Barnabe-Heider *et al*., 2010). Results described here are in agreement with these findings, where the percentage of total EdU^+ cells which were also immunopositive for OLC marker PanQKI was significantly greater than that of other glial markers. This trend continued throughout and was seen in all animals treated with EdU (Chapter 5).

The percentage of EdU^+ cells which colocalised with Iba1 was particularly low, suggesting that whilst repeated handling of animals and IP injections can increase stress (Yun *et al*., 2010; Lee, K. and Ko, 2018), the level of tissue reactivity by microglial proliferation was low. This was a trend which continued through these experiments.

Our work also showed that undifferentiated Sox2 cells were as abundant as $PanQKI^+$ OLCs, and particularly strong colocalisation of EdU was found with Sox2 at the CC. Sox2 is a neural progenitor marker as it is a transcription factor associated with maintenance of neural progenitor identity and inhibition of neural differentiation (Graham *et al*., 2003). Sox2 labelling in the WM, GM and in the ECs at the CC follows the same as the pattern of Sox2 staining found in both the rat and human spinal cord (Foret *et al*., 2010 2008 2008; Dromard *et al*., 2008). In these experiments, many EdU^+ cells colocalised with Sox2, where all ECs were $Sox2^+$, indicating the abundant proliferation of neural progenitors in both vehicle and VGB treated animals. Foret *et al*., (2010) also showed that $Sox2^+$ ECs also colocalised with S100β, which was also observed here.

There were however no EdU^+ cells which colocalised with the mature neuronal marker NeuN, this may be because of the short time frame used in this study of 5 days, where others have stated NeuN begins to be expressed in post-mitotic neurones at day 10 (Kim *et al*., 2009). Alternatively, few others have provided evidence for the proliferation of new neurones in the intact adult spinal cord, often showing that whilst proliferation of astrocytes and oligodendrocytes occurs, markers of proliferation such as BrdU and EdU are never found in $NeuN^+$ cells (Barnabe-Heider *et al*., 2010). It is therefore possible that the signals

required for neuronal differentiation may be absent in the adult spinal cord, instead providing a more gliogenic environment.

Whilst GABA has been shown to influence differentiation of new cells (Tozuka *et al*., 2005), VGB treatment did not result in any significant differences in number of EdU^+ the cells which co-labelled with either Sox2, PanQKI, S100B, Iba1, or NeuN compared to vehicle. As VGB increases GABA levels it could be hypothesised that the reduced level of proliferation would also result in more differentiation to more mature cell types, however this was not the case here. $Sox2/EdU^+$ cells showed a trend toward an increase, but this was not significant, however perhaps this indicates that the length of time following EdU administration and sacrifice was not long enough to observe sufficient differentiation as many undifferentiated $Sox2^+$ cells were still present. Further experiments could be carried out with a longer time to sacrifice following EdU to determine whether this increases the level of differentiated cells in the spinal cord from the boosted proliferative population.

In conclusion, whilst VGB treated animals may not have had significant changes in the differentiation potential of newly proliferated cells, these new cells are capable of differentiation into astrocytes, oligodendrocytes, and microglia.

3.6 Conclusion

In conclusion, the experiments carried out in this chapter have ultimately shown that EdU administration in the evening is superior in these types of experiments as animals show greater levels of proliferation in the evening whilst awake and active. Alternatively, light/dark cycle reversal could be carried out to allow working in normal hours with animals which are in their dark phase.

Experiments described here are the first to show that like in other CNS niches, GABA has a role in controlling *in vivo* postnatal spinal cord proliferation, as confirmed by both transgenic and pharmacological methods. These newly proliferated cells are also capable of

differentiation, where most EdU^+ cells are either PanQKI-IR oligodendrocytes or undifferentiated Sox2-IR neural progenitors.

Furthermore, GAD67-GFP and VGB show that GABA levels inversely affect proliferation, illustrating a bidirectional mechanism which can be used to either increase or decrease proliferation depending upon clinical need. For example, the ability to reduce proliferation in CNS cancers would be hugely beneficial. Results described here were the result of widespread changes in GABAergic neurotransmission, by increasing GABA availability. However, further work needs to be carried out using more specific modulators to probe the effects of GABA at GABAaR upon proliferation at specific allosteric binding sites. This work will also help determine whether the spinal cord also employs endogenous GABAergic modulators such as DBI for the control of proliferation and differentiation, as is seen in the brain.

Chapter 4 – DBI and TSPO are expressed in the postnatal spinal cord

4.1 Introduction and rationale

Work presented in chapter 3 showed that changes in ambient GABA in the spinal cord resulted in changes in the numbers of proliferative cells in the WM, GM, and CC. This work suggests that much like the brain, GABA also acts as a stop signal for proliferation within the spinal cord.

GABAaRs contain many allosteric binding sites for both pharmacological and endogenous agents, leaving a wide range of possible ways to further examine the effects of GABA on spinal cord proliferation. Endogenous BZ-like molecules of the CNS, endozepines, which bind to BZ sites and modulate GABAergic neurotransmission, are known to occur in the CNS (Guidotti *et al*., 1983; Alho *et al*., 1985; Bormann, 1991) and may provide a novel avenue for these investigations. DBI is the most well documented of the endozepines and indeed has already been shown to have a role in controlling proliferation and differentiation within the neurogenic niches of the brain (Alfonso *et al*., 2012, Dumitru *et al*., 2017). However, whether DBI is also expressed in the spinal cord is not yet known. Therefore, work described here investigates the expression of DBI in the spinal cord in an attempt to elucidate whether endozepinergic modulation of GABAaR may be a possible mechanism involved in the regulation of the GABA-mediated stop signal which restricts proliferation in the postnatal spinal cord.

4.1.1 What is known about DBI and TSPO in the spinal cord?

There have been many studies investigating the cellular location and distribution of DBI within the brain (Alho *et al*., 1985), in addition to pinpointing the essential expression of DBI within the SVZ and SGZ neurogenic niches (Alfonso *et al*., 2012, Dumitru *et al*., 2017). However, less is known about the pattern of DBI expression and cellular distribution in the spinal cord or its expression in spinal cord NSCs, the ECs. It evident that DBI expressed in other cells which also have NSC properties and is important in other proliferative niches to balance the effects of GABAergic signalling upon NSC proliferation and differentiation

(Alfonso *et al*., 2012; Dumitru *et al*., 2017). DBI may therefore have similar roles in the spinal cord. The full length DBI pro-peptide is a precursor to ODN, a smaller fragment of DBI which also has high affinity for GABAaR/CBR (Slobodyansky *et al*., 1989). ODN replicates the effects of DBI at CBR (Alfonso *et al*., 2013, Dumitru *et al*., 2013). Much like DBI, expression of ODN has been confirmed in the brain (Ferrero *et al*., 1984; Ferrero *et al*., 1986b; Tonon *et al*., 1990), however less is known about whether ODN is also present within the spinal cord.

Similarly, expression of the mitochondrial DBI receptor TSPO has also been well documented in the brain and the periphery (Gavish *et al*., 1999). Other work has focused on the upregulation of TSPO in response to EAE induced demyelination (Daugherty, D. J. *et al*., 2013) and other neuroinflammatory conditions (Liu, G.J. *et al*., 2014). Many studies have investigated the upregulation of TSPO in microglia during inflammatory processes and reactive gliosis following injury (Papadopoulos and Lecanu, 2009). Much less is known however about the cell types which express TSPO in the intact adult spinal cord.

4.1.2 Aims and objectives

Before we can consider utilising systems involving TSPO and DBI in the modulation of proliferation, we need to first characterise their expression within the spinal cord, and how these compare to other neurogenic niches. This study aims to investigate which specific cell types express DBI and TSPO within the spinal cord and whether NSCs of the spinal cord CC also express DBI, ODN, and TSPO. Immunohistochemical investigations using antibodies raised against the peptides DBI and ODN and the mitochondrial receptor TSPO were therefore carried out in the adult spinal cord.

This chapter will focus on the expression of DBI and TSPO within the CC, lamina X, and in select populations of neurones, astrocytes, and oligodendrocytes in both the WM and GM.

4.2 Methods

4.2.1 Animals

Wild-type adult C57BL/6 mice, GAD67-GFP, and nestin-GFP mice (4-6 weeks *N*=9, N=6 and *N*=9, respectively) of either sex were used in line with the UK Animals (Scientific Procedures) Act 1986 and ethical standards set out by the University of Leeds Ethical Review Committee. Further detail regarding the use of GAD67-GFP and nestin-GFP transgenic mice is represent in section 2.11 and 2.22. Briefly, GAD67-GFP animals were used in these studies to visualise GABAergic CSFcCs present at the CC. Nestin-GFP animals were used to label to EC layer of the CC.

4.2.2 Fluorogold-mediated tracing from the periphery to label motor neurones, sympathetic preganglionic neurones, and pericytes in the spinal cord

To fluorescently label motor neurones (MNs), sympathetic preganglionic neurones (SPNs), and pericytes by retrograde tracing from the periphery, (Edwards *et al*., 2013), C57BL/6 mice (4-6 weeks *N*=3) and GAD67-GFP mice (4-6 weeks *N*=3) received a single intraperitoneal (I.P) injection of FluoroGold (FG) (0.05 ml 1% in sterile saline, 25 mg/kg, hydroxystilbamadine, Abcam, UK). 72 hours post FG I.P injection animals were terminally anaesthetised, perfused with 4% paraformaldehyde, and 40 µm sections of spinal cord were generated for tissue analysis, as discussed in section 2.2.4.

4.2.3 Surgery to perform WM minimal stab injury to examine resultant changes in DBI- and TSPO-IR

Injury to the WM dorsal columns was carried out by stab injury in order to investigate whether the patterns of expression of DBI and/or TSPO are altered in such conditions. Surgery to perform such stab injuries was carried out via a modified version of the surgical methods used for the injection of LPC/saline for focal demyelination (section 2.3).

Briefly, the glass pipette was inserted at the midline to a depth of 300μm to reach the dorsal column without disturbing the ependyma, left in place for 2 minutes to allow the tissue to reseal around the pipette, and then withdrawn. Animals were sutured and allowed to recover for 3 days before being sacrificed and undergoing tissue analysis at the height of the injury response.

4.2.4 Immunohistochemistry

Tissue from wild-type C57Bl/6, GAD67-GFP, and nestin-GFP mice for IHC analysis was prepared as previously described (sections 2.2.4 and 2.2.7). Tissue from the thoracolumbar region was processed for DBI-IR (1:2000 Frontier Institute) and TSPO-IR (1:100, Abcam). Double labelling IHC was carried out to look for colocalisation of DBI and TSPO with various other specific cellular markers including; CD31 (1:500, BD Pharmingen) for endothelial cells, anti-ODN (1:250, gift of Dr. M.C Tonon, University of Rouen, France), cluster of differentiation 24 (CD24) (1:500 BD Pharmingen) for membranes of CSF-cCs and ECs, S100β for ECs, (1:750, Abcam), Sox2 (polyclonal,1:1000, monoclonal, 1:100, Santa Cruz) and for neural stem/progenitor cells, Nestin (1:1000 BD Pharmingen) for radial glia, glial fibrillary acid protein (GFAP) (1:100, Neuromab) for astrocytes, PanQKI (1:100 Neuromab) for oligodendrocytes, NeuN (1:1000, Millipore) for nuclei of mature neurones, and HuC/D (1:1000, Proteintech) for immature and mature neurones. More information on primary antibodies, secondary antibodies, and methods used are detailed in tables 2.3 and 2.4 and section 2.2.7.

4.2.5 Image capture and manipulation

Sections were viewed using a Zeiss LSM880 laser scanning confocal microscope, acquired using Zen software, and manipulated in CorelDRAW 2017 (section 2.2.10).

For FG labelled sections, images were also captured using the Nikon E600 microscope set up for epifluorescence at custom settings and Acquis image capture software (Synoptics,

Cambridge UK) (section 2.2.10). Images were adjusted and channels merged to create dual labelled images using Corel Photo Paint (Corel, Canada).

4.2.6 Cell counting and statistical analysis of FG/TSPO$^+$ cells

Using a Nikon E600 microscope, TSPO$^+$, FG$^+$, and GAD$^+$ labelled cells were counted in sections from cervical, thoracic, and lumbar regions of the adult spinal cord to determine the distribution and percentage colocalisation of TSPO within MNs and SPNs (*N*=3 *n*=18, where *N* refers to the number of animals and *n* refers to the total number of sections in which cells were counted).

Data were plotted and analysed using GraphPad Prism 6 software (GraphPad Software, California, USA). The data were expressed as mean ± SEM. For multiple comparisons, and evaluation of statistical differences between groups, one-way ANOVA was used followed by Tukeys post hoc testing for multiple comparisons. A p value of <0.05 was considered statistically significant.

4.3 Results

4.3.1 DBI and TSPO are expressed within the adult spinal cord CC

DBI and TSPO are both expressed within the postnatal murine spinal cord (figure 4.1). Intense DBI immunoreactivity (DBI-IR) appears to be preferentially located at the CC (figure 4.1A), with less intense staining appearing in both the WM and GM (figure 4.1Ai). TSPO exhibits a similar pattern of expression in the spinal cord to that of its ligand DBI, and is present in both WM and GM, with intense immunoreactivity at the CC (figure 4.1B and Bii).

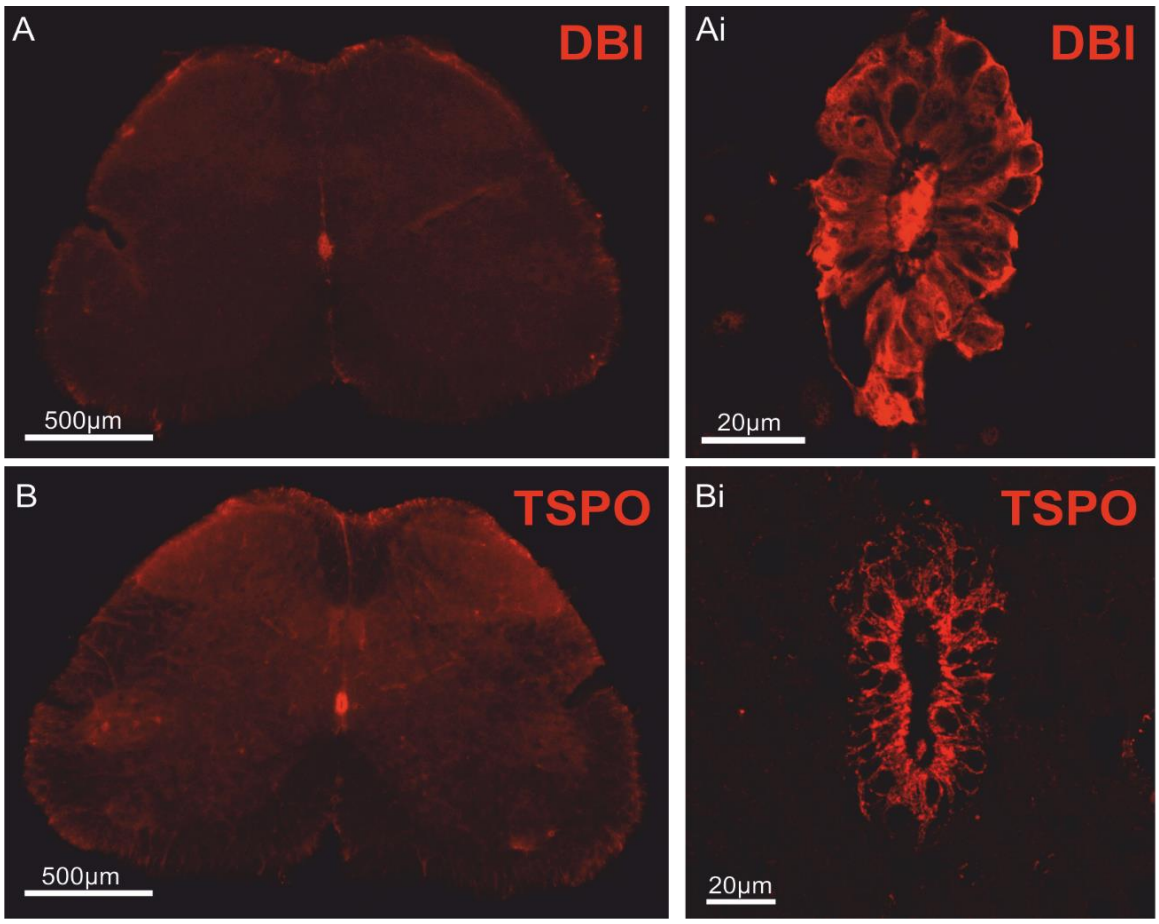

Figure 4.1 DBI and TSPO are expressed within the postnatal spinal cord CC

A: Representative image showing DBI expression in the postnatal spinal cord **Ai**: Representative confocal image of DBI expression at the CC **B**: Representative confocal image of TSPO expression in the adult spinal cord **Bi**: Representative confocal image of TSPO expression at the CC. Images in B-Bi are not taken from the same sections as A-Ai.

Whilst TSPO and DBI exhibit overall similar patterns of expression in the spinal cord, with strong labelling at the CC, DBI and TSPO are preferentially present in different cellular locations. DBI is expressed in both the cytoplasm and membranes of cells lining the CC (figure 4.1Ai). TSPO however appears to be more distinct at cell membranes, with a lack of staining in the cytoplasm (figure 4.1Bi). The distinct patterns of staining of DBI and TSPO are exemplified by double labelling IHC, as seen in figure 4.2A-Bii. TSPO and DBI are present in complementary locations to one another in the CC (figure 4.2Aii and Bii). When examining labelling at the CC in both transverse and sagittal planes (figure 4.2B-Bii), it becomes clear that TSPO is present within the membranes of the DBI^+ cells which surround the CC.

Immunohistochemical labelling using anti-sera raised in rabbit against rat ODN illustrated that much like DBI and TSPO ODN is also present cells lining the CC (figure 4.2C-Cii). ODN exhibits a similar cytoplasmic pattern of staining to that of DBI (figure 4.2A and C). TSPO is present in the membranes of these ODN^+ cells (figure 4.2C-Cii). A double labelling protocol using ODN and DBI was not possible due to species reactivity of ODN and DBI antibodies used in these experiments.

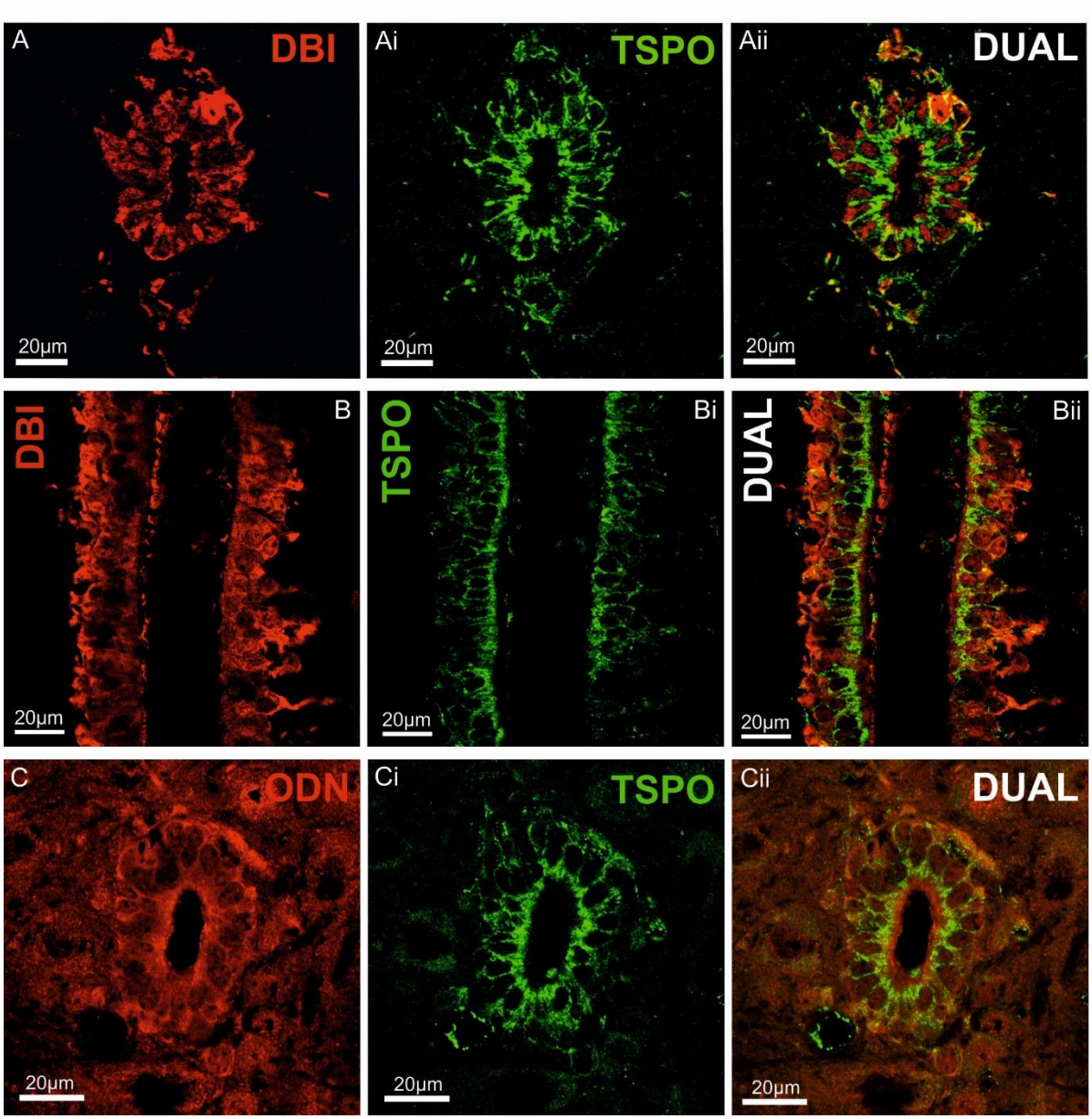

Figure 4.2 TSPO labelling is present at the CC alongside DBI$^+$ and ODN$^+$ areas

A-Ai: Representative confocal images showing staining for DBI (A), the mitochondrial DBI receptor TSPO (Ai), and dual labelling for both (Ai) at the CC **B-Bii**: Confocal images of DBI (B) and TSPO (Bi) labelled cells in sagittal spinal cord sections **C-Cii**: Confocal images showing staining for the DBI-fragment ODN (C), TSPO (Ci), and dual labelling for both (Cii)

4.3.2 DBI and TSPO colocalise in the WM

Labelling for DBI and TSPO were also found to be colocalised in the WM (figure 4.3A-Aii). Colocalisation of DBI- and TSPO-IR was observed in fibres (figure 4.3Aii, closed arrows), with absence of TSPO in DBI^{+} cell bodies (figure 4.3Aii, open arrows).

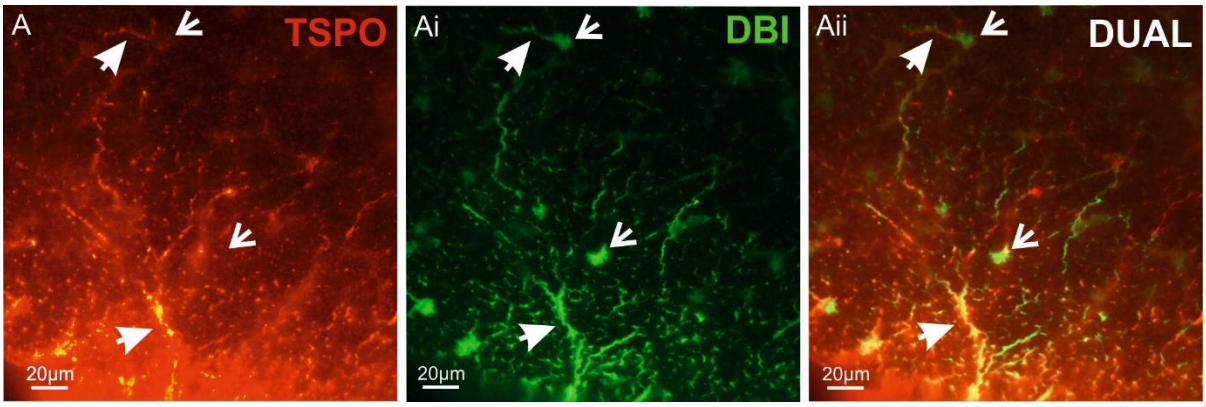

Figure 4.3 DBI and TSPO colocalise in cell projections within the WM

A-Aii: Representative confocal images illustrating labelling of TSPO (A), DBI (Ai), and dual labelling for both (A-Aii) in the spinal cord WM

4.3.3 TSPO is expressed in spinal cord vasculature where DBI is not

Whilst DBI and TSPO are expressed in complementary regions of ECs (figure 4.2A-Cii), which echoes their functional relationship as ligand and receptor, there are some cell types within the cord which do not express both TSPO and DBI. For example, unlike DBI, TSPO is strongly expressed within blood vessels, appearing in both larger and smaller diameter vessels (figure 4.4A-Ai). Colabelling for the endothelial cell marker CD31 (figure 4.4B-Bii), and absence of TSPO in FG labelled pericytes (data not shown), indicate that TSPO is expressed in vascular endothelial cells rather than perivascular cells within the spinal cord vasculature (figure 4.4C-Cii).

TSPO$^+$ blood vessels can also be seen adjacent to the CC in lamina X (figure 4Ci). Whilst DBI may not be putatively expressed alongside TSPO in vascular endothelial cells, DBI$^+$ cells at the CC do appear to make contact with these cells (figure 4.4Cii). Figure 4.4 illustrates that some DBI$^+$ cells at the CC send out lateral projections which are in close apposition with the TSPO$^+$ vasculature present in lamina X (figure 4.4C-Cii).

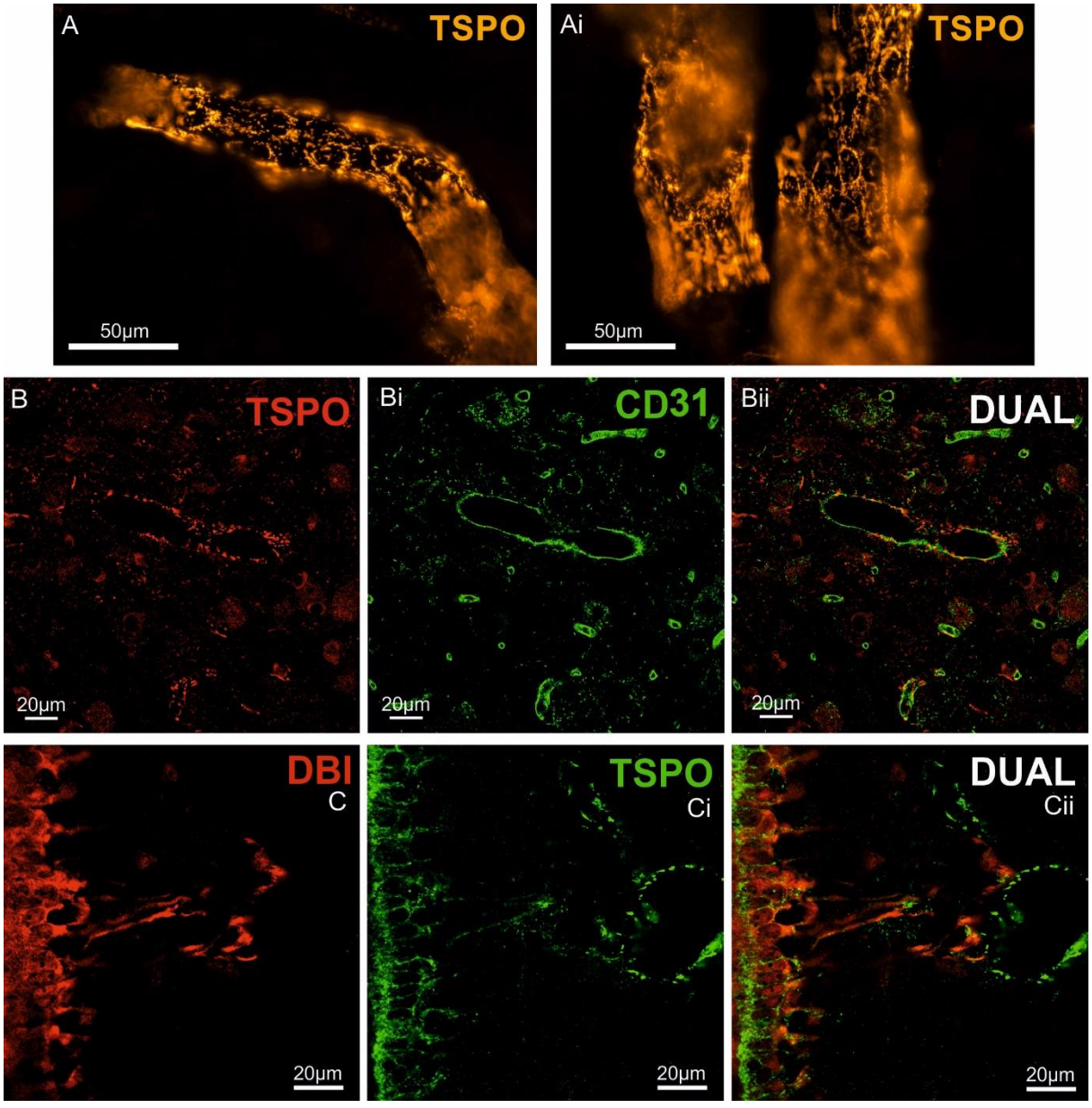

Figure 4.4 Epithelial cells of spinal cord vasculature are TSPO$^+$ and DBI$^+$ EC processes are in close apposition to TSPO$^+$ blood vessels

A-Ai: Confocal images of TSPO$^+$ labelling of large blood vessels in the spinal cord **B-Bi**: Representative confocal images of TSPO$^+$ cells surrounding vascular spaces (B), CD31$^+$ endothelial cells (B), and colocalisation of TSPO and CD31 (Bii) **C-Cii**: Representative confocal images of DBI$^+$ EC projections (C), TSPO $^+$ ECs and vessels (Ci), and colocalisation of these markers (Cii)

4.3.4 Intense DBI-IR and TSPO-IR are present within ECs

Whilst the CC generally appears to be strongly labelled for both TSPO and DBI, there are some regions within the CC where staining for both TSPO and DBI are absent. Therefore, coloabelling with markers which detect specific cell types present in the CC lining was perfomed to determine the specific populations which express DBI and/or TSPO.

Antibodies against the cell adhesion molecule CD24, to label ECs and CSFcCs, and the EC specific marker, S100β were used alongside double labelling for either DBI or TSPO. Results illustrated that both DBI and TSPO are preferentially expressed in ECs (figure 4.5, arrows). Areas which are CD24$^+$ but are TSPO- and DBI- are likely to represent CSFcC cell bodies which are present in the EC layer.

Findings from experiments using GAD67-GFP to selectively label GABAergic CSFcCs alongside DBI confirm that DBI is not expressed in GFP$^+$ CSFcC cell bodies present in the EC layer (figure 4.6A-Aii). CSFcCs are characterised by long apically projecting dendritic processes which terminate in an end bulb within the CC lumen (Hugnot and Franzen, 2011). DBI was also absent from these CSFcC bulbs within the CC lumen (figure 4.6A-Aii). Sagittal sections of the CC improved visualisation of the CC lumen, and therefore CSFcC end bulbs,

and confirmed that DBI was not expressed in either CSFcC cell bodies or end bulbs. (Figure 4.6B-Bii).

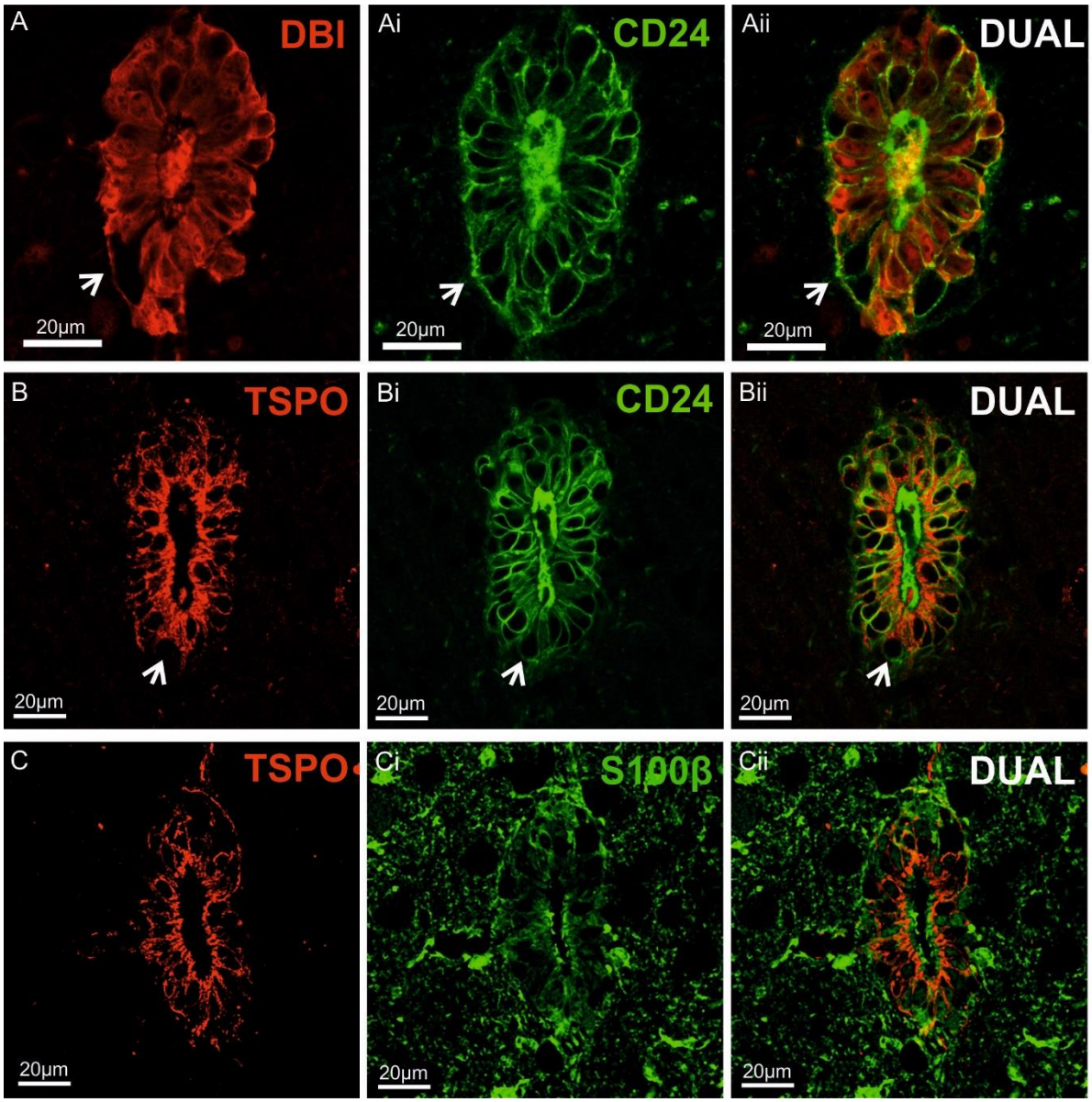

Figure 4.5 DBI and TSPO are expressed in ECs

A-Ai: Representative confocal images of DBI (A), CD24 (Ai), and dual labelling for both (C) at the spinal cord CC **B-Bi**: Representative confocal images of TSPO (B), CD24 (Bi), and dual labelling for both (Bii) within the CC **C-Cii**: Representative confocal images of labelling for TSPO (C), S100β (Ci), and dual labelling for both (C) at the spinal cord CC region. Open arrows denote non-colocalised cells which are $CD24^{+}$ but DBI-

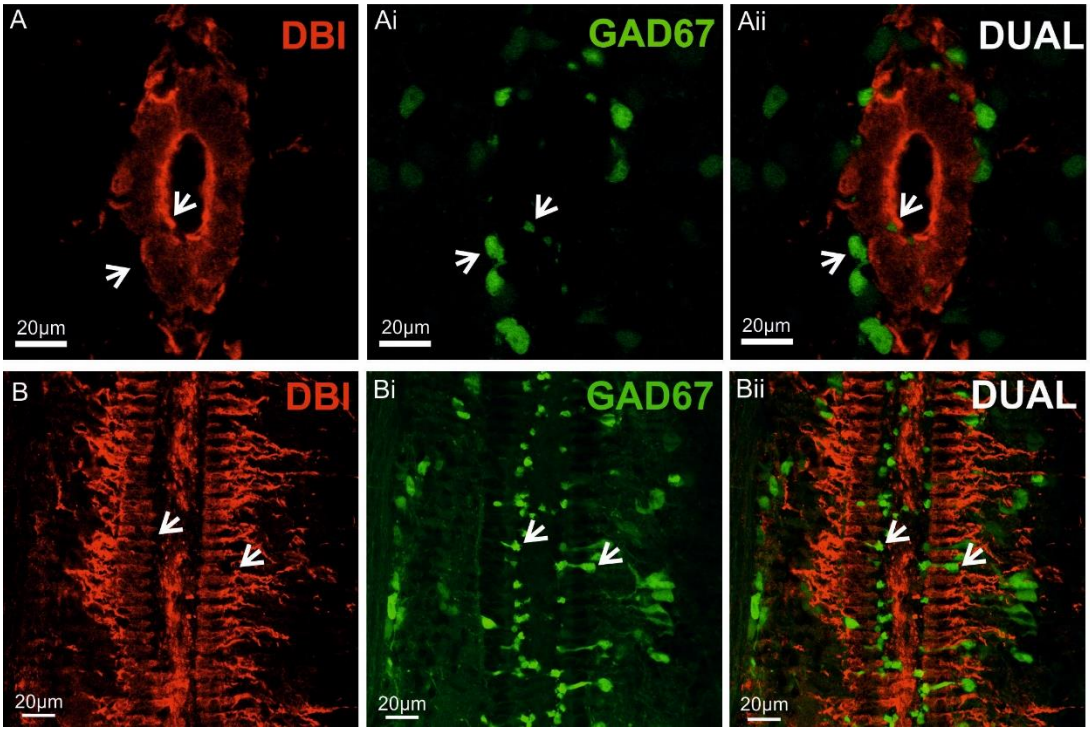

Figure 4.6 DBI is not expressed in CSFcCs

Representative confocal images showing DBI$^+$ (**A** and **B**), GFP$^+$ (**Ai** and **Bi**) and dual labelling for DBI and GFP (**Aii** and **Bii**) at the CC in both transverse (A-Aii) and sagittal (B-Bii) tissue sections from the spinal cord. Open arrows denote non-colocalised cells

Similarly to DBI, TSPO-IR is also absent from CSFcC cell bodies, confirmed by double labelling in GAD67-GFP mice (figure 4.7A-Aii, open arrows). However, unlike DBI, it appears that TSPO is expressed within CSFcC terminal projections as TSPO-IR colocalises with GFP in CSFcC end bulbs within the CC lumen (Figure 4.7A-Aii, closed arrows). These results were confirmed using double labelling for TSPO in sagittal sections of the CC from GAD67-GFP animals (figure 4.7B-Bii).

Together these results illustrate that DBI-IR is confined to the ECs of the CC region and is absent from CSFcCs. Unlike DBI however, TSPO is expressed in CSFcC end bulbs.

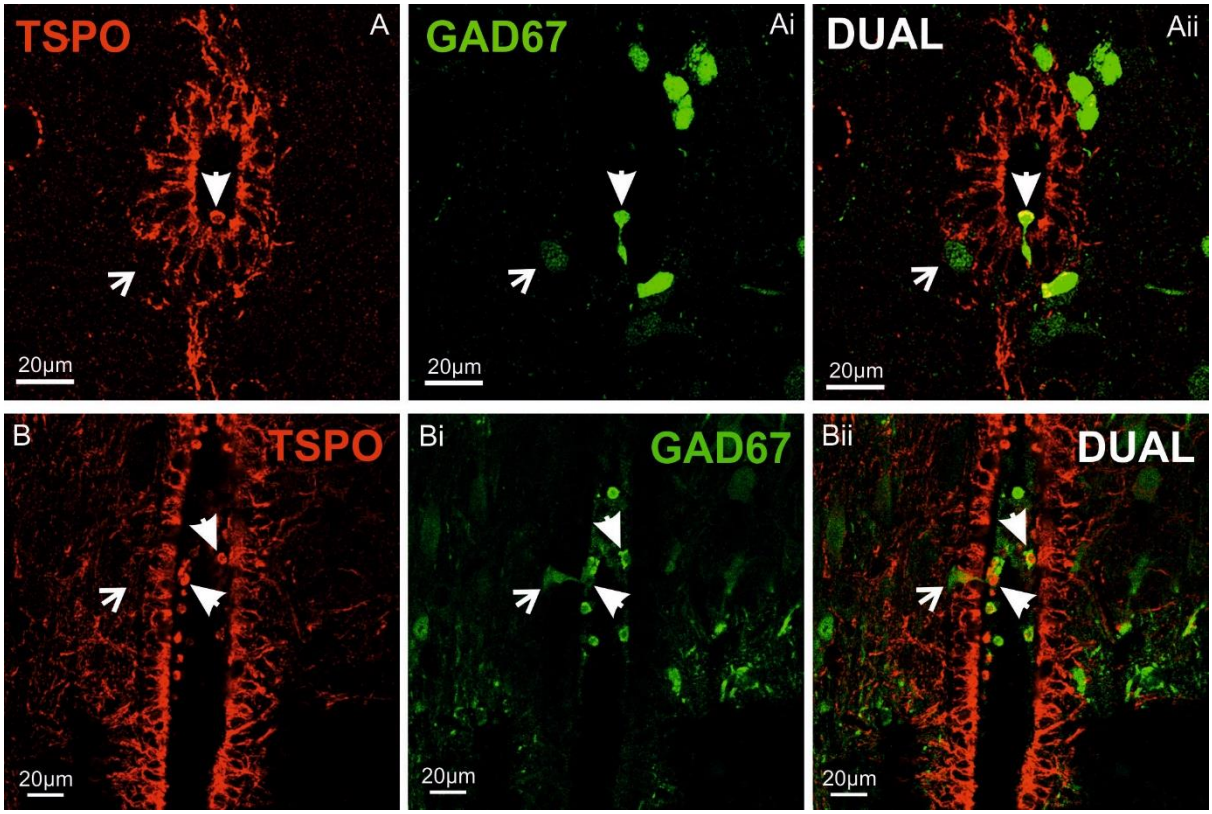

Figure 4.7 TSPO is expressed in CSFcC end bulbs

Representative confocal images showing TSPO$^+$ (**A** and **B**), GFP$^+$ (**Ai** and **Bi**) and dual labelling for TSPO and GFP (**Aii** and **Bii**) at the CC in both transverse (A-Aii) and sagittal (B-Bii) tissue sections from the spinal cord. Open arrows denote non-colocalised cells and closed arrows denote areas of colocalisation

4.3.5 DBI and TSPO$^+$ cells at the CC express the NSPC marker Sox2

Sox2 labelling of ECs provides further evidence for the presence of DBI and TSPO within the EC fraction of the CC region, as the Sox2$^+$ nuclei of ECs are located in the cytoplasm of DBI$^+$ cells (figure 4.8A-Aii). These findings are further strengthened by the colocalisation of the smaller fragment of DBI, ODN, with Sox2$^+$ ECs (figure 4.8B-Bii). Furthermore, whilst some CSFcCs are also labelled by Sox2, these are easily distinguished from ECs due to both the absence of DBI and ODN, and their less intense IHC labelling (figure 4.8A-Bii, open arrows).

TSPO also labels membranes of EC which possess Sox2^{+} nuclei (Figure 4.8C-Cii). These results illustrate that TSPO is also expressed in NSCs of the spinal cord, the ECs.

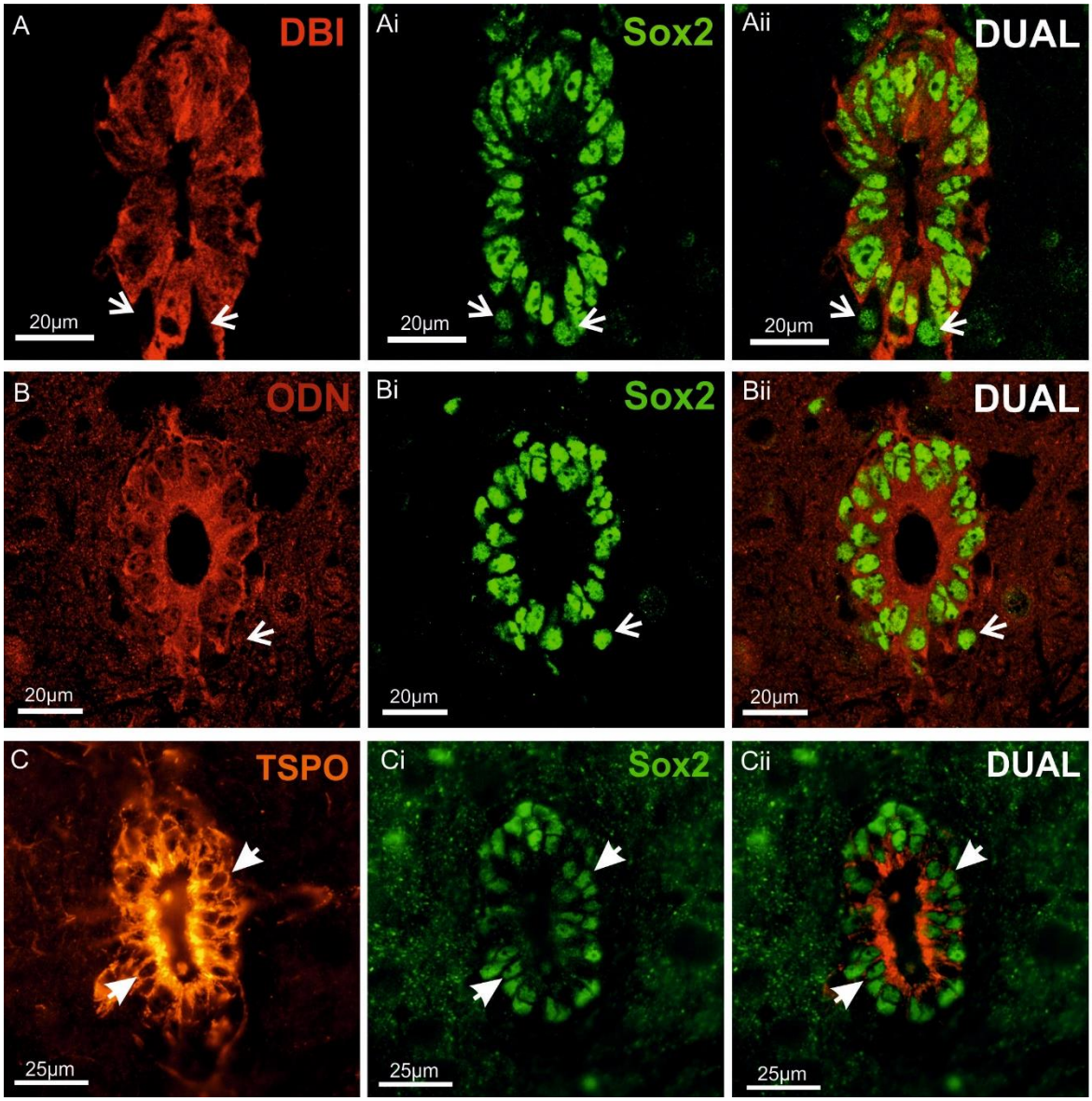

Figure 4.8 Sox2^{+} cells are present in areas of the CC which are also labelled by DBI, ODN, and TSPO

A-Ai: Representative confocal images of DBI (A) and Sox2 (Ai) and dual labelling for both markers at the CC (Pandamooz *et al*.) **B-Bii**: representative confocal images of ODN (B), Sox2 (B), and dual labelling (Bii) at the CC **C-Cii**: Representative confocal images of TSPO (C), Sox2 (Ci), and dual labelling for both at the CC (Cii) (Closed arrows non colocalised cells. Open arrows: colocalised cells)

4.3.6 DBI and TSPO labelling is present in GFP$^+$ ECs in nestin-GFP mice

Nestin-GFP mice were used to selectively label the nestin$^+$ EC population present at the CC. Examining both transverse and sagittal sections for double labelling for DBI and GFP in nestin-GFP mice shows that DBI is expressed in the GFP$^+$ EC population (figure 4.9A-Aii).

DBI is also expressed in GFP$^+$ fibres projecting from the dorsal pole of the CC (figure 4.9A-Aii). Furthermore, DBI also appears to be expressed in a subset of nuclei of small nestin-GFP$^+$ cells in lamina X (figure 4.9A-Aii, closed arrows and 8Aii, inset). However not all of these GFP$^+$ cells express DBI (figure 4.9Aii, open arrows).

The pattern of TSPO-IR in nestin-GFP ECs is similar to that of DBI (figure 4.9C-Dii), however TSPO does not label dorsal projections from the CC (figure 4.9C-Cii).

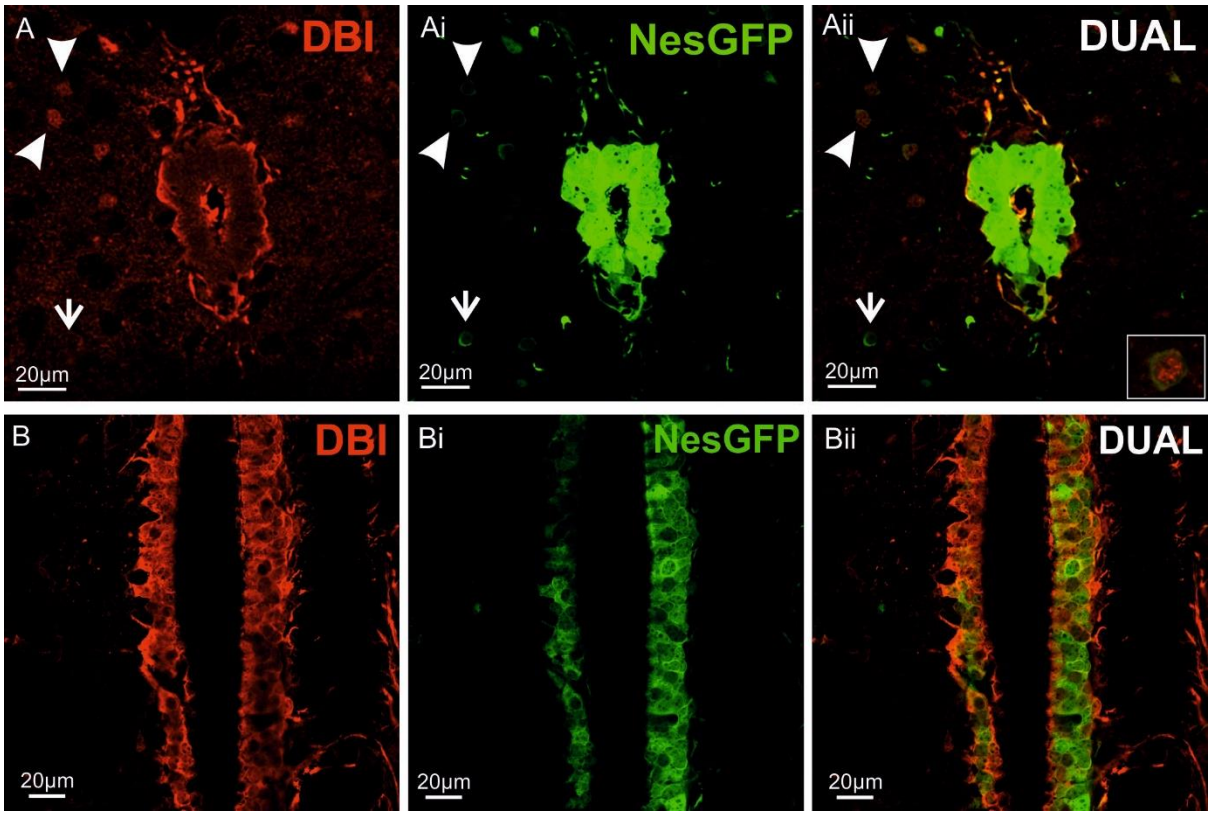

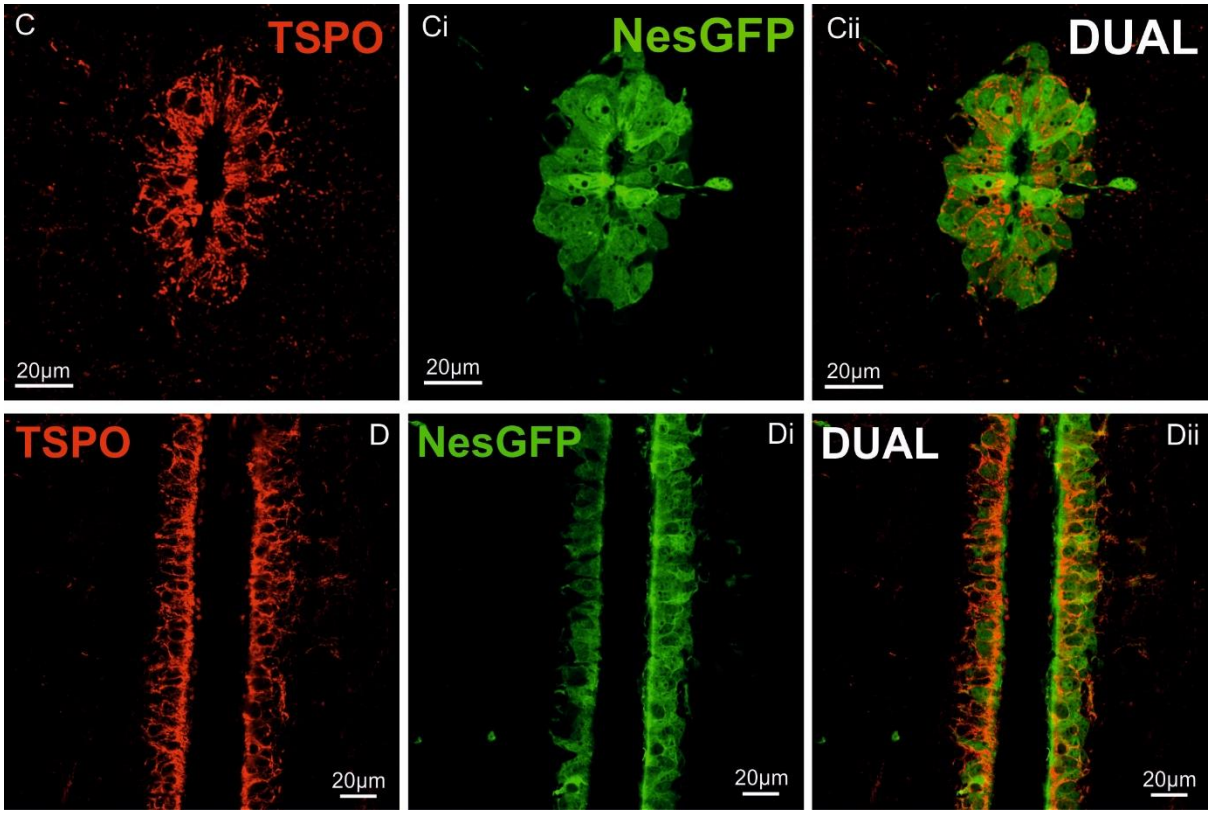

Figure 4.9 DBI and TSPO are expressed in GFP$^+$ ECs of nestin-GFP mice

A-Bii: Representative confocal images of DBI (A and B), GFP (Ai and Bi), and dual labelling for both (Aii and Bii) at the CC of nestin-GFP mice in transverse (A-Aii) and sagittal (B-Bii) sections **C-Cii**: Representative confocal images of TSPO (C and D), GFP (Ci and Di), and dual labelling for both (Cii and Dii) at the CC of nestin-GFP mice in transverse (C-Cii) and sagittal (D-Dii) sections (open arrows: colocalised cells, closed arrows: non-colocalised cells)

4.3.7 DBI and TSPO are expressed within astrocytes of the spinal cord WM but not oligodendrocytes

Whilst nestin-GFP mice label ECs, using a nestin antibody to label glial cells yields a different pattern of staining at the CC to that seen in nestin-GFP mice (figure 4.10A-Aii). Double labelling using an antibody directed against nestin confirms that DBI is expressed at the dorsal and ventral poles of the CC (figure 4.10A-Bii). DBI$^+$ fibres extend dorsally from the CC towards the posterior median sulcus and exhibit punctate nestin staining along their entire length (figure 4.10A-Bii). DBI is also expressed in glia within the WM (figure 4.10C-Cii). However, whilst DBI exhibits punctate staining in nestin$^+$ radial glial fibres at the CC, in

the WM DBI is expressed in both the cell body and fibres of nestin^{+} astrocytes (figure 4.10Cii, closed arrows).

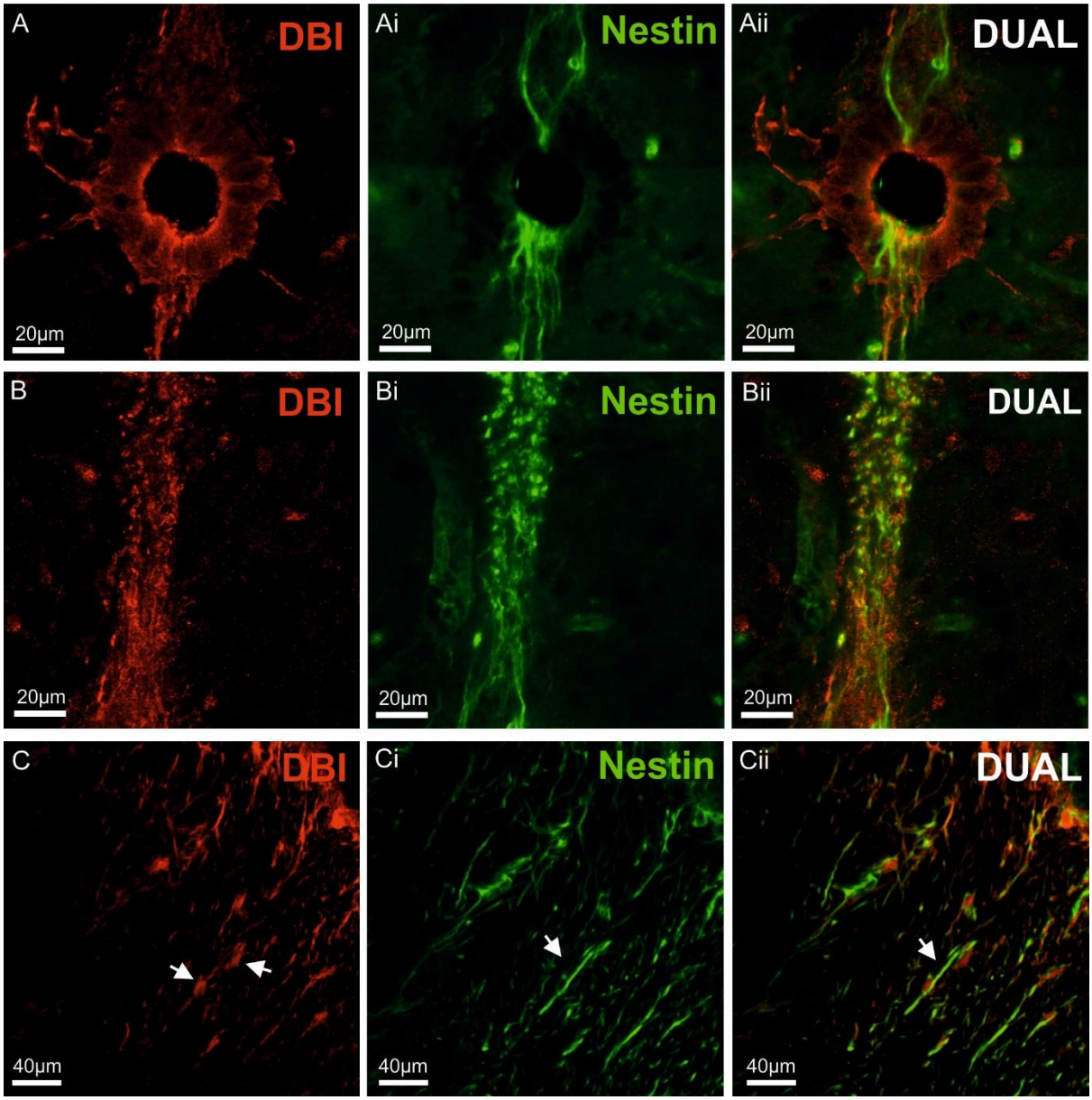

Figure 4.10 Nestin^{+} radial glia are DBI^{+} at the CC and WM

A-Aii: Representative confocal images of DBI (A), nestin (Ai) and dual labelling for both (Pandamooz *et al*.) at the CC of the spinal cord **B-Bii**: Representative confocal images of labelling for DBI and nestin within the fibres which extend from the dorsal pole of the CC **C-Cii**: Representative confocal images of DBI and nestin colabelling within the WM of the spinal cord (closed arrows: colocalised cells)

GFAP$^+$ astrocytic fibres are located within lamina X, and are in close apposition to the DBI and TSPO$^+$ EC layer of the CC region (figure 4.11A-Bii). GFAP$^+$ fibres often make contact with ECs and pass through the EC layer to contact the CC lumen (figure 4.11Aii), however GFAP is not expressed within DBI and TSPO$^+$ ECs (figure 4.11A-Bii). There are however, DBI/GFAP$^+$ astrocyte cell bodies present in close proximity to the CC, and GFAP$^+$ fibres from these cells often contact the EC layer (figure 4.11A-Aii, arrows).

In the WM DBI is also present within the cell bodies of GFAP$^+$ astrocytes (figure 4.11C-Ci). In contrast, TSPO colocalises with GFAP$^+$ fibres in the WM with minimal staining found in the soma of astrocytes (Figure 4.11D-Dii).

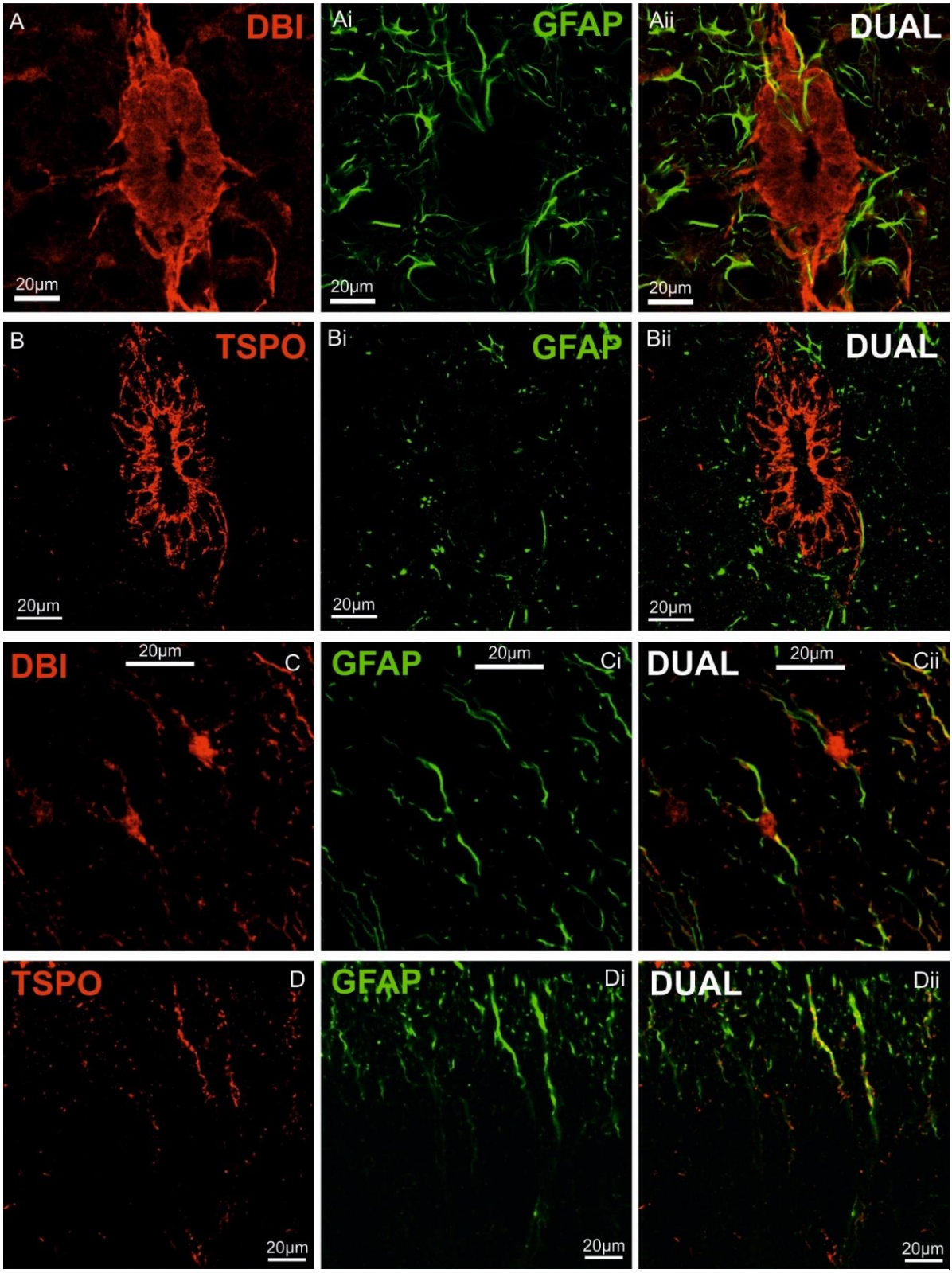

Figure 4.11 DBI and TSPO are expressed within GFAP$^+$ astrocytes of the spinal cord

A-Bii: Representative confocal images of labelling for DBI and GFAP (A-Aii) and TSPO and GFAP (B-Bii) at the CC region **C-Dii**: Representative confocal images of labelling for DBI and GFAP (C-Cii) and TSPO and GFAP (D-Dii) in the spinal cord WM

In addition to radial glia and astrocytes, oligodendrocytes are another cell type which contribute to the vast population of neuroglial cells within the spinal cord. Double labelling IHC for DBI, or TSPO, and the oligodendrocyte marker PanQKI, illustrates that in the WM there are some DBI and TSPO^{+} cells which also express PanQKI (figure 4.12A-Bii). In the dorsal columns there are also TSPO^{+} cells which colocalise with the oligodendrocyte transcription factor olig2 (figure 4.12C-Cii). DBI and TSPO were not found in PanQKI^{+} oligodendroctyes in lamina X (data not shown).

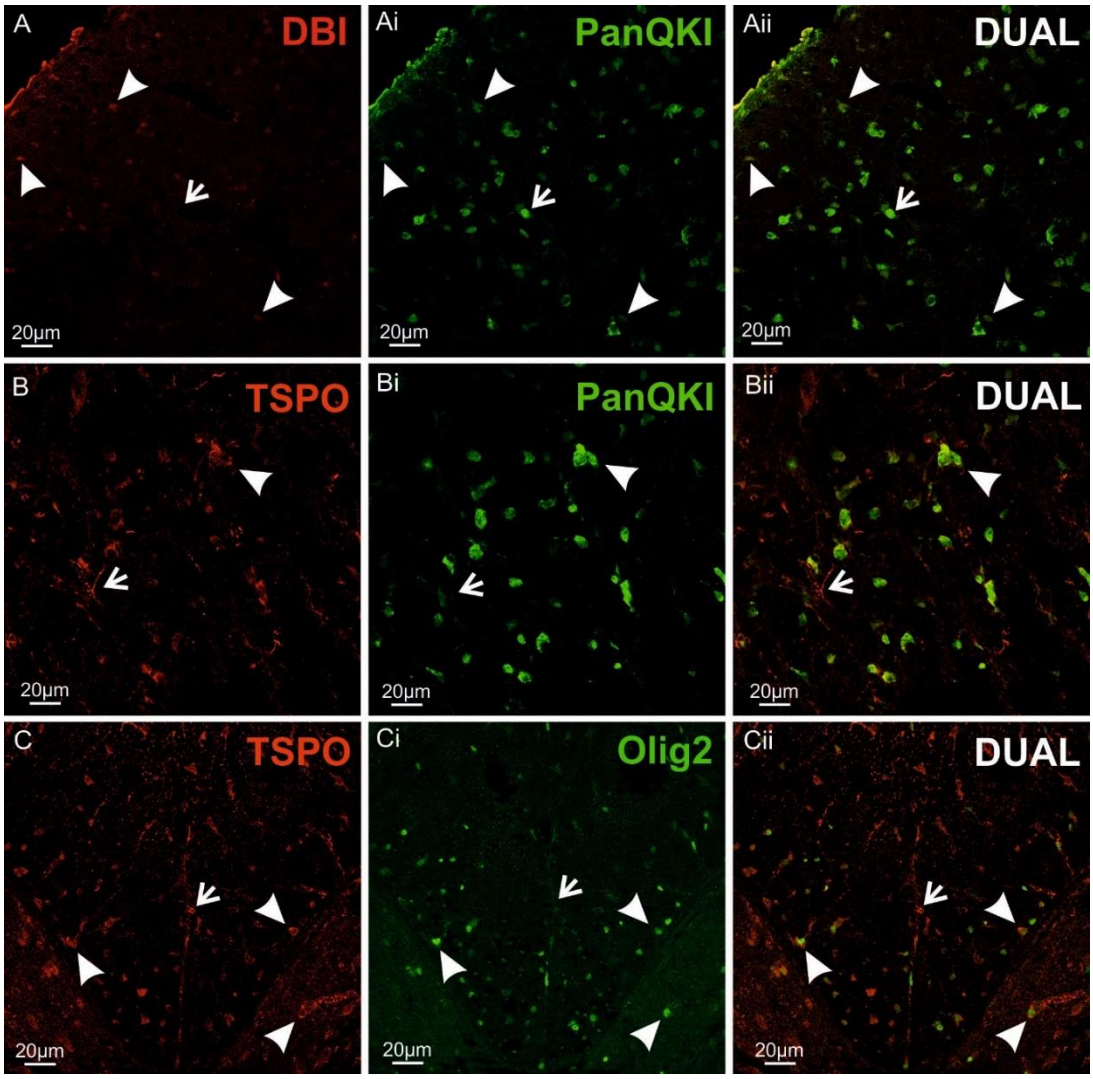

Figure 4.12 DBI and TSPO are expressed in a subset of PanQKI^{+} and Olig2^{+} oligodendrocytes

A-Bii: Representative confocal images of labelling for DBI and PanQKI (A-Aii) and TSPO and PanQKI (B-Bii) in the spinal cord WM **C-Cii**: Representative confocal images of TSPO and Olig2 labelling with the dorsal column WM (closed arrows: colocalised cells open arrows: non-colocalised cells)

Staining with the microglial marker Iba1 showed that TSPO is also expressed in microglia of the adult spinal cord (figure 4.13A-Aii).

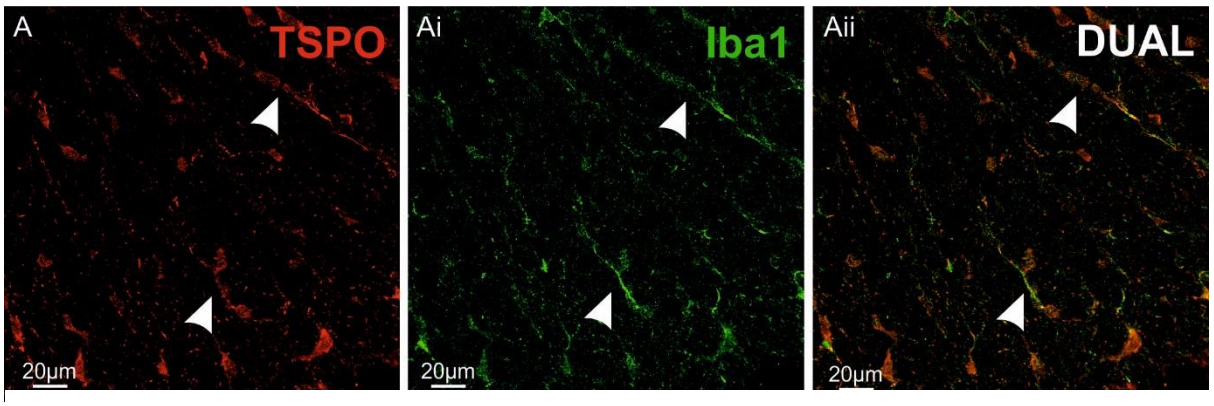

Figure 4.13 TSPO is expressed in Iba1$^+$ microglia

A-Aii: Representative confocal images of TSPO (A), Iba1 (Ai), and dual labelling for both (Aii) in the WM of the intact adult spinal cord

4.3.8 DBI is not expressed in mature neurones however TSPO is present in some MNs and SPNs

Double labelling IHC for the mature neuronal nuclei marker NeuN alongside DBI showed that DBI was not present in NeuN$^+$ neuronal populations of the spinal cord (Figure 4.14A-Aii). Furthermore, TSPO was also absent from NeuN$^+$ mature neurones which are present in lamina X (Figure 4.1412B-Bii). NeuN$^+$ neurones however appeared appear to make close contact with the TSPO and DBI$^+$ ECs (Figure 4.14Aii and Bii).

NeuN labels mature neurones, however HuC/D is present in both immature and mature neurones and therefore labels a greater neuronal population. TSPO expression was also absent in HuC/D labelled cells surrounding the CC (figure 4.1412C-Cii), indicating that TSPO is not present in the neuronal populations present in lamina X.

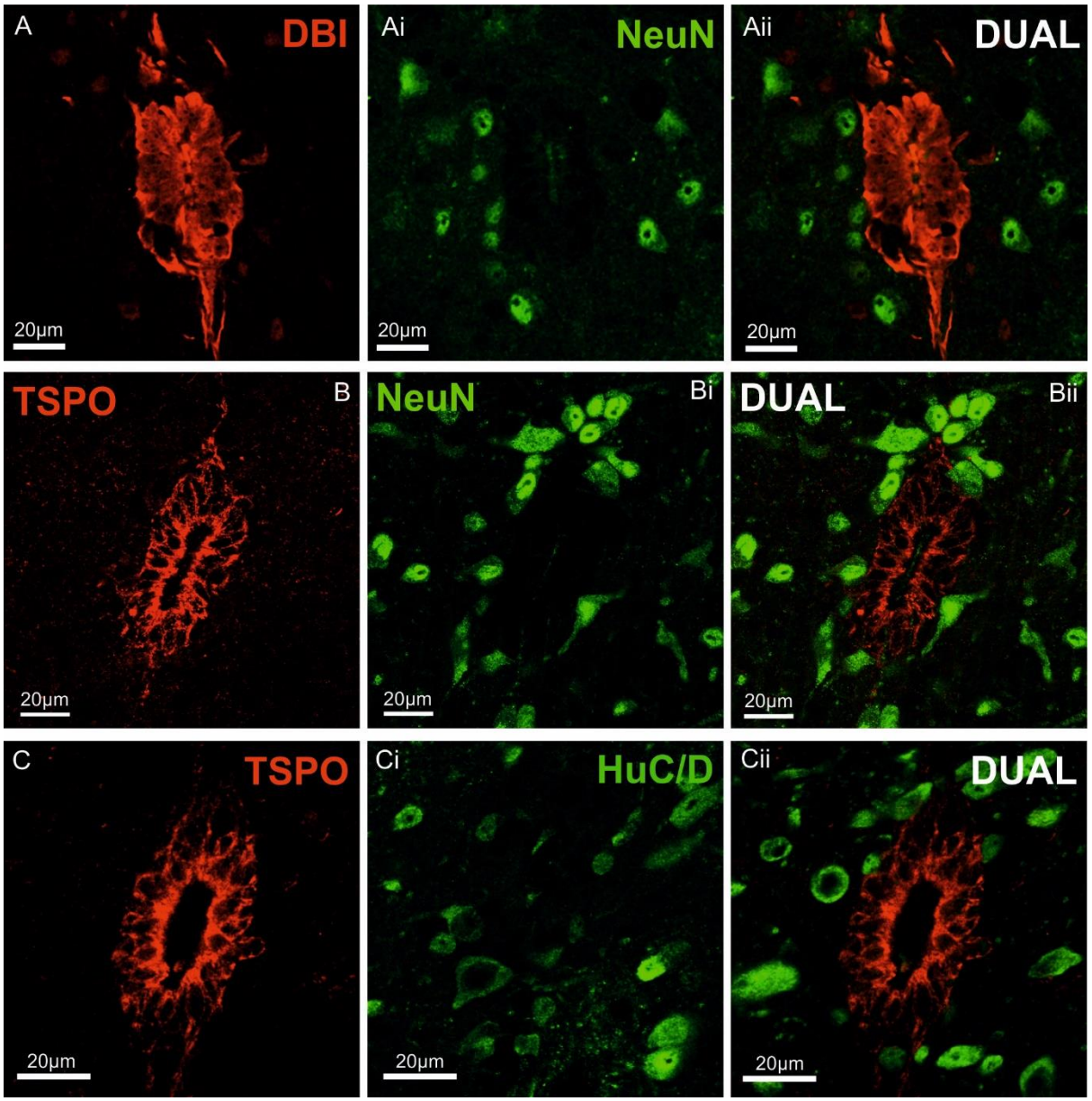

Figure 4 14 Mature and immature neurones surrounding the CC do not express DBI or TSPO

A-Bii: Representative confocal images of labelling for DBI and NeuN (A-Aii) and TSPO and NeuN (B-Bii) in the spinal cord WM **C-Cii**: Representative confocal images of TSPO and HucD labelling with the dorsal column WM

Interestingly, unlike the smaller NeuN$^+$ or HuC/D$^+$ neurones near the CC, a subset of large MNs, and their projections, within the ventral horns were determined to be TSPO$^+$ (figure 4.15). These TSPO$^+$ cells were mature NeuN$^+$ neurones (figure 4.15A-Aii, closed arrows) which were also colabelled by the retrograde neuronal tracer fluorogold (figure 4.15B-Bii, closed arrows), following peripheral IP injection. TSPO is not expressed by the entire ventral MN population, and instead appears to be localised to a subset of larger alpha MNs (figure 4.15, open arrows).

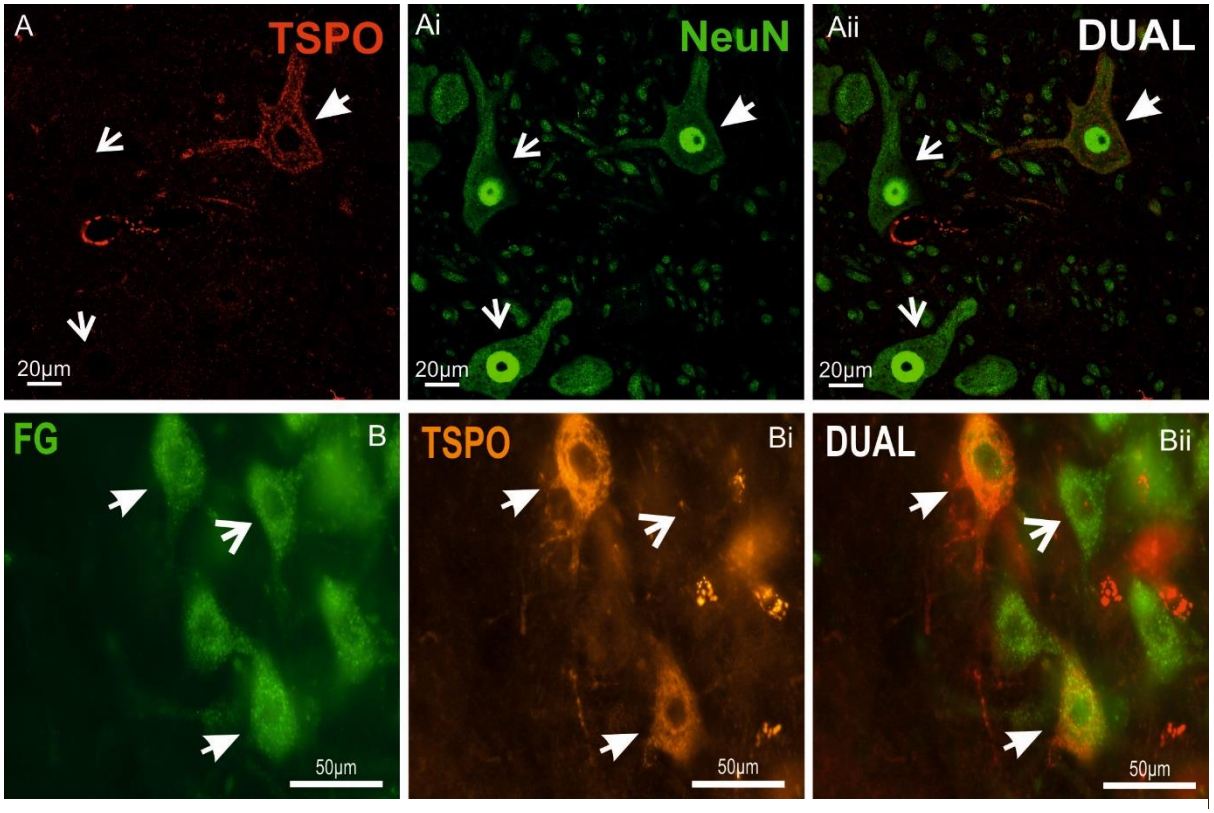

Figure 4.15 TSPO is expressed in a subset of ventral motor neurones

A-Aii: Representative confocal images of TSPO (A), NeuN (Ai), and dual labelling for both markers in the ventral horn of the spinal cord (Pandamooz *et al*.) B-Bii: Representative images of colocalisation of FG and TSPO in the ventral horn of the spinal cord (open arrows: non-colocalised cells closed arrows: colocalised cells)

TSPO-IR was also often found within a subpopulation of cells present adjacent to the CC in IMM, and laterally in IML. These TSPO^{+} cells were identified as SPNs based upon double labelling with FG, their morphology, and location within the thoracolumbar region of the spinal cord (Figure 14A-Bii).

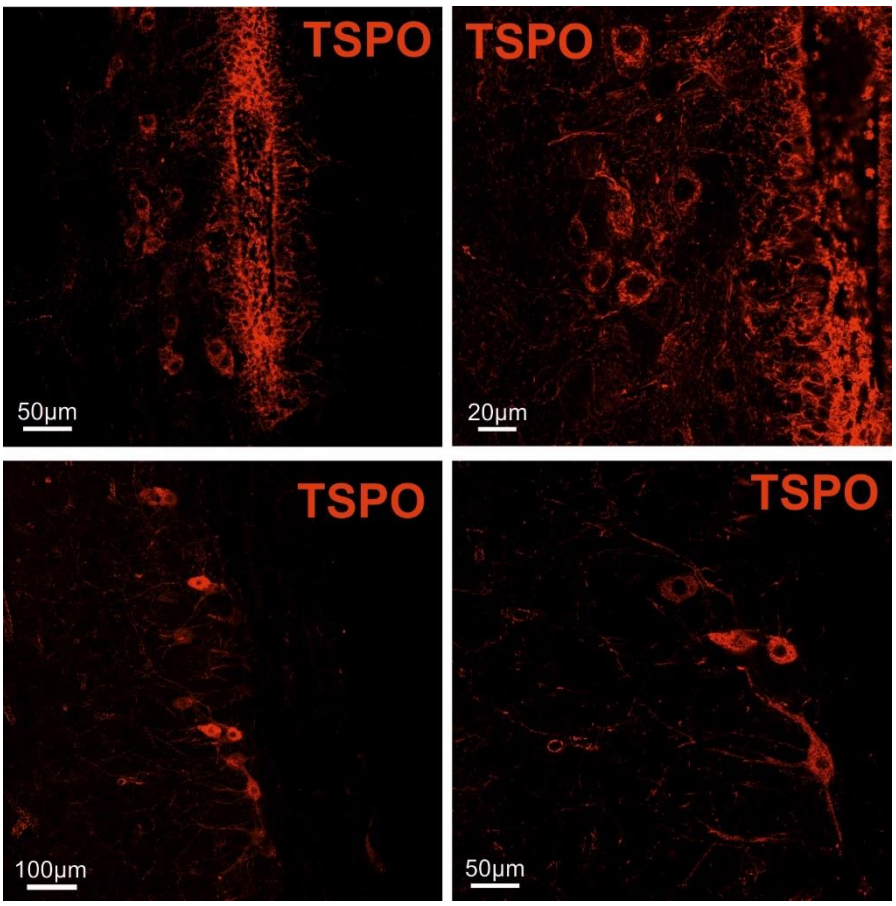

Figure 4.16 TSPO labels subsets of neurones within the IMM and IML

A-Ai: Confocal images showing TSPO labelling in the IMM, Ai is a higher magnification image of A **B-Bi**: Representative confocal images of TSPO labelling within the IML of sections taken from the thoracic segment of the spinal cord. Bi is a higher magnification image of B

DBI did not exhibit this same pattern of expression in MNs regardless of the level of spinal cord examined and was also absent from SPNs of the thoracolumbar region. Therefore, unlike TSPO, which appeared to be expressed in some of these neuronal cell types, DBI was absent from all neurones within the spinal cord.

4.3.8.1 Distribution of TSPO labelling in neurones in the spinal cord

In order to determine whether the subpopulations of $TSPO^+$ ventral MNs and SPNS were distributed along the entire rostrocaudal spinal cord axis, or were specific to the ventral horns of certain spinal regions, cell counts were performed in all spinal cord segments. TSPO-IR MNs of the ventral horn, and SPNs within both the IMM and IML, were counted in cervical, thoracic, and lumbar regions. Furthermore, the percentage of FG^+ cells which also expressed TSPO was calculated in each of segment region. There was no colocalisation of GAD67-GFP TSPO within these $TSPO/FG^+$ MNs. Furthermore, there were no instances of GFP/FG^+ SPNs in any section from any spinal segment during cell counting (data not shown).

TSPO was present in a subset of, but not all, ventral MNs, in cervical, thoracic, and lumbar regions of the spinal cord. The mean percentage of FG labelled MNs which were also $TSPO^+$ in cervical, thoracic, and lumbar segments was 31%, 22%, and 36%, respectively (figure 4.16). There were no significant differences in the percentage of FG^+ MNs which were also $TSPO^+$ in the cervical segment (31±2%) compared to thoracic regions (21±4%). There were no significant differences in the percentages of FG^+ MNs which also expressed TSPO in the ventral horn of cervical regions compared to lumbar regions (36±3%). However, there were significantly more FG^+ MNs which also expressed TSPO in the lumbar region compared to the thoracic region (21±4% v.s 36±3%, respectively, $p < 0.05$, students t-test, figure 4.17)

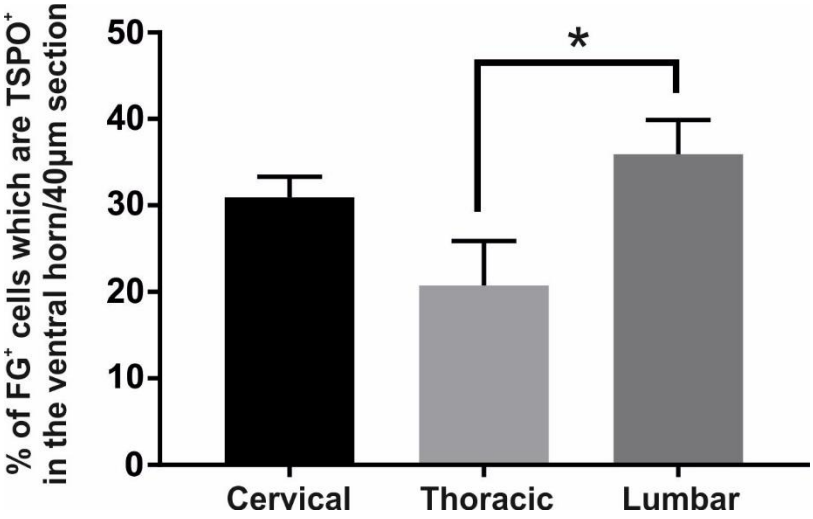

Figure 4.17 The percentage of total FG labelled cells which are also TSPO$^+$ is significantly greater in sections from the lumbar segment

When examining the distribution of TSPO in FG$^+$ SPNs, there were no significant differences in the percentages of FG$^+$ cells which were also and TSPO$^+$ in the IML between the thoracic (48±2%) and lumbar (42±5%) segments. Furthermore, there was no significant difference in the percentage of FG$^+$ cells which also expressed TSPO within the IMM between the thoracic (30±4%) and lumbar (18±5%) segments (figure 4.18A).

At the IML all FG$^+$ cells were TSPO$^+$, however there was another population of TSPO$^+$ cells present in the IML which were not FG$^+$ (figure 4.18B). In other words, FG$^+$ cells within the IML were always TSPO$^+$, however TSPO$^+$ cells at this location did not always contain FG. There were a significantly larger population of TSPO$^+$/FG- cells cells in the IML of the upper lumbar spinal segment compared to the thoracic segment (22±7% of TSPO$^+$ cells were FG- in the lumbar IML vs. 2±1% of TSPO$^+$/FG- in the thoracic IML, respectively, $p < 0.05$, students t-test, figure 4.18B).

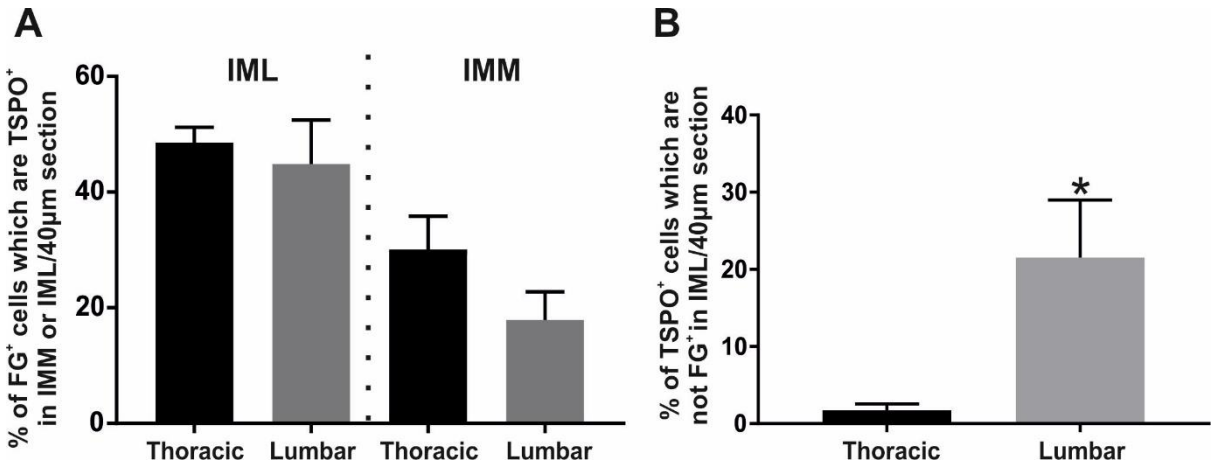

Figure 4.18 TSPO is expressed in FG labelled SPNs across the thoracolumbar region

A: Pooled data showing the percentage of total FG labelled cells which are also $TSPO^+$ in the IML and IMM in the thoracic and lumbar segments. **B**: Pooled data showing differences in the percentage of total $TSPO^+$ cells which are also FG^+ at the IML of sections taken from thoracic and lumbar segments

4.3.9 DBI-IR and TSPO-IR following stab injury to the spinal cord

Focal intraspinal stab injuries were performed in the dorsal column WM to examine changes in DBI-IR and TSPO-IR in response to environmental insult to the spinal cord. DBI-IR and TSPO-IR was examined 3 days post injury. Following injury to the cord there were varying observable changes in DBI-IR and TSPO-IR (figure 4.19).

At 3 dpi in sections taken from the injury site, the CC and DBI/$TSPO^+$ EC cells appeared distorted (figure 4.19), possibly due to mechanical trauma to the ependyma. Furthermore, following injury TSPO appeared to exhibit more diffuse staining at the CC and within the WM than is usually seen (figure 4.19). Whilst DBI and TSPO labelling appeared more intense, and in more regions, following WM injury, we were unable to quantify such changes, and therefore further work is required to more closely investigate how DBI and TSPO expression changes in such injurious situations.

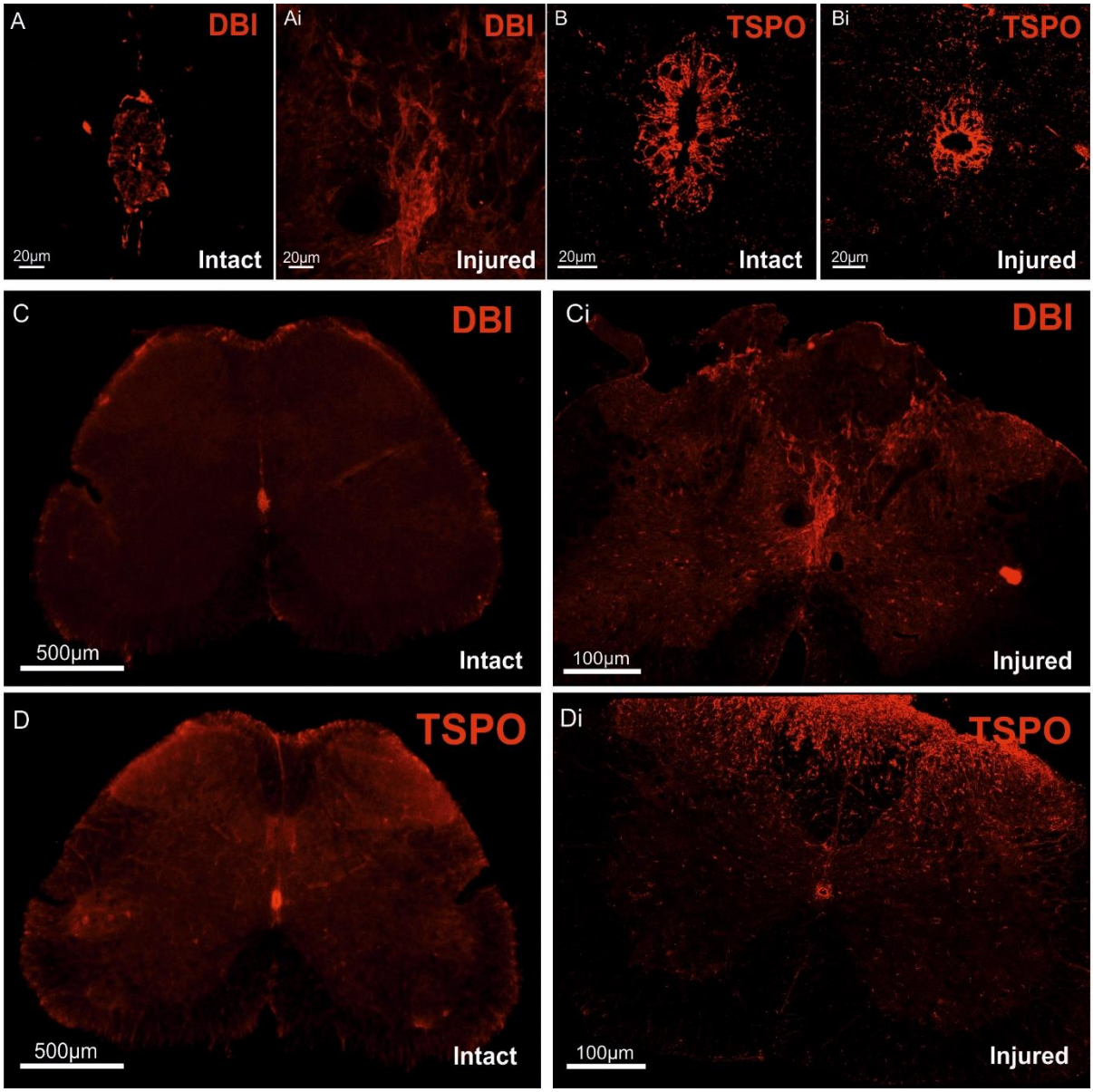

Figure 4.19 Patterns of DBI and TSPO staining appear to change following WM injury

A-Bi: Representative confocal images of DBI (A-Ai) and TSPO (B-Bi) labelling at the CC following WM injury (Ai and Bi) **C-Di**: Representative confocal images of DBI (C-Ci) and TSPO (D-Di) labelling in the WM and GM following WM injury (Ci and Di)

4.4 Discussion

4.4.1 DBI and TSPO are present in the adult spinal cord where they often are colocalised with one another

Many studies have characterised the expression of DBI and TSPO within the brain and peripheral organs, where they are often found in complementary regions to one another in tissues (Guidotti *et al*., 1983; Alho *et al*., 1988b; Tong, Y. *et al*., 1991; Gavish *et al*., 1992). For example, DBI and TSPO are both expressed in glial and ependymal cells in the brain and also colocalise in peripheral steroidogenic cells (Alho *et al*., 1991; Bovolin *et al*., 1990; Lihrmann *et al*., 1994; Malagon *et al*., 1993). These results may not be surprising as DBI is a known ligand for TSPO.

Results from this study are consistent with previous findings and show that, similarly to the brain, robust DBI- and TSPO-IR is also present in the intact adult spinal cord where they often colocalise. DBI and TSPO are colocalised within cells in the WM which have a glial-like morphology. In addition, DBI and TSPO are also coexpressed at the CC. The DBI metabolite ODN is also expressed in $TSPO^+$ ECs lining the CC.

Whilst DBI and TSPO are present in the same cells and regions, they show different cellular locations. TSPO has been previously detected at the plasma membrane in some CNS cell types and peripheral organs (Scarf *et al*., 2009; Oke *et al*., 1992). In the spinal cord TSPO is also located at the plasma membrane of ECs lining the CC. In $TSPO^+$ ECs DBI-IR is localised more diffusely in the cytoplasm, a pattern which echoes that of DBI^+ glial cells and ECs within the brain (Alho *et al*., 1991). ODN within ECs also exhibits a similar pattern to ODN labelling in ECs of the brain (Tonon *et al*., 1990). In the spinal cord WM, TSPO is present in glial-like fibres whereas DBI is concentrated within the cell soma.

Much like the brain, TSPO is also found in the endothelial cells of the spinal cord vasculature (Cosenza-Nashat *et al*., 2009). MRNA expression analysis of TSPO in different cell types of

the mouse cerebral cortex has shown that endothelial cells have the same basal levels of TSPO mRNA as microglia (Wimberley *et al*., 2018).

Unlike TSPO, endothelial cells within the spinal cord were not DBI^+. However, DBI is expressed in a subset of ECs which appear to send lateral projections from the CC to make contact with adjacent $TSPO^+$ vessels within lamina X. These DBI^+ cells are likely to be tanycytes which are laterally located ECs that contact the CC lumen and are characterised by a long basal process which terminates on the basal lamina of blood vessels (Hugnot and Franzen, 2011; Doetsch *et al*., 1997). Tanycytes have contact with both CSF and vessels, potentially linking the CSF, blood, and neuroendocrine system. The presence of TSPO in the vascular contacts of DBI^+ tanycytes only strengthens this possibility as DBI in these tanycytes could communicate changes sensed in the CSF to the vasculature by binding to TSPO in the endothelial cells.

Furthermore, tanycytes of the spinal cord also show strong IR for vasoactive intestinal polypeptide (VIP), a hypotensive and vasodilatory peptide found in the CSF (Fahrenkrug *et al*., 1977; Sharpless *et al*., 1984), where processes of VIP^+ tanycytes also terminate on blood vessels (Basbaum and Glazer, 1983; Chung and Lee, 1989). Tanycytes therefore may be able to control vascular tone of spinal blood vessels through the communication of DBI and TSPO which then leads to the release of VIP from these cells. Indeed, the TSPO specific antagonist PK11195 strongly dilates large arteries and arterioles (Gavish *et al*., 1992). In normal human volunteers, midazolam, which has actions at TSPO, is also a vasodilator (Colussi *et al*., 2011), indicating a link between DBI/TSPO and vascular control which may also extend to CNS vasculature.

Tanycytes also line the ventricles of the brain, and in particular tanycytes of the 3rd ventricle have been shown to express DBI-IR along the length of the ventricle (Dumitru *et al*., 2017) indicating that DBI expression is conserved between tanycytes of the brain and CC. DBI-IR tanycytes lining the 3rd ventricle also coexpress nestin and Sox2 much like DBI-IR ECs of

the CC. ODN is also expressed in tanycytes of the brain, indicating the importance of DBI and DBI metabolites as signalling mechanisms in this cell type (Gandolfo *et al*., 2000). TSPO is also present in the hypothalamus (Giannaccini *et al*., 2011; Gavish *et al*., 1992). Hypothalamic DBI/ODN^{+} tanycytes of the 3rd ventricle are thought to be glucosensing, communicating CSF nutrient availability to nearby hypothalamic neuronal nuclei, where DBI/ODN act as a 'relay' in glucose sensing and regulation of energy homeostasis (Lanfray *et al*., 2013; Guillebaud *et al*., 2017). These results indicate that DBI, its metabolites, and TSPO in tanycytes are a complementary sensing system in the brain, and results described here suggest that this function may also extend to the spinal cord.

4.4.2 Expression of DBI and TSPO in NSCs modulates proliferation

In the brain intense DBI expression is found in areas designated as postnatal neurogenic niches, including the dentate gyrus of the hippocampus and the ependyma of the SVZ of the lateral ventricle (Yanase *et al*., 2001; Tong, Y. *et al*., 1991; Alho *et al*., 1988a; Alfonso *et al*., 2012). Alfonso *et al*., (2012) and Dumitru *et al*., (2017) show that DBI is expressed in NSCs and the expression of DBI decreases in association with cellular differentiation. Results from these studies also show that DBI is necessary in these areas for balancing the paracrine activity of GABA, released from nearby neuroblasts, which keeps NSCs in an inactive state. Thus, following OE or KD of DBI, there are resultant changes in the proportion of proliferation of NSCs, migration of neuroblasts, and maturation of new neurones (Alfonso *et al*., 2012, Dumitru *et al*., 2017).

Findings from this study show that DBI is also located within the neurogenic niche of the spinal cord and is preferentially expressed within the ECs of the CC region. ECs constitute the NSC population of the spinal cord (section 1.5) and co-label with the NSC marker Sox2 alongside DBI. ODN, determined to be the 'active' fragment at GABAaR (Alfonso *et al*., 2012, Dumitru *et al*., 2017) is also present in Sox2^{+} ECs.

The presence of DBI within yet another neurogenic niche of the CNS highlights the importance of this endogenous protein in the maintenance of the postnatal stem cell niche. The presence of DBI may be essential to maintain the proliferative balance by offsetting the negative effects of GABA on proliferation (Alfonso *et al*., 2012; Bormann, 1991; Tozuka *et al*., 2005). Whilst ECs possess NSC properties and exhibit NSC behaviour, self-renewal and differentiation, following spinal cord injury their basal level of proliferation is low, Many different niche signals may be involved in this process (section 1.6), however as GABA is important in other niches for regulating proliferation and differentiation, and modulates proliferation in the spinal cord following manipulation of ambient GABA levels (chapter 3), perhaps GABA also suppresses EC NSC behaviour. Neighbouring GABAergic CSFcCs may provide the source of this GABA (section1.9), however processes which restrict EC proliferation, and whether DBI is involved in such processes, remain to be elucidated.

TSPO is robustly expressed at the plasma membrane of ECs and is colocalised with the NSC marker Sox2. TSPO mRNA and protein has also been shown to be expressed in NSCs and in post-mitotic neural precursors in primary neuron-enriched cultures *in vitro* (Varga *et al*., 2009). The DBI-derived TSPO ligand TTN stimulates proliferation in cultured rat astrocytes following binding to TSPO (Gandolfo *et al*., 2000), suggesting that TSPO is implicated in proliferation and differentiation in the CNS. Furthermore, TSPO is involved in the production of neurosteroids, such as allopregnanolone, which have profound effects on NSCs including influencing differentiation and suppressing genes that repress cell proliferation (Charalampopoulos *et al*., 2008b; Charalampopoulos *et al*., 2008a). Moreover, allopregnanolone increases oligodendrocyte proliferation and function (Daugherty, D. J. *et al*., 2013), indicating that it has multiple effects within both NSCs and also more mature lineage committed cell types. Therefore, TSPO may influence proliferation and differentiation in the CNS indirectly through neurosteroidogenesis.

Indeed, studies of glioma within the spinal cord give a perfect example of the power that DBI and TSPO may have over proliferation. Studies on these spinal cord tumours have shown

increased levels of DBI and its receptor TSPO (Alho *et al*., 1995; Miettinen *et al*., 1995), where perhaps unchecked expression of DBI and TSPO work in an autocrine manner to result in pathological tumorigenic proliferation. DBI and TSPO are therefore are expressed in areas involved in proliferation, differentiation, and migration, including spinal cord ECs.

4.4.3 DBI is not expressed in CSFcCs however CSFcC end bulbs are TSPO$^+$

The CC of the spinal cord is a heterogenous population of cells consisting of a variety of different cell types with different morphologies, functions, and expression of characteristic markers (Hugnot and Franzen, 2011). Areas devoid of DBI and TSPO may therefore represent these different cell types which have cell bodies within the EC layer but do not express DBI or TSPO such as CSFcCs.

CSFcCs are another cell type which are distributed around the CC with ependymal- or subependymally located soma. CSFcCs send a thick dendritic-like process into the lumen which terminates in a large ciliated end-bulb contacting the CSF (Hugnot and Franzen, 2011). There are 2 main types of CSFcCs, type-1 and type-2 CSFcCs, which are classified based on morphology, IHC, and electrophysiological properties, however both types are GABAergic (Barber *et al*., 1982) and can therefore be visualised as GFP$^+$ cells within the CC ependyma of GAD67-GFP mice. GFP is expressed in the entire CSFcC; in the cell body within the ependyma, the dendritic-like structure which projects through the ependyma and the terminal end-bulb which sits in the CC lumen contacting the CSF.

DBI is not expressed in either the cell body, dendritic-like projections or CSF-contacting end-bulbs of GFP$^+$ CSFcCs. CSFcCs are thought to represent a neuronal subtype, albeit with a less developed immature neural cell phenotype (Marichal, Nicolás *et al*., 2009). CSFcCs express the immature neuronal markers DCX, PSA-NCAM and HuC/D, but do not express the mature marker NeuN (Marichal, Nicolás *et al*., 2009; Stoeckel *et al*., 2003). CSFcCs also display electrophysiological properties of immature neurones (Marichal, Nicolás *et al*., 2009). In the brain DBI is expressed in few immature and mature neurones (Alho *et al*., 1988b),

therefore perhaps DBI is also absent from CSFcCs due to the neural similarities of these cells.

However, whilst TSPO is also absent from the soma of GFP^+ CSFcCs, TSPO-IR is found in GFP^+ CSFcC end bulbs within the CC lumen. Terminal bulbs of CSFcCs contain mitochondria (Leonhardt, 1976). TSPO is primarily expressed within mitochondria (Yasin *et al*., 2017; Gavish *et al*., 1999), where is it believed to play a role in the translocation of cholesterol from the outer mitochondrial membrane to the inner mitochondrial membrane, during steroid- and neurosteroidogenesis (Papadopoulos *et al*., 2018). As CSFcC end-bulbs are rich in mitochondria, and TSPO is normally expressed in mitochondria, it would therefore make sense that TSPO would be found in mitochondrial-rich CSFcC terminal bulbs.

In the brain, TSPO is present within the ventricular ependyma and choroid plexus of the brain (Benavides *et al*., 1983; Stephenson *et al*., 1995). Binding of the TSPO antagonist Ro 5-4864 decreases CSF formation by 48%, suggesting that $TSPO^+$ end bulbs of CSFcCs may also be related to modulation of CSF as seen in the brain. Whilst the precise function of CSFcCs is still enigmatic, they have been implicated in the sensing of CSF composition, pressure, and flow (Vigh *et al*., 1977; Vigh *et al*., 1983b). For example, CSFcCs have been shown to express both pH- and acid- sensing ASICs, $P2X_2$ receptors, and PKD2L1 channels which may be related to CSF chemosensing in CSFcCs (Marichal, N. *et al*., 2016; Marichal, Nicolás *et al*., 2009; Stoeckel *et al*., 2003; Huang, A.L. *et al*., 2006). The presence of TSPO within the end bulbs of CSFcCs, which are in direct contact with the CSF, may aid CSFcCs in sensing CSF composition and initiating downstream signalling processes in response to CSF components. For example, DBI is present in high levels within the mammalian CSF (Barbaccia *et al*., 1986), where it would be able to bind to TSPO within CSFcC end bulbs present within the CC lumen. ECs of the CC express high levels of DBI, however whether they secrete DBI into the CSF to influence TSPO present within CSFcC bulbs, or whether the source of DBI is located further away from the niche, is unknown.

In the SVZ GABA is released from nearby neuroblasts where it acts as a paracrine stop signal to limit proliferation of NSCs (Nguyen *et al*., 2003). ECs at the CC exhibit NSC properties, however in the intact cord their proliferation is restricted, occurring only for population maintenance (Barnabe-Heider *et al*., 2010). Work described in chapter 2 illustrates that proliferation in the spinal cord is also restricted by GABAergic signalling. Perhaps a mechanism exists in which DBI, or other CSF components, are able to bind to TSPO within CSFcC bulbs which regulates the level of GABA released from CSFcCs which inhibits EC proliferation in the intact cord by paracrine signalling on GABAaRs in ECs. If this were to be the case, then increased proliferation and differentiation of ECs following SCI could result from disruption of this system by either change in CSF composition following injury or by loss of CSFcCs. As yet the effects of DBI upon CSFcCs, EC proliferation, and changes in CSFcC behaviour following injury remain to be seen.

TSPO regulates the synthesis of neurosteroids and therefore it could be possible that expression of TSPO in CSFcC end-bulbs allows for neurosteroid synthesis in CSFcCs, where DBI in the CSF would then regulate this process by interacting with TSPO (Guarneri *et al*., 1990; Besman *et al*., 1989; George *et al*., 1994). Synthesis and secretion of neurosteroids by CSFcCs into the CC niche may then maintain the proliferative brake on nearby ECs by local PAM effects on GABAaRs in these cells. CSFcCs also express GABAaRs therefore a negative feedback loop could exist to regulate neurosteroid production in CSFcCs. Whether this is possible or does indeed occur is unknown and much more work is required to understand the patterns of DBI and TSPO expression in CSFcCs.

4.4.4 DBI and TSPO are expressed in certain glial populations of the spinal cord

In the brain, DBI and TSPO are preferentially located in glial populations. Astroglial cells have extremely high concentrations of DBI and DBI mRNA, and express the DBI gene (Costa, E. and Guidotti, 1991; Alho *et al*., 1994; Alho *et al*., 1985; Gandolfo *et al*., 2000). DBI

is exclusively located in glial cell populations of the brain including hypothalamic glial cells and Bergmann glia of the cerebellum (Tong, Y. *et al*., 1991). Cultured rat astroglial cells also contain and release substantial amounts of DBI-related peptides, TTN and ODN (Gandolfo *et al*., 2000), suggesting that DBI metabolites may not only be stored in astrocytes but that they may also regulate their local environment by secretion from these cells. Indeed, ODN has also been preferentially located in glial cells of the brain (Tonon *et al*., 1990). IHC shows that DBI and DBI-related peptides are also highly to moderately concentrated in the cytoplasm of astroglial cells in the cerebellum and dentate gyrus (Alfonso *et al*., 2012) (Yanase *et al*., 2002). TSPO is also most prevalent in glia, particularly within microglia and astrocytes (Gavish *et al*., 1992).

When examining expression of TSPO and DBI in the spinal cord, it was evident that DBI and TSPO were also expressed in glial-like cells of the spinal cord WM. TSPO appeared as punctate staining that was preferentially located in WM fibres, whereas DBI appeared to label cell bodies. In order to determine which glial populations may express DBI and TSPO in the spinal cord at the CC dorsal pole, lamina X GM, and WM double labelling for nestin and GFAP alongside DBI and TSPO were carried out. DBI- and TSPO-IR were also examined in Nestin-GFP mice

4.4.4.1 DBI and TSPO are expressed in nestin$^+$ radial glia

Dorsal projections which originate from the CC dorsal pole were DBI and TSPO$^+$ suggesting that DBI and TSPO may also be expressed in radial-glia like ECs, an EC subtype which possess long basal processes that extend along the dorsal midline and express the glial markers nestin and GFAP and (Hugnot and Franzen, 2011). Nestin-GFP mice possessed DBI/ GFP$^+$ dorsally located fibres at the CC, indicating that these dorsally projecting DBI/TSPO$^+$ ECs were nestin$^+$ as might be expected.

Nestin-GFP mice exhibit intense and specific GFP staining in ECs at the CC which colocalises with both DBI and TSPO, with some labelling of DBI$^+$ dorsally projecting fibres at

the CC dorsal pole. DBI also appeared to be expressed in small nestin-GFP$^+$ cells in lamina X. Labelling using a nestin antibody generated a different pattern of staining, where DBI$^+$ projecting fibres RG-like ECs at the dorsal pole were nestin$^+$, however all other DBI$^+$ ECs were nestin$^-$. Nestin-GFP mice also do not exhibit GFP-labelling in WM glial cells as seen in nestin antibody labelled sections. Despite these differences, results ultimately show that nestin$^+$ RG-like ECs are DBI$^+$ and that DBI is also present in nestin$^+$ radial glia of the WM.

4.4.4.2 DBI and TSPO are expressed in GFAP$^+$ astrocytes in the spinal cord

GFAP is another intermediate filament protein expressed by glial cells which is used to label astrocytes. GFAP is also present in RG-like ECs of the CC dorsal pole where it colocalises with DBI$^+$. There are GFAP$^+$ astrocytic fibres which are located within lamina X, and are in close apposition to the DBI$^+$ and TSPO$^+$ EC layer of the CC region. GFAP$^+$ fibres often appear to make contact with the EC layer, these CC-contacting astrocytes of lamina X express DBI in their cell body. TSPO is not seen in these GFAP$^+$ astrocytes close to the CC and neither DBI or TSPO colocalise with GFAP$^+$ astrocytic processes in this region. In the WM, DBI is expressed within the cell body and fibres of GFAP$^+$ astrocytes while TSPO colocalises with GFAP$^+$ fibres with minimal staining found in the soma. Despite differing patterns of cellular expression of GFAP, these results illustrate that DBI and TSPO are also expressed in astrocytes of the spinal cord.

In the brain, astrocytes are thought to synthesise, break down, (Loomis *et al*., 2010), and release substantial amounts of DBI and DBI-related peptides (Gandolfo *et al*., 2000; Patte *et al*., 1999; Christian *et al*., 2013) and this function may also occur in spinal cord DBI and TSPO$^+$ astroglial cells. In the brain TSPO and DBI expressing astrocytes are involved in the production of neurosteroids which then feedback to astrocytes and influence the production and secretion of DBI peptides (Loomis *et al*., 2010). DBI, ODN, and TTN have also been shown to protect neurones and astrocytes from oxidative stress-induced apoptosis (Ghouili *et al*., 2018; Hamdi *et al*., 2015). Whether these processes also occur in the spinal cord

DBI/TSPO$^+$ astrocytes remain to be seen, but could explain why DBI and TSPO are colocalised within glial cells of the spinal cord.

4.4.4.3 TSPO is expressed in Iba1$^+$ microglia of the spinal cord

In the brain TSPO is also expressed in microglia where it plays a role in microglia-macrophage interactions in response to injury and inflammation (Wang, M. *et al*., 2014; Daugherty, D. J. *et al*., 2013). TSPO was also found to be expressed in Iba1$^+$ microglial cells within the spinal cord, where it may perform similar functions following SCI as it does in peripheral nerve injury and inflammatory demyelinating lesions (Daugherty, D. J. *et al*., 2013)dau(Daugherty, Daniel J. *et al*., 2016; Girard *et al*., 2008).

4.4.4.4 A subset of PanQKI$^+$ oligodendrocytes colocalise with DBI and TSPO

QKI is an RNA binding protein which has been implicated in controlling the translation of many oligodendrocyte related genes, oligodendrocyte differentiation, and myelinogenesis (Hardy, 1998; Wu *et al*., 2001; Zhao, L. *et al*., 2006; Chen, Y. *et al*., 2007). Disruption of QKI results in dysmyelination (Hardy, 1998). DBI and TSPO were not found in PanQKI$^+$ oligodendroctyes in lamina X. There were however rare occurrences of small, less intense, DBI and TSPO$^+$ cells present in the WM, some of which appeared to colabel with PanQKI and the oligodendrocyte transcription factor olig2, suggesting that some oligodendrocytes may express DBI and TSPO in the spinal cord.

Previous studies have shown that TSPO and DBI peptides are expressed in Schwann cells of the peripheral nervous system (Lacor *et al*., 1999), however when examining myelinating cells in the brain, TSPO and DBI were rarely found in oligodendrocytes (Cosenza-Nashat *et al*., 2009), which fits with the case within the spinal cord. Many studies have reported the expression of DBI and TSPO in astrocytes and microglia, however a detailed picture of whether TSPO and DBI or DBI metabolites are expressed in oligodendrocytes of the brain is not yet available. However, a correlation has been found between TSPO expression, steroid

biosynthesis, and oligodendrocyte differentiation (Cascio *et al*., 2000), suggesting TSPO may also be involved in differentiation of this cell type.

4.4.5 TSPO is present in a subpopulation of motor neurones and SPNs whilst DBI is absent from all neuronal populations of the spinal cord

DBI IHC in the spinal cord echoes that of the brain, where DBI is preferentially expressed in glia and is absent from neurones. In the spinal cord DBI was also absent from CSFcCs, which express immature neuronal markers such as DCX and PSA-NCAM, suggesting that DBI is not expressed any cells with a neuronal phenotype. In the brain however DBI may be present in select neuronal populations such as pyramidal neurons of the cerebral cortex, hippocampal pyramidal cells, and neurons of the reticular thalamus (Alho *et al*., 1985; Ferrarese *et al*., 1987b; Costa, E. and Guidotti, 1991; Christian, Catherine A. and Huguenard, John R., 2013). When DBI is expressed in neurones, it is concentrated into synaptosomes where it is colocalised and co-released alongside GABA (Ferrarese *et al*., 1987b; Ferrarese *et al*., 1987a; Ferrarese *et al*., 1993). These findings suggest that whilst DBI and its proteolytic fragments are synthesised and released by glia, hence the strong labelling of glial populations throughout the brain, DBI can be taken up and retained by some neurons, which may explain the conflicting results found between some studies when examining expression of DBI in neurones (Tong, Y. *et al*., 1991).

However, this was not the case for DBI-IR in the spinal cord. IHC labelling for DBI was never seen in retrogradely labelled MNs and SPNS or in cells labelled with the mature neuronal marker NeuN. Staining for DBI in the GM was non-nucleic in nature and did not appear in cytoplasmic areas of large neurones, as often seen with TSPO. When DBI labelling was present in GM it appeared as diffuse cytoplasmic labelling in small cells with glial morphology. ODN was also absent from neurones in the spinal cord as is also seen in the brain (Vidnyánszky *et al*., 1994; Tonon *et al*., 1990). Furthermore, results examining the colocalisation of ODN-IR and GABA-IR in the cerebellar cortex of mice, where GABA is

always associated with neuronal elements, showed that whilst ODN-IR glial processes were located in close apposition to synaptic junctions, ODN and GABA did not colocalise. These findings therefore do not support the conclusion that DBI and DBI metabolites such as ODN are a neuronal processing product of DBI which are retained in some GABAergic neurones (Vidnyánszky *et al*., 1994). They do however support conclusions drawn here using IHC showing that DBI is also absent from spinal cord neurones.

In contrast to DBI, TSPO was expressed in a subset of large MNs of the ventral horn, SPNs in the lateral horn of the thoracolumbar segment, and SPNs in the IML. TSPO colocalised with FG^+ MNs in the ventral horn and FG^+ SPNs in the lateral horn. This was not specific to one particular spinal cord segment as TSPO/FG^+ MNs were found in cervical, thoracic, and lumbar sections, indicating that TSPO is not specific to the function of motor neurones at a particular spinal level to certain muscle effectors. There were however significantly more TSPO/FG^+ MNs in lumbar sections compared to thoracic sections. This finding may be simply a result of the increased size of the ventral horn in lumbar sections, and that the lumbar region is responsible for more motor output for controlling the lower limbs. Furthermore, fewer TSPO/FG labelled SPNs were present in the IMM compared to the IML in both thoracic and lumbar regions. Literature searches for TSPO/PBR in SPNs yield no results, therefore it does not appear that presence/expression of TSPO has as yet been documented/published in this cell type.

TSPO labelled a subset of MNs and SPNs, there were often cells which were $TSPO^+$ but FG negative or FG^+ and TSPO negative. At the IML there many $TSPO^+$ cells which were not FG^+, and there were significantly more $TSPO^+$/FG- cells in the lumbar region compared to thoracic. Retrograde labelling by IP FG injection should label the entire SPN population (Anderson, C. and Edwards, 1994), therefore these $TSPO^+$ cells at the IML and IMM are unlikely to be SPNs, and further investigation using markers of neurochemistry to elucidate the identity of these cells is required.

Double labelling for FG and TSPO and TSPO and NeuN indicate that not all motor neurones or SPNs of the spinal cord express TSPO and that TSPO is present in a subpopulation of large motor neurones. Further work is therefore required to examine TSPO-IR alongside other specific immunohistochemical markers to determine the neurochemistry of $TSPO^{+}$ motor neurones and SPNs, such as ChaT, GAT, parvalbumin, and somatostatin.

Very few other studies have examined the expression of TSPO in neurones, motor neurones, or SPNs and those which have report that TSPO is preferentially expressed in non-neuronal cells, with the greatest expression of TSPO in astrocytes and microglia (Cosenza-Nashat *et al*., 2009). This is in direct opposition to the pattern of TSPO-IR in the spinal cord, as discussed here. *In vitro* cultured cortical neurones have been shown to express TSPO, but this has not been replicated *in vivo* (Jayakumar *et al*., 2002). Whilst few have shown the expression of TSPO in neurones of the intact CNS *in vivo*, others have shown that TSPO, but not DBI, is expressed is induced in dorsal root ganglia neurones following peripheral nerve injury *in vivo* (Karchewski *et al*., 2004; Mills *et al*., 2005; Xiao *et al*., 2002). Moreover, treatment with the TSPO reported agonist Ro5-4864 result in enhanced mouse sensory axon regeneration following injury *in vivo* (Mills *et al*., 2005). Hernstadt *et al*., (2009) also report that TSPO is colocalised in $NeuN^{+}$ mature neurones of the dorsal horn following Complete Freund's Adjuvent-induced monoarthritis in mice (Hernstadt *et al*., 2009). Therefore, previous work shows that TSPO is expressed in neurones following nerve damage in a similar way to injury induced inflammatory upregulation of TSPO in microglia. However, whilst it is clear that some motor neurones and SPNs express TSPO, the reason for this, and whether their expression changes in these cell types following injury is unknown.

4.4.6 The pattern of DBI and TSPO IHC is changed following spinal cord WM injury

Following stab injury to the dorsal column of the spinal cord, DBI expression appeared to increase at 3dpi. ECs respond to injury by proliferation, differentiating into astrocytes, and migrating toward the lesion, and is possibly the reason for the new pattern of DBI-IR following injury to the dorsal columns. In sections more rostral to the injury, DBI-IR appeared to be more intense in the dorsal horns than in the same region in uninjured animals. There have been no previous studies investigating changes in DBI expression following SCI and whilst TSPO expression has been shown to increase following peripheral nerve injury, the same cannot be said for DBI (Karchewski *et al*., 2004). However, others have shown that ODN-IR increases in the sciatic nerve distal stump, and is expressed in Schwann cells, following transection of the sciatic nerve (Lacor *et al*., 1999). Results from this study shows that DBI may increase its expression following injury to the spinal cord WM and continues to be expressed in migrating activated ECs. However, such visual changes need to be quantified and work must be carried out to examine this phenomenon in greater detail, including lineage tracing the of DBI^+ EC progeny in injured spinal cord tissue.

Although very little is known about what may happen to DBI, or its metabolites, following injury, changes in TSPO expression have become a hallmark investigative feature in recent research in CNS injury and repair. Following stab injury to the spinal cord WM TSPO-IR appeared more intense, particularly at the site of injury. CNS pathologies which show an upregulation of TSPO are typically associated with microglial activation, neuroinflammation, and reactive gliosis (Papadopoulos and Lecanu, 2009). Increased spinal cord TSPO expression has also been seen following compression-induced SCI (Li, X.-m. *et al*., 2017). Moreover, treatment with the specific TSPO ligand ZBD-2 improved motor recovery after SCI and reduced mechanical allodynia and thermal hyperalgesia in these injured animals. ZBD-2 also attenuated GM damage and significantly reduced chronic reactive astrocytosis and

microgliosis, indicating that the TSPO ligand improved both functional motor outcomes and reactive gliosis and tissue damage after SCI (Li, X.-m. *et al*., 2017).

TSPO is thought to be involved in the regulation of reactive gliosis as PK11195 and etifoxine, reduce the level of reactive microglia and astroglia *in vivo* after a neurodegenerative insult (Ryu *et al*., 2005; Veiga *et al*., 2005; Veiga *et al*., 2007). Furthermore, PK11195 reduces the level of microglial reactivity by a mechanism which is independent of neuronal survival, indicating that a reduction in microglial reactivity by PK11195 is not simply due to increased apoptosis of microglial populations, but rather by a mechanism which regulates TSPOs control over gliosis, microglial proliferation and infiltration (Veiga *et al*., 2007). TSPO ligands also improve functional repair following peripheral nerve injury, SCI, and EAE-induced demyelination (Li *et al*., 2017, Girard 2011, Daugherty *et al*., 2013), suggesting that TSPO may be a future therapeutic target for treating CNS injury. The presence of TSPO and DBI in NSC-ECs, their upregulation following injury, and positive effects of TSPO ligand treatment in other studies, further strengthen this possibility.

4.5 Conclusion

In conclusion, DBI and TSPO are expressed in similar cell types of the spinal cord and brain, where both are found to be preferentially expressed in glial cells. Work discussed here has illustrated that similarly to cells of the 3rd ventricle, DBI/TSPO^{+} CSFcCs and tanycytes of the CC may also use DBI/TSPO and for environment sensing and information relay. DBI has been implicated in SVZ and SGZ neurogenic niche function, and remarkably is also expressed in the spinal cord NSC niche, suggesting that DBI may also be necessary for NSC niche behaviour in the cord. TSPO ligands may be a powerful tool for CNS recovery, elucidating a novel pathway for tissue repair. This work must therefore be carried further to determine whether DBI and TSPO within the spinal cord may be beneficial in other SC pathologies such as SCI, CNS tumours, and demyelinating conditions.

Chapter 5 – Modulation at central and peripheral diazepam binding sites alters the levels of proliferation, and differentiation, of new cells within the postnatal spinal cord

5.1 Introduction and rationale

Previous work has shown that GABA is an important signal in controlling proliferation and differentiation within the adult CNS (section 1.8 and 1.9). It also appears that regulation of GABAaR by the endogenous CBR site ligand DBI further modulates proliferation and differentiation by controlling GABAergic signalling (Alfonso *et al*., 2012; Dumitru *et al*., 2017)

GABA also appears to perform similar functions in the adult spinal cord, these findings are discussed at length in chapter 3. The endogenous GABAergic modulator DBI is also expressed in the adult spinal cord, with robust expression in the proliferative EC population, (Chapter 4). However, it is unknown whether modulation of GABAaR by endogenous CBR ligands such as DBI is also important in balancing the negative influence GABA also exerts upon proliferation in the intact adult spinal cord.

Therefore, experiments detailed in this chapter focus upon modulation of GABAaR via ligand binding at specific subunits to examine the effects upon postnatal proliferation and differentiation. As DBI also binds to the mitochondrial protein TSPO, the effects of modulation at TSPO upon postnatal proliferation are also considered.

5.1.1 Using pharmacology and transgenic mice to probe the contribution of GABAaR- and TSPO in the modulation of proliferation

To investigate this possibility, results presented below will discuss the effects of various different CBR and TSPO modulators upon proliferation and differentiation in the adult spinal cord. The mechanism of action (MOA) of these can be broadly split into 3 classes; 1. Mixed modulators which bind at both GABAaR and TSPO, such as etifoxine (ETX) and midazolam (MDZ) 2. Modulation specific to TSPO, such as PK-11195 3. Modulation specific to CBR binding, such as flumazenil and Ro15-4513. A summary of the pharmacological agents used, their administered dose (mg/kg), the vehicle in which they were dissolved and a brief overview of their MOA can be found in section 1.4 table 1.1

5.1.2 Mixed modulators of GABAaR and TSPO

5.1.2.1 The GABAaR and TSPO mixed modulators MDZ and ETX bind to and positively modulate GABAaR

MDZ was first developed in 1975 and is still used frequently in clinic today for its muscle relaxant, anticonvulsant, hypnotic, and sedative properties. MDZ belongs to the BZ class of drugs, binding to the CBR site of GABAaR to potentiate GABAergic signalling (Squires and Braestrup, 1977). MDZ results in a leftward shift of the GABA concentration-response curve, where saturating MDZ doses result in an increase in the maximal channel open probability by 10.2% (Rüsch and Forman, 2005). ETX is a structurally distinct positive GABAergic modulator which acts as an effective anxiolytic without the common BZ side effects (Kruse and Kuch, 1985; Schlichter *et al*., 2000; do Rego *et al*., 2015). BZ effects such as sedation, anterograde amnesia, and ataxia, are linked to binding to the α subunit of GABAaR (Tan *et al*., 2011), which forms one half of the CBR site alongside γ2 (Gunther *et al*., 1995). ETX however preferentially modulates β2-3 subunit containing GABAaRs which are less sensitive to typical BZ and neurosteroid modulation (Hamon *et al*., 2003).

5.1.2.2 The effects of ETX and MDZ upon GABAergic signalling are twofold due to neurosteroidogenesis

ETX and MDZ also bind to the mitochondrial DBI/endozepine receptor TSPO (Hamon *et al*., 2003; Schlichter *et al*., 2000; Verleye *et al*., 2001). It is therefore likely that ETX may mediate its anxiolytic effects via a combination of these two distinct binding mechanisms. Firstly, ETX enhances GABAergic neurotransmission by allosteric PAM of GABAaRs at β2-3 subunits (Schlichter *et al*., 2000; Verleye *et al*., 2002). However, ETX also activates TSPO, whereby it upregulates the production of GABAaR modulatory neuroactive steroids, such as AlloP and dehydroepiandrosterone (Aouad *et al*., 2014; Gunn *et al*., 2015; Verleye, M. *et al*., 2005; Liere *et al*., 2017).

The effects of ETX are not fully reversed by the either the BZ antagonist flumazenil or the TSPO antagonist PK11195 alone (Choi, Y.M. and Kim, 2015), however PK1195 suppresses the effect of ETX upon GABAaR transmission (do Rego *et al*., 2015). Therefore, there exists a likely scenario in which these two mechanisms are synergistic; where both direct allosteric modulation of GABAaR, and indirect modulation of GABAaR by stimulation of neurosteroidogenesis at TSPO, modulate GABAergic neurotransmission to a greater degree than either mechanism alone (Tokuda, K. *et al*., 2010). Furthermore, it has been reported that the anxiolytic action of ETX is potentiated by allopregnanolone (Verleye *et al*., 2001; Ugale *et al*., 2007).

MDZ is also able to influence GABAergic signalling by either binding to the CBR site of GABAaR itself and/or indirectly by binding to TSPO to promote the synthesis of GABAaR modulatory neurosteroids (Bender and Hertz, 1987; Tokuda, K. *et al*., 2010; So *et al*., 2010). MDZ enhances the synthesis of 5-α reduced neurosteroids, such as AlloP, in hippocampal neurones in *ex-vivo* brain slices, where the effects of MDZ upon synaptic inhibition require both neurosteroidogenesis by TSPO activation and PAM of GABAaR (Tokuda, K. *et al*., 2010). Interaction with TSPO is also required for the anticonvulsant, antidepressant, and anxiolytic activity of MDZ (Dhir and Rogawski, 2012; Qiu *et al*., 2015).

5.1.2.3 Effects of ETX and MDZ upon proliferation

Although little work has been done to investigate the effects of MDZ upon NSC proliferation, studies of highly proliferative cancer cell lines show that MDZ can influence proliferation, as MDZ inhibits highly-proliferative tumour cell-lines of varying tissue origin, including CNS-derived gliobastoma (Chen, Jingkao *et al*., 2016). Experiments described here attempt to determine whether MDZ produces similar effects upon the postnatal proliferation of neurones, astrocytes, and oligodendrocytes in the adult spinal cord. The effects of *in vivo* MDZ treatment upon EC proliferation, the NSC-like cells spinal cord, are also reported here.

Much work focuses on the effects of ETX as a reparative agent following injury, therefore there is less information concerning how ETX affects intact tissue. It is also currently unknown whether the effects of ETX at both GABAaR and/or TSPO can affect postnatal proliferation, differentiation, or even neurogenesis. Neurosteroids influence proliferation and differentiation of NSCs *in vitro* (Varga *et al*., 2009). AlloP influences proliferation and differentiation of both human and murine neuronal precursor cells *in vitro* (Wang, D.D. and Kriegstein, 2009). These findings therefore suggest that ETX and MDZ may influence proliferation and differentiation through their effects upon neurosteroidogenesis. The PAM of GABAaR by ETX and MDZ may also influence postnatal proliferation and differentiation as suggested by results discussed earlier in Chapter 3 which show that GABA influences postnatal proliferation in the intact adult spinal cord.

5.1.3 TSPO-specific modulation may affect neuroinflammation and proliferation

In order to determine whether effects of ETX and MDZ upon proliferation in the spinal cord were due to their binding at TSPO, the effects of the specific TSPO ligand PK-11195 upon proliferation were also examined. PK-11195 is an isoquinoline carboxamide which binds selectively to TSPO with nanomolar affinity, and exhibits antagonist properties (Le Fur *et al*., 1983). Others however have provided evidence that PK-11195 may also act as a partial weak agonist in some systems (Park, S.Y. *et al*., 2005; Mackowiak *et al*., 2017). It is therefore difficult to predict the effects that PK-11195 will have in a novel system, such as proliferation and differentiation in the adult spinal cord, as investigated here. The majority of work referencing the use of PK-11195 is directed toward the use of labelled PK-11195 for the assessment of CNS inflammation *in vivo* in both humans and animals (Betlazar *et al*., 2018; Chen, M.K. and Guilarte, 2008). TSPO expression has been reported to increase in stroke patients (Cerami and Perani, 2015), traumatic brain injury (Donat *et al*., 2016), in CNS

tumours such as glioblastoma (Roncaroli *et al*., 2016), and in patients with chronic neurodegenerative conditions such as MS (Herranz *et al*., 2016).

Early autoradiographic studies using tritiated PK-11195 ([3H]-PK11195) in rodents have shown that in the healthy CNS, TSPO is primarily expressed in the ependymal walls, choroid plexus, and olfactory bulb (Williams *et al*., 1990; Anholt *et al*., 1984; Benavides *et al*., 1983). Using this method TSPO expression has been shown to be specific to glial cells, showing little to no expression in neurones (Betlazar *et al*., 2018). However, results described in chapter 4 show that TSPO is expressed in a subset of MNs and SPNs within the adult spinal cord.

Following injury to the CNS, for example in models of MS and PNI, there is a widespread upregulation in [3H]-PK11195 binding (Daugherty, D. J. *et al*., 2013; Daugherty, Daniel J. *et al*., 2016; Girard *et al*., 2008). Higher levels of TSPO density via radiolabelled PK11195 ([11C]-PK11195) PET have also been used as a marker of neuroinflammation in humans (Liu, G.J. *et al*., 2014). The injury-induced increase in TSPO expression may be due to either upregulation of TSPO in glial cells, or more likely as a result of the increased proliferation of $TSPO^{+}$ proinflammatory activated microglia and reactive astrocytes (Cosenza-Nashat *et al*., 2009; Betlazar *et al*., 2018).

Less is known however about the effects of PK-11195 on cell proliferation, although, much like MDZ, PK-11195 has also been shown to inhibit cell proliferation in a dose dependent manner in some *in vitro* cancer cell lines (Maaser *et al*., 2001; Campbell *et al*., 2006; Mendonça-Torres and Roberts, 2013; Bode *et al*., 2012).

The TSPO specific ligand TTN increases intracellular [Ca^{2+}] (Gandolfo *et al*., 2001) and stimulates proliferation in cultured rat astrocytes (Gandolfo *et al*., 2000). This pro-proliferative effect was determined to be due to TTN binding at TSPO as these effects were abolished by PK11195 but not by the CBR specific antagonist flumazenil (Gandolfo *et al*., 2000). Furthermore, increased levels of TSPO expression have been found in high-grade

gliomas (Roncaroli *et al*., 2016; Miettinen *et al*., 1995). TSPO has also been implicated in neurosteroidogenesis (Papadopoulos *et al*., 2018; Wolf *et al*., 2015), where neurosteroids such as AlloP have been shown to strongly modulate GABAaR activity and influence NSC differentiation and proliferation (Wolf *et al*., 2015; Varga *et al*., 2009). These results suggest that TSPO may also influence postnatal proliferation so this was a feasible target for my studies.

5.1.4 Effects of CBR site specific modulation by endogenous and exogenous ligands upon proliferation and differentiation in the CNS

It is evident that BZs bind to CBR and exert their effects through PAM of GABAaR activity. However, the existence, function, and necessity of binding of an endogenous positive GABAaR-modulatory BZ-like molecule, or endozepine, is still controversial. Furthermore, it is also still unknown whether endozepines exhibit basal levels of binding to GABAaR which is essential for normal network functioning and regulation of proliferation and differentiation.

Existence of the elusive endozepinergic molecule, defined as an endogenous ligand for the CBR site, was first demonstrated in 1983, when DBI was isolated and characterised based on its ability to bind to and displace radio labelled diazepam from GABAaR in the adult rat brain (Guidotti *et al*., 1983) Since its discovery, DBI has been shown to be widely expressed in the CNS, where, upon binding to CBR within GABAaRs, it acts as a NAM, reducing GABAaR activity and dampening GABAergic signalling (Bormann, 1991; Olsen, 2018; Guidotti *et al*., 1983; Slobodyansky *et al*., 1989; Alfonso *et al*., 2012; Dumitru *et al*., 2017). Most importantly DBI has functional effects on GABAergic control over proliferation and differentiation in the SVZ neurogenic niches of the lateral ventricle SVZ and SGZ of the hippocampus dentate gyrus (Alfonso *et al*., 2012, Dumitru *et al*., 2017). In addition, GABAergic modulation by DBI is essential for the neurogenic effects of enriched environment upon hippocampal neurogenesis (Dumitru *et al*., 2017). These findings raise an important question; could endozepinergic modulation of GABAaR function, which contributes

to the balance of proliferation vs. differentiation, also occur in the spinal cord neurogenic niche?

DBI is robustly expressed in the NSC-like ECs and the glial cells of the spinal cord (Chapter 4), however whether it negatively modulates GABA to ease the proliferative brake in the spinal cord in the same way as in the SVZ and SGZ is unknown. DBI can also act as a PAM, for example in the thalamic nucleus, where, following secretion from astrocytes, it potentiates inhibitory GABAergic signalling and suppresses absence seizures in a mouse model of epilepsy (Christian, Catherine A. and Huguenard, John R., 2013; Christian *et al*., 2013). These results indicate that DBI does not act as a NAM throughout the entire CNS, and indeed areas may exist where it acts as a PAM, likely dependent upon the specific subunit composition of the local GABAaRs in that region. The specific action of endogenous CBR site ligands, such as DBI, upon GABAergic signalling in the spinal cord is entirely speculative. Furthermore, it is also unknown whether inverse agonists of GABAaR, such as Ro15-4513, which also bind to the CBR site, would have similar effects to DBI to influence the level of proliferation and differentiation of new cells.

Therefore, the effects of the CBR competitive antagonist flumazenil, the inverse agonist Ro15-4513, and reduced CBR binding affinity in mutant G2F77I animals upon postnatal proliferation and differentiation within the spinal cord were investigated here.

5.1.4.1 Selective CBR antagonists influence proliferation

Flumazenil is an imidazobenzodiazepine derivative which acts as a selective CBR site antagonist to competitively inhibit activity of BZ and BZ-like compounds at the CBR site of GABAaR (Votey *et al*., 1991; Kucken *et al*., 2003). Flumazenil is therefore used in the reversal of BZ-induced anaesthesia and as an antidote to BZ overdose (Amrein *et al*., 1988; Chern *et al*., 1998; Sage, 1988).

Flumazenil is considered a neutral allosteric modulator at the CBR site with selective antagonism at α1 and partial agonism at α2, α3, α5 subunit subtypes (Sivilotti, 2016).

Radiolabelled [C^{11}-Flumazenil] has therefore been used to examine the distribution and subunit composition of GABAaRs in the brain, much like the use of [C^{11}-PK11195] to visualise TSPO (Yankam Njiwa *et al*., 2013).

DBI and ODN influence the proliferation and differentiation of NSCs within the SVZ and SGZ, acting to dampen the inhibitory GABAergic tone within the niche to delicately balance the numbers and fate of NSCs and neural progenitor pools. Concomitant flumazenil treatment alongside lentiviral mediated DBI or ODN OE or KD determined that these effects were specific to the DBI/ODN binding at the CBR site of GABAaR (Dumitru *et al*., 2017; Alfonso *et al*., 2012). It would therefore appear that endogenous modulation of GABAaR by CBR binding acts as a negative feedback mechanism to maintain proliferative homeostasis within the niche.

Ro15-4513 is structurally similar to flumazenil and therefore also acts as competitive antagonist at the CBR site of GABAaR (Syapin *et al*., 1990). Ro15-4513 is also a weak partial inverse agonist of GABAaR (Mereu *et al*., 1987; Bonetti *et al*., 1988), which lowers seizure threshold to bicuculline and pentylenetetrazole (Nutt and Lister, 1987; Lister and Nutt, 1988). Ro15-4513 also exhibits antagonist properties at the ethanol binding site of extrasynaptic GABAaRs (Nutt *et al*., 2007; Bonetti *et al*., 1988; Suzdak *et al*., 1986; Glowa *et al*., 1988; Olsen *et al*., 2007).

Studies described here attempt to examine the effects of flumazenil and Ro15-4513 upon postnatal proliferation and differentiation in the spinal cord, to determine whether the inverse agonist or competitive antagonist properties of these drugs are able to influence proliferation in a similar way to DBI or ODN.

5.1.4.2 Mutations of the γ2 subunit of GABAaR can affect proliferation

Binding of BZs to GABAaR occurs at the CBR site, where the γ2 subunit is essential for the actions of BZs upon GABAaR (Sigel, E., 2002; Ernst *et al*., 2003). γ2F77I mice possess a phenylalanine (F) to isoleucine point mutation (I) at position 77 in the N-terminal domain of

the Gabrg2 gene which alters the affinity and specificity of the drug binding site within the γ2 subunit (Buhr and Sigel, 1997; Cope *et al*., 2004; Ogris *et al*., 2004). Whilst cerebella of mutant mice show a 15% reduction in γ2 subunit expression, γ2F77I mice breed normally and behave similarly to control C57BL/6 mice when examined with a range of behavioural observational tests (Cope *et al*., 2004). GABAaRs within these mice however, show altered responses various CBR ligands including, but not limited to, zolpidem, zopiclone (Cope *et al*., 2004), diazepam (Ramerstorfer *et al*., 2010), flunitrazepam (Buhr and Sigel, 1997; Wingrove *et al*., 1997) and flumazenil (Cope *et al*., 2004). G2F77I mice therefore demonstrate the importance of phenylalanine expression for the formation of the CBR binding pocket in GABAaR (Cope *et al*., 2004; Ogris *et al*., 2004; Ramerstorfer *et al*., 2010).

The endogenous proteins DBI and ODN also bind to, and modulate, GABAaR through the CBR site (Bormann, 1991; Alfonso *et al*., 2012). In WT mice, electrophysiological experiments demonstrate that hyperpolarising GABA-induced currents within SVZ transit amplifying cells are significantly decreased following application of ODN, indicating that DBI and ODN inhibit GABAergic signalling in these progenitor cells (Alfonso *et al*., 2012). However, this effect was almost abolished in G277I mutant hippocampal NSCs. In addition, whilst DBI OE normally results in an expansion of the $Sox2^{+}$ progenitor pool in WT mice, by NAM of GABAaR, the effects of DBI OE are mitigated in G2F77I mice (Dumitru *et al*., 2017). These experiments illustrate the utility of G2F77I when investigating the contribution of CBR-site binding in modulating postnatal proliferation and differentiation.

5.2 Aims

The aim of the work described in this chapter was to determine whether the CBR/DBI/endozepine binding sites of GABAaR are also important in the regulation of postnatal proliferation and differentiation in the intact adult spinal cord, as has been suggested for other neurogenic niches such as the SGZ and SVZ (Dumitru *et al*., 2017, Alfonso *et al*., 2013).

DBI and its derivatives are also TSPO ligands (Slobodyansky *et al*., 1989), therefore the effects of TSPO specific modulation were also examined to determine whether the effects DBI/endozepines may be having on proliferation are also related to TSPO.

5.3 Methods

5.3.1 Animals

To determine the effects of *in vivo* administration of various CBR- and TSPO- ligands upon proliferation and differentiation within the adult spinal cord, adult (6-8 weeks) C57Bl/6 mice (N=38) of either sex were used in line with the UK animals (Scientific Procedures) Act 1986 and ethical standards set out by the University of Leeds Ethical Review Committee. Every effort was made to minimise the number of animals used and their suffering. Animals were given ad libitum access to food and water and were housed in a 12-hour light dark cycle.

Collaboration with groups at UC Davis, California and Heidelberg, Germany provided us with an opportunity to examine spinal cord proliferation in transgenic mice with global TSPO KO and transgenic mice with a point mutation within the G2 subunit of GABAaR which disrupts binding affinity at CBR, respectively. These animals were used in order to determine whether perturbation of TSPO and GABAergic signalling pathways in these animals results in differences in spinal cord proliferation compared to WTs.

EdU treated spinal cord tissue from adult (~8-12 weeks) G2F77I mice (Buhr and Sigel, 1997) (*N*=5) was a kind gift of I. Dumitru (Prof. H. Monyer's Lab, DKFZ, Heidelberg, Germany).

Adult (4-8 weeks) heterozygous TSPOflox (*N*=4) mice were generated using Cre-LoxP technology and crossed with Cre-expressing mice to generate TSPO global KO mice (Wang, H. *et al*., 2016). Mice with floxed TSPO which was not yet excised were used as controls in these experiments (*N*=4) Tissue from these animals was a kind gift of O. Chechneva (Dr W. Deng's lab, UC Davis, Sacramento, California, USA).

GAD67-GFP knock in mice (Tamamaki *et al*., 2003) (*N*=3) were also used in experiments using ETX, further details about these animals can be found in chapter 3.

5.3.2 *In vivo* drug and EdU administration

Experiments using the thymidine analogue EdU (100ul at 10mM) were carried out as previously described (section 2.2.1). In addition to EdU, drug-treated animals were also given either ETX (50 mg/kg), MDX (0.3 mg/kg), PK11195 (3 mg/kg), flumazenil (5 mg/kg), Ro15-4513 (5 mg/kg). Control animals received an equivalent volume of vehicle IP (table 1.1). The doses of the drugs used in these experiments were determined based upon previous studies in mice.

Table 1.1. Details of drugs used and their mechanism of action

Name	Abbreviation	Dose (mg/kg)	Vehicle	MOA
Etifoxine	ETX	50	1% TWEEN-80 in sterile saline	TSPO ligand and GABAaR PAM (β subunits)
Midazolam	MDZ	0.3	0.9% sterile saline	TSPO ligand and GABAaR (CBR)
PK11195	N/A	3	4% DMSO/0.8% TWEEN-80 in Saline	TSPO specific antagonist
Flumazenil	N/A	5	0.1% TWEEN-80 in sterile saline	Competitive inhibitor at CBR site
Ro15-4513	N/A	5	4% TWEEN-80/3%DMSO in sterile saline	Inverse agonist at CBR site

5.3.3 Tissue preparation, EdU detection, and immunohistochemistry

Tissue from the thoracolumbar region (T11-L4) was prepared as described previously (section 2.2.4) and underwent post-hoc Cu^{2+} catalysed click-chemistry mediated detection of EdU-incorporation to visualise newly proliferated cells (section 2.2.5).

Following EdU localisation, sections were incubated with primary antibodies to determine the identity of any new EdU^+ cells. Immunofluorescence was performed with antibodies against NeuN, for mature neurones (mouse, 1:1000, Millipore, Watford, UK), Tuj or HucD for immature and mature neurones (rabbit, 1:1000, and rabbit 1:1000, for Tuj and HucD, respectively, Proteintech, Manchester, UK), Sox2, for undifferentiated stem-progenitor cells, (goat, 1:1000, Santa Cruz), PanQKI, for oligodendrocytes, (mouse, 1:100, UC Davis/NIH Neuromab Facility, Davis, CA), S100β, for astrocytes, (rabbit, 1:750, Abcam, Cambridge, UK), and Iba1, for microglia (rabbit, 1:1000, Wako, Japan). Further details are present in table 2.3 and 2.4.

5.3.4 Cell counts, statistical analysis, image capture and processing

Cell counts, including colocalisation of EdU and specific cellular markers, were performed as described previously (section 2.2.8). The percentage of total EdU^+ cells which colocalised with the marker in question was determined for each section. Occasionally the raw number of EdU^+/differentiation $marker^+$ cells were also examined. Cell counts are given as mean number of EdU^+ cells per 40µm section where *n*=number of sections counted in each condition and *N*=number of animals included in each experimental group.

Data were collated in Microsoft Excel and analysed using GraphPad Prism 7 software (GraphPad Software, California, USA). Data are presented as means ± SE. Student's t-tests and one-way ANOVA and post-hoc Tukey's testing for multiple comparisons were carried out and were carried out to determine significant differences between vehicle and drug treated animals. Data were considered significant when $p < 0.05$ (denoted by *); $p < 0.05$ (denoted by **), $p < 0.005$ (denoted by ***); or $p < 0.0001$ (denoted by ****).

Representative images of colocalised cells were acquired using Carl Zeiss ZEN software (Zeiss microscopy, Germany) and edited using CorelDRAW 2017.

5.4 Results

5.4.1 ETX and MDZ modulate spinal cord proliferation

Following treatment with 50 mg/kg ETX, animals showed reduced levels of proliferation (figure 5.1A-Ai). In WT C57Bl/6 mice, the total number of EdU^+ cells, which included both the WM and GM regions was significantly lower in ETX treated animals compared to vehicle treated (38.6 ± 1.9 vs. 84.4 ± 4.7, for ETX and vehicle treated animals, respectively, $p < 0.0001$, student's t-test, N=3, n=12). Proliferation of ECs, as assessed by changes in the number of EdU^+ cells at the CC, was also significantly reduced in ETX treated animals (1.3 ± 0.2 vs. 2.9 ± 0.4 vs., for ETX and vehicle treated animals, respectively, $p < 0.01$, student's t-test, N=3, n=12). The number of total EdU^+ cells was reduced by 54% in ETX treated animals while CC-specific proliferation was reduced by 55% compared to vehicle treated animals (figure 5.1Ai).

Experiments were repeated in GAD-GFP transgenic animals which produce significantly less GABA in the brain and spinal cord compared to WT counterparts (section 3.3.4). Much like WT mice, GAD67-GFP animals treated with ETX possessed significantly fewer total EdU^+ cells (48 ± 2.3 vs. 68 ± 1.8, $p < 0.0001$, student's t-test, N=3 n=*10*) and EdU^+ cells at the CC (1.1 ± 0.1 vs. 3.4 ± 0.3, $p < 0.0001$, student's t-test, N=3 n=*10*) compared to vehicle treated animals (figure 5.1B-Bi). ETX reduced total proliferation by 29% in GAD67-GFP mice, which is smaller than that seen in ETX treated WT mice. However, GAD67-GFP mice had a greater reduction in CC proliferation at 67% compared to 55% for WT mice.

Animals treated with MDZ also had significantly fewer total EdU^+ cells in the spinal cord compared to vehicle treated animals (42 ± 2.1 cells for MDZ vs. 67.5 ± 3.4 cells for vehicle, $p < 0.05$, student's t-test, N=3 n=30) (figure 5.1C). Animals treated with MDZ also possessed

fewer EdU$^+$ cells within the EC layer of the CC (0.4 ± 0.1 cells at the CC for MDZ vs. 2 ± 0.2 cells at the CC for vehicle, $p < 0.05$, student's t-test, N=3 n=30), compared to vehicle treated animals (figure 5.1Ci). The total number of EdU$^+$ cells was 38% smaller in MDZ treated animals. MDZ treated animals also possessed 80% fewer EdU$^+$ cells at the CC.

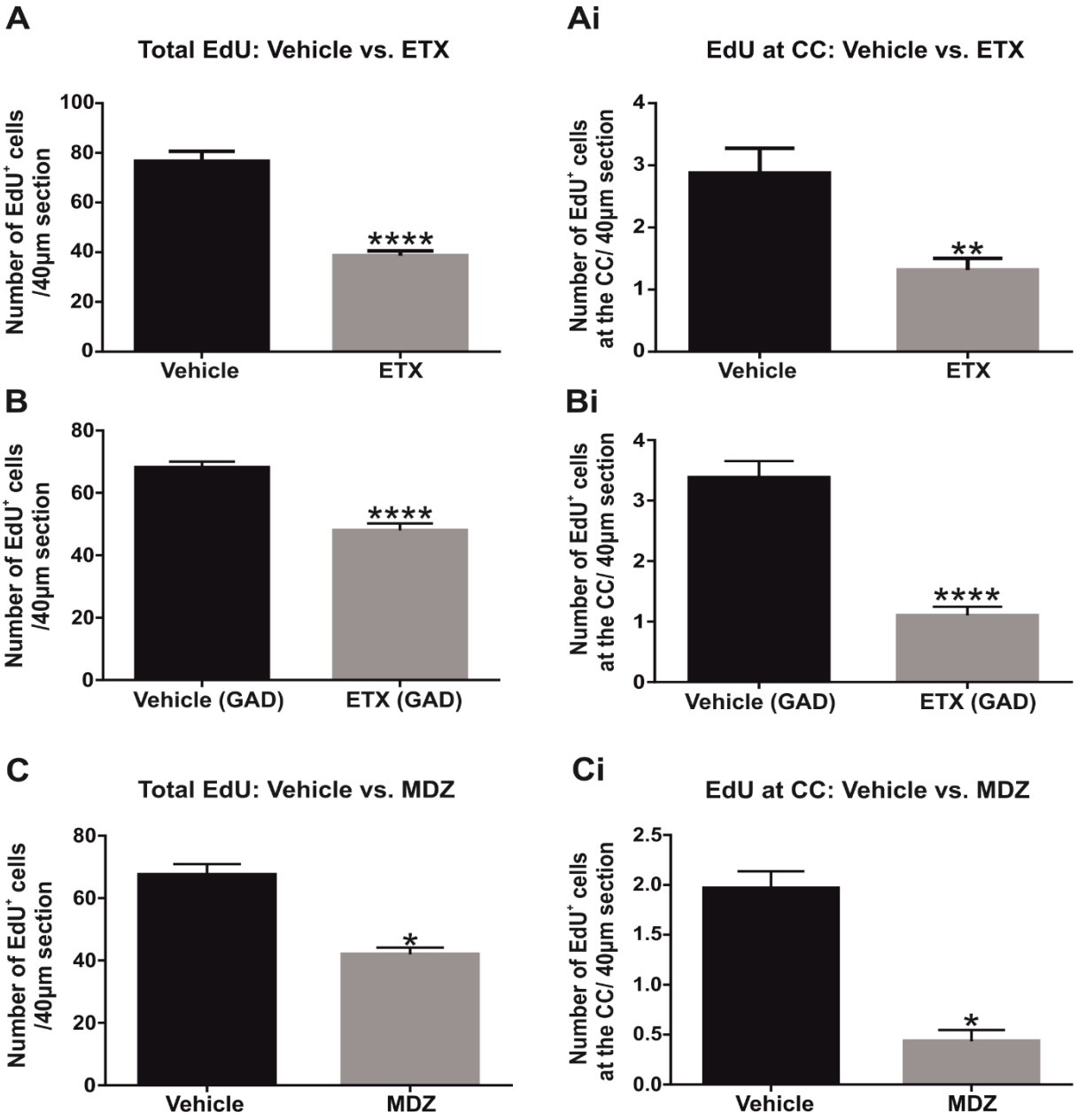

Figure 5.1 Both ETX and MDZ treatment significantly reduces proliferation in the adult murine spinal cord compared to vehicle treatment

A-Ai: Effect of ETX (50 mg/kg) in WT mice upon the number of proliferative cells in the spinal cord, including cell counts of EdU^+ cells specifically located at the CC compared to vehicle treatment. **B-Bi**: Effects of ETX in GAG67-GFP mice upon the number of EdU^+ cells in the WM and GM and CC compared to vehicle treatment. **C-Ci**: Effects of MDX (0.3 mg/kg) upon numbers of EdU^+ cells in the spinal cord and spinal cord CC compared to vehicle treatment. (* = $p < 0.05$, ** = $p < 0.01$, **** = $p < 0.0001$, student's t-test, N= 3 n=30)

5.4.2 Effects of ETX and MDZ treatment upon differentiation of newly proliferated EdU^+ cells

In ETX treated animals the proportion of total EdU/$PanQKI^+$ cells was significantly smaller than that of vehicle treated animals (49.7 ± 4.8% vs. 64.9 ± 5.2%, $p < 0.05$, student's t-test, N=3 n=12, figure 5.2B). The raw number of EdU/$PanQKI^+$ cells was also significantly lower in ETX treated animals compared to vehicle treated animals, however unlike percentage colocalisation, EdU and PanQKI colabelled cells were significantly lower ($p < 0.0001$, student's t-test, N=3 n=12) in total counts (14.83 ± 2.3 cells vs. 64.9 ± 5.2 cells), WM- (8.8 ± 1.5 cells vs. 30 ± 2.4 cells), and GM-specific counts (6.2 ± 1.1 cells vs. 30.2 ± 2.1 cells) (figure 5.2Bi) Furthermore, the proportion of EdU^+ cells which were also colabelled with PanQKI was also significantly reduced (p <0.005, student's t-test, N=3 n=9) in the GM of MDZ treated animals (18.0 ± 7.0%) compared to those treated with vehicle (50.5 ± 7.7%). However, the proportion of EdU/$PanQKI^+$ cells was significantly greater in the WM of MDZ vs. vehicle treated animals (82.0 ± 7.0% vs. 49.5 ± 7.7%, $p < 0.01$, student's t-test, N=3 n=9, figure 5.2Bii).

There was no significant difference in the percentage of EdU^+ cells which were also labelled with GFAP in either region for ETX treated vs. vehicle treated animals (figure 5.3A). However, animals treated with ETX had significantly greater percentage of total EdU^+ cells

which were colabelled with NeuN in the WM (4.2 ± 1.2% vs. 0% $p < 0.05$, student's t-test, N=3 n=9, figure 5.3B)

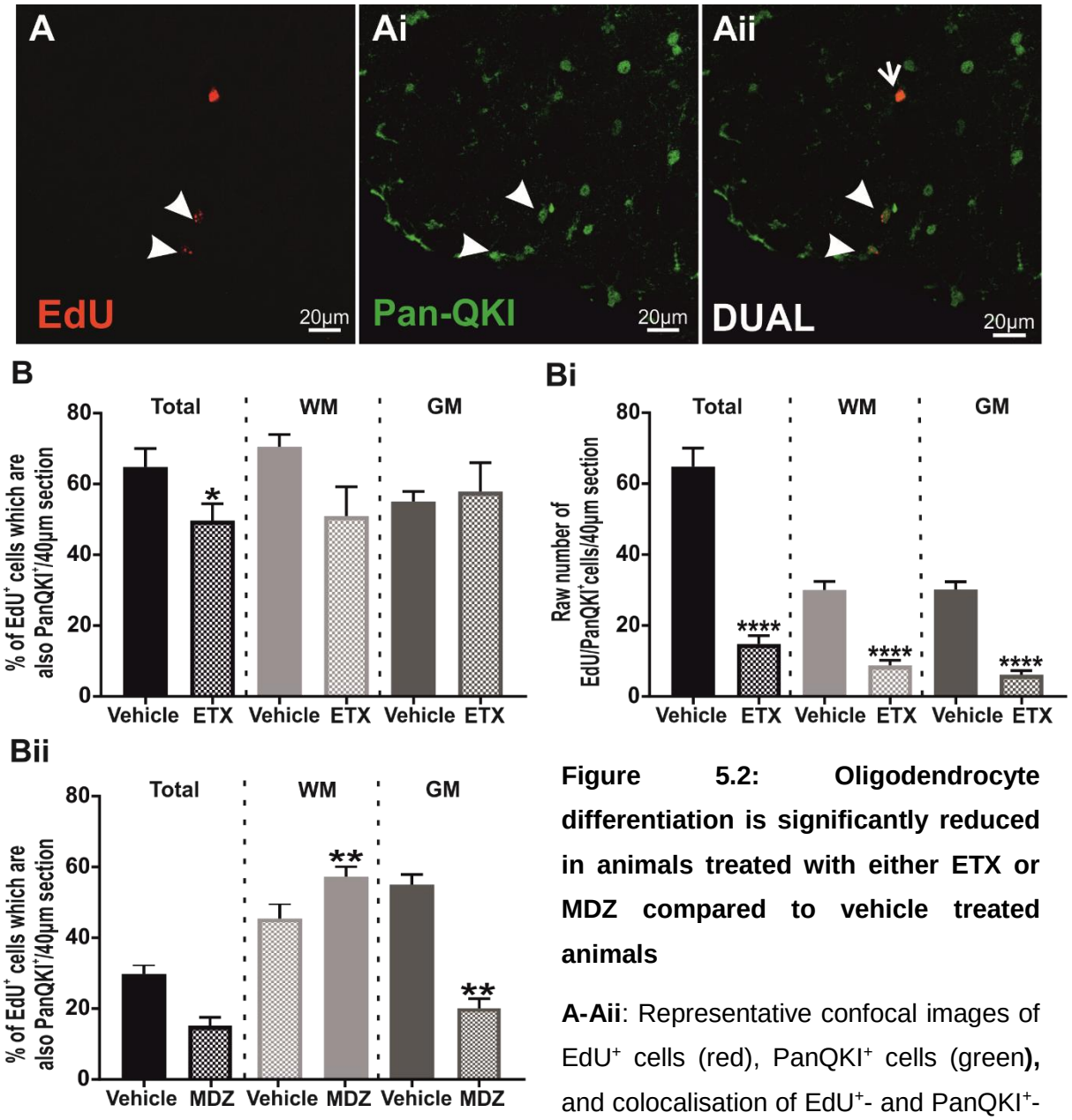

Figure 5.2: Oligodendrocyte differentiation is significantly reduced in animals treated with either ETX or MDZ compared to vehicle treated animals

A-Aii: Representative confocal images of EdU$^+$ cells (red), PanQKI$^+$ cells (green**),** and colocalisation of EdU$^+$- and PanQKI$^+$-PanQKI$^+$ cells (dual) in the ventral WM region of the spinal cord (closed arrows: EdU$^+$/PanQKI$^+$ cells, open arrows: EdU$^+$/PanQKI- cells). **B-Bi**: Graphs showing the total percentage of EdU/PanQKI$^+$ cells and the percentages of EdU/PanQKI$^+$ cells in WM and GM of ETX and vehicle treated animals (**B**) and raw numbers of EdU/PanQKI$^+$ cells in ETX vs vehicle treated animals (**Bi**). **Bii**: Percentages of EdU/PanQKI$^+$ cells in the WM and GM of MDZ and vehicle treated animals. Solid bars represent vehicle treated animals. Hatched bars are ETX and MDZ treated animals (* = $p < 0.05$, ** = $p < 0.01$, **** = $p < 0.0001$, student's t-test, N=3 n=9)

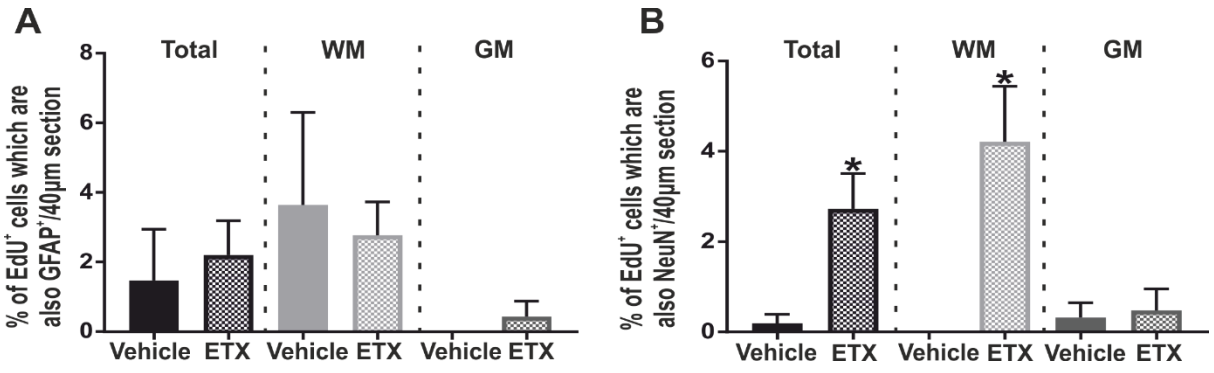

Figure 5.3 Animals treated with ETX exhibit unaltered glial differentiation but significantly more EdU/NeuN$^+$ cells compared to vehicle treated animals

A: Pooled cell counts showing the percentage of EdU$^+$ cells which are also GFAP$^+$ in the WM and GM in ETX and vehicle treated animals. **B**: Graph showing the average percentages of EdU$^+$ cells which are also NeuN$^+$ in the WM and GM of ETX and vehicle treated animals. Vehicle treated animals are represented by solid bars and ETX treated animals are represented by hatched bars. (* = p <0.05, student's t-test, N=3 n=9)

5.4.3 Perturbation of TSPO function significantly alters proliferation

Animals treated with PK11195 (3 mg/kg) had significantly fewer EdU$^+$ cells in both the WM and GM (60.9 ± 2.9 vs. 86.8 ± 3.8, p < 0.0001, student's t-test N=3, n=10) and at the CC (0.7 ± 0.1 vs. 4.2 ± 0.3, p < 0.0001, student's t-test N=3, n=10), compared to vehicle (4% DMSO/ 0.8% TWEEN-80 in sterile saline) treated littermates (figure 1.4A-Ai). The total number of EdU$^+$ cells in PK1195 treated mice was 30% lower compared to vehicle (figure 5.4A) while proliferation at CC was 83% lower in PK11195 treated animals compared to vehicle (figure 5.4Ai).

In contrast however, mice with global KO of TSPO exhibited significantly higher numbers of EdU$^+$ cells, compared to WT animals (54.6 ± 2.4 vs. 47.4 ± 2, p < 0.05, student's t-test, N=4 n=18, figure 5.4B). This difference was specific to the WM region (35.5 ± 1.5 vs. 29.4 ± 1.4 EdU$^+$ cells, p < 0.001, N=4, n=18, figure 5.4B), as the numbers of EdU$^+$ cells in the GM of TSPO KO mice were not significantly different from WT. There were also no differences in

the numbers of EdU$^+$ at the CC in TSPO KO animals compared to WTs (1.6 ± 0.2 vs. 1.9 ± 0.2, n.s, $p > 0.05$, student's t-test, N=4 n=18, figure 5.4Bi

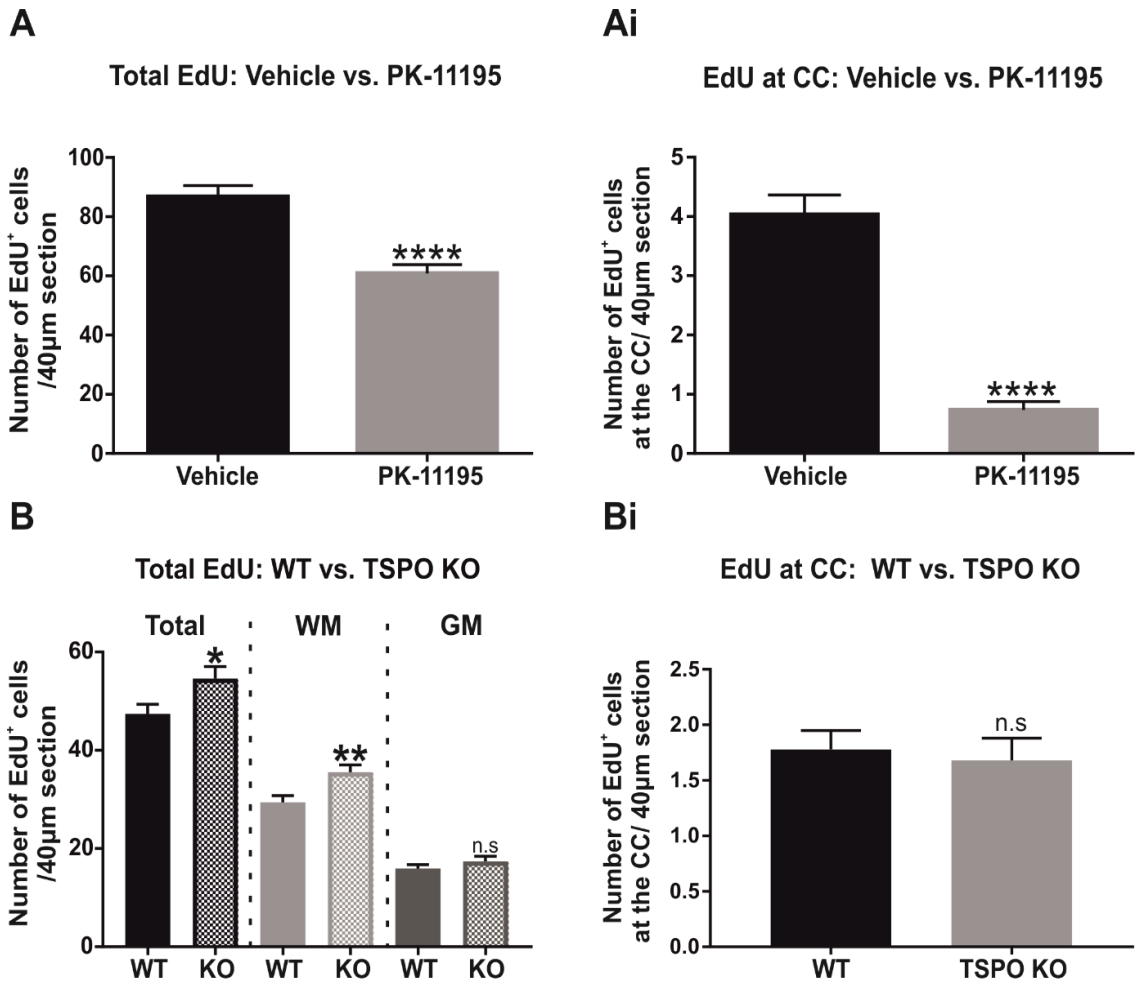

Figure 5.4 Effects of TSPO modulation on proliferation in the postnatal spinal cord

A-Ai: Effects of the TSPO specific ligand PK11195 (hatched bars) upon the number of EdU$^+$ proliferative cells in the WM and GM combined and the CC compared to vehicle treated animals (solid bars). **B-Bi**: Numbers of EdU$^+$ cells in the WM, GM, and CC of animals with global TSPO KO vs. WT animals (n.s = $p > 0.05$, * = $p < 0.05$, ** = $p < 0.01$, **** $p < 0.0001$, student's t-test, N=3, n=9 and N=4, n=18 for PK11195 vs. vehicle and TSPO KO vs. WT, respectively)

5.4.4 Global TSPO KO alters differentiation in the spinal cord

There were no NeuN/EdU$^+$ cells present in any of the sections examined from either TSPO KO or WT animals and therefore but these data are not further examined. It was found that for every other marker tested there was at least one example of a mature cell which colocalised with EdU (figure 5.5A-Ai)

The percentage colocalisation of PanQKI/EdU$^+$ and Sox2/EdU$^+$ cells was significantly greater than the colocalisation of any other markers studied, independent of region studied or experimental condition (figure 5.5A). There were no differences between the percentage colocalisation of EdU$^+$ cells with either Sox2, HucD, Tuj, or S100β in animals with TSPO KO compared to WT mice (figure 5.5).

There was however a significantly smaller percentage of EdU$^+$ cells which colocalised with PanQKI in TSPO KO animals compared to WT mice (45.7 ± 2.6% vs. 56.1 ± 4.1%, $p < 0.05$, student's t-test, N=4 n=12, figure 5.5). This represents a 19% reduction in EdU$^+$ cells which are PanQKI$^+$ compared to vehicle. These results illustrate that whilst overall differentiation of newly proliferated astrocytes and mature or immature neurones is not affected by TSPO KO, the number of proliferating PanQKI$^+$ OLCs in the WM is reduced following TSPO KO despite an overall increase in EdU$^+$ cells.

EdU/Sox2$^+$ and EdU/S100β$^+$ were found scattered throughout the WM and GM. However, newly proliferated EdU$^+$ cells at the CC exclusively colocalised with Sox2 (figure 5.6A-Aii) indicating that NSC-like ECs were also proliferating in the intact cord. Moreover, whilst there was no significant difference in the numbers of proliferating cells at the CC in TSPO KO mice compared to WT mice, in experiments detailed throughout this chapter it is highly likely that these pharmacologically induced changes in proliferation at the CC are due to direct effects upon EC proliferation as EdU$^+$ cells frequently colocalise with both Sox2 (figure 5.6A-Aii). For example, in this case the percentage of EdU$^+$ cells which were also Sox2$^+$ accounted for

57.6 ± 11.6 % and. 63 ± 11% of total EdU$^+$ cells at the CC in TSPO KO and WT mice, respectively (figure 5.5A).

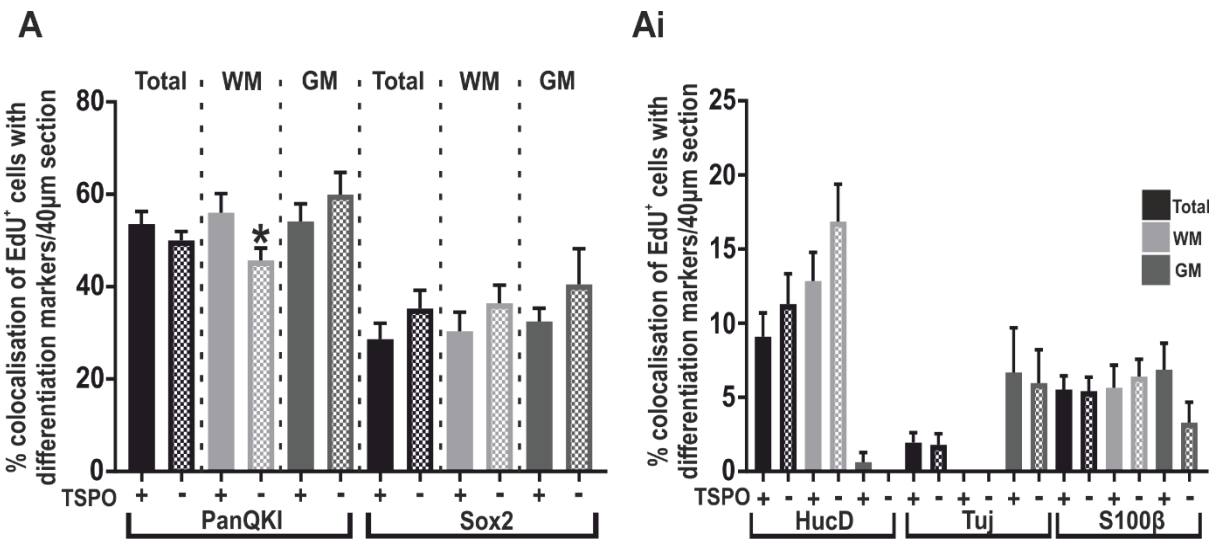

Figure 5.5 TSPO KO reduces the number of new PanQKI$^+$ cells in the spinal cord WM

A-Ai: Percentages of total EdU$^+$ cells which colocalise with either PanQKI, Sox2, HucD, Tuj, or S100β in WT (solid bars) and TSPO KO (hatched bars). Values for PanQKI and Sox2 are shown on a larger y-axis due to higher percentage values. (* p <0.05, one-way ANOVA)

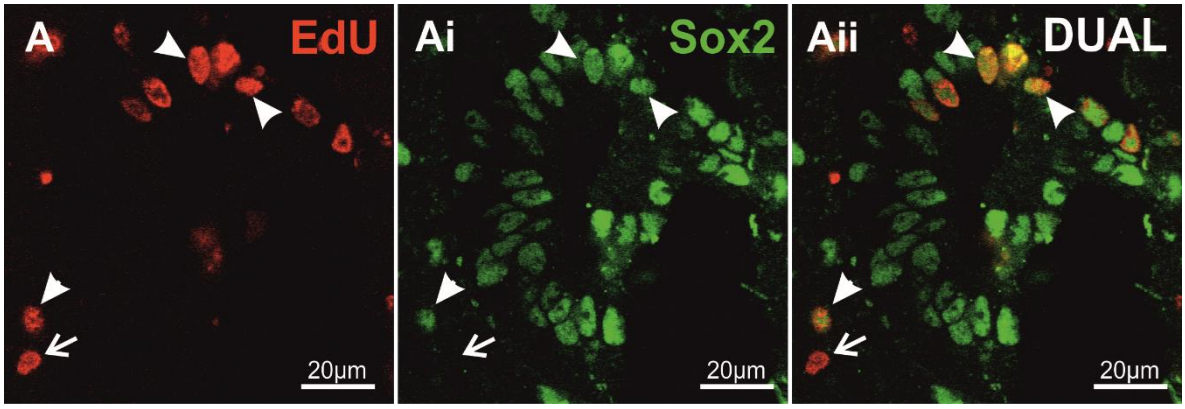

Figure 5.6 EdU$^+$ cells at the central canal are Sox2$^+$ ECs

A-Aii: Representative confocal images of EdU$^+$ cells (red) and Sox2$^+$ cells (green) located at the spinal cord CC. EdU/Sox2$^+$ cells are also present (dual). Closed arrows mark colocalised cells. Open arrows mark non-colocalised cells.

5.4.5 Modulation of the GABAaR CBR site affects numbers of EdU$^+$ cells

Three experimental conditions were used to assess the effects of manipulation of the CBR site, and therefore GABAaR function, upon baseline proliferation in the intact adult spinal cord 1. Treatment with the CBR site competitive antagonist flumazenil vs vehicle treatment, 2. Treatment with the CBR site inverse agonist Ro15-4513 vs. vehicle treatment, or 3. Transgenic mutagenesis to reduce ligand binding affinity at CBR in G2F77I mice vs. WT littermates

Animals treated with flumazenil (5 mg/kg), a CBR specific antagonist, exhibited a significant increase in the total number of EdU$^+$ cells within the spinal cord compared to vehicle (0.1% TWEEN-80/sterile saline) treated animals (132.1 ± 4.4 vs. 112 ± 2.1, for flumazenil and vehicle treated animals, respectively, p <0.001, student's t-test, N=3 n=*15*, figure 5.7A). Flumazenil treated mice exhibited an 18% increase in proliferating EdU$^+$ cells. These effects were specific to proliferating cells within the WM (77.3 ± 3.6 vs. 63 ± 1.7, for flumazenil and vehicle treated animals, respectively, p < 0.001, student's t-test, N= 3 n=15, figure 5.7A) as increases in EdU$^+$ cells within the GM did not reach statistical significance.

Ro15-4513 is a weak partial inverse agonist at CBR and was used to investigate and compare the effects of a drug with a similar MOA to flumazenil.

Following treatment with Ro15-4513 (5 mg/kg) there were significantly more total EdU$^+$ cells in the spinal cord (104.2 ± 3.8 vs. 85.6 ± 2.9 cells for Ro15-4513 and vehicle treated mice, respectively, $p < 0.001$, student's t-test, N=3 n=18, figure 5.7B), indicating an increase in proliferation in Ro15-4513 treated animals compared to vehicle. These results were similar to those seen in flumazenil treated animals, however there were significantly more EdU$^+$ cells in the GM following Ro15-4513 treatment compared to vehicle (41.8 ± 1.8 vs. 30.7 ± 1.4 cells respectively, $p < 0.0001$, student's t-test, N=3 n=18). Ro15-4513 induced a 22% increase in total EdU$^+$ cells and a 36% increase in the GM specifically (figure 5.7B).

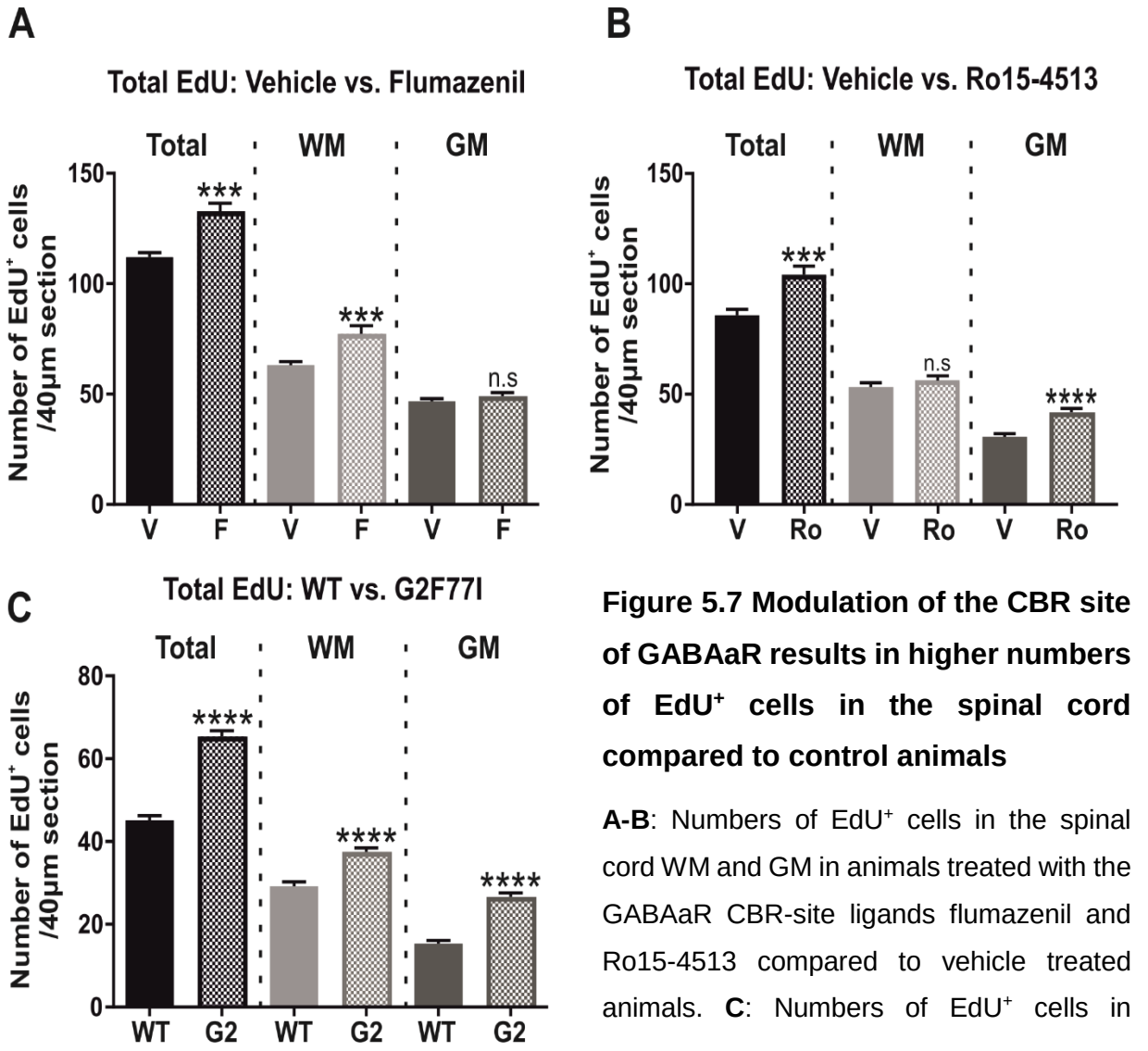

Figure 5.7 Modulation of the CBR site of GABAaR results in higher numbers of EdU$^+$ cells in the spinal cord compared to control animals

A-B: Numbers of EdU$^+$ cells in the spinal cord WM and GM in animals treated with the GABAaR CBR-site ligands flumazenil and Ro15-4513 compared to vehicle treated animals. **C**: Numbers of EdU$^+$ cells in transgenic G2F77I in the WM and GM compared to WT littermates. Hatched bars: treated or transgenic animals Solid bars: vehicle or WT animals. (*** = $p < 0.001$, ****, $p< 0.0001$, student's t-test)

Similarly, animals with the G2F77I point mutation exhibited significantly greater average numbers of total EdU^+ cells per section compared to control animals (65.9 ± 1.4 cells vs. 45.1 ± 1.1 cells in G2F77I mice (*N*=5 *n*=60) and WT mice (*N*=4 *n*=60), respectively, $p < 0.0001$, student's t-test, figure 5.7C). G2F77I mutant mice also had significantly ($p < 0.0001$) higher numbers of EdU^+ cells in both the WM and the GM (37.5 ± 0.9, n=60, 26.6 ± 1, *n*=60, for WM and GM respectively) compared to WT controls (29.2 ± 1.1, *n*=60, 15.3 ± 0.8, *n*=60 for WM and GM, respectively, figure 5.7C). G2F77I animals had 46% more total EdU^+ cells, WM 28% more EdU^+ cells in the WM and 42% more EdU^+ cells in the GM compared to WT animals.

Thus, both pharmacological and transgenic manipulation of binding to the CBR site within GABAaR increases proliferation within the intact adult spinal cord.

5.4.6 Effects of CBR modulation upon EC proliferation

Flumazenil treatment also resulted in significantly greater levels of proliferation at the CC compared to vehicle (5.7 ± 0.4 vs. 2.5 ± 0.2 EdU^+ cells, for flumazenil and vehicle treated animals, respectively, $p < 0.0001$, student's t-test, *N*=3 *n*=15), a change of 128% (figure 5.8A-Ai).

Animals treated with Ro15-4513 also had significantly more EdU^+ cells at the CC (3.1 ± 0.2 cells vs. 1.7 ± 0.2 cells, $p < 0.0001$, student's t-test, *N*=3 *n*=18). Treatment with Ro15-4513 therefore resulted in 82% more proliferative cells at the CC compared to vehicle treated animals (figure 5.8B-Bi).

Proliferation at the CC was also significantly greater in G2F77I mice than in WT control animals (1.3 ± 0.2 EdU^+ cells at the CC in G2F77I mice (*N*=5 *n*=60) vs. 0.63 ± 0.1 EdU^+ cells

at the CC in WT animals (N=4 n=60) student's t-test, $p < 0.0001$) (figure 5.8C-Ci). The number of EdU$^+$ cells at the CC was 106% higher in G2F77I mice.

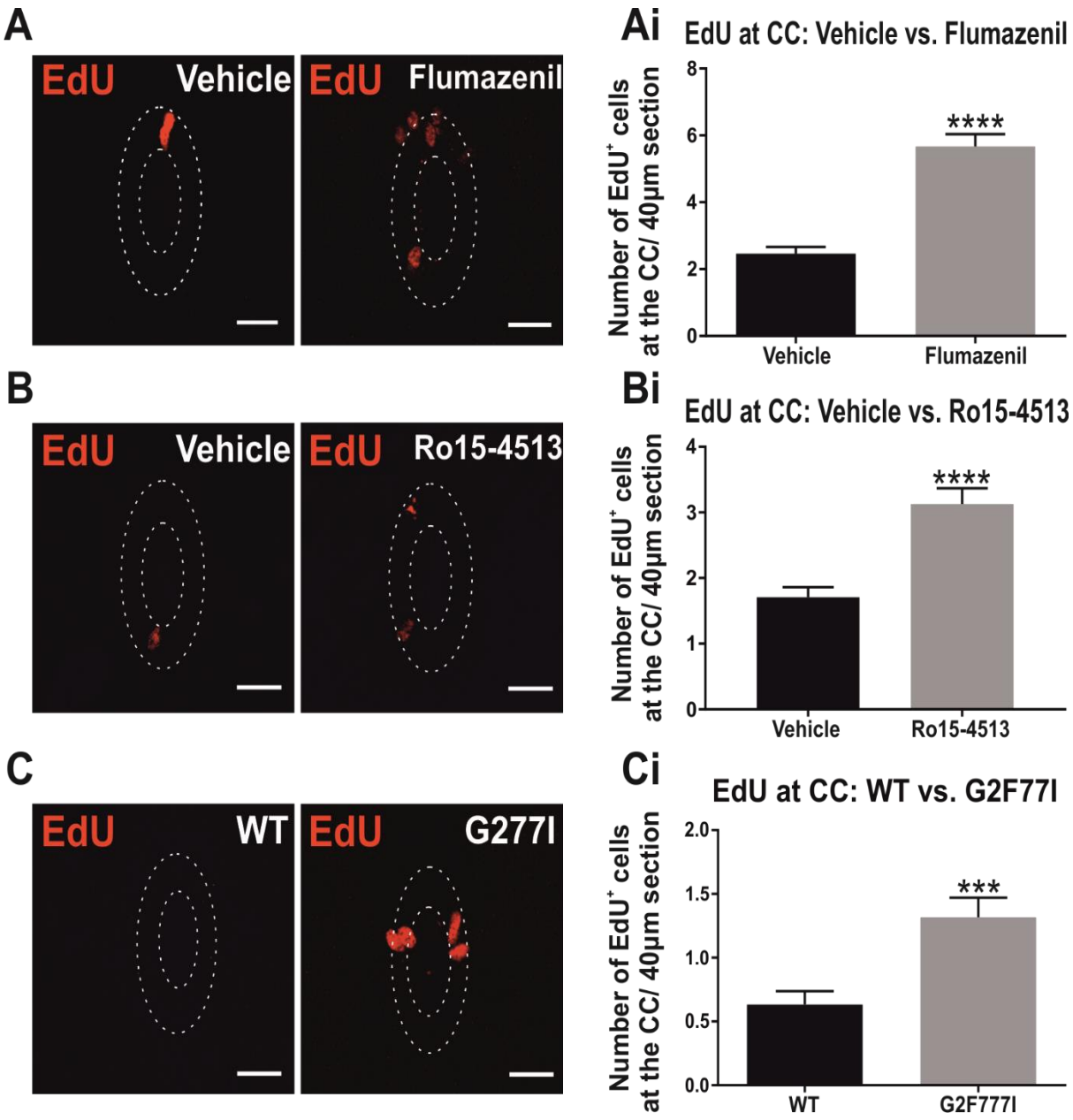

Figure 5.8 Alteration in CBR function results in greater levels of proliferation at the CC

A, B: Representative confocal images of the CC region illustrating the presence of EdU$^+$ cells at the CC in animals treated with either flumazenil or Ro-154513 compared to vehicle treated animals. **Ai, Bi**: Pooled data showing the numbers of EdU$^+$ cells at the CC of flumazenil and Ro15-4513 treated animals vs. vehicle treatment. **C**: Representative confocal images of EdU$^+$ cels at the CC of WT and G2F77I animals **Ci**: Cell counts of EdU$^+$ cells at the CC of WT and G2F77I animals. (*** = $p < 0.001$, **** = $p < 0.0001$, student's t-test)

5.4.7 Oligodendrogenesis is altered following CBR modulation

In both control and treated animals EdU/PanQKI$^+$ cells were frequently observed in both the WM and GM (figure 5.9A-Aii, closed arrows) with between 31-36.7% of newly proliferated cells differentiating into PanQKI$^+$ oligodendrocytes.

Although flumazenil and Ro15-4513 treated animals showed a slight trend toward a decrease in the percentage of EdU$^+$ cells which were also PanQKI$^+$ compared to vehicle treated animals, there were no significant differences in the percentage of EdU/PanQKI$^+$ cells in flumazenil or Ro15-4513 treated animals compared to vehicle (figure 5.9B). However, when looking at raw numbers of EdU/marker$^+$ cells, rather than the percentage of entire EdU$^+$ cell population which were also PanQKI$^+$, there were some significant differences between vehicle and Ro15-4513 (figure 5.9Bi). Ro15-4513 treated animals had significantly more total EdU/PanQKI$^+$ cells compared to vehicle treated animals (17.5 ± 2.4 cells vs. 11.2 ± 1.7 cells, in Ro15-4513 treated animals and vehicle treated animals, respectively, p <0.05, student's t-test, N=3 n=9, figure 5.9Bi).

However, whilst PanQKI$^+$ cells also represented the greatest proportion of newly proliferated EdU$^+$ cells in the cord of G2F77I mice these animals had a significantly smaller proportion of total EdU/PanQKI$^+$ cells than WT mice (25.5 ± 2.2% vs. 33.7 ±1.7%, p < 0.05, student's t-test, N=5 n=15, figure 5.9B). There was also a significantly smaller percentage of EdU$^+$/PanQKI$^+$ cells in the GM of G2F77I mice compared to that of WT littermates (19.1 ± 1.8% vs. 29.9 ± 4.1%, p <0.05, student's t-test, N=5 n=15) (figure 5.9B). These results indicate that whilst G2F77I exhibit significantly greater levels of proliferation in the postnatal spinal cord, the differentiation of these cells into PanQKI$^+$ oligodendrocytes is decreased compared to their level of differentiation in WT animals.

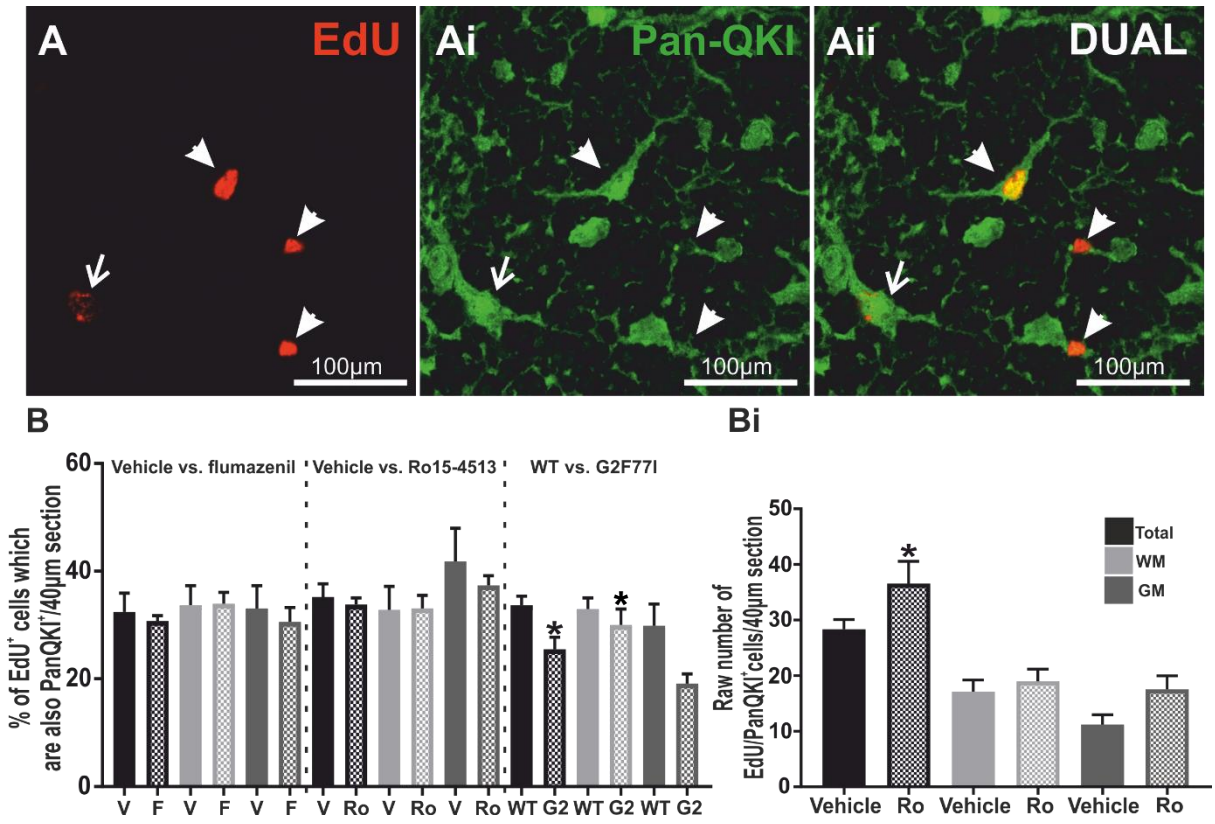

Figure 5.9 Effects of alteration of CBR function on oligodendrocyte differentiation

A-Aii: Representative confocal images illustrating the presence of EdU/PanQKI$^+$ cells in the dorsal WM (dual) Colocalised cells are labelled with closed arrows. Open arrows denote non-colocalised cells. **B**: Pooled data showing the percentages of EdU$^+$ cells which are also PanQKI$^+$ in flumazenil and Ro15-4513 treated animals vs. vehicle treatment. The percentages of EdU/PanQKI$^+$ cells in G2F77I and WT animals are also shown. **Bi**: Raw numbers of EdU/PanQKI$^+$ cells in Ro15-4513 treated animals vs. vehicle treatment. Solid bars represent control animals. Hatched bars represent data from flumazenil-, Ro15-4513-treated, and G2F77I animals. (* = $p < 0.05$, student's t-test)

5.4.8 CBR modulation alters the level of glial proliferation compared to control treated animals

Astrocytes represent the third largest population of proliferating cells in the intact adult spinal cord following PanQKI$^+$ oligodendrocytes, and Sox2$^+$ NSCs. The glial markers GFAP and S100β were used here to identify EdU$^+$ cells belonging to the astrocyte lineage. The 'classic'

glial cell marker GFAP was utilised in early experiments, however due to the nature of GFAP labelling it was difficult to confidently identify EdU/GFAP$^+$ cells due to the lack of staining of the cell soma. Therefore, in later experiments S100β, a cytoplasmic/nuclear specific stain was used.

In both vehicle and flumazenil treated animals there were instances of EdU$^+$ cells which were also GFAP$^+$ in both the WM and GM, indicating the presence of astroglial differentiation in the mature spinal cord of both flumazenil and vehicle treated animals (figure 5.10A-Aii). However, there were no significant differences in the percentages of EdU$^+$ cells which were also GFAP$^+$ in flumazenil treated animals compared to vehicle treatment (figure 5.10D), despite the changes in the overall number of EdU$^+$ cells compared to vehicle.

Animals treated with Ro15-4513 however showed a reduction in the percentage of total EdU/S100β$^+$ cells compared to vehicle treated animals (2.4 ± 0.4% vs. 5 ± 1%, $p < 0.01$, student's t-test, N=3 n=9, figure 5.10B-Bii,D). In G2F77I mice the proportion of EdU$^+$ cells which were colabelled with S100β was also decreased at both the total cord level, looking at WM and GM together (1.5 ± 0.4% vs. 3.9 ± 1.1% for G2F77I and WT animals, respectively $p < 0.05$, student's t-test, N=4 n=12) and also more specifically within the GM alone (1.6 ± 0.7% vs. 6.8 ± 2.4%, $p < 0.05$, student's t-test, N=4 n=12, figure 5.10D). The differentiation of newly proliferated EdU$^+$ cells into S100β$^+$ astrocytes was therefore decreased in both Ro15-4513 treated animals and G2F77I mutant mice compared to control animals.

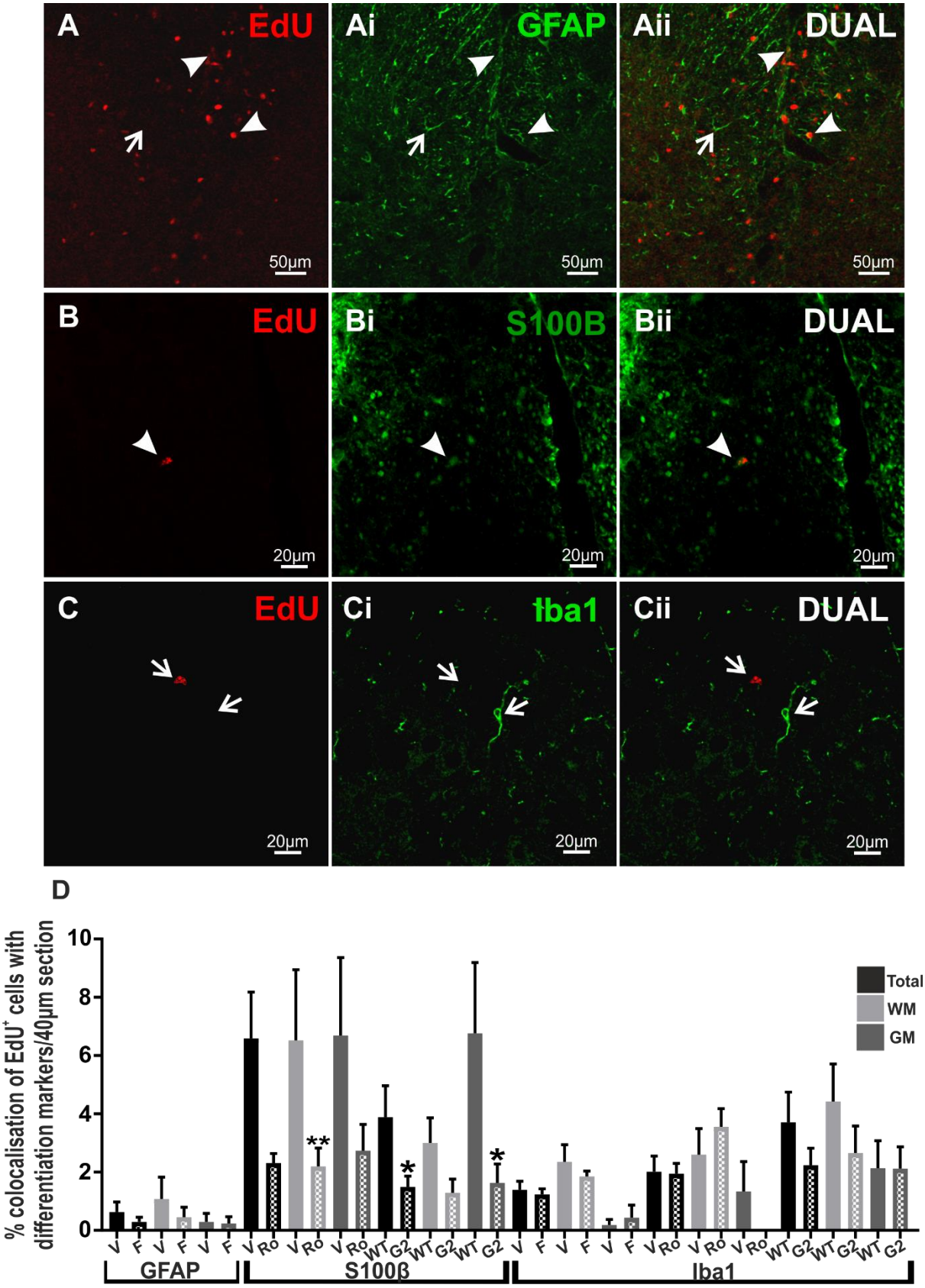
A
EdU
Ai
GFAP
Aii
DUAL
50µm
B
EdU
Bi
S100B
Bii
DUAL
20µm
C
EdU
Ci
Iba1
Cii
DUAL
20µm
D
% colocalisation of EdU+ cells with differentiation markers/40µm section
Total
WM
GM
GFAP
S100β
Iba1
V F V F V F V Ro V Ro V Ro WT G2 WT G2 WT G2

Figure 5.10 Ro15-4513 and G2F77I animals exhibit decreased proliferation of S100b$^+$ astrocytes compared to control animals

A-Bii: Representative confocal images illustrating the presence of EdU/GFAP$^+$ cells and EdU/S100β in the intact postnatal spinal cord **C-Cii**: Representative confocal images illustrating the presence of Iba1$^+$ microglia in the WM. Non-colocalised cells are labelled with open arrows. Closed arrows denote colocalised cells **D**: Average percentages of EdU$^+$ cells which were also either GFAP$^+$, S100 β$^+$, or Iba1$^+$ in both the WM and GM in each experimental condition (solid bars: vehicle treated/WT animals and hatched bars: experimental group, * $p <$ 0.05, ** $p <$0.01, one way ANOVA).

Iba1 was used to investigate microglial proliferation in the intact cord in an effort to determine whether changes in proliferation may be related to astrogliosis and microglial reactivity. Labelling with the microglial specific marker Iba1 revealed WM and GM which were sparsely populated with activated Iba1$^+$ microglia (figure 5.10C-Ci). which is common in healthy intact CNS tissue. The total percentage of EdU$^+$ cells which were also Iba1$^+$ was not significantly different from the percentage of EdU$^+$ cells which colocalised with either GFAP or S100β, indicating that reactive microglial proliferation was not increased in any of the groups examined when compared to proliferation of other 'healthy' glial cell types. Furthermore, although animals exhibited increased proliferation compared to controls, the percentages of EdU$^+$ cells which were Iba$^+$ were not significantly altered in either flumazenil, Ro15-4513 treated animals, or G2F77I mutant mice, compared to control (figure 5.10D).

5.4.9 Ro15-4513 treatment significantly increases proliferation of Sox2$^+$ NSCs in the spinal cord compared to vehicle

In these experiments there was frequent colocalisation of EdU$^+$ cells with S100B, Iba1, and PanQKI, indicating progression and differentiation of new EdU$^+$ cells into microglia, oligodendrocyte lineage cells, and astroglial. However, Sox2 /EdU$^+$ cells were the second largest population when compared to colocalisation of other markers with EdU (figure 5.12), indicating that a large proportion of the EdU$^+$ cells in both control and experimental groups

remained as undifferentiated NSCs which still expressed the stem cell marker Sox2. Sox2/EdU$^+$ cells were located in both the WM and GM (figure 5.11A-Aii and B-Bii). Furthermore, EdU$^+$ cells surrounding the CC were consistently immunoreactive for the transcription factor Sox2, thereby confirming the stem cell identity of these newly proliferated cells within the ECL of the CC region (figure 5.11B-Bii).

Flumazenil treated animals did not show any significant differences in the percentage of EdU$^+$ cells which were also Sox2$^+$ in either the WM, GM, or CC, compared to vehicle treated animals (figure 5.11C). The total percentage of EdU$^+$ new cells which were still residing in an undifferentiated state of stem cell readiness was also similar in both WT and G2F77I animals, 19% for WTs, and 20% for G277I animals, indicating that the proportion of newly proliferated Sox2$^+$ NSCs was not significantly different in G2F77I compared to WT littermates (figure 5.11C). Ro15-4513 treated animals however exhibited an increase in the percentage of EdU/Sox2$^+$ cells in the GM compared to vehicle treated animals (figure 5.11C). Animals treated with Ro15-4513 also had significantly more EdU/Sox2$^+$ cells at the CC compared to vehicle treated animals (2.2 ± 0.4 cells vs. 1.1 ± 0.3 cells, p <0.05, student's t-test, N=3 n=9, figure 5.11Ci).

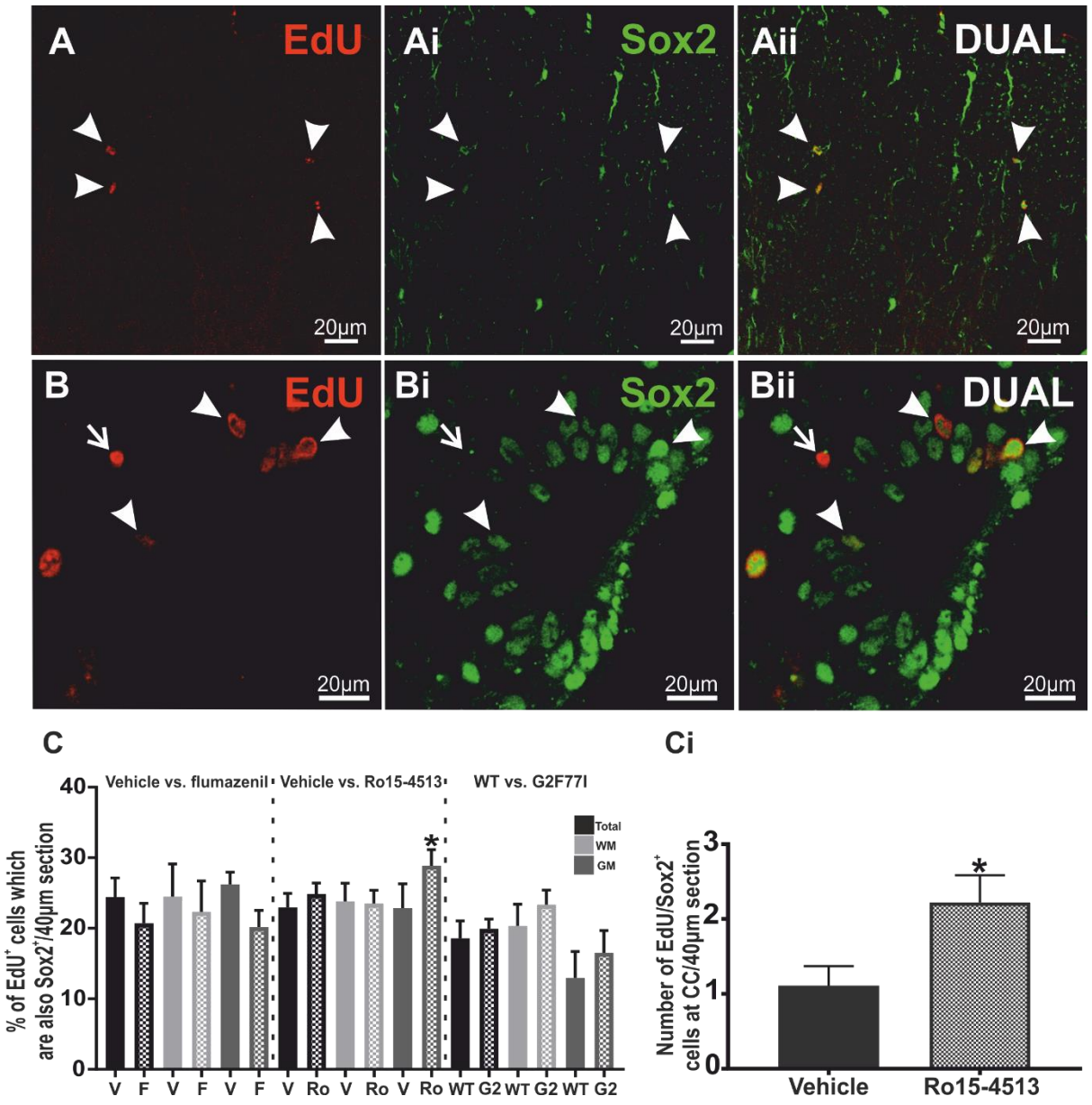

Figure 5.11 Proliferation of Sox2$^+$ NSCs is greater in Ro15-4513 animals vs. vehicle treated animals, this effect is specific to the GM and CC

A-Aii: Representative confocal images illustrating the presence of EdU$^+$ cells and Sox2$^+$ cells the WM. **B-Bii**: Representative confocal images of EdU$^+$ and Sox2$^+$ cells surrounding the CC. Colocalisation of EdU and Sox2 in the WM and CC are also shown (dual, closed arrows. Non-colocalised cells: open arrows) **C**: Pooled cell count data of EdU/Sox2$^+$ cells from the WM and GM of control (solid bars) vs. experimental animals (hatched bars) **Ci**: Pooled data for percentages of EdU$^+$ cells that are also Sox2$^+$ in the CC of vehicle and Ro15-4513 treated animals. (* p <0.05, student's t-test, N=3 n=9)

5.4.10 CBR modulation had mixed effects on neuronal cell differentiation

In all groups examined, evidence of neuronal differentiation of newly proliferated EdU^+ cells was very rare, that is very few EdU^+ cells were colocalised with the mature marker NeuN (figure 5.12). In both flumazenil vs vehicle treated animals and G2F77I vs WT animals, evidence of NeuN immunoreactivity within EdU^+ cells was absent in both the WM and GM regions, indicating a lack of neural differentiation in these experiments (data not shown).

However, in the GM of both vehicle and Ro15-4513 treated mice there were rare occurrences of EdU/$NeuN^+$ cells within the GM (~0.2% in both vehicle and Ro15-4513 treated mice). Upon inclusion of immature neurones in staining using Tuj, the average percentage of EdU^+ cells which colocalised with neuronal markers was increased to 0.9% in both vehicle and Ro15-4513 mice, indicating the importance of labelling for immature neuronal cells.

Ro15-4513 treated animals also showed a significant increase in the percentage of EdU/Tuj^+ compared to vehicle treatment suggesting a slight increase in neuronal proliferation, likely immature neurones as the same changes were not seen with the mature neuronal marker NeuN. Ro15-4513 treatment also resulted in significantly greater total numbers of EdU/Tuj^+ cells (1.3 ± 0.4 cells vs. 0.3 ± 0.12 in Ro15-4513 treated animals and vehicle treated animals, respectively, $p < 0.05$, N=3 n=9, figure 5.12A) and EdU/Tuj^+ cells specifi**c** to GM, compared to vehicle treated animals (1.3 ± 0.4 vs. 0.2 ± 0.2 cells, $p < 0.05$, N=3 n=9, figure 5.12A).

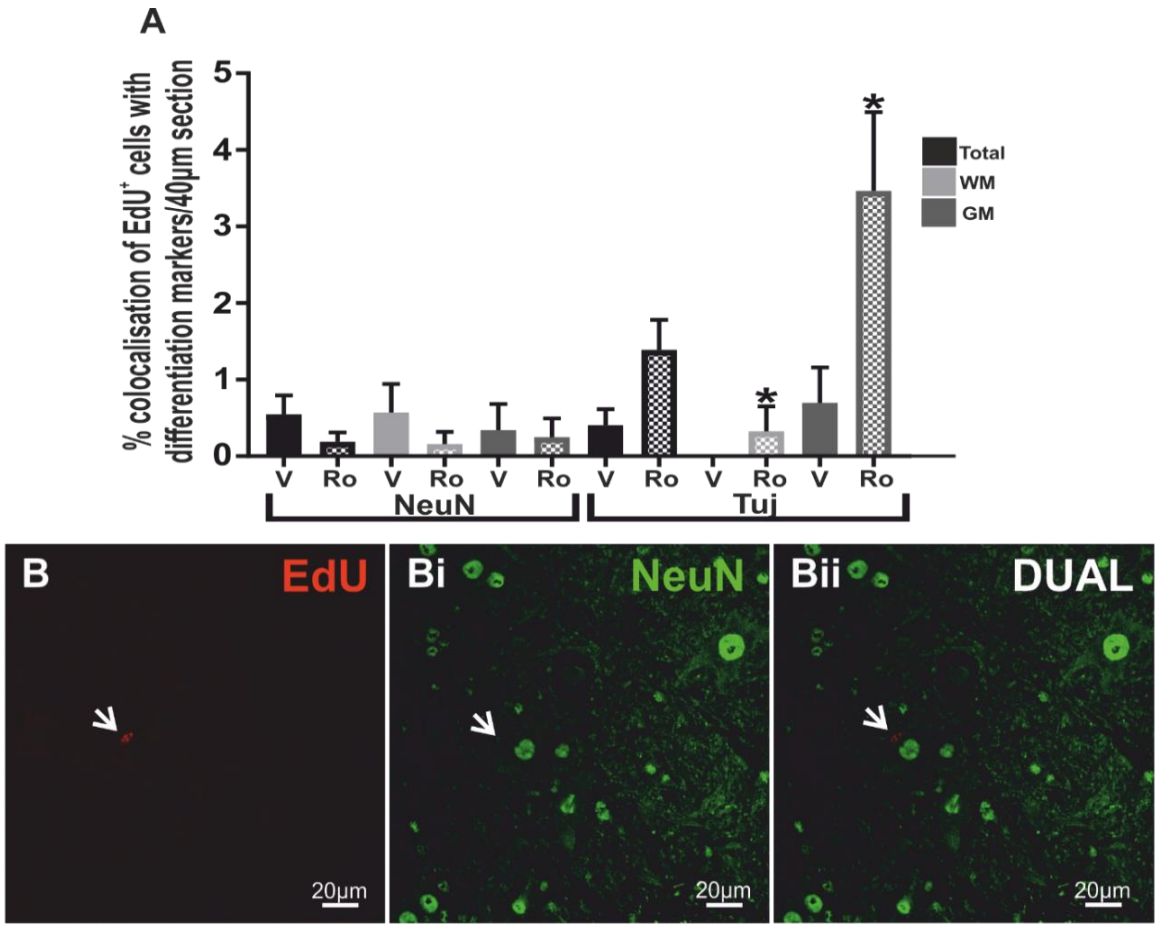

Figure 5.12 Ro1504513 treated animals possess a significantly greater percentage of EdU$^+$ cells which coexpress the imature neuronal cell type marker TuJ1 compared to vehicle treated animals

A: Pooled data illustrating percentages of EdU/NeuN$^+$ and EdU/Tuj$^+$ cells in the WM and GM of both vehicle (solid bars) and Ro15-4513 treated (hatched bars) animals. **B-Bii**: Representative confocal images illustrating that EdU$^+$ cells rarely colocalise with the mature neuronal marker NeuN (open arrows) (* = $p < 0.05$, student's t-test, N=3 n=9)

5.5 Discussion

5.5.1 Mixed modulation at TSPO and GABAaR reduces the level of postnatal proliferation in the spinal cord

Results described here provide evidence that proliferation within the adult spinal cord can be modulated by pharmacological agents which also bind at the endozepine-specific binding sites at GABAaR and TSPO. Much like DBI, MDZ and ETX are also able to bind and

modulate both GABAaRs and TSPO. Therefore, understanding the effects that these drugs have upon proliferation and differentiation within the adult spinal cord may provide insights into how these endogenous ligands may influence the postnatal proliferation within the intact spinal cord.

Following treatment with either MDZ or ETX, animals showed a significant reduction in proliferation within both the WM and GM compared to vehicle treated animals. Proliferation of cells within the NSC-containing EC layer of the CC was also curbed in animals treated with either MDZ or ETX compared to vehicle. These findings are the first to show that following binding at GABAaR and TSPO, MDZ and ETX negatively affect proliferation within the intact adult spinal cord. Furthermore, MDZ and ETX also act to significantly reduce proliferation within the already relatively dormant NSC-containing EC layer of the CC.

Results detailed here support the hypothesis that GABAaR and TSPO play a regulatory role in spinal cord proliferation. It is possible that both GABAaR and TSPO are influenced by endogenous modulators such as DBI, and upon binding to these same sites by MDZ and ETX, the regulation is lost, leading to a change in proliferation. In other neurogenic NSC-containing regions such as the SVZ and SGZ, GABAergic signalling negatively affects the level of cell turnover, restricting proliferation of NSCs, the findings from chapter 3 suggest that this may also be the case in the adult spinal cord. The negative effect of ETX and MDZ upon proliferation complements the results described in chapter 3 and strengthens the notion that much like other proliferative niches of the CNS, GABA is also an important regulatory signal of proliferation in the adult spinal cord.

5.5.1.1 ETX and MDZ may help reduce aberrant neoplastic proliferation

Although few have investigated the effects of MDZ upon NSC proliferation, many studies have investigated the effects of MDZ upon proliferation of tumour cells as a hopeful anti-proliferative agent for cancer therapy (Jiao *et al*., 2017). These reports show that MDZ reduces proliferation in a squamous cell carcinoma cell line (Dou *et al*., 2014), a malignant

glioblastoma line (Chen, Jingkao *et al*., 2016), and 2 different murine myeloid leukaemia cell lines (Mak *et al*., 1997; Jiao *et al*., 2017). Such findings highlight the importance of considering the use of endogenous regulators of proliferation such as GABA for reducing proliferation in situations of aberrant proliferation such as cancer. For example, TSPO, DBI and CBR sites have all been shown to be upregulated in human glioma and astrocytomas, where expression levels are linked to tumour malignancy and poor prognosis (Miettinen *et al*., 1995; Alho *et al*., 1995). It is possible that the high expression of DBI, TSPO, and CBR may play a role in the neoplastic growth of glial cells via GABAergic signalling, and that modulation of such pathways using drugs such as MDZ and ETX may suppress tumour proliferation in these cases.

5.5.1.2 The effect of MDZ upon proliferation negatively affects neonatal brain development

Others have shown that exposure to MDZ in developing brains reduces NSC proliferation *in vivo*, resulting in neurodegenerative (Duerden *et al*., 2016) and neuroapoptotic effects (Stevens *et al*., 2011). Early MDZ exposure and its effects upon proliferation and neurogenesis lead to future neurofunctional deficits (Xu, J. *et al*., 2019; Giri *et al*., 2018; Kang *et al*., 2017). These effects are particularly pronounced in preterm infants exposed to MDZ during procedures involved in neonatal intensive care. For example, preterm MDZ exposure is associated with macro- and microstructural alterations in hippocampal development, hippocampal dysmaturation, and poorer cognitive scores in later life (Duerden *et al*., 2016).

Furthermore, neonatal MDZ exposure in rats leads to decreased proliferation in the SVZ and SGZ and progressively poorer performances in the Morris water maze, in adulthood, suggesting impaired learning and memory/cognitive functions. The deleterious effects of neonatal MDZ exposure upon NSC proliferation and cognition in adulthood were ameliorated by the, previously reported neuroprotective agent, minocycline (Giri *et al*., 2018). These

effects are therefore likely a result of the detrimental effect of MDZ on NSC proliferation, leading to stunted hippocampal neurogenesis and development (Duerden *et al*., 2016). It would also appear that MDZ is having similar effects in the adult spinal cord.

GABA acts as a crucial signalling molecule to influence both the proliferation and differentiation of neural- and embryonic stem cells (Nguyen *et al*., 2003; Varju *et al*., 2001; Bolteus and Bordey, 2004), therefore it is unsurprising that MDZ, which mediates its effects through GABAergic modulation, can have profound effects on the normal proliferation and differentiation of neural cell types during development. Results described here are the first to show that, much like in the brain, MDZ also negatively impacts proliferation within the adult spinal cord, further illustrating the importance of GABA as a regulator of postnatal proliferation in the CNS.

5.5.1.3 ETX and MDZ may be affecting NSC proliferation by $Ca2^+$ mediated secondary signalling cascades

Zhao *et al*., (2012) examine the effects of MDZ on NSC proliferation, using cultured hippocampal NSCs. Similar to results described here MDZ treatment significantly reduced proliferation of hippocampal NSCs *in vitro*. MDZ also decreased the proportion of NSCs in the S-phase of the cell cycle and evoked a rapid increase in the intracellular calcium concentration within NSCs. Pre-treatment with the GABAaR antagonist bicuculline or the NKCC2 cotransporter furosemide partially rescued the MDZ-induced reduction in NSC proliferation and inhibited the increase in intracellular $Ca2^+$. These findings suggest that the effects of MDZ upon proliferation within cultured hippocampal slices were mediated by the activation of GABAaR, which is likely communicated to intrinsic secondary signalling cascades by the rise in intracellular $Ca2^+$ (Zhao, S. *et al*., 2012). Intracellular $Ca2^+$ signalling is essential for cell cycle progression and regulation of proliferation (Roderick and Cook, 2008). TSPO-specific ligands such as TTN have been shown to mediate their effects upon proliferation through their effects on $Ca2^+$ signalling (Gandolfo *et al*., 2001). It is therefore

possible that MDZ also reduces proliferation in the spinal cord as a result of changes in intracellular $Ca2^{+}$.

MDZ has also been shown to block voltage-dependent $Ca2^{+}$ channels in neurones, which is related to the caspase-8-independent proapoptotic pathway (Cheung So *et al*., 2013). This mechanism may also explain the beneficial effect of MDZ in tumour proliferation, as tumors are often found to over express $Ca2^{+}$ channels (Panner and Wurster, 2006). ETX has been shown to decrease the force of muscle contraction by inhibiting voltage dependent $Ca2^{+}$ channels (Zagorchev *et al*., 2018), and the beneficial effects of ETX in the amelioration of nerve damage and axonal recovery in animal models of both MS and traumatic brain injury have been hypothesised to be in part related to changes in $Ca2^{+}$ and its effect on secondary inflammatory cascades (Zagorchev *et al*., 2018; Sama and Norris, 2013). Therefore, much like MDZ, ETX may also influence proliferation via changes in intracellular calcium signalling cascades. However, whether this is also the case within the spinal cord is currently unknown

5.5.1.4 ETX and MDZ augment neurosteroidogenesis which may further influence proliferation

ETX and MDZ also have binding affinity at TSPO, where they have been shown to increase levels of the neuroactive steroids such as AlloP (Costa, B. *et al*., 2017; Liere *et al*., 2017; Verleye, Marc *et al*., 2005; Qiu *et al*., 2015). AlloP is an allosteric GABAergic modulator (Rupprecht and Holsboer, 1999; Lambert *et al*., 2009). The selective TSPO ligands PK11195 and 4'-cholorodiazepam mimic the neurotrophic effect of etifoxine, whereas the selective $GABA_A$ receptor ligands muscimol and bicuculline are ineffective at stimulating axonal repair and reducing the inflammatory environment (Girard *et al*., 2008). These results therefore suggest that the neurotrophic and neuroprotective effects of ETX could be mediated by TSPO and the concomitant stimulation of neurosteroidogenesis.

The unique duality of the mechanism of actions of MDZ and ETX therefore makes their effects upon proliferation and differentiation difficult to predict, especially as findings showed

that ETX had similar effects in GAD67-GFP animals with perturbed GABA levels. Therefore, whether the effects described here are the result of MDZ and ETX acting alone at GABAR, or a consequence of enhancement of the production GABAergic modulatory neurosteroids, such as AlloP, by binding to TSPO, or a synergistic effect of both, as seen in hippocampal long-term potentiation (Tokuda, K. *et al*., 2010), is as yet unknown. Further experiments using specific CBR or TSPO antagonists such as flumazenil or PK11195, respectively, or through attenuation of neurosteroidogenesis, by finasteride-induced inhibition of 5α-reductase, alongside MDZ and ETX treatment are therefore required to elucidate such mechanisms further.

Pharmacological treatment with the neurosteroid AlloP however has been found to enhance NSC proliferation and differentiation (Varga *et al*., 2009; Wang, Mingde, 2011; Wang, J.M. *et al*., 2010), promote neurogenesis, and positively influence learning and memory in trace eye-blink conditioning in mice (Wang, J.M. *et al*., 2010). It would therefore seem that the effect of neurosteroids upon GABAergic modulation of NSC proliferation and differentiation, as well as their increased synthesis by drugs such as MDZ and ETX, are not as simple as previously imagined. It is also currently unclear how the reported effects of AlloP upon NSC proliferation and differentiation would take place alongside the inhibition of proliferation by increased GABAergic signalling as previously reported.

5.5.1.5 Concomitant TSPO and GABAaR modulation decreases the level of oligogenesis in the spinal cord whilst increasing neurogenesis

In addition to the effects GABA has upon proliferation GABA also promotes differentiation of new born cells, processes which are also likely regulated by endozepinergic modulation of GABAergic signalling. Song *et al*., (2012) propose that a reduction in GABAergic signalling to NSCs increases symmetric and asymmetric division, thus augmenting the NSC pool and astrocyte production, respectively. Furthermore, Dumitru *et al*., (2017) report that a reduction in GABAergic signalling by OE of DBI in the SVZ leads to expansion of the NSC pool and a depletion of new born neurones, whereas DBI KD causes a reduction in the early progenitor pool with a concomitant shift toward neuronal differentiation. These findings illustrate the role GABA plays in the differentiation of postmitotic NSCs, where DBI acts to regulate this pathway, acting as a potent regulator of NSC self-renewal to delicately balance stem cell and mature populations (Dumitru *et al*., 2017).

Results described here suggest that GABA may also play a similar regulatory role in the spinal cord as animals treated with ETX exhibited an increase in EdU/NeuN^{+} cells, despite an overall decrease in proliferation, compared to vehicle treated animals. Furthermore, ETX treatment also resulted in a reduction in oligodendrocyte proliferation, despite others showing that ETX and enhances the proliferation and differentiation of new Olig2^{+} OPCs for myelin repair in an animal model of MS (Daugherty, D. J. *et al*., 2013). Previous studies have also shown that neurosteroids such as pregnanolone promote myelin repair after sciatic nerve injury in the same way as ETX (Girard *et al*., 2008; Schumacher *et al*., 2012; Koenig *et al*., 1995). Furthermore, administration of the steroid hormones oestrogen and testosterone has also been shown to be beneficial in treating MS symptoms (Gold *et al*., 2009; Soldan *et al*., 2003), while the neuroactive steroids progesterone and allopregnanolone have been effective in EAE (Yates *et al*., 2010). Neurosteroids have also been shown to increase oligodendrogenesis and expression of MBP, suggesting that they may aid in oligodendrocyte regeneration and remyelination in the spinal cord (Ghoumari *et al*., 2003; Ghoumari *et al*.,

2005). Results described here however show that ETX treatment significantly reduced the number of proliferating oligodendrocytes compared to vehicle, therefore further work is required to examine the effects of neurosteroidogenesis in the intact spinal cord

These findings may suggest that potentiation of GABAergic signalling in the spinal cord, either by direct modulation of GABAaR itself or by increased synthesis of GABAaR modulatory neurosteroids, results in a reduction in gliogenesis and an increase in neurogenesis. It therefore would appear that GABAergic mechanisms which regulate the NSC pool and the differentiation of new cells in the neurogenic niches of the SVZ and SGZ, and their regulation by endozepines such as DBI (Alfonso *et al*., 2013, Dumitru *et al*., 2017), are also important in the adult spinal cord.

Following ETX treatment there were significantly more EdU^+ cells which were colabelled with the mature neurone marker NeuN, suggesting that ETX treatment increased the number of new neurones in the adult spinal cord compared to vehicle. Although generally accepted to be the case in the SVZ and SGZ, and despite evidence that latent multipotent NSCs reside in the spinal cord, the existence of postnatal neurogenesis in the adult spinal cord is often contested. Whilst much work has shown that ECs constitute the NSC population of the cord which proliferate and differentiate to contribute to the glial scar following injury (Barnabe-Heider *et al*., 2010; Cregg *et al*., 2014; Sabelstrom *et al*., 2013) as yet there have been no conclusive *in vivo* studies which have detailed the birth of new neurones in the adult intact spinal cord. Furthermore, although ECs exhibit tripotent potential *in vitro*, these results have not been replicated *in vivo*, where lineage tracing studies of EC progeny show glial-restricted potential (Barnabe-Heider *et al*., 2010).

It is therefore surprising that the percentage of $EdU/NeuN^+$ cells in the adult spinal cord was seen to increase following ETX treatment and therefore further work must be carried out to confirm this finding. ETX however, has been shown induce axonal repair and neuronal recovery in animal models of MS (Daugherty *et al*., 2013) and peripheral nerve injury (Girard

et al., 2008), possibly due to its effects upon neurosteroidogenesis. Indeed, AlloP has been shown to induce neurogenesis and suppresses genes that repress cell proliferation (Charalampopoulos *et al*., 2008b; Charalampopoulos *et al*., 2008a).

It is possible however that ETX also acts as a neurogenic agent in the intact spinal cord Further work which also examines colocalisation of immature neuronal markers such as Tuj/b-tubulin III with EdU^+ cells, alongside that of mature neuronal markers such as NeuN, is required to determine whether these results are replicable Coadministration of ETX alongside blockers of neurosteroidogenesis, such as finasteride, would also help to determine whether the effects of ETX are a result of the attenuated synthesis of pro-neural neurosteroids such as AlloP, as is suggested in animal models of MS and peripheral nerve injury.

5.5.2 TSPO specific modulation by either -PK11195 or global TSPO KO gave diametrically opposed effects upon proliferation in the spinal cord

The binding of ETX and MDZ to TSPO and GABAaR resulted in a significant decrease in the number of EdU^+ cells in the spinal cord, indicating a reduction in the level of proliferation in the WM, GM, and at the CC. As ETX and MDZ have effects at both TSPO and GABA, it is difficult to determine which receptor may be causing these changes. Previous work has shown that GABA influences proliferation in the spinal cord (chapter 3), therefore more specific investigation into the effects of TSPO upon proliferation in the spinal cord was essential. To this end, the number of EdU^+ cells were examined in animals treated with the specific TSPO ligand PK11195 and in animals with global KO of TSPO compared to control. It was found that PK11195-treated animals had significantly fewer EdU^+ cells, and therefore a reduced level of proliferation, in the WM, GM, and CC regions of the spinal cord compared to vehicle treated animals. TSPO KO animals however possessed significantly greater numbers of EdU^+ cells in the WM and GM compared to WT littermates. There were no significant differences in the number of EdU^+ cells at the CC in TSPO KO animals compared

to control. The original hypothesis was that similar results would be found for both PK11195 treatment and following global TSPO KO as the mechanism of both includes the perturbation of TSPO function, however it seems that this is not the case.

5.5.2.1 PK-11195 treatment inhibits proliferation in both *in vitro* and *in vivo* models

In agreement with the findings presented here, previous work has shown that PK-11195 inhibited proliferation of human colorectal carcinoma cells (Maaser *et al*., 2001) and growth of multiple myeloma cells growth *in vitro*. PK-11195 has also been shown to chemosensitise drug-resistant human-derived multiple myeloma tumours in immunodeficient mice (Campbell *et al*., 2006), leading to marked inhibition of tumour growth in animals treated with both PK-11195 and melphalan compared to animals treated with melphalan alone (Campbell *et al*., 2006). Similar effects have also been seen following PK-11195 treatment of pre- and post-relapse neuroblastoma cell lines (Mendonça-Torres and Roberts, 2013), and in glioblastoma cell lines (Bode *et al*., 2012; Chen, J. *et al*., 2013). Bruce *et al*., (1991) also illustrate that PK-11195 inhibits proliferation of astrocytes *in vitro*, suggesting that PK-11195 may not only inhibit proliferation of neoplastic tumour cells, but also 'healthy' glial cells (Bruce *et al*., 1991). It is possible that the effects of PK11195 in our experiments were the result of a reduction in glial cell proliferation in particular, and therefore more work using markers of glial differentiation such as S100β or GFAP alongside EdU labelling is necessary to investigate this further.

In contrast to the above findings, PK11195 has been shown to be anti-apoptitic when used at concentrations close to its affinity for TSPO whereupon administration at higher concentrations elicits pro-apoptotic effects which does not appear to be related to TSPO binding (Veenman and Gavish, 2012; Veenman *et al*., 2007). This dose-dependent mechanism may explain why PK11195 reduced proliferation in the spinal cord, whereas TSPO KO increased proliferation.

Analysis of the thermodynamic properties of PK1195 has suggested that it acts as a TSPO antagonist (Le Fur *et al*., 1983), leading to the hypothesis that TSPO KO would produce similar results to PK11195. However, later *in vivo* and *in vitro* studies have shown that this broad pharmacological classification of these compounds is not always applicable, and that PK111195 also acts as a weak partial agonist at TSPO (Papadopoulos *et al*., 1990). Furthermore, recent work has also shown that hepatic metabolism of PK-11195 causes a switch in the pharmacological properties of the ligand at TSPO, where *N*-demethylation of PK11195 alters the interaction with the binding pocket of the constitutive androstane receptor causing PK11195 to act as an agonist (Mackowiak *et al*., 2017). Such a metabolic switch may explain the opposing pharmacological properties of PK11195 in different systems. Therefore, predicting the antagonist effect PK11195 may have upon spinal cord proliferation, and that TSPO KO would cause similar effects was too simplistic, leading to the opposing results described here. Additional experiments comparing the effects of the TSPO agonist FGIN-127 upon proliferation in the spinal cord to those seen in TSPO KO mice would help determine if PK11195 is indeed acting as an agonist here.

5.5.2.2 TSPO and neurosteroidogenesis

TSPO is an evolutionarily well conserved outer mitochondrial membrane OMM protein which is highly expressed in steroidogenic cells of the adrenal glands and testis (De Souza *et al*., 1985; Veenman and Gavish, 2012). Exposure to TSPO ligands at close to their binding affinities was found to stimulate steroid synthesis in adrenal cortical cells (Mukhin *et al*., 1989), testicular Leydig cells (Papadopoulos *et al*., 1990), and neurosteroid production in glial cells (Costa, E. and Guidotti, 1991; Papadopoulos, 1993) which lead to the hypothesis that TSPO was involved in steroidogenesis, including neurosteroidogenesis in the CNS. For example, DBI and TTN have been shown to stimulate steroidogenesis in glioma originating mitochondria (Papadopoulos *et al*., 1991; Costa, E. and Guidotti, 1991).

Neurosteroids exhibit neuroprotective, anti-inflammatory, and neurogenic effects within the CNS, as described previously (Borowicz *et al*., 2011; Varga *et al*., 2009; Noorbakhsh *et al*., 2014). It was therefore hypothesised that inhibition of TSPO function by PK11195 may influence proliferation of NSCs of the spinal cord by inhibiting the production of neurosteroids. Indeed, PK11195 did result in a significant reduction in proliferation in the spinal cord, however as TSPO KO did not produce the same results, instead resulting in an increase in proliferation, it is unlikely that effects of PK11195 on proliferation are a result of a simple inhibition of neurosteroidogenesis. In order to assess this possibility further, coadministration of PK11195 alongside compounds to inhibit neurosteroidogenesis, such as finasteride, would elucidate the effects PK11195 may have upon neurosteroidogenesis in this system and the effects this may have upon proliferation and differentiation.

The dogma that TSPO function is essential for steroidogenesis was born when experiments which attempted to generate TSPO KO mice illustrated that heterozygous global TSPO KO was embryonic lethal (Papadopoulos *et al*., 1997). However, more recently animals with global TSPO KO from birth have shown to be viable, indeed the TSPO KO model here was one of the first to show that pups with global TSPO KO were possible. Viable global TSPO KO mice therefore cast doubt on the idea that TSPO function, and the irrefutable role it plays in steroidogenesis and neurosteroidogenesis is essential for survival.

Therefore, the effects described here may be unrelated to neurosteroidogenesis and the effects these compounds have upon proliferation and instead could a result of one of the many other proposed functions of TSPO, including inducing apoptosis by the increased production of reactive oxygen species. For example, the TSPO agonist FGIN-127 has been shown to induce apoptosis in cancer cells by this signalling mechanism (Maaser *et al*., 2001; Sutter *et al*., 2003; Veenman *et al*., 2007; Santidrian *et al*., 2007). It is therefore possible that PK11195 significantly reduces the number of EdU^+ cells compared to vehicle treatment by inducing apoptosis of NSCs, whereas TSPO KO increases the proliferation within the spinal cord compared to WT by attenuation of the pro-apoptotic TSPO-mediated pathways.

5.5.3 Changes in proliferation and differentiation following CBR modulation suggests endozepinergic regulation of GABAergic signalling in the adult spinal cord

Previous work has shown that GABA is also an important modulator of proliferation in the intact postnatal spinal cord (chapter 3), where an increase in the level of ambient GABA by vigabatrin significantly decreased the number of proliferative EdU^+ cells. Work described here has also shown that PAM of GABAaR by the CBR-specific ligand MDZ also results in a reduction in the number of EdU+ proliferating cells, suggesting that this modulatory region of the GABAaR may be involved in the inhibitory GABAergic tone which appears to dampen proliferation in the spinal cord.

The endogenous CBR ligand DBI is robustly expressed in the spinal cord. Utilising the CBR site ligands flumazenil and Ro15-4513 allowed for investigation to determine whether endogenous binding at CBR in the spinal cord may also balance proliferation and differentiation via GABAaR, as in SVZ and SGZ. Indeed, flumazenil and Ro15-4513 treated animals exhibited greater levels of proliferation compared to vehicle treated animals. Differentiation of EdU^+ cells into $S100b^+$ glial cells was reduced in Ro15-4513 treated animals compared to control, however the proportion of EdU^+/Tuj^+ cells increased. The percentage of EdU^+ cells which were $sox2^+$ was also greater in Ro1504513 treated mice vs. vehicle treatment. Using G2F77I mice to alter the binding affinity to CBR also increased proliferation in the spinal cord, with a decrease in gliogenesis, compared to WT animals. These results therefore suggest that modulation of GABAergic signalling by endogenous CBR ligand binding may also influence proliferation in the spinal cord.

5.5.3.1 Does flumazenil show intrinsic efficacy without exogenous BZ binding?

As flumazenil mediates its effects by competitive inhibition at the CBR site it is debated whether flumazenil itself has intrinsic activity, or produces behavioural effects, in the absence of exogenous BZ administration. For example, Marten *et al*., (1993) report that

flumazenil has no effect in rotarod testing of motor deficits and offers no protection against pentylenetetrazole- or audiogenic-induced seizures in mice, and therefore conclude that flumazenil exhibits little to no intrinsic efficacy in these cases (Martens, F. *et al*., 1990). Flumazenil has also been shown to have no effect upon anxiety-like states in rodents exposed to the open field test (Nazar *et al*., 1997) and did not evoke anxiety in quiescent human volunteers (Darragh *et al*., 1983).

In direct contrast to these findings however, it was shown that flumazenil reduced social interaction in rats and mice, suggesting an increase in 'anxiety' (File and Pellow, 1985; Uhlirova *et al*., 2004). Flumazenil also exhibited an anxiogenic-like profile in the elevated plus maze (Lee, C. and Rodgers, 1991). Others however, have shown that in rodents flumazenil also produces anxiolysis in several behavioural tests including the elevated plus maze (Belzung *et al*., 2000) and measurements of ultrasonic vocalisation (Hess *et al*., 2013). These findings therefore suggest that flumazenil has inconsistent behavioural effects which may be dependent upon several factors, including the behavioural paradigm in question, the basal level of anxiety, or the result of the different doses of flumazenil used in such studies (Uhlirova *et al*., 2004). However, such results suggest that flumazenil may indeed have intrinsic efficacy in certain neurological systems and lend support to the existence of endogenous CBR ligand modulation of GABAaR.

Results described here also give evidence for intrinsic efficacy of flumazenil as flumazenil treatment significantly increased the number of EdU^+ cells in the spinal cord of adult animals compared to vehicle. This effect may be mediated by the effects flumazenil would have upon endogenous CBR ligand binding.

5.5.3.2 Endozepines and CBR ligands

The presence of endogenous ligand binding to the CBR site of GABAaR may explain why flumazenil has been shown to have intrinsic activity and behavioural effects in the absence of exogenous BZ admin. Flumazenil may also exhibit inconsistent behavioural effects due to the presence of endogenous ligands of the CBR site in the CNS, for example the endozepines DBI and the CBR site-specific fragment ODN. The action of flumazenil, which inhibits binding of these endogenous peptides to the CBR site (Slobodyansky *et al*., 1989), is therefore likely to be dependent upon the effect of DBI and ODN upon GABAaR signalling. However, the effects of endozepines upon GABAergic signalling are still undefined many systems/regions, therefore making it difficult to predict the effects flumazenil may have without exogenous BZ administration.

For example, if DBI or ODN act as inverse agonists/NAMs at GABAaR, then removal of basal binding of these ligands by flumazenil could be hypothesised to lead to an anxiolytic profile of flumazenil. Indeed, some studies have reported flumazenil to act as an axiolytic and also as a sedative (Hess *et al*., 2013), which could also be explained by the removal of a NAM at CBR by flumazenil. Many studies have shown that ODN and DBI act as inverse agonists/NAMs at GABAaRs both *in vitro* and *in vivo* (Costa and Guidotti, 1991; Alfonso *et al*. 2012; Dumitru *et al*., 2017; Bormann *et al*.,1991; Slobodyansky *et al*., 1989). For example, studies conducted by Bormann *et al*., (1988) and MacDonald *et al*., (1986) show that micromolar concentrations of rat brain DBI, which were insufficient to affect the gating of $GABA_AR$ channels, reduced the GABA-activated Cl^- current in a dose dependent manner, as measured by whole-cell patch clamp electrophysiology in primary cultures of mouse embryonic spinal cord. Bormann *et al*., (1985) not only provided seminal findings illustrating the NAM action of DBI, but also showed that reduction of GABA responses by DBI did not occur in the presence of flumazenil, indicating that DBI affects GABA-induced Cl^- currents by direct interaction with the CBR site of $GABA_AR$. It is currently unknown whether this is the

case in all regions of the CNS, particularly as heterogeneity in specific alpha subunit expression is seen in different areas of the CNS.

Whilst it may be difficult to predict the effects of DBI in all CNS regions/systems Alfonso *et al*, (2012) and Dumitru *et al*., (2017), show that DBI and ODN do indeed act as NAMs at CBR and regulate the level of proliferation and differentiation in the neurogenic niches of the SVZ and SGZ. It appears that DBI and ODN are important regulators of postnatal neurogenesis; acting to balance the inhibitory nature of GABAergic signalling upon NSC proliferation to increase the proliferating NSC pool. These effects are attenuated however following flumazenil treatment or disruption to CBR site binding by mutation of crucial amino acids for the formation of the CBR site in G2F77I mice. (Alfonso *et al*., 2012; Dumitru *et al*., 2017). Results described here are the first to show that similar mechanisms involving endozepinergic modulation of GABAergic signalling may also control the basal level of proliferation in the spinal cord as proliferation was significantly greater in both flumazenil treated and G2F77I mutant mice compared to control.

DBI and ODN have been shown to induce anxiety and pro-conflict behaviour (De Mateos-Verchere *et al*., 1998) further suggesting inverse agonist activity of endozepines. Increased levels of DBI-like immunoreactivity have been found in the CSF of patients with severe depression and anxiety (Barbaccia *et al*., 1986) and following psychological stress in mice (Katsura *et al*., 2002) and rats (Sudakov *et al*., 2001). Differences in baseline levels of anxiety, perhaps related to the level of endogenous DBI or ODN binding to CBR, therefore also appear to affect the actions of flumazenil. It appears that when anxiety is high, such as during benzodiazepine withdrawal, flumazenil appears as an anxiolytic: however, when anxiety is low, flumazenil increases anxiety (Uhlirova *et al*., 2004; File *et al*., 1990). For example, in sociable mouse strains, flumazenil produced anxiogenic-like effects by inducing timidity (Uhlirova *et al*., 2004). However, flumazenil produced anxiolytic effects in the elevated plus maze and the light/ dark test in BALB/c mice, a more ‘anxious’ mouse strain but not in ‘low-anxiety’ C57BL/6 mice (Belzung *et al*., 2000; Belzung and Griebel, 2001).

Significant differences in brain levels of DBI have been found in two inbred rat strains which exhibit different basal levels of anxiety-like behaviour (Suzdak *et al*., 1986). The biphasic effect of flumazenil upon anxiety could therefore be explained by the difference in the level of DBI/ODN binding, and its effect upon GABAaR signalling, in anxious vs. non-anxious subjects.

However, if endozepines are primarily agonists/PAMs of GABAaR signalling flumazenil would be expected to induce anxiety by reducing the inhibitory GABAergic tone following removal of DBI/ODN binding at CBR. Whilst most studies have shown that DBI and ODN act as NAMs of GABAaR and that flumazenil has anxiolytic properties (Alfonso *et al*. 2012; Dumitru *et al*., 2017; Bormann *et al*.,1991; Slobodyansky *et al*., 1989) others have reported that DBI acts as a PAM of GABAaR signalling in select neuronal populations. For example, Christian *et al*., (2013) show that DBI potentiates GABAergic signalling in the reticular thalamic nucleus of the hypothalamus, and that this effect is blocked by flumazenil (Christian *et al*., 2013).

It therefore appears that endozepines such as DBI and ODN are able to act as both PAMs and NAMs of GABAaR depending upon the specific system in which the GABAergic signalling is implicated. The dual action of DBI and ODN upon modulation of GABAergic signalling may also explain why flumazenil also has seemingly contradictory behavioural effects. It is also possible that the subunit heterogeneity of GABAaRs, and therefore the different ways in which the CBR site can be formed, may be the cause of such diametrically opposed effects of the CBR ligands; endozepines and flumazenil.

5.5.3.3 Is the endogenous CBR ligand a GABAaR PAM in the spinal cord?

Although Alfonso *et al*., (2012) and Dumitru *et al*., (2017) show that DBI and ODN are potent regulators of proliferation and differentiation in the SGZ and SVZ, respectively, less it known about how regulation of GABAaR by CBR site binding may affect these processes in the

adult spinal cord. Work detailed in this chapter is the first to show that these mechanisms may also be important in the spinal cord

Following alteration of CBR function by a variety of means, these results strengthen the hypothesis that endogenous modulation of GABAaR by endozepinergic compounds influences basal proliferation and differentiation in the postnatal spinal cord. For example, in instances of decreased binding affinity to CBR as seen in G2F77I mutant mice, or competitive antagonist activity at CBR following flumazenil treatment, the basal level of proliferation is significantly greater compared to control animals. These results suggest the presence of an endogenous molecule bound to CBR, which influences GABAergic tone to negatively modulate basal proliferation in the postnatal intact spinal cord, which, following interruption or blocking of its binding to CBR, in G2F77I mutant- and flumazenil treated animals, respectively, releases the negative GABAergic tone on proliferation and therefore proliferation increases. A similar mechanism has been described in the both the hippocampus and SVZ for DBI, where DBI OE leads to an expansion of the NSC pool, via a reduction in GABAergic signalling, in the SVZ, this effect is blocked by flumazenil and attenuated in G2F77I mice (Alfonso *et al*., 2013; Dumitru *et al*., 2017). However, if this were also the case for the spinal cord, the endozepinergic molecule in question would be acting as a PAM, rather than the NAM action described in the hippocampus and SVZ. Indeed, PAM activity of endozepines such as DBI is evident in the reticular thalamic nucleus, where is it secreted by nearby astrocytes to influence GABAergic tone (Christian, Catherine A. and Huguenard, John R., 2013; Christian *et al*., 2013). Glial cells of the spinal cord also express DBI (Chapter 4) and so a similar paracrine feedback loop may also exist within the spinal cord to regulate proliferation and differentiation.

Furthermore, animals treated with the CBR-specific inverse GABAaR agonist Ro15-4513 also have greater levels of proliferation, $Sox2^{+}$ NSCs, and a reduced level of gliogenesis compared to vehicle treated animals. These results further suggest the existence of a positive endogenous CBR-specific molecule which is involved in the GABAaR mediated

dampening of proliferation in the adult spinal cord by PAM of GABAaR at CBR. For example, inverse agonist functionality requires constitutive receptor activity (Khilnani and Khilnani, 2011; Kenakin, 2001), therefore Ro15-4513 reverses CBR mediated inhibitory GABAergic tone, resulting in an increase in proliferation and a decrease in differentiation.

In conclusion, whilst it appears that modulation of GABAaR at CBR is an important mechanism in the control GABA exerts over proliferation in the spinal cord the exact molecule responsible for the actions in the spinal cord is still elusive. Although results described here have illustrated that it is an endozepinergic-like compound, we are unable to conclude with absolute certainty that it is DBI or its derivatives, despite robust expression of these proteins within the postnatal spinal cord Further work is required to determine the molecular identity of this particular modulator and specific effects it has upon proliferation and differentiation in the CNS

5.6 Conclusion

The experiments carried out in this chapter have shown that endozepines may be present in the spinal cord to regulate proliferation by acting in concert at both TSPO and GABAaR. Furthermore, experiments using the GABAaR CBR site antagonist flumazenil suggest that endogenous ligand binding at the CBR site may regulate quiescence in the spinal cord as seen in other neurogenic niches.

Chapter 6 – CBR modulation does not boost the number of new oligodendrocytes produced in the spinal cord following focal LPC-induced demyelination

6.1 Introduction and rationale

Work presented in Chapter 5 showed that modulation of GABAaR by the endogenous CBR site competitive antagonist flumazenil significantly increased the number of EdU^+ cells in the intact spinal cord of adult animals compared to vehicle treatment. On average animals treated with flumazenil had 18% more EdU^+ cells in the spinal cord compared to vehicle treated animals. This change was specific to the WM as there was no significant difference in the numbers of EdU^+ cells present in the GM of flumazenil treated animals compared to vehicle treatment.

It was hypothesised that the WM-specific increase in EdU^+ cells may represent an increase in the proliferation of OLCs in flumazenil treated animals. Staining for the mature and immature oligodendrocyte marker PanQKI was therefore carried out to examine whether flumazenil treated animals had a significantly greater percentage of EdU^+ cells which were also $PanQKI^+$ compared to vehicle treated animals. However, there were no significant differences in the proportion of EdU^+ cells which were $PanQKI^+$ OLCs, therefore indicating that whilst flumazenil treated animals had more EdU^+ cells in the WM, these cells did not differentiate into $PanQKI^+$ OLCs to increase the population of $EdU/PanQKI^+$ cells compared to vehicle treated animals in the intact spinal cord.

Preliminary results from our lab have shown that although it is possible to increase proliferation in the intact adult spinal cord by modulation of neurotransmission, the numbers of EdU^+ cells appear to decrease and return to a baseline level of proliferation by 14 days post EdU treatment (Deuchars lab, unpublished observation). Genetic fate mapping experiments have illustrated that proliferation within the intact adult spinal cord is limited and occurs only for the purpose of self-renewal and cell population maintenance (Barnabe-Heider *et al*., 2010; Meletis *et al*., 2008). Whilst proliferation increases exponentially following spinal cord injury, these cells differentiate and migrate toward the injury site, replacing lost astrocytes and oligodendrocytes and contribute to the sealing of the lesion

cavity by formation of the glial scar (McDonough, Ashley and Martínez-Cerdeño, 2012; Barnabe-Heider *et al*., 2010; Meletis *et al*., 2008; Sabelstrom *et al*., 2013). Indeed, it has also been shown that injury-induced proliferation in the spinal cord also dissipates over time (McDonough, Ashley and Martínez-Cerdeño, 2012; Lacroix *et al*., 2014), suggesting that as the need for increased numbers of astrocytes and oligodendrocytes for tissue repair wanes in the time after injury, so too does the increased level of proliferation.

It is therefore unsurprising that in the intact spinal cord, where maintenance of the cell population size is crucial, flumazenil-induced increases in the proliferative cell population does not also result in differentiation of these new cells. In these animals the oligodendrocyte population is likely already at its peak, and therefore these new cells are surplus to the needs of the intact cord. Indeed, recent *in vivo* imaging work has shown that oligodendrocyte apoptosis frequently occurs in the adult rodent brain, where most OLCs die prior to committing to myelination (Hill *et al*., 2018; Hughes *et al*., 2018). This therefore sparks the question as to what would happen if we were to give flumazenil, and boost the cell population, in a situation where more cells, and their differentiation, would be beneficial. For example, what would happen if we were to induce demyelination and tissue injury to the WM and then boost the numbers of proliferative cells by flumazenil? Work presented here aims to examine the effects of demyelination upon proliferation within the postnatal spinal cord. The effect of demyelination upon the proliferation and differentiation of cells, particularly of EdU/PanQKI$^+$ OPCs in the spinal cord of flumazenil vs. vehicle treated animals is also considered.

Our experiments were particularly focused on looking at the numbers of new EdU/PanQKI$^+$ oligodendrocytes after LPC induced focal demyelination, using CBR site manipulation via flumazenil in an attempt to increase the level of proliferation and differentiation of these crucial cells for repair of demyelinated lesions. In order to determine whether demyelination-induced oligodendrocyte death results in the differentiation of EdU$^+$ cells to replace the cells which have been lost by the demyelination, a model of focal demyelination was employed

here. Focal areas of demyelination were induced by direct intraspinal injection of the gliotoxin lysophosphatidylcholine (LPC) into the spinal cord dorsal column WM of adult mice (figure 5.1)

LPC is a bioactive lipid with detergent-like activity which is capable of solubilizing membranes and producing rapid demyelination of WM tracts at the injection site (Hall, 1972). Focal Injection of 1% LPC results in demyelination in the spinal cord (Hall, 1972; Keough *et al*., 2015), brainstem (Pratt *et al*., 1991), caudal cerebellar peduncle (Woodruff and Franklin, 1999), and the corpus callosum (Sahel *et al*., 2015). LPC selectively targets myelin and leaves other cellular components relatively unaffected, resulting in the recruitment of T and B immune cells, microglia and macrophages to the lesion site (Keough *et al*., 2015; E Marzan *et al*., 2018). This procedure therefore produces a well characterized and focused demyelinating injury consisting of macrophage/microglial infiltration and activation (E Marzan *et al*., 2018; Miron *et al*., 2013; Kotter *et al*., 2001), reactive astrogliosis, disruption of axonal homeostasis and axonal injury, and OPC proliferation and migration (Keough *et al*., 2015; Lau *et al*., 2012).

The LPC lesion exhibits precise temporal regulation over a period of a few weeks and is eventually capable of full remyelination, a process which begins at the end of the first week following removal of myelin debris (Woodruff and Franklin, 1999; Ghasemlou *et al*., 2007; Blakemore and Franklin, 2008; Keough *et al*., 2015). At 1-3dpi days there is active demyelination at the site of LPC injection. During days 3-7, OLCs proliferate extensively and are recruited to the lesion site which then differentiate into mature myelinating oligodendrocytes by 7-10 dpi. At 10-21 dpi there is evidence of active remyelination (Keough *et al*., 2015). Remyelination following LPC injection is faster compared to other toxin-induced demyelination models as OPCs are unaffected (Blakemore and Franklin, 2008). Furthermore, LPC does not induce loss of astrocytes or macrophages which also facilitates faster remyelination (Bjelobaba *et al*., 2018).

In vivo models of demyelination are frequently used to investigate the processes of demyelination and remyelination in the CNS in order to understand the processes which govern the proliferation and differentiation of OPCs and their ability to generate and remodel axonal myelin throughout the lifespan of the CNS (Young, K.M. *et al*., 2013; Osorio-Querejeta *et al*., 2017). These models also provide clues as to ways in which new therapeutic strategies could be employed to promote the proliferation and maturation of OPCs to replace lost myelin in diseases such as MS.

MS is a chronic demyelinating disease of the CNS which is characterised by immune cell infiltration, oligodendrocyte death, and neuronal and axonal degeneration. MS typically follows a relapsing-remitting disease course consisting of inflammatory relapses and periods of neurological decline, followed by periods of symptom remission (Keough *et al*., 2015). Remyelination in MS does occur in humans, however in the majority of patients, this process is incomplete (Patrikios *et al*., 2006; Goldschmidt *et al*., 2009). Remyelination is also present in animal models of demyelination, however its efficiency declines with age and disease severity (Blakemore, 1977; Jeffery and Blakemore, 1995; Shields *et al*., 1999). Myelin provides metabolic support to underlying axons (Funfschilling *et al*., 2012; Lee, Y. *et al*., 2012), and with an absence of treatments that halt disease progression, patients with MS eventually exhibit progressive neurological decline likely due to neuroaxonal degeneration as a result of chronic demyelination (Irvine and Blakemore, 2008). New treatments to boost the endogenous OPC population to enhance remyelination in these patients is therefore essential. Modulation of GABAaR niche signalling to enhance the endogenous proliferating cell population in the spinal cord may provide a new source of reparative cells for this purpose.

For successful remyelination several processes must occur; OPCs need to proliferate, migrate toward the demyelinating lesion site, and mature into myelinating oligodendrocytes which contact and enwrap axons (Harlow *et al*., 2015; Osorio-Querejeta *et al*., 2017). Although flumazenil is capable of increasing the number of proliferative EdU^+ cells in the

intact spinal cord, where 30% of these new cells are PanQKI$^+$ OLCs (Chapter 5), the numbers of new PanQKI$^+$ OLCs were unchanged compared to vehicle treatment. It was hypothesised that this is because these new cells are not necessary in the intact cord as cell population size is strictly controlled to balance self-renewal and cell death. Therefore, in conclusion, work described here attempts to use intraspinal LPC treatment to recapitulate demyelinating lesions seen in MS *in vivo,* and examine whether demyelination provides differentiating cues for the replacement of lost myelin by flumazenil-induced augmentation of proliferation.

6.2 Aims

The aim of the work described in this chapter was to investigate whether flumazenil was also capable of increasing proliferation following focal LPC-induced demyelination in the spinal cord. Proliferation of PanQKI$^+$ oligodendrocytes following focal LPC injection in animals treated with either vehicle or flumazenil was also investigated in order to determine whether modulation of GABAaR by blocking endogenous ligand binding to the CBR site may be a possible mechanism for increasing the numbers of oligodendrocytes after a demyelinating insult to the adult spinal cord.

6.3 Methods

6.3.1 Animals

Adult (6-8 weeks) male C57Bl/6 mice (*N*=12) were used in line with the UK animals (Scientific Procedures) Act 1986 and ethical standards set out by the University of Leeds Ethical Review Committee. Every effort was made to minimise the number of animals used and their suffering. Animals were given ad libitum access to food and water and were housed in a 12-hour light dark cycle.

6.3.2 Experimental design

Full details of the materials and methods used for the *in vivo* intraspinal LPC injection, postoperative care, treatment with EdU and flumazenil, and post-hoc tissue processing and analysis are present in section 2.4. The rationale for these methods is also discussed.

Animals were randomly assigned to 3 experimental groups: 1. intraspinal LPC injection and I.P flumazenil (*N*=3), 2. intraspinal saline injection and I.P flumazenil (*N*=3), and 3. intraspinal LPC injection and I.P vehicle (*N*=3). Animals that had received 5 days of EdU and flumazenil treatment, but had not received intraspinal injections, were used as intact controls (*N*=3).

6.3.3 Thoracolumbar intraspinal injections of either saline of LPC

Animals received direct intraspinal injections to the dorsal column at a depth of 300 μm, of 1 μl of either 1% LPC, to induce focal demyelinated lesions, or saline, in the dorsal column of the thoracolumbar region of the spinal cord (figure 6.1).

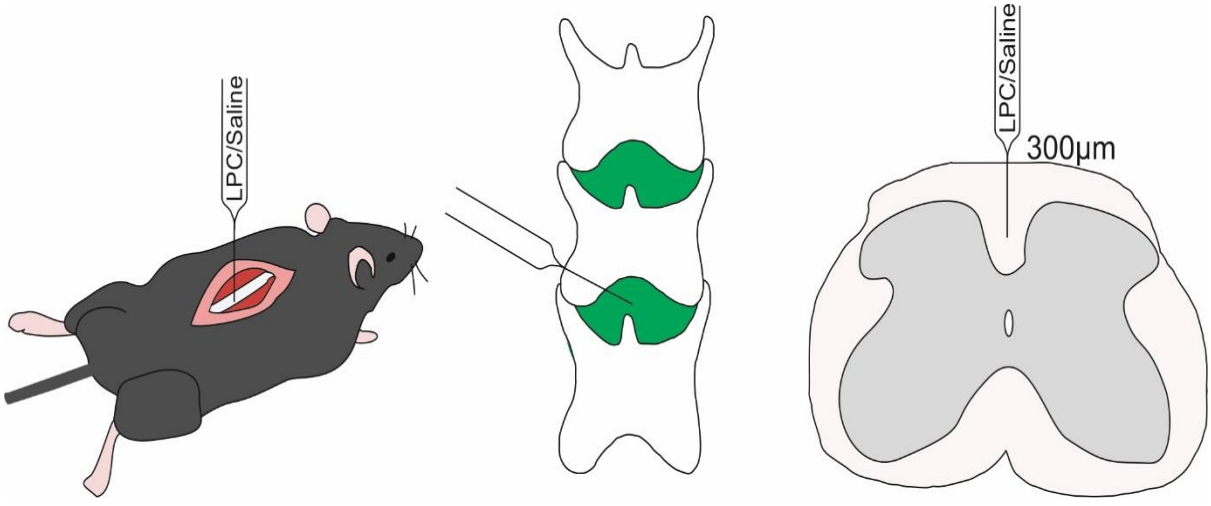

Figure 6.1 LPC or saline were injected directly into the spinal cord through the intervertebral space

Diagram showing the injection paradigm for the *in vivo* focal injection of either LPC or saline into the dorsal column of the spinal cord

6.3.4 *In vivo* injection paradigm for introduction of drugs and EdU

Following intraspinal LPC or saline treatment animals were treated with I.P injections of EdU and either flumazenil or saline and underwent sacrifice and processing for IHC as outlined (figure 6.2).

6.3.5 Processing of tissue for EdU and immunohistochemistry

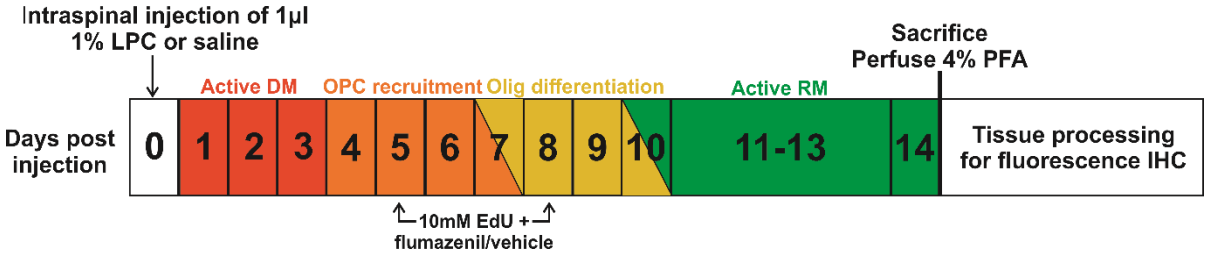

Figure 6.2 Timeline of experimental paradigm

Diagram of the experimental timeline showing the time following intraspinal injection of LPC or saline, the effects of LPC, and the period in which animals were treated with EdU alongside flumazenil or saline. The diagram also shows the length of the experiment and details timing of sacrifice, perfusion, and tissue processing for IHC.

Tissue was sectioned at 40 µm on a vibrating microtome and processed for post-hoc detection of newly proliferated EdU^+ cells and markers of oligodendrocyte differentiation as previously described (section 2.2.5).

Intraspinal LPC/saline injection sites were situated at approximately mid-lumbar level and were determined by the presence of a slight pinprick sized bruise on the cord surface which made the area appear irregular and distinct from the rest of the tissue. Injection sites were isolated from each spinal cord to give an ~3mm tissue block and were sectioned and analysed as detailed below.

Animals which had not received an intraspinal infusion but which were treated with EdU and flumazenil for 4 days were used intact/control animals to examine the effects of intraspinal injection upon the level of proliferation in the spinal cord.

6.3.6 Analysis of spinal cord sections following LPC induced demyelination or saline infusion

Following tissue processing, sections from the injection sites of each animal (*N*=3 N=30) were imaged using a Zeiss LSM880 upright confocal laser scanning microscope with Airyscan equipped with argon and He-Ne lasers. ZEN software (Carl Zeiss, Germany) was used to acquire z-plane tile scan stacks of entire spinal cord sections imaging Alexa-Fluor555 and Alexa-Fluor488, to capture EdU and PanQKI^{+} cells, from the entire injection site. Images were processed using ZEN to stitch tiles together and generate maximum intensity projections before exporting the final images for analysis in Fiji.

Sections were also imaged using the Axio Scan.Z1 slide scanner microscope for high throughput collection of tiles and z-stacks of sections taken from the injection site of all experimental groups. The centre of each section, determined by the Z-plane position in which EdU^{+} cells were most in focus, were exported and EdU^{+} cells in the WM, GM, and CC were counted using the cell counter plugin in Fiji. Cells located specifically within the dorsal columns were also counted to determine if there were differences in proliferation and differentiation specifically within the lesion site. To examine colocalisation of PanQKI^{+} and EdU^{+} cells images were converted to single channel images and PanQKI^{+} cells were marked in the green channel using the cell counter plugin. EdU^{+} cells in the red channel were then counted in the same way. Overlaying the red and green channel allowed the counting of cells which were both PanQKI^{+} and EdU^{+}. Cell counts of EdU^{+} and PanQKI/EdU^{+} cells in images acquired using the LSM880 confocal microscope were also carried out using this method.

Data were collated and analysed as described previously (Chapter 2: section #). Data were considered significant when $p < 0.05$ (denoted by *); $p < 0.01$ (denoted by **), $p < 0.001$) (denoted by ***); or $p < 0.0001$ (denoted by ****).

6.4 Results

6.4.1 Effects of intraspinal injection upon proliferation within the adult spinal cord

Injections were targeted to the dorsal column of the spinal cord and as such many EdU^+ cells were often found clustered at the dorsal surface of the cord following intraspinal injection of saline, whereas in intact/control animals EdU^+ cells were more sparsely spread throughout the entire section (figure 6.3 A-Ai). Animals which received an intraspinal injection of saline into the dorsal column possessed significantly greater numbers of total EdU^+ cells in the spinal cord compared to animals that did not receive an intraspinal injection (748.9 ± 0.4 EdU^+ cells in saline injected animals vs. 132.1 ± 4.4 EdU^+ cells in intact animals, p <0.0001, student's t-test, N=3 n=45, figure 6.3A-B). The number of EdU^+ cells was significantly greater in both the WM and GM regions of the spinal cord in animals which received intraspinal saline injection compared to control/'intact' animals (495.8 ± 27.3- vs. 77.31 ± 3.6 EdU^+ cells in the WM and 247.7 ± 15.5- vs.113.8 ± 19.4 EdU^+ in saline treated and control/'intact' animals respectively, p < 0.0001, student's t-test, N=3 n=45, figure 6.3A-Ai and Bi). However, there was no significant difference in the number of EdU^+ cells which were present at the CC in animals which received an intraspinal injection of saline compared to animals which did not (figure 6.3Bii)

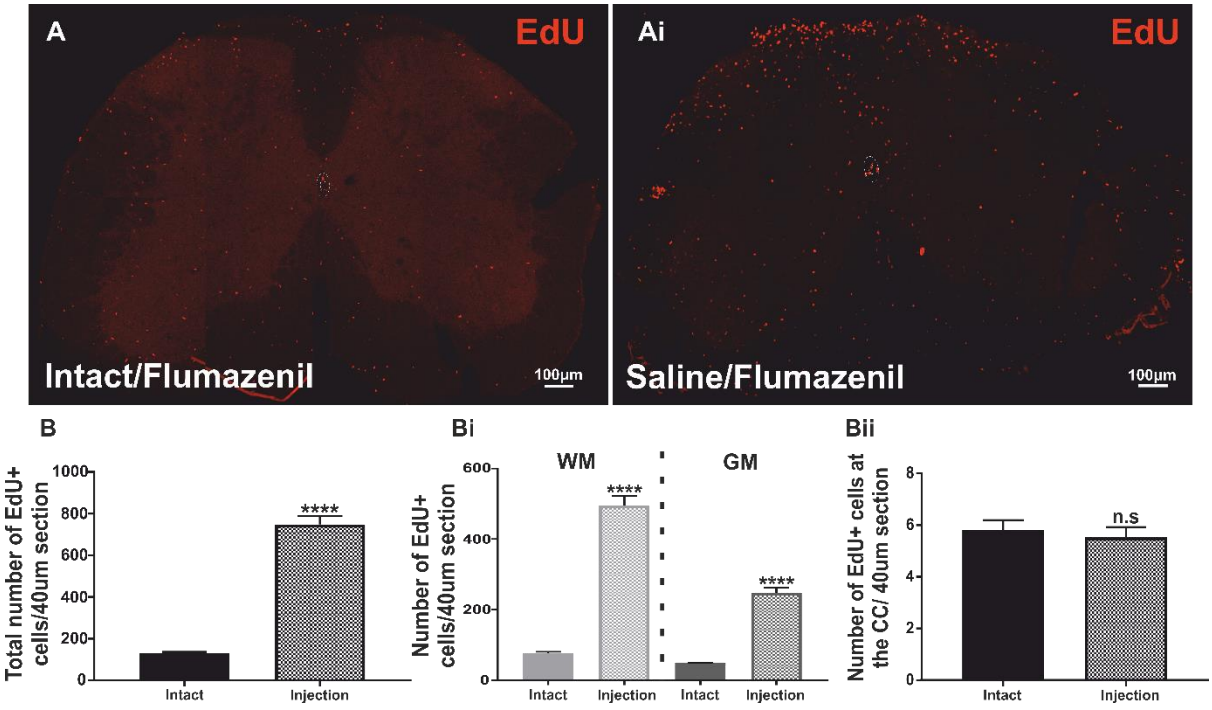

Figure 6.3 Animals which received an intraspinal injection of saline had significantly higher numbers of EdU⁺ cells in the WM and GM of the spinal cord

A: Representative confocal image of the presence and distribution of EdU⁺ cells in the intact spinal cord of adult mice treated with flumazenil. **Ai**: Representative confocal image of the increased numbers of EdU⁺ cells in the spinal cord of flumazenil treated animals that received an intraspinal infusion of saline. **B**: Pooled data of counts of total EdU⁺ cells in the spinal cord of control and intraspinal treated animals. **Bi**: EdU⁺ cell counts in the WM and GM of control and intraspinal treated animals. **Bii**: Counts of EdU⁺ cells at the CC of control and intraspinal treated animals. Solid bars: intact/control animals. Hatched bars: intraspinal saline injected animals (**** = $p < 0.0001$, student's t-test)

Both groups were treated with the CBR site antagonist flumazenil, as later experiments were interested in investigating the effects of flumazenil upon proliferation of PanQKI⁺ oligodendrocytes following focal demyelination by intraspinal LPC injection.

6.4.2 Focal intraspinal LPC injection results in fewer EdU$^+$ cells in the spinal cord compared to intraspinal saline injection

Animals that underwent intraspinal injection of saline exhibited higher numbers of EdU$^+$ cells in the spinal cord compared to 'intact' animals. Therefore, animals that received intraspinal dorsal column injections of saline were used as controls to examine the baseline effects of focal demyelination in the spinal cord by LPC in flumazenil treated animals.

Whilst the injection method itself resulted in significantly more EdU$^+$ cells in both the WM and GM of the spinal cord in flumazenil treated animals, animals receiving an intraspinal infusion of LPC had significantly fewer EdU$^+$ cells in the WM compared to control animals given intraspinal saline (327.4 ± 27.8 vs. 428.6 ± 22.3 EdU$^+$ cells in animals treated with LPC and saline, respectively, p <0.01, students t-test, N=3 n=30, figure 6.4A-B). There were no significant differences in the number of EdU$^+$ cells within the GM of LPC treated- vs saline treated animals (figure 6.4A-B).

In addition, animals which received intraspinal LPC treatment also had significantly fewer EdU$^+$ cells surrounding the CC compared to saline treated animals (3 ± 0.3 vs. 5.2 ± 0.3 EdU$^+$ cells at the CC of animals treated with LPC or saline, respectively, p <0.0001, N=3 n=*30,* figure 6.4Bi).

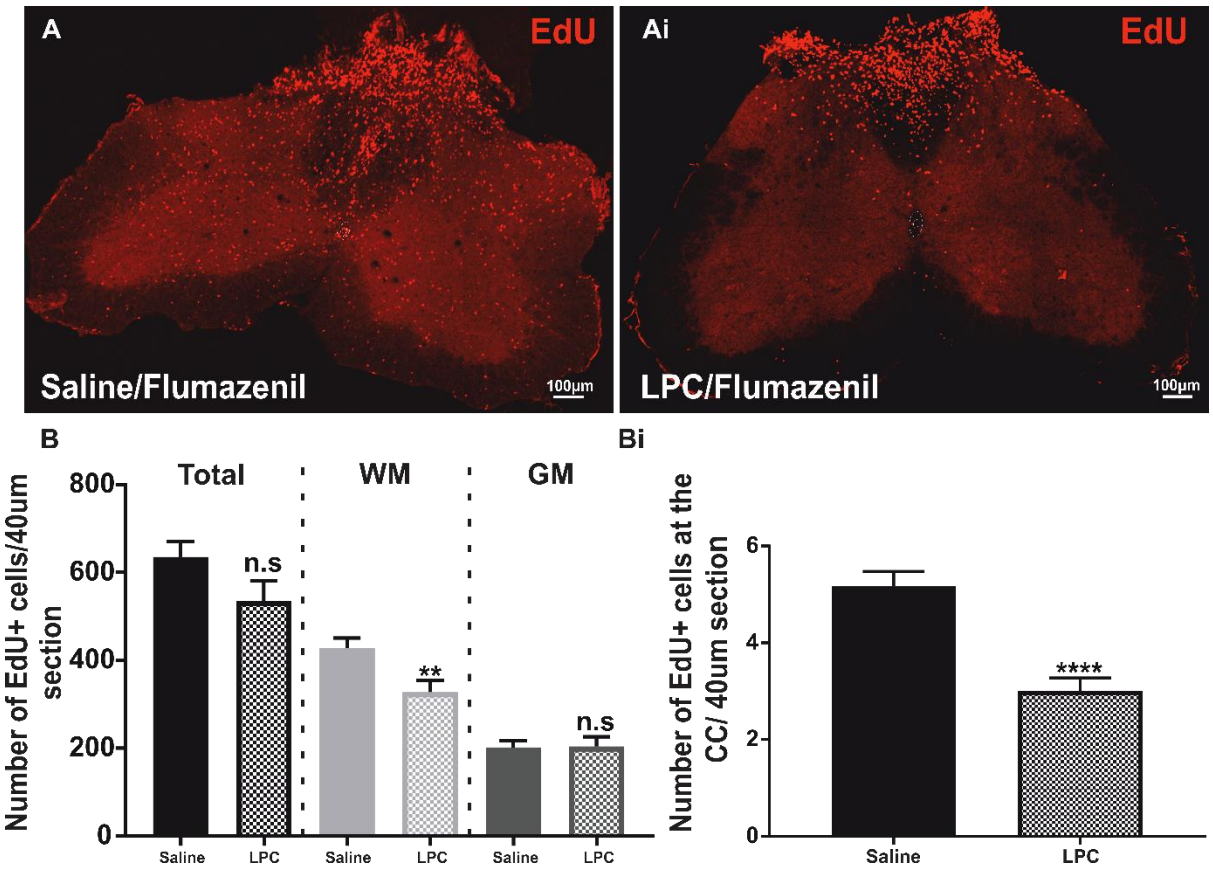

Figure 6.4 Intraspinal LPC treatment results in fewer EdU⁺ cells in the WM and at the CC compared to saline treatment

A – Ai: Representative confocal images of the spinal cord showing EdU⁺ cells following intraspinal injection of either saline or LPC, respectively. **B**: Pooled data of EdU⁺ cell counts in the spinal cord of both saline and LPC treated animals. **Bi**: Pooled data of EdU⁺ cell counts at the CC. Solid bars are saline treated animals. Hatched bars are LPC treated animals (** = p <0.01, **** = p <0.0001, student's t-test)

6.4.3 Intraspinal LPC results in focal areas of MBP-ve labelling where EdU$^+$ cells are also located

Direct injection of LPC into the WM results in the recruitment of macrophages and microglia which phagocytose nearby myelin, leading to focal areas of demyelination. MBP labelling was therefore was used as a marker of LPC-induced demyelination in the spinal cord.

In saline treated animals there was strong MBP immunoreactivity present throughout the WM of the spinal cord (figure 6.5A and 6.6A). Following intraspinal injection of LPC into the dorsal columns, MBP staining appeared absent from focal regions of the WM where the toxin had been introduced (figure 6.5Ai and 6.6B). Examining such changes in labelling for MBP in the WM therefore suggest that, as expected, LPC infusion resulted in focal demyelination in the spinal cord.

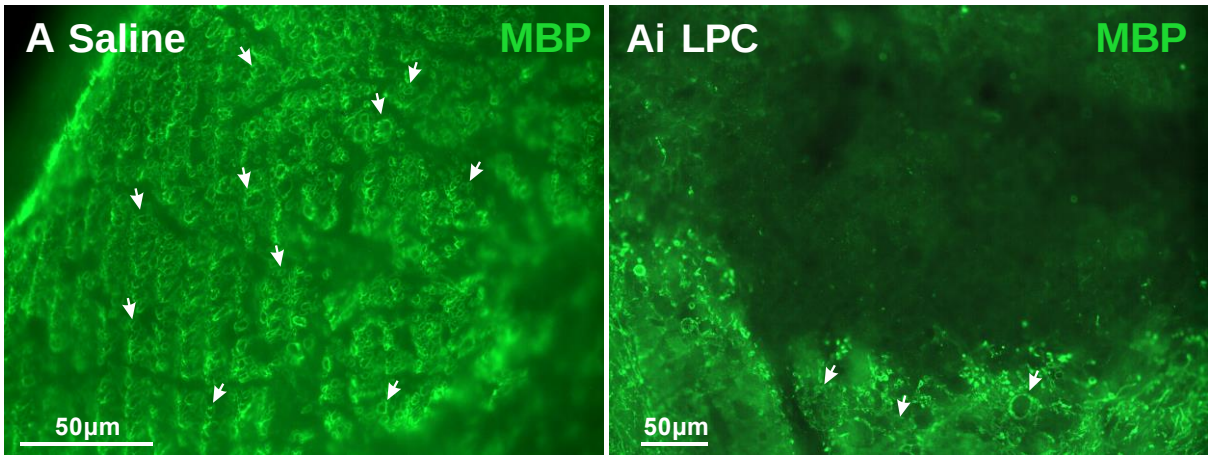

Figure 6.5 Animals which received intraspinal LPC injection possessed areas devoid of MBP labelling indicative of LPC-induced focal demyelination

A: Representative confocal image of MBP labelling in the WM of the spinal cord of animals treated with intraspinal saline, illustrating the presence of MBP$^+$ myelin rings (arrows). **B**: Representative confocal image showing areas within the WM of LPC-treated animals which no longer possess MBP

Following intraspinal injection of 1% LPC there was a decrease in the level of proliferation in the spinal cord WM, with clustering of EdU$^+$ cells near the injection site (figure 6.3Ai). LPC treatment significantly reduced the level of proliferation in the spinal cord compared to saline, however, despite this, EdU$^+$ cells were present within focal areas which were MBP- (figure 6.6). These findings suggest that despite an overall loss of EdU$^+$ cells in the spinal cord in animals which possess areas of LPC-induced demyelination, proliferating cells are present at the lesion site (figure 6.6). Therefore, these results illustrate the potential for LPC lesion-induced migration of newly proliferated cells to regions of demyelination in the dorsal column which may be beneficial for tissue repair.

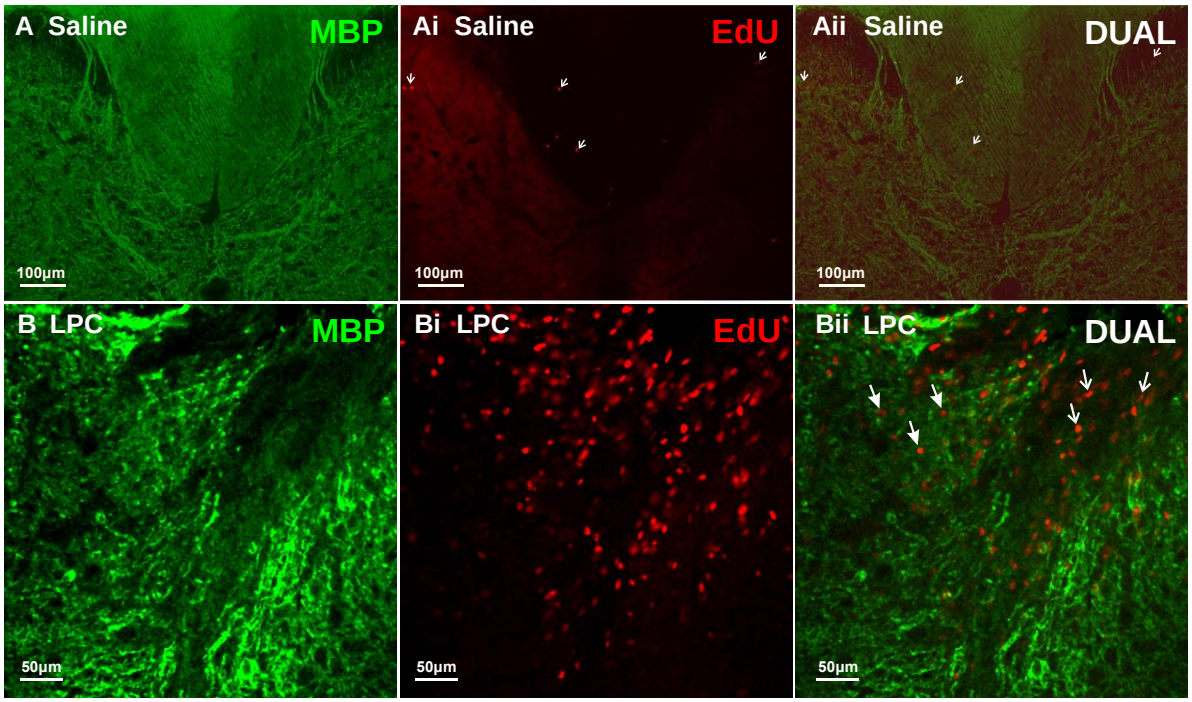

Figure 6.6 Newly born EdU$^+$ cells are present in areas of demyelination following intraspinal LPC treatment

A-Aii: Representative confocal images of the spinal cord DC of intraspinal saline treated animals showing labelling for MBP (green) and EdU (red), and dual labelling for both. Open arrows mark EdU$^+$ cells. **B-Bii**: Representative confocal images showing areas which are MBP$^+$ and MBP- (green) in the DC of animals treated with LPC. EdU$^+$ cells (red) in this region are present in both MBP$^+$ and MBP- regions (dual). Closed arrows label EdU$^+$ cells in MBP$^+$ regions. Open arrows label EdU$^+$ cells in MBP- regions

6.4.4 EdU$^+$ cells at the LPC-lesion site are also PanQKI$^+$

EdU$^+$ cells are found at the lesion site following LPC injection (figure 6.7B-Bi). In LPC treated mice labelling with PanQKI illustrates that many of these cells EdU$^+$ cells belong to the oligodendrocyte cell lineage as they are also PanQKI$^+$ (figure 6.7Bii and Cii, closed arrows represent colocalised cells). These results show that new PanQKI$^+$ oligodendrocytes are present in the dorsal column WM areas targetted by LPC-induced demyeination, therefore suggesting that whilst LPC induces oligodendrocyte death, new oligodendrocytes are present at the lesion site in the days following demyelination. This finding provides a window of opportunity for WM repair, whereby augmenting the proliferative population of the spinal cord may lead to greater numbers of oligodendrocytes which could contribute to remyelination following LPC-induced demyelination.

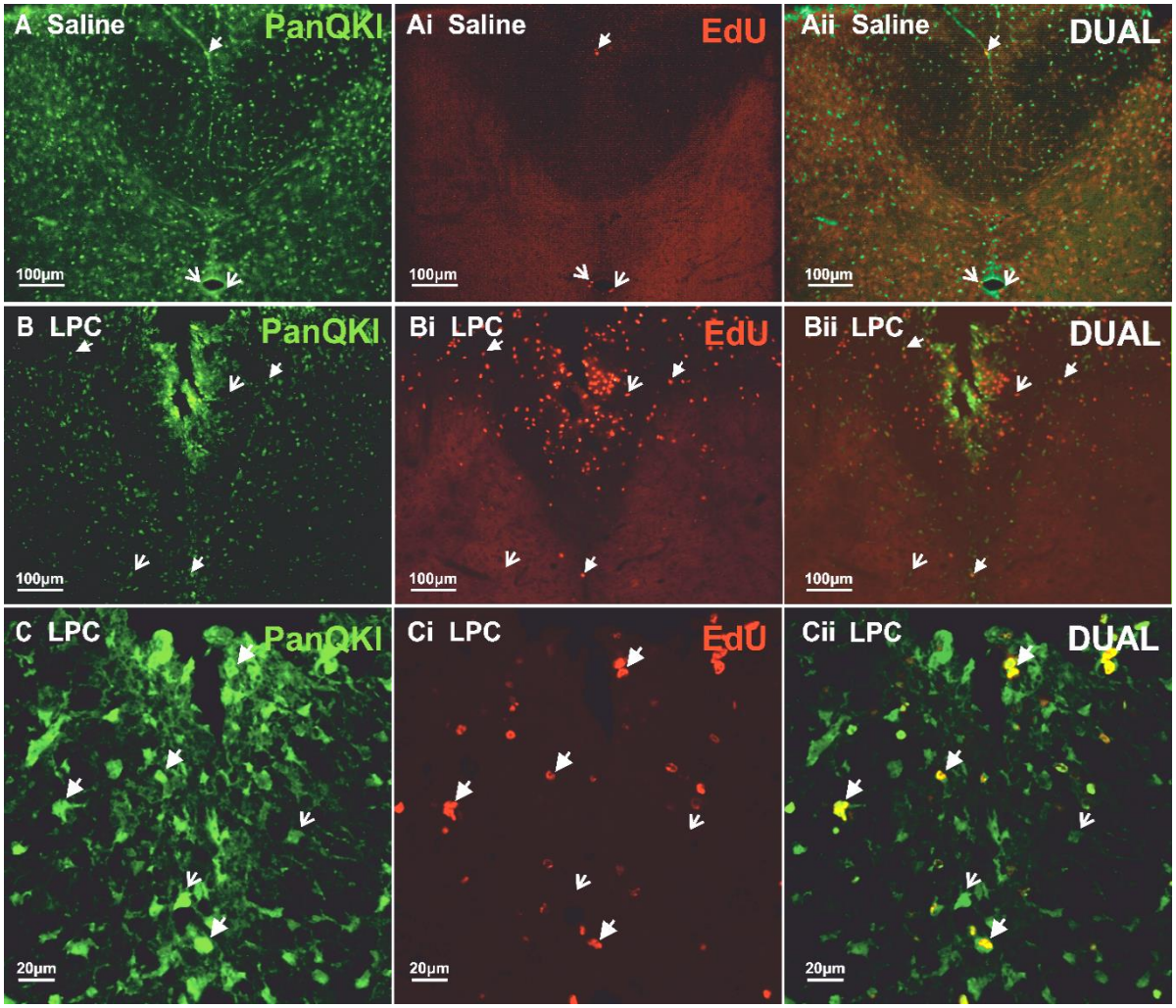

Figure 6.7 EdU$^+$ cells present at the DC of LPC-treated animals are also PanQKI$^+$

A-Aii: Representative confocal images illustrating the presence of PanQKI$^+$ (green) and EdU$^+$ (red) cells at the DC of the spinal cord of intraspinal saline treated animals. Colocalisation of EdU and PanQKI can also be seen (dual). **B-Bii**: Representative confocal images showing colocalisation of EdU and PanQKI$^+$ cells in the DC of LPC treated animals. **C-Cii**: Higher magnification of sections shown in B-Bii. Open arrows mark non-colocalised cells. Closed arrows represent EdU/PanQKI$^+$ colocalised cells

6.4.5 Following LPC injection flumazenil treated animals exhibit greater numbers of EdU$^+$ cells compared to vehicle

Following intraspinal LPC injection there were significantly fewer proliferating EdU$^+$ cells compared to animals injected with saline (figure 6.4). In the intact cord flumazenil significantly increases the level of proliferation in the WM, GM, and CC regions compared to vehicle treatment (Chapter 5). The effects of flumazenil upon proliferation were therefore examined in animals which had received intraspinal LPC treatment. In these animals, EdU was administered at 5 days post-LPC injection in an effort to avoid labelling the immediate post-injection induced peak in proliferation which is frequently seen following injury to the spinal cord.

Animals treated with flumazenil possessed significantly more EdU$^+$ cells compared to animals which received vehicle following intraspinal LPC treatment (327.4 ± 27.8 vs. 168.1 ± 16.8 total EdU$^+$ cells in animals treated with flumazenil or saline following intraspinal LPC injection, respectively, $p < 0.0001$, student t-test, N=3 n=30, figure 6.8A-B). In flumazenil treated animals the numbers of EdU$^+$ cells were significantly higher in both the WM (327.4 ± 27.8 vs. 168.1 ± 16.8 EdU$^+$ cells, p <0.0001, student's t-test, N=*3* n=30, , figure 6.8B) and GM (204.4 ± 22.1 vs 58.7 ± 6.7 EdU$^+$ cells p <0.0001, student's t-test, N=*3* n=30) of the post-LPC spinal cord compared to vehicle treated animals

Although there was a trend toward an increase in the number of EdU$^+$ cells surrounding the CC in flumazenil treated animals, this was not statistically significant (figure 6.8Bi).

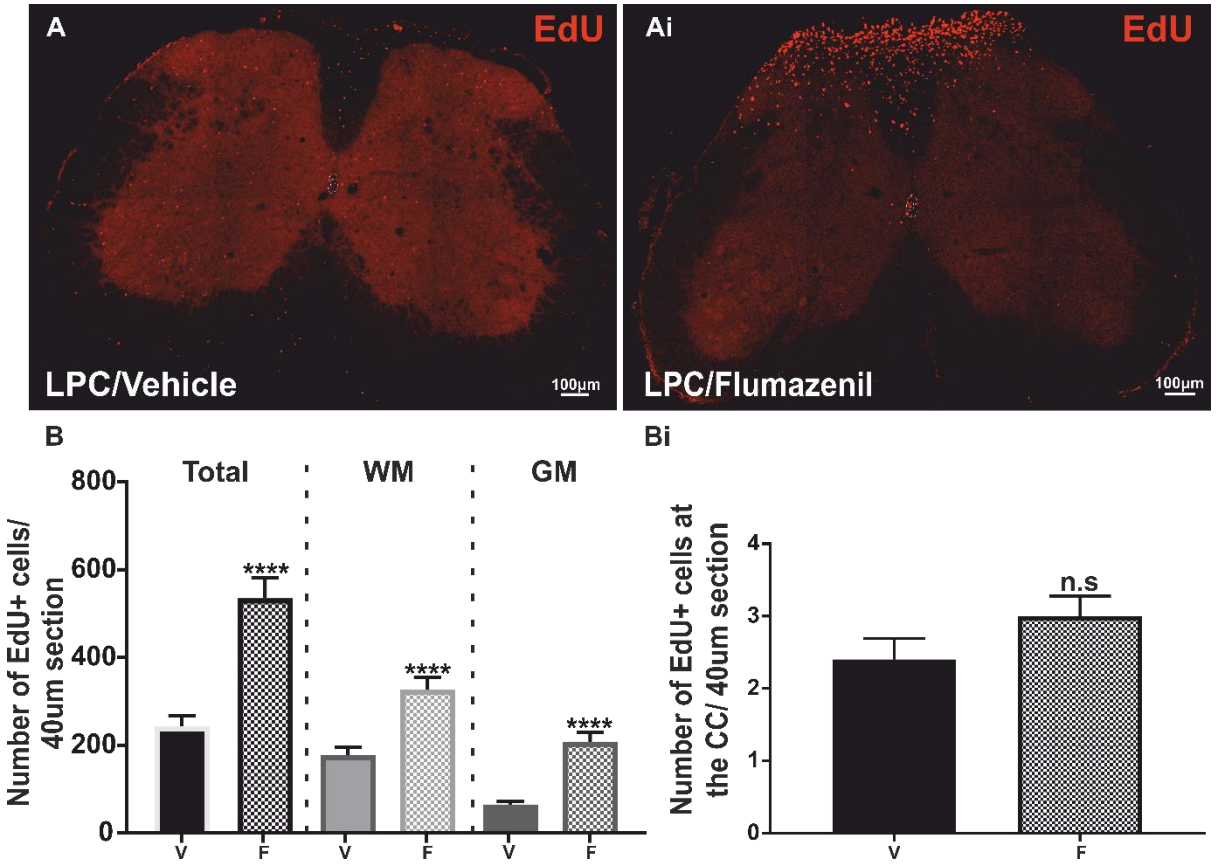

Figure 6.8 Following intraspinal LPC infusion animals treated with flumazenil possess significantly more EdU⁺ cells compared to vehicle treated animals

A-Ai: Representative confocal images of EdU⁺ cells in the spinal cord of LPC-treated animals following either vehicle or flumazenil I.P treatment, respectively. **B**: Average numbers of EdU⁺ cells in the spinal cord of LPC-vehicle and LPC-flumazenil treated animals. **Bi**: Pooled data showing numbers of EdU⁺ cells at the CC specifically. Solid bars represent LPC/vehicle treated animals. Hatched bars are LPC/flumazenil treated animals (**** = $p < 0.0001$, student's t-test)

6.4.6 Effects of LPC treatment on the number and percentage of EdU/PanQKI⁺ cells in the spinal cord

In the intact cord EdU⁺ cells most frequently colocalise with PanQKI, illustrating that PanQKI⁺ oligodendrocytes contribute the greatest number of proliferating cells in the adult spinal cord. Animals that received intraspinal injection of either saline or LPC also possessed many EdU⁺ cells which were also PanQKI⁺ (figure 6.9A-Bii, closed arrows

represent EdU and PanQKI colocalised cells). In these animals 19-37% of total EdU^+ cells were also $PanQKI^+$ (figure 6.9Ci)

In the spinal cord of LPC treated animals there were significantly fewer EdU^+ cells which were also $PanQKI^+$ (46.2 ± 14.3 vs. 97.1 ± 18.1 total EdU/$PanQKI^+$ cells in LPC and saline injected mice, respectively, $p < 0.05$, student's t-test, N=3 n=10, figure 6.9C). The number of newly proliferated $PanQKI^+$ cells was significantly lower in the WM (31.7 ± 10.6 vs. 65.5 ± 9.3 EdU/$PanQKI^+$ cells, p <0.05, student's t-test, N=3 n=30) and in the GM (14.6 ± 3.8 vs. 49 ± 9.9 EdU/$PanQKI^+$ cells, p <0.01, student's t-test, N=3 n=30) in animals which received intraspinal LPC compared to those injected with saline (figure 6.9C)

These results are likely explained by the finding that LPC-treatment significantly reduced the overall number of EdU^+ cells compared to saline treatment (figure 6.4B). Therefore, it is important to consider percentage of total EdU^+ cells which are also $PanQKI^+$ in both saline and LPC treated animals to examine the numbers of EdU/$PanQKI^+$ cells relative to the overall number of EdU^+ cells in each condition (figure 6.9Ci). The percentages of total EdU/$PanQKI^+$ cells in LPC and saline treated animals show that despite an overall decrease in the number of EdU^+ cells in LPC treated animals, the proportion of EdU^+ cells which were also $PanQKI^+$ were significantly greater in LPC treated animals vs. saline treated animals (35.8 ± 4% vs. 16.6 ± 2.6% of total EdU^+ cells which were also $PanQKI^+$, $p < 0.01$, student's t-test, N=3 n=30, figure 6.9Ci). The percentage of EdU^+ cells which were also $PanQKI^+$ was significantly greater in both the WM (39.7 ± 6.6% vs. 18.3 ± 3.3%, $p < 0.05$, student's t-test,

N=3 *n*=30) and GM (36.1 ± 2.1% vs. 20.6 ± 2.1%, $p < 0.0001$, student's t-test, *N*=3 *n*=30) of LPC- vs saline treated animals (figure 6.9Ci).

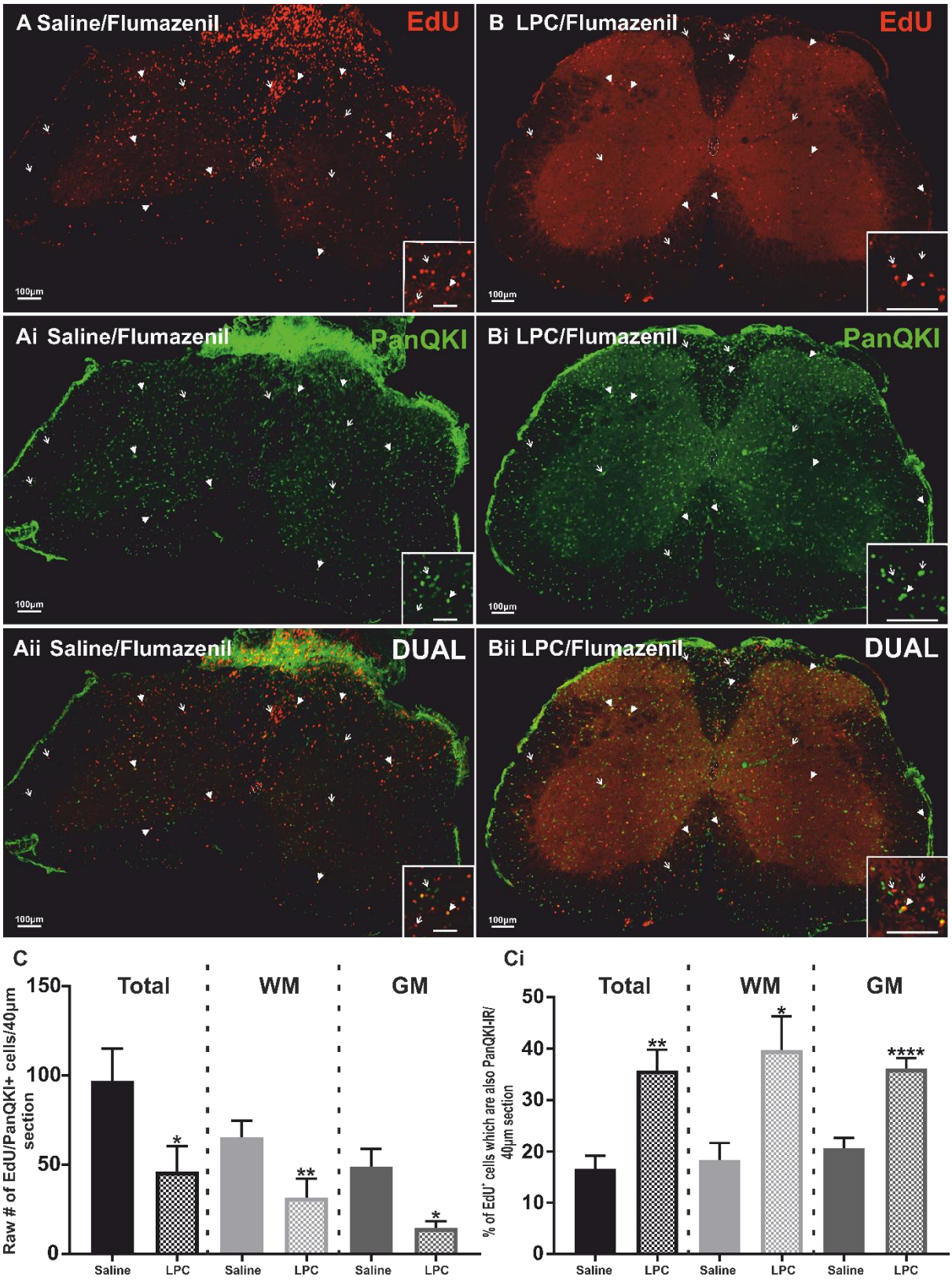

Figure 6.9 Intraspinal LPC-treatment significantly affects oligodendrocyte lineage acquistion of EdU$^+$ cells compared to saline treatment

A-Aii: Representative confocal images showing the expression of both EdU (red) and PanQKI (green) in saline/flumazenil treated animals. Dual labelling illustrates colocalisation of EdU$^+$ and PanQKI$^+$ cells in the spinal cord of these animals. **B-Bii**: Representative confocal images also illustrating the colocalisation of EdU$^+$ and PanQKI$^+$ cells in the spinal cord of LPC/flumazenil treated animals. Open arrows represent non-colocalised cells. Closed arrows represent EdU/PanQKI$^+$ colocalised cells. **C**: Counts of total EdU$^+$ cells which are also PanQKI$^+$. The numbers of EdU/PanQKI$^+$ cells in the WM and GM are also shown. **Ci**: Pooled data showing the percentage of total EdU$^+$ cell which are also PanQKI$^+$ in the WM and GM combined, and the WM and GM specifically. Solid bars represent saline/flumazenil treated animals. Hatched bars are LPC/flumazenil treated animals (* = $p < 0.05$, ** = $p < 0.01$, **** = $p < 0.0001$, student's t-test)

6.4.7 Effects of flumazenil treatment on the number and percentage of EdU/PanQKI$^+$ cells in LPC treated mice

It was hypothesised that as flumazenil increased the number of proliferating EdU$^+$ cells in the spinal cord following LPC infusion, and that EdU/PanQKI$^+$ cells were frequently seen at the site of LPC-induced demyelinated lesions, flumazenil may be able to boost the numbers of newly proliferated PanQKI$^+$ OPCs to contribute toward remyelination following LPC treatment.

However, in animals which received an intraspinal LPC infusion, there were no significant differences were found in the number of EdU/PanQKI$^+$ cells in animals treated with LPC/flumazenil vs LPC/vehicle treated animals (figure 6.10A). There were also no significant differences in the percentage of total EdU$^+$ cells which were also PanQKI$^+$ in LPC/flumazenil vs LPC/vehicle treated animals (figure 6.10Ai).

It was hypothesised that as counts of EdU^{+} cells were counted in the entire spinal cord section and that LPC results in a discrete area of demyelination, including counts of other regions may be masking the effects of LPC at the lesion site. However, when analysing the numbers of EdU^{+} cells and EdU/PanQKI^{+} located at the lesion site there were no significant differences in animals treated with LPC/flumazenil vs. saline/flumazenil (figure 6.10B-Bi). There were also no significant differences in the percentage of total EdU^{+} cells which were PanQKI^{+} at the lesion site. These results therefore show that flumazenil did not significantly increase the population of proliferating PanQKI^{+} cells compared to vehicle following LPC induced demyelination in the dorsal column of the adult spinal cord.

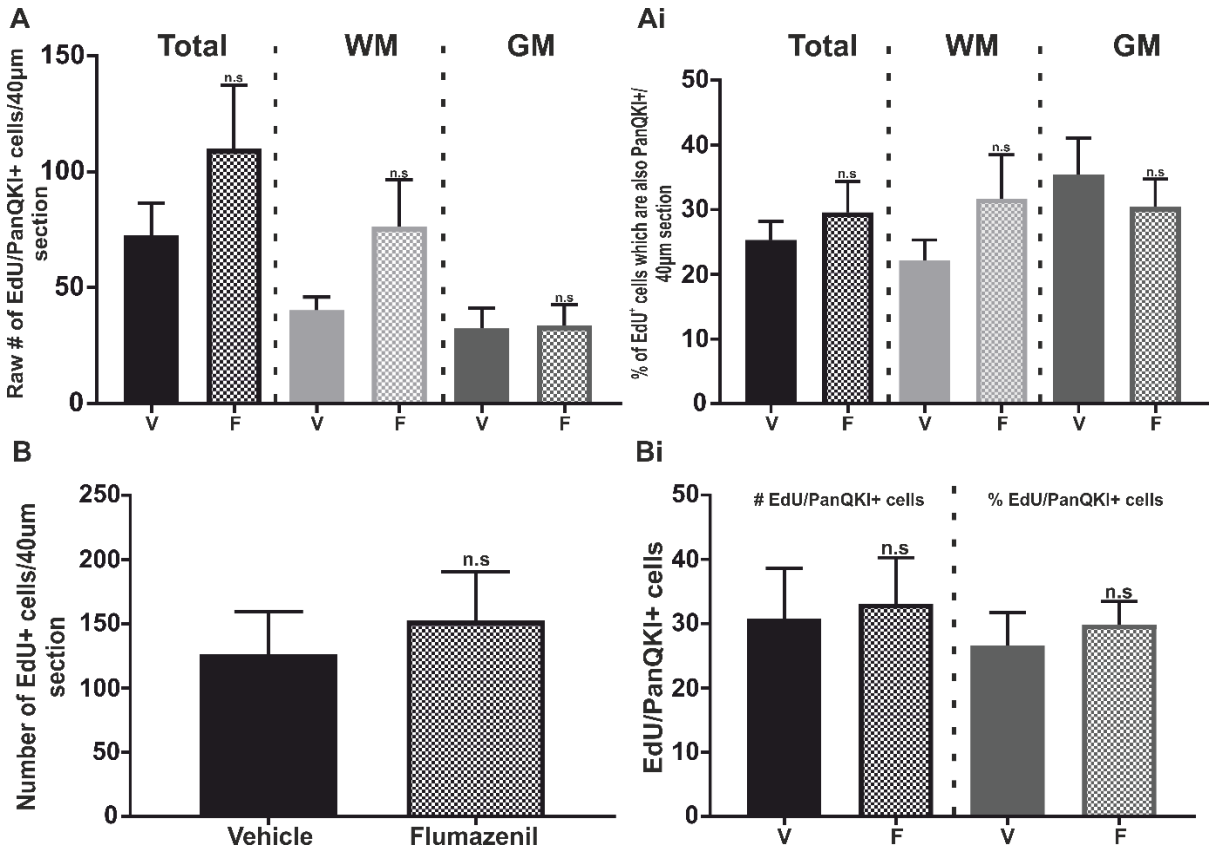

Figure 6.10 There are no significant differences in the numbers or percentages of EdU/PanQKI$^+$ cells in the spinal cord of flumazenil vs. saline treated animals following intraspinal LPC infusion

A: Pooled data showing total counts of EdU/PanQKI$^+$ cells in the spinal cord of LPC/vehicle and LPC/flumazenil treated animals. Cell counts specific to the WM and GM are also shown. **Ai**: Pooled data showing the percentage of total EdU$^+$ cells which are also PanQKI$^+$ in the spinal cord of LPC/vehicle and LPC/flumazenil treated animals. Solid bars represent counts from LPC/vehicle treated animals. Hatched bars represent counts from LPC/flumazenil treated animals **B-Bi**: Pooled data of EdU$^+$ (B) and EdU/PanQKI$^+$ cell counts and the percentage of total EdU$^+$ cells which are PanQKI$^+$ at the lesion site (Bi) in LPC/vehicle vs. LPC/flumazenil treated animals : (n.s = $p > 0.05$, student's t-test, N=3, n=9)

6.5 Discussion

6.5.1 Proliferation in the postnatal spinal cord is markedly increased in the WM and GM following intraspinal injection of saline

In these experiments focal demyelinated lesions were induced by direct injection of LPC into the spinal cord dorsal column of adult mice. Intraspinal treatments were delivered to the spinal cord by a glass capillary broken back to a sharp tip. It is therefore important to consider the effects of the injection procedure itself upon the level of proliferation within the spinal cord as the spinal cord responds to tissue disruption and trauma with a marked increase in the number of proliferative cells (Johansson *et al*., 1999; Meletis *et al*., 2008; Barnabe-Heider *et al*., 2010; Mothe and Tator, 2005).

As a result of the capacity of the spinal cord to respond to injury in this way, it is possible that the intraspinal injection method may resemble a stab injury which causes an increase proliferation via an injury-induced proliferative response. Indeed, animals which received an intraspinal infusion of saline exhibited higher numbers of proliferative EdU$^+$ cells compared to animals which did not. It is therefore likely that a proportion of the EdU$^+$ cells which are

present following intraspinal injection of either saline or LPC are the result of reactive proliferation as a result of injury to the spinal cord itself.

6.5.2 Are EdU$^+$ cells at the CC migrating toward the 'injury' site?

In animals receiving intraspinal saline, the proliferation was greater in both the WM and GM compared to intact animals. Interestingly however, there were no significant differences in the number of EdU$^+$ cells which were located at the CC in intact vs. intraspinal treated animals. This is in contrast with other studies which have shown that spinal cord injury reactivates the NSC properties of the normally quiescent ECs which reside at the CC, causing this dormant population to proliferate extensively, migrate to the lesion site, and differentiate into oligodendrocytes and astrocytes (Mothe and Tator, 2005; Johansson *et al*., 1999; Lytle and Wrathall, 2007; McDonough, A. *et al*., 2013; Meletis *et al*., 2008; Barnabe-Heider *et al*., 2010; Sabelstrom *et al*., 2013). Genetic fate mapping studies have shown that following dorsal funiculus transection the majority of new glial cells are derived from ECs (Barnabe-Heider *et al*., 2010), where injury-induced proliferation, migration, and differentiation of ECs is essential to prevent secondary tissue damage and cavitation at the lesion site (Barnabe-Heider *et al*., 2010).

Following stab injury at T8, DiI-labelled ECs begin to migrate away from the CC toward the site of injury by 3dpi, where the distance of migration and number of migratory cells occurs in a time-dependent manner. By 14dpi DiI-labelled ECs are found at a distance of 140um from the CC (Mothe and Tator, 2005). In our experiments proliferating ECs are labelled by EdU during days 4-8 post saline injection, however animals are not sacrificed until day 14, giving EdU$^+$ ECs time to migrate away from the CC and toward the dorsal column. Indeed, there were many EdU$^+$ cells present at the dorsal surface of the cord where the capillary would have pierced the WM during saline infusion. It is therefore possible that EdU$^+$ ECs could have migrated to the injection site, making it appear as though there was no difference in the

level of proliferation at the CC at 14dpi. In addition, injury induced proliferation occurs in a spatiotemporal wave-like pattern which may also explain such findings (Lacroix *et al*., 2014).

Further experiments using genetic fate mapping by tamoxifen-dependent Cre-recombination under the control of the EC-specific promotor FoxJ1 would help determine whether ECs are indeed migrating toward the injection site. Lineage tracing of glial progeny alongside EC progeny would also elucidate whether the increased proliferation seen in the WM and GM of intraspinal saline treated animals is the result of proliferation of native glial cells or infiltration of newly proliferated EC progeny.

6.5.3 Does EC proliferation following injury require ependymal disruption?

Recent work however has challenged the role that ECs play in tissue repair following injury, suggesting that ECs do not constitute a dormant NSC population which are reactivated following injury (Ren *et al*., 2017). Contrary to previous findings, using BrdU in *Foxj1*^{CreERT2}-tdT transgenic animals, Ren *et al*., (2017) illustrate that, following either lateral or midline stab injuries which are near to, but do not directly impact the CC ependyma, there were no tdT^{+} EC-derived progeny at the lesion site. Such injuries contained many newly proliferated, scar-forming astrocytes that were positive for both BrdU and GFAP, but did not contain any tdT positive cells, with or without BrdU, even when lesions came within less than 150 μm of the lateral edge of the EC layer. However, Foxj1-tdT mice receiving midline radially orientated stab injuries that penetrated the ependyma exhibited BrdU/tdT^{+} cells which extended from the EC layer along the injury margins (Ren *et al*., 2017), echoing the findings of previous studies which have also observed reactive EC proliferation, migration, and differentiation following SCI.

Taken together, these findings demonstrate that ECs do not contribute any cells to stab injury response unless the ependyma itself is directly injured (Ren *et al*., 2017), and may also explain why EC proliferation has not been seen in humans following SCI (Paniagua-Torija *et al*., 2018). In our study the injection was performed at a depth of 300 μm from the

dorsal surface to target the dorsal column. Successful injection should therefore leave CC intact and the ependyma undamaged and so may explain why there were no significant differences in the number of EdU^+ cells at the CC in intact vs. intraspinally injected animals. If this is the case it would also mean that any changes seen at the CC following LPC injection are more likely the result of the LPC rather than the injection method itself.

6.5.4 Effects of intraspinal LPC upon the numbers of EdU^+ cells in the postnatal spinal cord

6.5.4.1 Intraspinal injection of LPC results in significantly fewer EdU^+ cells in the spinal cord

Whilst intraspinal injection itself resulted in greater numbers of EdU^+ cells in the WM and GM compared to intact animals, animals which received intraspinal injection of 1% LPC possessed fewer EdU^+ cells compared to animals which were injected with saline. Furthermore, in LPC treated animals there were fewer EdU^+ cells in the WM compared to animals treated with intraspinal saline infusion.

Intraspinal LPC injection results in marked astrocyte loss and death of OLCs in the WM, as measured by GFAP, Olig2, and PDGFRα IHC (Plemel *et al*., 2017; Keough *et al*., 2015). As OLCs and astrocytes make the largest contribution to the proliferating population of the spinal cord (Barnabe-Heider *et al*., 2010), it is possible that animals treated with LPC possessed fewer EdU^+ proliferating cells compared to saline-treated animals due to the oligo- and gliotoxic properties of LPC in the WM.

However, the remyelinating properties of LPC-induced demyelinating lesions by 14-21dpi are well described (Hall, 1972; Woodruff and Franklin, 1999; Blakemore and Franklin, 2008; Ghasemlou *et al*., 2007; Keough *et al*., 2015), where there is a significant increase in both the total number of OLCs at 14 days compared to 7 days, as well as the proportion of mature oligodendrocytes compared to OPCs (Keough *et al*., 2015). These results suggest that it is therefore unlikely that at the time of EdU injection, 5-8dpi, there would have been fewer

proliferating oligodendrocytes in LPC treated animals than in those which were treated with intraspinal saline injection as this has been shown to be the period in which OLCs are proliferating and migrating to the lesion site. Further investigation, using IHC for OLC markers specific to oligodendrocyte maturity alongside markers of cell death, is necessary to confirm whether or not differences in the numbers of EdU^+ cells in the WM of LPC treated animals are due to OLC death.

Animals treated with intraspinal LPC also possessed fewer EdU^+ cells at the CC compared to animals treated with saline. Previously, Lacroix *et al*., (2014) illustrated that LPC-induced demyelinating lesions did not result in greater numbers of proliferative $Ki67^+$ cells at the CC compared to PBS injection. LPC injections were performed at the dorsal lateral funiculus as it was noted that dorsal column injections occasionally penetrated too deeply, contacting the CC, and resulting in needle damage to the ependyma which itself caused an increase in baseline Ki67 staining at the CC (Lacroix *et al*., 2014). Animals injected with saline at the dorsal column in our experiments did not show greater numbers of proliferative cells at CC compared to non-injected intact animals, therefore it is unlikely that the reduction in the EdU^+ cells at the CC of LPC treated animals is related to traumatic perturbation to the CC itself. Proliferating ECs may have provided a population of migratory cells which moved toward the lesion site, however genetic fate mapping of EC progeny following LPC-induced demyelination would be required to investigate this possibility further.

6.5.5 Can we augment OPC proliferation for more oligodendrocytes following LPC?

6.5.5.1 LPC-treated animals possess a greater proportion of EdU/PanQKI$^+$ cells in the spinal cord following demyelination

IHC for MBP and $PanQKI^+$ illustrate that LPC infusion did indeed result in demyelination within the dorsal column and that new EdU/$PanQKI^+$ OLCs were present within the lesion site. Furthermore, despite showing an overall decrease in the number of new cells in the

WM, LPC-treated animals possessed a greater proportion of EdU^+ cells which were $PanQKI^+$. These findings suggest an increase in the proportion of EdU^+ cells that differentiated into $PanQKI^+$ oligodendrocytes compared to saline treated animals, likely as a result of the need to replace the OLC population which undergo cell death during LPC-induced demyelination (Plemel *et al*., 2017).

Whilst it is known that OPC proliferation and differentiation does occur following LPC-induced demyelination, which ultimately leads to remyelination (Keough *et al*., 2015), the well documented choreography of myelin repair following LPC infusion allows investigation into ways in which this process of endogenous remyelination could be enhanced for therapeutic gain. For example, work described here attempts to determine whether modulation of GABAergic signalling by perturbation of binding of endogenous CBR ligands by flumazenil can enhance the proliferation of OLCs for remyelination.

6.5.5.2 Effects of flumazenil upon proliferation of PanQKI+ cells following LPC-induced demyelination

Whilst animals treated with intraspinal LPC were found to have fewer EdU^+ cells than intraspinal saline treated counterparts, flumazenil treatment following LPC infusion resulted in greater numbers of new cells compared to animals receiving vehicle following LPC treatment.

Therefore, this study is the first to show that modulation of GABAaR signalling by the CBR antagonist flumazenil can result in a greater number of cells in the spinal cord following LPC-induced demyelination. These results suggest that modulation of GABAaR by its endogenous ligands may be important in the post-injury response to LPC-infusion in the spinal cord, where the CBR antagonist flumazenil prevents this and augments the proliferating cell population.

It was hypothesised that whilst flumazenil results in more EdU^+ cells in the WM, GM, and CC compared to vehicle treatment in the intact cord the proportion of these cells which are

also PanQKI$^+$ is unchanged as these cells are surplus to the needs of the intact cord and so do not undergo differentiation (Hill *et al*., 2018; Hughes *et al*., 2018; Sun, L.O. *et al*., 2018). This study showed that flumazenil can also increase the number of proliferative cells in the cord after LPC infusion to perhaps augment the endogenous pool of cells which could be used for repair in cases of demyelinating injury such as MS.

However, whilst flumazenil increased the number of EdU$^+$ cells following LPC-induced demyelination compared to vehicle treatment, there were no significant differences in either the number or proportion of EdU/PanQKI$^+$ cells. There were also no changes in the numbers of new PanQKI$^+$ cells specifically at the site of LPC-induced demyelination in flumazenil vs. vehicle treated animals. Therefore, despite the hypothesis that loss of OLCs by LPC-induced demyelination may influence the differentiation of the greater population of EdU$^+$ cells in flumazenil treated animals, this was not the case.

Indeed others have shown that endogenous GABA alters neuronal firing in OPCs which may alter OPC proliferation and myelination (Lin and Bergles, 2004; Gibson, E. M. *et al*., 2014). Furthermore, GABA release is essential for OPC maturation and development of fully mature myelinating oligodendrocytes (Zonouzi *et al*., 2015; Hamilton, N.B. *et al*., 2017). In flumazenil treated animals alteration in GABAergic signalling by antagonist activity at the CBR site animals, there were more proliferative cells, but these were not PanQKI+, which may be the result of a reduction GABAergic stop signal for proliferation but a loss of the GABAergic maturation signals. However, it is possible that proliferation of ECs and cells within the WM and GM may still contribute to repair, without their maturation into differentiated progeny. For example, Sabelstrom *et al*., (2013) illustrated that without EC proliferation, animals with SCI exhibited worse functional outcomes, and poorer tissue repair.

6.5.6 How can we accurately quantify remyelination?

Examining the number and proportion of EdU/PanQKI$^+$ cells in LPC/flumazenil treated animals vs LPC/vehicle treated animals provides an insight into whether flumazenil increased the level of oligodendrocyte proliferation and differentiation following LPC treatment. QKI is an RNA-binding protein that is upregulated in myelinating oligodendrocytes to which the commonly used mature oligodendrocyte marker APC/CC1 binds (Bin *et al*., 2016). This provides an indirect measure of repair as oligodendrocytes are capable of forming a wide number of remyelinated internodes (Keough *et al*., 2015), however it is not able to provide exact information on the level of remyelination.

Animals were sacrificed at 14dpi and injection sites were stained for MBP in order to quantify the level of remyelination in LPC/flumazenil vs. LPC/vehicle treated animals at a time point when remyelination has begun but some demyelination remains for comparison (Keough *et al*., 2015). However, technical issues during imaging prevented the gathering of this data and therefore it was not possible to determine whether flumazenil had any effect on the level of remyelination in these animals compared to vehicle treatment outside of the effects upon EdU/PanQKI$^+$ cell counts. Therefore, further experiments must be undertaken in order to provide more insight into the effects, if any, that flumazenil may have had upon the speed and efficiency of remyelination in these animals.

The ‘gold-standard- method for quantification of remyelination is based on the central dogma that remyelinated segments are shorter in length and thinner than their healthy counterparts (Gledhill *et al*., 1973; Harrison and McDonald, 1977). An increase in the g-ratio (axon diameter divided by axon $^+$ myelin diameter) is a morphological indication of the presence of axons which have undergone remyelination (Crawford *et al*., 2013; Franklin and Goldman, 2015; Duncan *et al*., 2017). Calculation of the g-ratio of cross-sectional semi- or ultrathin sections stained with toluidine blue would therefore provide an accurate measure of the presence and extent of remyelination in animals treated with LPC/flumazenil vs.

LPC/vehicle. Analysis of the prevalence of shorter internodes and thinner myelin sheaths could therefore be employed in future experiments to determine whether remyelination is improved in flumazenil treated animals (Duncan *et al*., 2017; Crawford *et al*., 2013).

Remyelination has been linked to restoration of saltatory conduction (Smith, K.J. *et al*., 1979) and therefore the level of repair following models of demyelination are likely best quantified by the level of functional neurological recovery. However, as a result of the focal nature of LPC-induced demyelinating lesions there are no overt observable neurological or motor deficits compared to more robust demyelination models such as experimental autoimmune encephalitis (Keough *et al*., 2015).

Hamaguchi *et al*., (2017) however have developed a protocol for the assessment of behavioural deficits following demyelination of the corticospinal tract by injection of LPC into the dorsal column, illustrating that assessment of sensorimotor impairment following LPC-induced demyelination is possible. Demyelination of the corticospinal tract leads to motor impairment as assessed by hindlimb function by correct stepping during beam walking and ladder walking behavioural test. Sensorimotor deficits partially recover over time due to spontaneous remyelination, however significant recovery of motor function is detectable by 10dpi (Hamaguchi *et al*., 2017; Matoba *et al*., 2017). Utilising behavioural analyses such as these in future work, alongside IHC analysis of remyelination, would be further help determine whether modulation of GABAaR by endogenous CBR ligands, and their perturbation by antagonists such as flumazenil, are mechanisms which could be harnessed for repair following demyelination.

6.6 Conclusion

Work described in this chapter has shown that intraspinal LPC infusion results in fewer EdU^+ cells in the spinal cord compared to saline infusion. The numbers of EdU^+ cells are greater in animals which receive flumazenil treatment following LPC infusion vs. animals which are

treated with vehicle, however, flumazenil treatment did not result in greater numbers of new EdU/PanQKI^{+} oligodendrocytes as hypothesised. Technical issues prevented the quantification of remyelination in these animals, and therefore we are still unable to determine whether modulation of GABAaR by perturbation of endogenous binding to CBR by flumazenil resulted in improved remyelination in these animals following LPC. Further work which employs the use of more sensitive methods of remyelination quantification alongside behavioural assessment of sensorimotor functional recovery is therefore necessary.

Despite this, work described here is the first to show that preventing binding to the GABAaR CBR site by flumazenil treatment results in a greater number of proliferative cells following LPC-induced demyelinating lesions in the spinal cord. Knowledge of ways to augment the endogenous proliferating population following demyelination is essential as research into future therapies for MS are beginning focus on ways to improve endogenous remyelination. It is possible that combinatorial therapies, involving a proliferative boost and a differentiating-promoting agent may be the future of MS therapy to slow or even halt the progressive neurological decline by chronic demyelination and neuroaxonal degradation.

Chapter 7 – General discussion

7.1 Introduction

It has been long contested as to whether postnatal proliferation and neurogenesis occurs outside of the well- defined neurogenic niches of the brain. However, there is much evidence illustrating that new cells are continually added to the intact adult spinal cord and that ECs possess NSC capabilities (section 1.5). Cell turnover occurs very slowly in the intact cord, where most cells undergo self-renewal for population maintenance, oligodendrocytes are the exception to this rule and also produce new progeny (Meletis *et al*., 2008; Barnabe-Heider *et al*., 2010). Whilst injury results in the expansion of the normally dormant cell populations, most progeny differentiate into scar-forming astrocytes, and although this is essential for damage control and lesion sealing, the new cells do not appear to contribute to the replacement of lost myelinating oligodendrocytes or neurones.

Therefore, rather than a lack of neurogenic potential, instead the spinal cord appears to possess a proliferation-restrictive and gliogenic environment which prevents the realisation of NSC-potential in the intact adult spinal cord and neurogenic- and oligogenic- potential in the injured cord. Hopes that the endogenous proliferating population of cells which are augmented following injury could be used for self-repair therefore feel short-sighted. However, if we determine the niche signalling mechanisms which contribute to the restrictive environment in the postnatal spinal cord to modulate proliferation and differentiation this would renew hope in the self-regenerative capabilities of the adult spinal cord. Work presented here illustrates that GABA is, at least one of, these restrictive signals in the spinal cord.

7.2 GABAergic signalling influences proliferation in the WM, GM, and CC region of the intact adult spinal cord

The numbers of EdU^+ cells in the WM, GM, and CC were examined in GAD67-GFP animals compared to WT animals. GAD67-GFP mice exhibit decreased levels of ambient GABA in

their spinal cord compared to WT and as a result possess greater numbers of EdU^+ cells in the spinal cord WM, GM, and CC, compared to WT animals (table 7.1). Increasing the levels of ambient GABA by treatment with vigabatrin significantly decreased the numbers of EdU^+ cells in the WM, GM, and CC compared to vehicle treatment (table 7.1). These results illustrate the inhibitory effect of the basal GABAergic tone in the adult spinal cord upon proliferation of cells in the WM and GM, but also that GABAergic signalling may be one of the signals within the CC neurogenic niche which keeps the NSC-like ECs in a quiescent state.

Table 7.1 Effects of various modulators upon proliferation in the postnatal spinal cord

Summary of the effects of different experimental conditions upon the number of EdU^+ cells located within the WM, GM, and CC of experimental vs. control animals. + = significantly greater numbers of EdU+ cells. - = significantly fewer EdU+ cells. N.s = no significant difference between groups

Experiment	Effect on numbers of EdU^+ cells
Day vs. Night (WT)	Total **+** CC **+**
Day vs. Night (GADs)	Total **+** CC **n.s**
WT vs. GAD in light hours	Total **+** CC **+**
WT vs. GAD in dark hours	Total **n.s** CC **+**
VGB vs. Vehicle	Total **-** WM **-** GM **-** CC **-**
ETX vs. Vehicle (WT and GAD)	Total **-** CC **-**
MDZ vs. Vehicle	Total **-** CC **-**
PK11195 vs vehicle	Total **-** CC **-**
TSPOKO vs TSPOflox	Total **+** WM **+** GM **n.s** CC **n.s**
Flumazenil vs. Vehicle	Total **+** WM **+** GM n.s CC **+**
Ro15-4513 vs. Vehicle	Total **+** WM **n.s** GM **+** CC **+**
G2F77I vs WT	Total **+** WM **+** GM **+** CC **+**

7.3 DBI and TSPO may be involved in the regulation of GABAergic modulation of proliferation in the cord

7.3.1 DBI and TSPO are expressed in the adult spinal cord

Work described in chapter 4 illustrates that the allosteric GABAaR modulator DBI is expressed within the postnatal spinal cord and is also robustly expressed in ECs. GABAergic signalling modulates proliferation in the spinal cord; the presence of DBI within the spinal cord therefore suggests that DBI may also serve as a master regulator of GABAaR to balance quiescence, proliferation, and differentiation. Indeed, this is the case in both the SVZ and SGZ, where DBI negatively modulates GABA to increase the NSPC pool and decrease the young neurone population (Alfonso *et al*., 2012; Dumitru *et al*., 2017).

The spinal cord also expresses the mitochondrial DBI receptor TSPO where it frequently colocalises with DBI (chapter 4). It is therefore possible that in the spinal cord DBI may also have effects at TSPO which could influence proliferation either by changes in $Ca2^{+}$ signalling (Gandolfo *et al*., 2000), or through the production of neurosteroids which are modulators of GABA (Varga *et al*., 2005).

Work in presented in chapter 3 illustrates that a basal inhibitory GABAergic tone modulates proliferation in the postnatal spinal cord. The presence of the endogenous CBR site ligand DBI suggests that similarly to the SGZ and SVZ the spinal cord may also modulate GABAaR through endogenous CBR site binding. The expression of TSPO in complementary regions of DBI-IR may also suggest the involvement of TSPO, and its role in GABAergic neurosteroidogenesis, in modulation of postnatal proliferation and differentiation in the adult spinal cord.

7.3.2 TSPO is involved in spinal cord proliferation

Animals treated with mixed modulators of GABAaR and TSPO, ETX and MDZ, possessed fewer EdU^{+} cells in the WM, GM, and CC, compared to vehicle treated animals (table 7.1).

The TSPO specific ligand PK11195 also resulted in fewer EdU^+ cells in the spinal cord compared to vehicle (table 7.1). These results are the first to show that that ligand binding at TSPO is involved in the modulation of proliferation within the adult spinal cord, however whether this is the result of DBI binding and/or the production of neurosteroids cannot be determined. Further work using the α5-reductase inhibitor finasteride would further elucidate the role neurosteroidogenesis may play in controlling proliferation in the intact spinal cord.

7.3.3 Perturbation of endogenous binding to CBR alters proliferation and differentiation in the adult spinal cord

Perturbation of ligand binding to the CBR site, by treatment with either the CBR specific antagonist flumazenil or the inverse agonist Ro15-4513 results in greater numbers of EdU^+ cells in the WM, GM, and CC compared to vehicle treatment (table 7.1). G2F77I animals also possessed greater numbers of EdU^+ cells in the spinal cord compared to WT animals (table 7.1). These results illustrate the importance of endogenous CBR-ligand binding in the control of levels of basal proliferation in the adult spinal cord as when this is prevented by either pharmacological or transgenic means there is an increase in proliferation compared to control.

It would therefore appear that endogenous ligand binding at CBR which modulates the inhibitory basal GABAergic tone acting on proliferation, as is seen in other neurogenic regions (Alfonso *et al*., 2012; Dumitru *et al*., 2017), is a likely mechanism which also occurs in the spinal cord However, such a mechanism would involve DBI acting as a PAM at GABAaR to keep GABAergic signalling high to maintain quiescence in the spinal cord, whereas in the SVZ and SGZ, DBI negatively modulates GABA to suppress its inhibitory proliferative brake (Alfonso *et al*.,2012; Dumitru *et al*., 2017). DBI has been shown to be released by astrocytes and potentiate GABAergic signalling in the reticular thalamic nucleus (Christian *et al*., 2013; Christian, C. A. and Huguenard, J. R., 2013). Although the expression of DBI within astrocytes and ECs could be hypothesised to be for this purpose, further work

is required to determine if DBI does show PAM activity at GABAaR in the spinal cord and its effects upon ECs. It is also not yet known whether specific peptide fragments of DBI are involved in such effects or whether these fragments exhibit preferential activity at subunit specific GABAaR CBR sites.

7.3.4 Clinical significance of the effects of GABA modulation upon proliferation in the postnatal spinal cord

Controlling NSC quiescence is extremely important, as unchecked proliferation may lead to tumorigenesis and GABAergic signalling may hold the key to such regulation. It has been hypothesised that endozepines such as DBI and GABAergic signalling may be involved in the high proliferative rate of anaplastic tumour cells, as there is a significant increase in DBI expression in various human brain tumours, including astrocytomas, glioblastomas and medulloblastomas (Alho *et al*., 1995). Tumours with high DBI expression also express the mitochondrial DBI receptor TSPO at a high level. The level of TSPO expression is strongly associated with the histological grade of the tumour, greater level of proliferation and malignancy, and tendency toward poor patient survival (Miettinen *et al*., 1995). Results presented in chapter 3 and 5 illustrate that modulation of GABAergic signalling in the spinal cord is able to influence proliferation in either direction. Such findings indicate that modulation of GABAaR by binding of endogenous CBR site antagonists such as flumazenil could be investigated as a means to reduce aberrant proliferation in CNS cancers

7.4 GABA and differentiation in the spinal cord

In all of the experiments described there was evidence of co-labelling of EdU^+ cells with markers of either astrocyte, oligodendrocyte, microglial, or neuronal differentiation. The majority of EdU^+ cells were either $Sox2^+$ or $PanQKI^+$ independent of experimental group, indicating that newly proliferated EdU^+ cells either remained as undifferentiated $Sox2^+$ NSCs or differentiated into $PanQKI^+$ oligodendrocytes. This is in agreement with findings from other

studies which have shown that in the intact adult spinal cord, OPCs consistently produce new oligodendrocytes and therefore make up 80% of the proliferating population (Barnabé-Heider *et al*., 2010).

The percentage and/or numbers of EdU^+ cells which were also positive for markers of differentiation were often not significantly different in experimental vs. control animals. However, fate acquisition of EdU^+ cells was altered in some experimental conditions vs. control (table 7.2).

Table 7.2 Summary of effects upon differentiation

Table showing the effects of different experimental conditions upon either the number of EdU/differentiation marker$^+$ cells (#) or the percentage of total EdU^+ cells which were colabelled with a particular marker of differentiation (%)

Experimental group	Marker of differentiation	Effect on EdU/marker # or %
ETX	PanQKI	# and % decreased
ETX	NeuN	% increased
MDZ	PanQKI	% increased
TSPO KO	PanQKI	% decreased
G2F77I	PanQKI	% decreased
G2F77I	S100β	% decreased
Ro15-4513	PanQKI	# increased
Ro15-4513	S100β	% decreased
Ro15-4513	Sox2	% increased
Ro15-4513	Tuj	% increased

Glial cell fate acquisition by newly proliferated EdU^+ cells was most affected as differences in the number and/or percentage of EdU^+ cells which expressed either S100b or $PanQKI^+$ changes in experimental vs control animals were more frequently observed (table 7.1). Whether these results reflect the effect that GABA has on differentiation of newly proliferated

cells in the spinal cord in creating a gliogenic environment is not clear and further work is required to determine whether this is the case.

Flumazenil treated animals possessed significantly more EdU^+ in the spinal cord compared to vehicle treated animals, however there were no differences in the fate acquisition of these newly proliferated cells. It was hypothesised that in flumazenil treated animals with greater numbers of EdU^+ cells, cell death by LPC-induced demyelination, may provide an environment for differentiation of these new cells to replace those which had been lost to demyelination. However, this was not the case (section 6.5.5.1)

GABAergic signalling, possibly modulated by endogenous ligands such as DBI, is likely involved in the control of proliferation and differentiation within the spinal cord. However, further work is required to determine how best to influence such signals to direct differentiation for repair following cell depletion in times of injury. For example, overexpression of the transcription factor Sox2 has been shown to induce the differentiation of resident astrocytes to DCX+ neurones in the injured adult spinal cord (Su *et al*., 2014). These 'directed-neurones' showed features of GABAergic interneurons and illustrate how the proliferative gliogenic environment following injury can be used for good. In a mouse model of demyelination, reactive astrocytes were converted to myelinating mature oligodendrocytes by injection of Sox10 into the lesion site. Such results hold promise for the future of CNS repair, where transdifferentiation of resident astrocytes which proliferate following injury could be employed *in situ* to enhance tissue repair

7.5 Considerations

7.5.1 Is EdU the best method to assess proliferation?

In all experiments described here, proliferation in the spinal cord was quantified by detecting incorporation of the thymidine analogue EdU. Examining thymidine incorporation in dividing cells has been used for the investigation of cell proliferation since the early work of Altman and Das who utilised autoradiography to detect cell division by the incorporation of [^{3}H]-thymidine and showed that proliferation does occur in the adult CNS (Altman and Das, 1965). This method was largely replaced by detection of BrdU incorporation in diving cells by IHC due to convenience and compatibility with high-resolution microscopy and colocalisation of up to 3 cell type markers (Breunig *et al*., 2008). However, assessing proliferation by BrdU detection can be problematic as it requires strong DNA-denaturing conditions to unmask and label the BrdU epitope within the new cell.

Assessing proliferation by incorporation of the thymidine analogue EdU, and its detection by 'click-chemistry', retains the benefits of BrdU-labelling in double labelling cell fate studies, but circumvents such methodological issues (Buck, S.B. *et al*., 2008; Salic and Mitchison, 2008; Chehrehasa *et al*., 2009). EdU incorporation has been frequently used for studying proliferation in the adult CNS (Zeng *et al*., 2010). However, recent work has suggested that EdU may not be the best way to investigate proliferation and may induce experimental artefacts caused by labelling DNA repair and damaging DNA.

EdU labels proliferating cells by replacing thymidine nucleosides during the s-phase of cell division, however nucleosides are also incorporated into DNA during DNA repair (Kao *et al*., 2005; Lee, Y.-H. and Stallcup, 2011; Lowndes and Murguia, 2000). There have been concerns that this is the case for BrdU (Cooper-Kuhn and Georg Kuhn, 2002), and as EdU only differs from BrdU in its post-hoc detection method, it is therefore possible that EdU also labels cells undergoing DNA repair. Inclusion of cells undergoing DNA repair would mean that we are overestimating the amount of proliferation in the adult CNS. This would be of

particular concern in experiments where tissue damage is induced, for example following LPC-induced demyelination (chapter 6).

Copper-Kuhn and Kuhn (2002) argue against DNA repair being a major contribution of $BrdU^+$ cells as double labelling IHC and analysis by EM illustrate that $BrdU^+$ cells exhibit maturation from dividing precursors to fully mature neurones. Apoptotic cell death is accompanied by activation of DNA repair mechanisms (Norbury and Zhivotovsky, 2004), however co-labelling with apoptotic markers such as active caspase-3 and TUNEL with BrdU was not observed in the SVZ, indicating that BrdU is not being incorporated into cells undergoing DNA repair before apoptosis (Cooper-Kuhn and Georg Kuhn, 2002). Neurones immediately activate DNA repair pathways to detect and correct DNA damage in response to ionising radiation (Gobbel *et al*., 1998; Leadon, 1996). Ionizing radiation dose-dependently increases DNA damage followed by DNA repair (Li, L. *et al*., 2001). However, when the number of $BrdU^+$ cells is measured in the SVZ following irradiation, there was an immediate dose dependent decline in $BrdU^+$ cells and a significant increase in the number of apoptotic cells (Bellinzona *et al*., 1996). Together these findings confirm that changes in the numbers of thymidine-analogue labelled cells are not an artefact or false-positive induced by the labelling of cells undergoing DNA repair.

EdU has recently been suggested however to possess cytotoxic properties, where its incorporation into dividing cells leads to cell cycle arrest and/or cell death (Diermeier-Daucher *et al*., 2009; Kohlmeier *et al*., 2013). It has been shown that EdU incorporation may slow cell replication, induce DNA damage signalling pathways, induce G2 cell cycle arrest and ultimately lead to apoptosis (Zhao, H. *et al*., 2013). EdU has also been observed to decrease survival of myogenic stem cell survival following transplantation into regenerating muscle (Andersen *et al*., 2013). These findings illustrate the need to reconsider EdU as an inert indicator in experimental settings. However, as they are based on the effects of EdU upon cell growth *in vitro*, where the dose of EdU used and the method of application, and length of exposure to EdU, differ from *in vivo* settings, further work is therefore required to

determine whether this is also a problem when using EdU to assess proliferation *in vivo*. Nevertheless, animals in all experimental groups studied here received EdU and this would control for any confounding cytotoxic effects that EdU may have *in vivo*.

7.5.2 Migration of ECs

Colabelling with the GFAP was used to determine whether any newly proliferated cells in the spinal cord were astrocytes. However, due to the fibrillary nature of $GFAP^+$ staining the soma of $GFAP^+$ cells was difficult to determine, and therefore colocalisation of EdU and GFAP could be easily over- or underestimated during cell counting. Later experiments used the calcium binding protein S100β as a marker of astrocytic differentiation in EdU^+ cells which vastly improved visualisation of EdU^+ astrocytes. However, S100b is also expressed in ECs (Canova *et al*., 2006) and therefore some of the EdU/$S100b^+$ cells may represent migrating ECs rather than astroglial proliferation.

Following injury, astrocytes and ECs proliferate, differentiate, and migrate to the centre of the lesion site to contribute to wound sealing and repair (Mothe and Tator, 2005; Meletis *et al*., 2008; Barnabe-Heider *et al*., 2010; Sabelstrom *et al*., 2013). Clustering of many EdU^+ cells was also seen at the dorsal columns following LPC-induced demyelination. However, due to the inability to track specific neural cell type progeny in our experiments we were unable to determine which populations of cells were most involved in the LPC-induced proliferative response. For this reason, it was also not possible to determine whether new EdU^+ cells present at the dorsal columns were glial cells native to the dorsal column WM or if it other cells migrated to the lesion site.

It has been repeatedly shown that EC proliferation increases markedly following injury to the spinal cord, however in animals which received an intraspinal injection, there were no more EdU^+ cells in at the CC compared to intact animals. Furthermore, following intraspinal LPC injection there were fewer EdU^+ cells in the CC compared to saline injected animals. It is possible that these results are due to the migration of newly proliferated cells to the injured

dorsal columns, resulting in fewer EdU^+ cells present at the CC, so that overall the level of proliferation in this area does not appear greater than in control conditions. However, without labelling of EC progeny in order to track their migration toward the dorsal column and their differentiation, we are unable to determine whether this is indeed the case.

Barnabe-Heider *et al*., (2010) performed genetic fate mapping using tamoxifen-dependent Cre-recombination under the control of cell type specific promotors such as FoxJ1 to label ECs (Barnabe-Heider *et al*., 2010; Meletis *et al*., 2008). Genetic fate mapping of $FoxJ1^+$ EC progeny would enable us to investigate the effects of GABAergic modulation of proliferation and differentiation in the intact spinal cord specifically in ECs. Such experiments would complement work presented here by further elucidating whether a basal GABAergic tone is responsible for the slow turnover of ECs in the intact cord. These experiments would further elucidate whether latent NSC properties of ECs can activated in the intact cord under conditions which modulate GABAergic signalling e.g. with CBR site modulation or KD or OE of DBI. As ECs are not the only proliferating cells in the postnatal spinal cord, genetic fate mapping would also allow more detailed investigation into the effects of GABAergic modulation of proliferation and differentiation of oligodendrocytes, astrocytes, and neurones in the intact spinal cord.

7.6 Function of DBI in the intact adult spinal cord

Work in presented in chapter 4 illustrates that DBI is expressed within the adult spinal cord and is present within the NSC-like ECs at the CC. In the SVZ and SGZ, DBI modulates the inhibitory effect of GABAergic signalling to balance NSC proliferation and neuroblast maturation (Alfonso *et al*., 2012; Dumitru *et al*., 2017). However, whether DBI is expressed in the spinal cord for the same purpose is not yet known.

Flumazenil treated and G2F77I mice possessed significantly more EdU^+ cells in the WM, GM, and CC compared to control animals, illustrating that attenuation of endogenous ligand

binding to the CBR site of GABAaR in the spinal cord by either pharmacological or transgenic means results in greater numbers of proliferative cells. These results suggest that an endogenous ligand exists at CBR in the spinal cord, which also modulates the basal inhibitory GABAergic tone to induce quiescence in the postnatal spinal cord, as perturbation of binding to CBR leads to more EdU^+ cells in the spinal cord. However, whether flumazenil treated mice or G2F77I mice exhibit reduced binding of DBI to GABAaR in the spinal cord is not known. If the ligand modulating GABAaRs control of proliferation in the spinal cord is DBI then unlike effects seen in the SVZ and SGZ, it would be acting as a positive modulator of GABAaR in the spinal cord as proliferation is greater in animals with alterations in CBR site binding. Although ECs express DBI and respond to GABA, the effects of DBI on GABAergic currents in ECs, and whether DBI augments these, remains to be seen. Further work examining the effects of DBI upon the electrophysiological behaviour of ECs is therefore essential.

Whilst work described in chapter 5 suggests that there is some form of endogenous ligand binding at the CBR site which modulates the inhibitory GABAergic tone in the adult spinal cord to keep cell turnover low in the intact cord, the effect of DBI on proliferation and differentiation was not specifically tested. Alfonso *et al*., (2012) and Dumitru *et al*., (2017) assess the effects of DBI on proliferation and differentiation in the neurogenic niches of the SVZ and SGZ using lentiviral mediated KD or OE of DBI. Collaboration with Prof. H. Monyer and Dr. I Dumitru allowed us to test these same DBI OE or DBI KD lentiviruses in the spinal cord in order to assess the contribution of DBI to the modulation of proliferation and differentiation in the intact postnatal spinal cord.

There were few instances of successful transfection of ECs by either virus, as assessed by the expression of GFP or RFP, following injections targeted to the CC. However, transfection was largely unsuccessful and propagation to cells outside of the injection site was rarely seen (data not shown). ECs divide slowly (Alfaro-Cervello *et al*., 2012; Barnabe-Heider *et al*., 2010), however as lentiviruses are capable of infecting non-dividing cells (Vodicka, 2001), it

is unlikely that slow turnover of ECs is to explain for poor transduction of these viruses following injection. Instead missed injections due to difficulty in exact targeting of injections to the CC or poor transfection by injection of too small a viral titre may explain why these experiments were unsuccessful. Ren *et al*., (2017) show that the proliferative response of EC following injury is due to direct damage to the CC ependyma (Ren *et al*., 2017). Therefore, if lentiviral mediated DBI OE or KD had been successful in the spinal cord, investigation into how DBI influences proliferation and differentiation within the intact adult spinal cord may have been confounded by the damage sustained by the ependyma during the viral injection itself. Martens *et al*., (2002) illustrated that *in vivo* infusions of exogenous growth factors into 4th ventricle resulted in changes in the proliferative capacity of cells in the spinal cord CC despite their introduction at a most rostral location. Injections of DBI OE/KD lentiviruses could be instead focused at the 4th ventricle, in an attempt to label ECs without the damage caused by direct injection to the ependyma (Ren *et al*., 2017).

7.6.1 GABAaR expression in the spinal cord

ECs respond with robust depolarisations in response to application of GABA, an effect which is mainly mediated by GABAaR (Corns *et al*., 2013). The numbers of EdU^{+} cells in the WM, GM, and CC are significantly higher in GAD67-GFP mice which possess lower levels of GABA in their spinal cord compared to WT animals. Together these results suggest that ambient GABA acting via GABAaRs influence proliferation in the adult spinal cord. However, the identity and specific subunit composition of GABAaRs in the proliferating cells of the spinal cord remain undetermined at present. Further investigation into the expression of specific GABAaR subunits in proliferating populations such as OPCs and ECs is needed in order to understand the effects of flumazenil, Ro15-4513, and G2F77I mutation, and possibly DBI, upon proliferation and differentiation in the spinal cord. For example, single cell RNA sequencing has already been used to analyse singe cell transcriptomics of ECs close to the SVZ neurogenic niche in relation to their neurogenic potential (Shah *et al*., 2018).

Therefore, such methods could also be used to investigate the expression profile of GABAaR subunits in ECs.

7.6.2 Can we determine the source of GABA in the spinal cord?

Neighbouring GABAergic CSFcCs have been hypothesised to be the source of the inhibitory GABA acting on ECs to induce quiescence, similar to that of neuroblasts in the SVZ (Daynac *et al*., 2013). Evidence for this hypothesis is discussed in detail in section 1.9 and section 3.5.2.1.

Irradiation of fast dividing progenitors results in depletion of the GABA-secreting neuroblast population and the activation of normally quiescent NSCs within the SVZ niche (Daynac *et al*., 2013). CSFcCs however do not show the same cell-cycle dynamics and have not been shown to incorporate markers of cell division in the intact postnatal spinal cord (Daniels, 2015), therefore this method would not be applicable to the spinal cord. Instead of trying to selectively remove the GABA source by selective ablation of CSFcCs, recording ECs and GCaMP3$^+$ CSFcCs in acute slices from VGAT-Cre/GCaMP3 mice would instead show whether activity of CSFcCs induces activity in ECs. VGAT/GCamp3 mice express the fluorescent calcium indicator in cells which express the vesicular GABA transporter VGAT, therefore activity of GABAergic cells, i.e. CSFcCs, can be measured in real time by changes in fluorescence intensity (Seo *et al*., 2016; Zariwala *et al*., 2012). Alternatively, expression of light activated channel rhodopsin in VGAT$^+$ cells in VGAT-cre/ChR-tdtomato animals could provide another method to probe the effect of CSFcC activity upon ECs, where CSFcCs could be activated by blue light and resultant changes in electrical activity could be recorded in the nearby ECs (Cohen *et al*., 2012).

If activity of CSFcCs does influence EC activity, it could be hypothesised that CSFcCs change in some way following SCI and this is why ECs are able to realise their NSC potential proliferate, differentiate, and migrate to the lesion site. Investigation into whether there are changes in the presence of GAD67-GFP$^+$ CSFcCs at the CC following SCI would

show whether these cells die following injury or migrate to release ECs from CSFcC-mediated inhibitory paracrine GABAergic signalling. A simpler explanation could involve a SCI-induced signalling pathway which inhibits GABA secretion by CSFcCs, leading to disinhibition of EC proliferation.

7.7 Applicability of findings to humans

Dromard *et al*., (2008) and Mothe *et al*., (2011) have demonstrated that the adult human spinal cord harbours cells which possess *in vitro* NSC potential. These studies show that self-renewing, multipotent NSCs can be passaged from adult human spinal cord which are able to differentiate into neurones and glia following transplantation into rats with SCI (Mothe *et al*., 2011). Such work suggests that endogenous NSCs from the spinal cord may be utilised for repair in conditions such as SCI or MS in humans.

Interestingly however, arguments about whether ECs possess NSC potential which could be manipulated for therapeutic gain may be moot according to findings from Garcia-Ovejero (2014) regarding the cytoarchitecture of the human spinal cord CC ependymal region. The function of the CC in humans in not yet well understood (Saker *et al*., 2016). It is often thought to be a vestigial structure which loses patency over time and is gradually replaced by ependymal cells, where occlusion or stenosis is thought to occur in 70 to 80% of normal adults, as seen by high resolution MRI (Saker *et al*., 2016; Milhorat *et al*., 1994; Garcia-Ovejero *et al*., 2015). MRI and post-mortem immunohistochemical investigations have also suggested that ECs within human spinal cords are distinct from those seen lining the CC in other species. A notable gliosis, formed by a dense mesh of $GFAP^+$ astrocytic processes is found at the adult human CC region. The $GFAP^+$ gliotic mesh surrounds and infiltrates EC accumulations within this area and is a characteristic believed to be unique to this region in humans (Garcia-Ovejero *et al*., 2015) $Vimentin^+$ cells arranged in a perivasuclar pseudorosette structures, a characteristic diagnostic feature of low-grade ependymoma, have also been found to be specific to the human CC region.

These findings are still debated however, with some claiming that CC occlusion and changes to the ependymal region architecture are a pathologic post-mortem finding, rather than an accepted degenerative process associated with normal aging (Cramer *et al*., 2005). It is thought that these changes may be associated with acquired ependymitis caused by common viruses contracted throughout life (Saker *et al*., 2016). Indeed, there is evidence that some viruses including influenza A, poxviruses, measles, mumps, selectively target ECs and replicate within ECs which results in their destruction without other clinically relevant disease (Milhorat *et al*., 1994; Mims, 1960).

Furthermore, whilst Garcia-Ovejaro (2015) show that the CC architecture may be distinct from other species, the vimentin^{+} ependymocytes present at the human CC show expression of CD15 and glutamate aspartate transporter which have been related to stem/precursor cell phenotypes in other NSC niches (Garcia-Ovejero *et al*., 2015). Cannabinoid receptor type 1, another molecular marker associated with NSC regulation, has also been shown to be enriched in the ependymal region of human CCs which retain patency (Paniagua-Torija *et al*., 2015) indicating that whilst differences in the ependymal region cytoarchitecture between different species, the ECs may still possess NSC capabilities which may be reparative, in humans as seen in animal models. Cawsey *et al*., 2015 illustrate that following SCI in humans, ECs respond by upregulating their expression of the neural progenitor cell marker nestin, with significantly more ECs positive for nestin post injury, where there is a positive correlation between the percentage of nestin positive ECs and post-injury survival time (Cawsey *et al*., 2015). These findings further illustrate that whilst the ependymal region may differ between species, it appears that ECs within humans also respond to injury, perhaps adopting a more neural progenitor-like phenotype, as illustrated by an increase in EC nestin expression (Cawsey *et al*., 2015).

Activation of ECs for functional gain has been explored in humans using infusion of growth hormone (GH) in a 9 month old infant with caudal regression syndrome (Devesa *et al*., 2017). Caudal regression syndrome is a foetal malformation characterised by incomplete

spinal cord development, resulting in interruption of the SC at L2-L3 level, lack of innervation to lower limbs, and neurogenic bowel and bladder in the patient treated in this study (Devesa *et al*., 2017). GH is known to have positive effects on NSCs in other niches (Martens, D.J. *et al*., 2002), therefore the patient was treated with GH plus rehabilitation over a course of 5 years. At the end of the 5-year experimental protocol, significant sensorial and motor improvements had been reached, with the gross motor function test-88 improving from 12.31% to 78.48% (where the maximum = 100). The patient gained control over his sphincters and could walk when aided with crutches, suggesting significant reinnervation occurring below the lesion level (Devesa *et al*., 2017). Treatment of caudal regression syndrome is usually supportive to improve quality of life and whilst it is difficult to assess the exact effects of GH in this situation, it appears that treatment with GH alongside rehabilitation at an early age when the CNS is still highly plastic, may have aided recovery. Brain GH has been shown to induce proliferation and differentiation of NSCs, and although less is known about the effects of GH on ECs, it seems possible that it may also have positive effects in the spinal cord if ECs are indeed NSCs. Devasa *et al*., (2017) argue that GH may act in the spinal cord as it does in the brain, increasing proliferation and differentiation of the spinal cord NSCs, allowing the formation of neural components which provide new innervation distal to the lesion level and therefore improve sensory and motor outcomes when supported by rehabilitation. Whilst this is an isolated case study, examining a disease known to have a spectrum of pathology, initial results suggest that manipulation of EC NSC properties by exogenous means may have contributed to the degree of functional recovery seen here. This is the ultimate goal for work described in this thesis, where investigation into how endogenous signalling in the spinal cord influences the cellular response, and how to manipulate these processes with clinically available drugs, may inform further work for therapeutic gain.

Overall, these results suggest that ECs in humans may also be important for repair following CNS trauma, and may be able to be manipulated to improve this process. Recent work

however has shown that ECs in humans do not proliferate in response to SCI, suggesting that ECs do not constitute an endogenous pool of cells for repair and that other avenues to replace cells lost in injury should be considered (Paniagua-Torias *et al*., 2018). However, ECs are not the only proliferative cell in the spinal cord (Barnabe-Heider *et al*., 2010; Horner *et al*., 2000). Work described here shows that modulation of GABAergic signalling influences proliferation of cells present in the WM and GM which may also be involved in the post-injury proliferative boom. Furthermore, GABA can decrease proliferation in the spinal cord, a finding which may be important in informing future CNS cancer therapies. Therefore, we must not ignore the importance of understanding the proliferative behaviour of different cell types in the adult spinal cord.

7.8 Conclusions

In conclusion, studies in this thesis have elucidated new information regarding how proliferation in the postnatal spinal cord may be modulated by GABAergic signalling. Results described here illustrate that GABA and its modulation by endozepines such as DBI may be one of the mechanisms which restrict proliferation of cells in the neurogenic niche surrounding the CC of the mammalian spinal cord. Although the postnatal spinal cord exhibits low levels of proliferation, this thesis has shown that proliferation within the intact adult spinal cord is not a rigid entity. Furthermore, alterations in either ambient GABA or modulation of GABAergic signalling by ligand binding to the CBR site of GABAaR can influence proliferation in a bidirectional manner. Work presented here illustrates that the postnatal spinal cord and NSC properties of ECs should not be overlooked when considering the possibility of self-regenerative therapies in future clinically relevant studies for spinal cord repair, it simply requires more attention.

References

Abematsu, M., Tsujimura, K., Yamano, M., Saito, M., Kohno, K., Kohyama, J., Namihira, M., Komiya, S. and Nakashima, K. 2010. Neurons derived from transplanted neural stem cells restore disrupted neuronal circuitry in a mouse model of spinal cord injury. *J Clin Invest.* **120**(9), pp.3255-3266.

Abla, A.A. and Sanai, N. 2013. GFP+ cells in nestin-GFP adult mouse hippocampus are radial glia-like quiescent neural stem cells capable of gamma-aminobutyric acid-mediated regulation by parvalbumin-expressing interneurons. *World Neurosurg.* **79**(2), pp.216-217.

Alfaro-Cervello, C., Soriano-Navarro, M., Mirzadeh, Z., Alvarez-Buylla, A. and Garcia-Verdugo, J.M. 2012. Biciliated ependymal cell proliferation contributes to spinal cord growth. *The Journal of comparative neurology.* **520**(15), pp.3528-3552.

Alfonso, J., Le Magueresse, C., Zuccotti, A., Khodosevich, K. and Monyer, H. 2012. Diazepam binding inhibitor promotes progenitor proliferation in the postnatal SVZ by reducing GABA signaling. *Cell Stem Cell.* **10**(1), pp.76-87.

Alho, H., Bovolin, P. and Slobodyansky, E. 1990. Diazepam binding inhibitor (DBI) processing: immunohistochemical studies in the rat brain. *Neurochem Res.* **15**(2), pp.209-216.

Alho, H., Costa, E., Ferrero, P., Fujimoto, M., Cosenza-Murphy, D. and Guidotti, A. 1985. Diazepam-binding inhibitor: a neuropeptide located in selected neuronal populations of rat brain. *Science.* **229**(4709), pp.179-182.

Alho, H., Fremeau, R.T., Jr., Tiedge, H., Wilcox, J., Bovolin, P., Brosius, J., Roberts, J.L. and Costa, E. 1988a. Diazepam binding inhibitor gene expression: location in brain and peripheral tissues of rat. *Proc Natl Acad Sci U S A.* **85**(18), pp.7018-7022.

Alho, H., Fremeau, R.T., Jr., Tiedge, H., Wilcox, J., Bovolin, P., Brosius, J., Roberts, J.L. and Costa, E. 1988b. Diazepam binding inhibitor gene expression: location in brain and peripheral tissues of rat. *Proceedings of the National Academy of Sciences of the United States of America.* **85**(18), pp.7018-7022.

Alho, H., Harjuntausta, T., Schultz, R., Pelto-Huikko, M. and Bovolin, P. 1991. Immunohistochemistry of diazepam binding inhibitor (DBI) in the central nervous system and peripheral organs: Its possible role as an endogenous regulator of different types of benzodiazepine receptors. *Neuropharmacology.* **30**(12, Part 2), pp.1381-1386.

Alho, H., Kolmer, M., Harjuntausta, T. and Helen, P. 1995. Increased expression of diazepam binding inhibitor in human brain tumors. *Cell Growth Differ.* **6**(3), pp.309-314.

Alho, H., Varga, V. and Krueger, K.E. 1994. Expression of mitochondrial benzodiazepine receptor and its putative endogenous ligand diazepam binding inhibitor in cultured primary astrocytes and C-6 cells: relation to cell growth. *Cell Growth Differ.* **5**(9), pp.1005-1014.

Altman, J. 1969. Autoradiographic and histological studies of postnatal neurogenesis. III. Dating the time of production and onset of differentiation of cerebellar microneurons in rats. *J Comp Neurol.* **137**, pp.433-458.

Altman, J. and Das, G.D. 1965. Autoradiographic and histological evidence of postnatal hippocampal neurogenesis in rats. *J Comp Neurol.* **124**(3), pp.319-335.

Amrein, R., Hetzel, W., Hartmann, D. and Lorscheid, T. 1988. Clinical pharmacology of flumazenil. *Eur J Anaesthesiol Suppl.* **2**, pp.65-80.
Andersen, D.C., Skovrind, I., Christensen, M.L., Jensen, C.H. and Sheikh, S.P. 2013. Stem cell survival is severely compromised by the thymidineanalog EdU (5-ethynyl-2'-deoxyuridine), an alternative to BrdU for proliferation assays and stem cell tracing. *Anal Bioanal Chem.* **405**(29), pp.9585-9591.
Anderson, C. and Edwards, S. 1994. *Intraperitoneal injections of FluroGold reliably label all sympathetic preganglionic neurons in the rat.*
Anderson, M.A., Burda, J.E., Ren, Y., Ao, Y., O'Shea, T.M., Kawaguchi, R., Coppola, G., Khakh, B.S., Deming, T.J. and Sofroniew, M.V. 2016. Astrocyte scar formation aids central nervous system axon regeneration. *Nature.* **532**(7598), pp.195-200.
Anholt, R.R., Murphy, K.M., Mack, G.E. and Snyder, S.H. 1984. Peripheral-type benzodiazepine receptors in the central nervous system: localization to olfactory nerves. *J Neurosci.* **4**(2), pp.593-603.
Ante, T. and Ljiljana, P. 2016. Neurosteroids, GABAA receptors and neurosteroid based drugs: are we witnessing the dawn of the new psychiatric drugs? *Endocrine Oncology and Metabolism.* **2**(1), pp.49-60.
Aouad, M., Petit-Demoulière, N., Goumon, Y. and Poisbeau, P. 2014. *Etifoxine stimulates allopregnanolone synthesis in the spinal cord to produce analgesia in experimental mononeuropathy.*
Asada, H., Kawamura, Y., Maruyama, K., Kume, H., Ding, R.-g., Ji, F.Y., Kanbara, N., Kuzume, H., Sanbo, M., Yagi, T. and Obata, K. 1996. Mice Lacking the 65 kDa Isoform of Glutamic Acid Decarboxylase (GAD65) Maintain Normal Levels of GAD67 and GABA in Their Brains but Are Susceptible to Seizures. *Biochemical and Biophysical Research Communications.* **229**(3), pp.891-895.
Asada, H., Kawamura, Y., Maruyama, K., Kume, H., Ding, R.G., Kanbara, N., Kuzume, H., Sanbo, M., Yagi, T. and Obata, K. 1997. Cleft palate and decreased brain gamma-aminobutyric acid in mice lacking the 67-kDa isoform of glutamic acid decarboxylase. *Proc Natl Acad Sci U S A.* **94**(12), pp.6496-6499.
Asher, G. and Sassone-Corsi, P. 2015. Time for Food: The Intimate Interplay between Nutrition, Metabolism, and the Circadian Clock. *Cell.* **161**(1), pp.84-92.
Asrican, B., Paez-Gonzalez, P., Erb, J. and Kuo, C.T. 2016. Cholinergic Circuit Control of Postnatal Neurogenesis. *Neurogenesis (Austin, Tex.).* **3**(1), pe1127310.
Barbaccia, M.L., Costa, E., Ferrero, P., Guidotti, A., Roy, A., Sunderland, T., Pickar, D., Paul, S.M. and Goodwin, F.K. 1986. Diazepam-Binding Inhibitor: A Brain Neuropeptide Present in Human Spinal Fluid: Studies in Depression, Schizophrenia, and Alzheimer's Disease. *Archives of General Psychiatry.* **43**(12), pp.1143-1147.
Barber, R.P., Vaughn, J.E. and Roberts, E. 1982. The cytoarchitecture of GABAergic neurons in rat spinal cord. *Brain Res.* **238**(2), pp.305-328.
Barnabe-Heider, F., Goritz, C., Sabelstrom, H., Takebayashi, H., Pfrieger, F.W., Meletis, K. and Frisen, J. 2010. Origin of new glial cells in intact and injured adult spinal cord. *Cell Stem Cell.* **7**(4), pp.470-482.
Barnabé-Heider, F., Göritz, C., Sabelström, H., Takebayashi, H., Pfrieger, F.W., Meletis, K. and Frisén, J. 2010. Origin of New Glial Cells in Intact and Injured Adult Spinal Cord. *Cell Stem Cell.* **7**(4), p470.
Basbaum, A.I. and Glazer, E.J. 1983. Immunoreactive vasoactive intestinal polypeptide is concentrated in the sacral spinal cord: a possible marker for pelvic visceral afferent fibers. *Somatosens Res.* **1**(1), pp.69-82.

Baumann, S.W., Baur, R. and Sigel, E. 2003. Individual Properties of the Two Functional Agonist Sites in GABA_A Receptors. *The Journal of Neuroscience.* **23**(35), p11158.
Belelli, D., Harrison, N.L., Maguire, J., Macdonald, R.L., Walker, M.C. and Cope, D.W. 2009. Extrasynaptic GABAA receptors: form, pharmacology, and function. *J Neurosci.* **29**(41), pp.12757-12763.
Bellinzona, M., Gobbel, G.T., Shinohara, C. and Fike, J.R. 1996. Apoptosis is induced in the subependyma of young adult rats by ionizing irradiation. *Neuroscience Letters.* **208**(3), pp.163-166.
Belluzzi, O., Benedusi, M., Ackman, J. and LoTurco, J.J. 2003. Electrophysiological differentiation of new neurons in the olfactory bulb. *J Neurosci.* **23**(32), pp.10411-10418.
Belzung, C. and Griebel, G. 2001. Measuring normal and pathological anxiety-like behaviour in mice: a review. *Behav Brain Res.* **125**(1-2), pp.141-149.
Belzung, C., Le Guisquet, A.M. and Crestani, F. 2000. Flumazenil induces benzodiazepine partial agonist-like effects in BALB/c but not C57BL/6 mice. *Psychopharmacology (Berl).* **148**(1), pp.24-32.
Ben-Menachem, E. 2011. Mechanism of action of vigabatrin: correcting misperceptions. *Acta Neurol Scand Suppl.* (192), pp.5-15.
Ben-Menachem, E., Hamberger, A. and Mumford, J. 1993. Effect of long-term vigabatrin therapy on GABA and other amino acid concentrations in the central nervous system--a case study. *Epilepsy Res.* **16**(3), pp.241-243.
Benavides, J., Quarteronet, D., Imbault, F., Malgouris, C., Uzan, A., Renault, C., Dubroeucq, M.C., Gueremy, C. and Le Fur, G. 1983. Labelling of "peripheral-type" benzodiazepine binding sites in the rat brain by using [3H]PK 11195, an isoquinoline carboxamide derivative: kinetic studies and autoradiographic localization. *J Neurochem.* **41**(6), pp.1744-1750.
Bénavidès, J., Savaki, H.E., Malgouris, C., Laplace, C., Daniel, M., Begassat, F., Desban, M., Uzan, A., Dubroeucq, M.C., Renault, C., Guérémy, C. and Le Fur, G. 1984. Autoradiographic localization of peripheral benzodiazepine binding sites in the cat brain with [3H]PK 11195. *Brain Research Bulletin.* **13**(1), pp.69-77.
Bender, A.S. and Hertz, L. 1987. Pharmacological characteristics of diazepam receptors in neurons and astrocytes in primary cultures. *J Neurosci Res.* **18**(2), pp.366-372.
Besman, M.J., Yanagibashi, K., Lee, T.D., Kawamura, M., Hall, P.F. and Shively, J.E. 1989. Identification of des-(Gly-Ile)-endozepine as an effector of corticotropin-dependent adrenal steroidogenesis: stimulation of cholesterol delivery is mediated by the peripheral benzodiazepine receptor. *Proc Natl Acad Sci U S A.* **86**(13), pp.4897-4901.
Betlazar, C., Harrison-Brown, M., Middleton, R.J., Banati, R. and Liu, G.-J. 2018. Cellular Sources and Regional Variations in the Expression of the Neuroinflammatory Marker Translocator Protein (TSPO) in the Normal Brain. *International journal of molecular sciences.* **19**(9), p2707.
Bin, J.M., Harris, S.N. and Kennedy, T.E. 2016. The oligodendrocyte-specific antibody 'CC1' binds Quaking 7. *J Neurochem.* **139**(2), pp.181-186.
Bjelobaba, I., Begovic-Kupresanin, V., Pekovic, S. and Lavrnja, I. 2018. Animal models of multiple sclerosis: Focus on experimental autoimmune encephalomyelitis. *J Neurosci Res.* **96**(6), pp.1021-1042.

Blakemore, W.F. 1977. Remyelination of CNS axons by Schwann cells transplanted from the sciatic nerve. *Nature.* **266**(5597), pp.68-69.
Blakemore, W.F. and Franklin, R.J. 2008. Remyelination in experimental models of toxin-induced demyelination. *Curr Top Microbiol Immunol.* **318**, pp.193-212.
Blanchart, A., Fernando, R., Haring, M., Assaife-Lopes, N., Romanov, R.A., Andang, M., Harkany, T. and Ernfors, P. 2016. Endogenous GABAA receptor activity suppresses glioma growth. *Oncogene.*
Bode, J., Veenman, L., Caballero, B., Lakomek, M., Kugler, W. and Gavish, M. 2012. The 18 kDa translocator protein influences angiogenesis, as well as aggressiveness, adhesion, migration, and proliferation of glioblastoma cells. *Pharmacogenet Genomics.* **22**(7), pp.538-550.
Bolger, G.T., Mezey, E., Cott, J., Weissman, B.A., Paul, S.M. and Skolnick, P. 1984. Differential regulation of 'central' and 'peripheral' benzodiazepine binding sites in the rat olfactory bulb. *Eur J Pharmacol.* **105**(1-2), pp.143-148.
Bolteus, A.J. and Bordey, A. 2004. GABA release and uptake regulate neuronal precursor migration in the postnatal subventricular zone. *J Neurosci.* **24**(35), pp.7623-7631.
Bonaguidi, M.A., Wheeler, M.A., Shapiro, J.S., Stadel, R.P., Sun, G.J., Ming, G.L. and Song, H. 2011. *In vivo* clonal analysis reveals self-renewing and multipotent adult neural stem cell characteristics. *Cell.* **145**(7), pp.1142-1155.
Bond, A.M., Ming, G.-L. and Song, H. 2015. Adult Mammalian Neural Stem Cells and Neurogenesis: Five Decades Later. *Cell stem cell.* **17**(4), pp.385-395.
Bonetti, E.P., Burkard, W.P., Gabl, M., Hunkeler, W., Lorez, H.P., Martin, J.R., Moehler, H., Osterrieder, W., Pieri, L., Polc, P. and *et al*. 1988. Ro 15-4513: partial inverse agonism at the BZR and interaction with ethanol. *Pharmacol Biochem Behav.* **31**(3), pp.733-749.
Bonner, J.F., Connors, T.M., Silverman, W.F., Kowalski, D.P., Lemay, M.A. and Fischer, I. 2011. Grafted neural progenitors integrate and restore synaptic connectivity across the injured spinal cord. *The Journal of neuroscience : the official journal of the Society for Neuroscience.* **31**(12), pp.4675-4686.
Bormann, J. 1991. Electrophysiological characterization of diazepam binding inhibitor (DBI) on GABAA receptors. *Neuropharmacology.* **30**(12, Part 2), pp.1387-1389.
Bormann, J., Hamill, O.P. and Sakmann, B. 1987. Mechanism of anion permeation through channels gated by glycine and gamma-aminobutyric acid in mouse cultured spinal neurones. *J Physiol.* **385**, pp.243-286.
Borowicz, K.K., Piskorska, B., Banach, M. and Czuczwar, S.J. 2011. Neuroprotective actions of neurosteroids. *Front Endocrinol (Lausanne).* **2**, p50.
Bouchard-Cannon, P., Mendoza-Viveros, L., Yuen, A., Kaern, M. and Cheng, H.Y. 2013. The circadian molecular clock regulates adult hippocampal neurogenesis by controlling the timing of cell-cycle entry and exit. *Cell Rep.* **5**(4), pp.961-973.
Bovolin, P., Schlichting, J., Miyata, M., Ferrarese, C., Guidotti, A. and Alho, H. 1990. Distribution and characterization of diazepam binding inhibitor (DBI) in peripheral tissues of rat. *Regulatory Peptides.* **29**(2), pp.267-281.
Braz, J.M., Sharif-Naeini, R., Vogt, D., Kriegstein, A., Alvarez-Buylla, A., Rubenstein, J.L. and Basbaum, A.I. 2012. Forebrain GABAergic neuron precursors integrate into adult spinal cord and reduce injury-induced neuropathic pain. *Neuron.* **74**(4), pp.663-675.

Bregman, B.S., Kunkel-Bagden, E., Reier, P.J., Dai, H.N., McAtee, M. and Gao, D. 1993. Recovery of function after spinal cord injury: mechanisms underlying transplant-mediated recovery of function differ after spinal cord injury in newborn and adult rats. *Exp Neurol.* **123**(1), pp.3-16.
Breunig, J.J., Sarkisian, M.R., Arellano, J.I., Morozov, Y.M., Ayoub, A.E., Sojitra, S., Wang, B., Flavell, R.A., Rakic, P. and Town, T. 2008. Primary cilia regulate hippocampal neurogenesis by mediating sonic hedgehog signaling. *Proceedings of the National Academy of Sciences.* **105**(35), p13127.
Bruce, J.H., Ramirez, A.M., Lin, L., Oracion, A., Agarwal, R.P. and Norenberg, M.D. 1991. Peripheral-type benzodiazepines inhibit proliferation of astrocytes in culture. *Brain Res.* **564**(1), pp.167-170.
Bruni, J.E. and Reddy, K. 1987. Ependyma of the central canal of the rat spinal cord: a light and transmission electron microscopic study. *Journal of anatomy.* **152**, pp.55-70.
Buck, K.J. and Harris, R.A. 1990. Benzodiazepine agonist and inverse agonist actions on GABAA receptor-operated chloride channels. II. Chronic effects of ethanol. *J Pharmacol Exp Ther.* **253**(2), pp.713-719.
Buck, S.B., Bradford, J., Gee, K.R., Agnew, B.J., Clarke, S.T. and Salic, A. 2008. Detection of S-phase cell cycle progression using 5-ethynyl-2'-deoxyuridine incorporation with click chemistry, an alternative to using 5-bromo-2'-deoxyuridine antibodies. *Biotechniques.* **44**(7), pp.927-929.
Buhr, A. and Sigel, E. 1997. A point mutation in the γ(2) subunit of γ-aminobutyric acid type A receptors results in altered benzodiazepine binding site specificity. *Proceedings of the National Academy of Sciences of the United States of America.* **94**(16), pp.8824-8829.
Calzolari, F., Michel, J., Baumgart, E.V., Theis, F., Gotz, M. and Ninkovic, J. 2015. Fast clonal expansion and limited neural stem cell self-renewal in the adult subependymal zone. *Nat Neurosci.* **18**(4), pp.490-492.
Campbell, R.A., Sanchez, E., Chen, H., Turker, L., Trac, O., Li, M., Shalitin, D., Gordon, M.S., Pang, S., Bonavida, B., Said, J., Berenson, R.J. and Berenson, J.R. 2006. PK11195, a Ligand of the Peripheral Benzodiazepine Receptor, Inhibits Myeloma Cell Growth *In vitro* and Chemosensitizes Myeloma Cells *In vivo* in SCID-hu Models of Human Multiple Myeloma. *Blood.* **108**(11), p3459.
Canova, C., Neal, J.W. and Gasque, P. 2006. Expression of innate immune complement regulators on brain epithelial cells during human bacterial meningitis. *Journal of neuroinflammation.* **3**, pp.22-22.
Cao, G., Edden, R.A.E., Gao, F., Li, H., Gong, T., Chen, W., Liu, X., Wang, G. and Zhao, B. 2018. Reduced GABA levels correlate with cognitive impairment in patients with relapsing-remitting multiple sclerosis. *Eur Radiol.* **28**(3), pp.1140-1148.
Carleton, A., Petreanu, L.T., Lansford, R., Alvarez-Buylla, A. and Lledo, P.M. 2003. Becoming a new neuron in the adult olfactory bulb. *Nat Neurosci.* **6**(5), pp.507-518.
Cascio, C., Brown, R.C., Liu, Y., Han, Z., Hales, D.B. and Papadopoulos, V. 2000. Pathways of dehydroepiandrosterone formation in rat brain glia. *The Journal of Steroid Biochemistry and Molecular Biology.* **75**(2), pp.177-186.
Catavero, C., Bao, H. and Song, J. 2018. Neural mechanisms underlying GABAergic regulation of adult hippocampal neurogenesis. *Cell Tissue Res.* **371**(1), pp.33-46.
Cawley, N., Solanky, B.S., Muhlert, N., Tur, C., Edden, R.A., Wheeler-Kingshott, C.A., Miller, D.H., Thompson, A.J. and Ciccarelli, O. 2015. Reduced gamma-

aminobutyric acid concentration is associated with physical disability in progressive multiple sclerosis. *Brain.* **138**(Pt 9), pp.2584-2595.
Cawsey, T., Duflou, J., Weickert, C.S. and Gorrie, C.A. 2015. Nestin-Positive Ependymal Cells Are Increased in the Human Spinal Cord after Traumatic Central Nervous System Injury. *J Neurotrauma.* **32**(18), pp.1393-1402.
Cerami, C. and Perani, D. 2015. Imaging neuroinflammation in ischemic stroke and in the atherosclerotic vascular disease. *Curr Vasc Pharmacol.* **13**(2), pp.218-222.
Chandra, D., Korpi, E.R., Miralles, C.P., De Blas, A.L. and Homanics, G.E. 2005. GABAA receptor gamma 2 subunit knockdown mice have enhanced anxiety-like behavior but unaltered hypnotic response to benzodiazepines. *BMC Neurosci.* **6**, p30.
Chang, W.P. and Sudhof, T.C. 2009. SV2 renders primed synaptic vesicles competent for Ca2+ -induced exocytosis. *J Neurosci.* **29**(4), pp.883-897.
Charalampopoulos, I., Margioris, A.N. and Gravanis, A. 2008a. Neurosteroid dehydroepiandrosterone exerts anti-apoptotic effects by membrane-mediated, integrated genomic and non-genomic pro-survival signaling pathways. *Journal of Neurochemistry.* **107**(5), pp.1457-1469.
Charalampopoulos, I., Remboutsika, E., Margioris, A.N. and Gravanis, A. 2008b. Neurosteroids as modulators of neurogenesis and neuronal survival. *Trends in Endocrinology & Metabolism.* **19**(8), pp.300-307.
Chehrehasa, F., Meedeniya, A.C.B., Dwyer, P., Abrahamsen, G. and Mackay-Sim, A. 2009. EdU, a new thymidine analogue for labelling proliferating cells in the nervous system. *Journal of Neuroscience Methods.* **177**(1), pp.122-130.
Chen, J., Dou, Y., Zheng, X., Leng, T., Lu, X., Ouyang, Y., Sun, H., Xing, F., Mai, J., Gu, J., Lu, B., Yan, G., Lin, J. and Zhu, W. 2016. TRPM7 channel inhibition mediates midazolam-induced proliferation loss in human malignant glioma. *Tumor Biology.* **37**(11), pp.14721-14731.
Chen, J., Ouyang, Y., Cao, L., Zhu, W., Zhou, Y., Zhou, Y., Zhang, H., Yang, X., Mao, L., Lin, S., Lin, J., Hu, J. and Yan, G. 2013. Diazepam inhibits proliferation of human glioblastoma cells through triggering a G0/G1 cell cycle arrest. *J Neurosurg Anesthesiol.* **25**(3), pp.285-291.
Chen, M.K. and Guilarte, T.R. 2008. Translocator protein 18 kDa (TSPO): molecular sensor of brain injury and repair. *Pharmacol Ther.* **118**(1), pp.1-17.
Chen, Y., Tian, D., Ku, L., Osterhout, D.J. and Feng, Y. 2007. The selective RNA-binding protein quaking I (QKI) is necessary and sufficient for promoting oligodendroglia differentiation. *J Biol Chem.* **282**(32), pp.23553-23560.
Chern, C.H., Chern, T.L., Wang, L.M., Hu, S.C., Deng, J.F. and Lee, C.H. 1998. Continuous flumazenil infusion in preventing complications arising from severe benzodiazepine intoxication. *Am J Emerg Med.* **16**(3), pp.238-241.
Cheung So, E., Wu, K.-C., Chen Kao, F. and Wu, S.-N. 2013. *Effects of midazolam on ion currents and membrane potential in differentiated motor neuron-like NSC-34 and NG108-15 cells.*
Chhabra, H.S. and Sarda, K. 2017. Clinical translation of stem cell based interventions for spinal cord injury — Are we there yet? *Advanced Drug Delivery Reviews.* **120**, pp.41-49.
Chiara, D.C., Jayakar, S.S., Zhou, X., Zhang, X., Savechenkov, P.Y., Bruzik, K.S., Miller, K.W. and Cohen, J.B. 2013. Specificity of intersubunit general anesthetic-binding sites in the transmembrane domain of the human α1β3γ2 γ-aminobutyric

acid type A (GABAA) receptor. *The Journal of biological chemistry.* **288**(27), pp.19343-19357.
Choi, Y.-A., Keem, J.O., Kim, C.Y., Yoon, H.R., Heo, W.D., Chung, B.H. and Jung, Y. 2015. A novel copper-chelating strategy for fluorescent proteins to image dynamic copper fluctuations on live cell surfaces. *Chemical science.* **6**(2), pp.1301-1307.
Choi, Y.M. and Kim, K.H. 2015. Etifoxine for pain patients with anxiety. *The Korean journal of pain.* **28**(1), pp.4-10.
Christian, C.A., Herbert, A.G., Holt, R.L., Peng, K., Sherwood, K.D., Pangratz-Fuehrer, S., Rudolph, U. and Huguenard, J.R. 2013. Endogenous positive allosteric modulation of GABA(A) receptors by diazepam binding inhibitor. *Neuron.* **78**(6), pp.1063-1074.
Christian, C.A. and Huguenard, J.R. 2013. Astrocytes potentiate GABAergic transmission in the thalamic reticular nucleus via endozepine signaling. *Proceedings of the National Academy of Sciences of the United States of America.* **110**(50), pp.20278-20283.
Christian, C.A. and Huguenard, J.R. 2013. Astrocytes potentiate GABAergic transmission in the thalamic reticular nucleus via endozepine signaling. *Proc Natl Acad Sci U S A.* **110**(50), pp.20278-20283.
Chung, K. and Lee, W. 1989. *Vasoactive intestinal peptide (VIP) immunoreactivity in the ependymal cells of the rat spinal cord.*
Cizkova, D., Nagyova, M., Slovinska, L., Novotna, I., Radonak, J., Cizek, M., Mechirova, E., Tomori, Z., Hlucilova, J., Motlik, J., Sulla, I., Jr. and Vanicky, I. 2009. Response of ependymal progenitors to spinal cord injury or enhanced physical activity in adult rat. *Cell Mol Neurobiol.* **29**(6-7), pp.999-1013.
Cohen, J.Y., Haesler, S., Vong, L., Lowell, B.B. and Uchida, N. 2012. Neuron-type-specific signals for reward and punishment in the ventral tegmental area. *Nature.* **482**(7383), pp.85-88.
Colussi, G.L., Di Fabio, A., Catena, C., Chiuch, A. and Sechi, L. 2011. *Involvement of endothelium-dependent and -independent mechanisms in midazolam-induced vasodilation.*
Compagnone, N.A., Bulfone, A., Rubenstein, J.L. and Mellon, S.H. 1995. Expression of the steroidogenic enzyme P450scc in the central and peripheral nervous systems during rodent embryogenesis. *Endocrinology.* **136**(6), pp.2689-2696.
Cooper-Kuhn, C.M. and Georg Kuhn, H. 2002. Is it all DNA repair?: Methodological considerations for detecting neurogenesis in the adult brain. *Developmental Brain Research.* **134**(1–2), pp.13-21.
Cope, D.W., Wulff, P., Oberto, A., Aller, M.I., Capogna, M., Ferraguti, F., Halbsguth, C., Hoeger, H., Jolin, H.E., Jones, A., McKenzie, A.N., Ogris, W., Poeltl, A., Sinkkonen, S.T., Vekovischeva, O.Y., Korpi, E.R., Sieghart, W., Sigel, E., Somogyi, P. and Wisden, W. 2004. Abolition of zolpidem sensitivity in mice with a point mutation in the GABAA receptor gamma2 subunit. *Neuropharmacology.* **47**(1), pp.17-34.
Corns, L.F., Atkinson, L., Daniel, J., Edwards, I.J., New, L., Deuchars, J. and Deuchars, S.A. 2015. Cholinergic Enhancement of Cell Proliferation in the Postnatal Neurogenic Niche of the Mammalian Spinal Cord. *Stem Cells.* **33**(9), pp.2864-2876.
Corns, L.F., Deuchars, J. and Deuchars, S.A. 2013. GABAergic responses of mammalian ependymal cells in the central canal neurogenic niche of the postnatal spinal cord. *Neurosci Lett.* **553**, pp.57-62.

Corotto, F.S., Henegar, J.A. and Maruniak, J.A. 1993. Neurogenesis persists in the subependymal layer of the adult mouse brain. *Neuroscience Letters.* **149**(2), pp.111-114.
Cosenza-Nashat, M., Zhao, M.L., Suh, H.S., Morgan, J., Natividad, R., Morgello, S. and Lee, S.C. 2009. Expression of the translocator protein of 18 kDa by microglia, macrophages and astrocytes based on immunohistochemical localization in abnormal human brain. *Neuropathol Appl Neurobiol.* **35**(3), pp.306-328.
Coskun, V., Wu, H., Blanchi, B., Tsao, S., Kim, K., Zhao, J., Biancotti, J.C., Hutnick, L., Krueger, R.C., Jr., Fan, G., de Vellis, J. and Sun, Y.E. 2008. CD133+ neural stem cells in the ependyma of mammalian postnatal forebrain. *Proc Natl Acad Sci U S A.* **105**(3), pp.1026-1031.
Costa, B., Cavallini, C., Da Pozzo, E., Taliani, S., Da Settimo, F. and Martini, C. 2017. The Anxiolytic Etifoxine Binds to TSPO Ro5-4864 Binding Site with Long Residence Time Showing a High Neurosteroidogenic Activity. *ACS Chem Neurosci.* **8**(7), pp.1448-1454.
Costa, E. and Guidotti, A. 1991. Diazepam binding inhibitor (DBI): a peptide with multiple biological actions. *Life Sci.* **49**(5), pp.325-344.
Cramer, S.C., Lastra, L., Lacourse, M.G. and Cohen, M.J. 2005. Brain motor system function after chronic, complete spinal cord injury. *Brain.* **128**(Pt 12), pp.2941-2950.
Crawford, A.H., Chambers, C. and Franklin, R.J. 2013. Remyelination: the true regeneration of the central nervous system. *J Comp Pathol.* **149**(2-3), pp.242-254.
Cregg, J.M., DePaul, M.A., Filous, A.R., Lang, B.T., Tran, A. and Silver, J. 2014. Functional regeneration beyond the glial scar. *Exp Neurol.* **253**, pp.197-207.
Crestani, F., Lorez, M., Baer, K., Essrich, C., Benke, D., Laurent, J.P., Belzung, C., Fritschy, J.M., Luscher, B. and Mohler, H. 1999. Decreased GABAA-receptor clustering results in enhanced anxiety and a bias for threat cues. *Nat Neurosci.* **2**(9), pp.833-839.
Crowe, M.J., Bresnahan, J.C., Shuman, S.L., Masters, J.N. and Beattie, M.S. 1997. Apoptosis and delayed degeneration after spinal cord injury in rats and monkeys. *Nat Med.* **3**(1), pp.73-76.
Cummings, B.J., Uchida, N., Tamaki, S.J., Salazar, D.L., Hooshmand, M., Summers, R., Gage, F.H. and Anderson, A.J. 2005. Human neural stem cells differentiate and promote locomotor recovery in spinal cord-injured mice. *Proceedings of the National Academy of Sciences of the United States of America.* **102**(39), pp.14069-14074.
Cusimano, M., Brambilla, E., Capotondo, A., De Feo, D., Tomasso, A., Comi, G., D'Adamo, P., Muzio, L. and Martino, G. 2018. Selective killing of spinal cord neural stem cells impairs locomotor recovery in a mouse model of spinal cord injury. *Journal of Neuroinflammation.* **15**(1), p58.
D'Hulst, C., Atack, J.R. and Kooy, R.F. 2009. The complexity of the GABAA receptor shapes unique pharmacological profiles. *Drug Discov Today.* **14**(17-18), pp.866-875.
Danilov, A.I., Covacu, R., Moe, M.C., Langmoen, I.A., Johansson, C.B., Olsson, T. and Brundin, L. 2006. Neurogenesis in the adult spinal cord in an experimental model of multiple sclerosis. *Eur J Neurosci.* **23**(2), pp.394-400.
Darragh, A., Lambe, R., Kenny, M. and Brick, I. 1983. Tolerance of healthy volunteers to intravenous administration of the benzodiazepine antagonist Ro 15-1788. *Eur J Clin Pharmacol.* **24**(4), pp.569-570.
Daugherty, D.J., Chechneva, O., Mayrhofer, F. and Deng, W. 2016. The hGFAP-driven conditional TSPO knockout is protective in a mouse model of multiple sclerosis. *Scientific Reports.* **6**, p22556.

Daugherty, D.J., Selvaraj, V., Chechneva, O.V., Liu, X.B., Pleasure, D.E. and Deng, W. 2013. A TSPO ligand is protective in a mouse model of multiple sclerosis. *EMBO Mol Med.* **5**(6), pp.891-903.
Daynac, M., Chicheportiche, A., Pineda, J.R., Gauthier, L.R., Boussin, F.D. and Mouthon, M.-A. 2013. Quiescent neural stem cells exit dormancy upon alteration of GABAAR signaling following radiation damage. *Stem Cell Research.* **11**(1), pp.516-528.
De Mateos-Verchere, J.G., Leprince, J., Tonon, M.C., Vaudry, H. and Costentin, J. 1998. The octadecaneuropeptide ODN induces anxiety in rodents: possible involvement of a shorter biologically active fragment. *Peptides.* **19**(5), pp.841-848.
De Souza, E.B., Anholt, R.R., Murphy, K.M., Snyder, S.H. and Kuhar, M.J. 1985. Peripheral-type benzodiazepine receptors in endocrine organs: autoradiographic localization in rat pituitary, adrenal, and testis. *Endocrinology.* **116**(2), pp.567-573.
Deisseroth, K. and Malenka, R.C. 2005. GABA excitation in the adult brain: a mechanism for excitation- neurogenesis coupling. *Neuron.* **47**(6), pp.775-777.
Deisseroth, K. and Malenka, R.C. 2005. GABA Excitation in the Adult Brain: A Mechanism for Excitation- Neurogenesis Coupling. *Neuron.* **47**(6), pp.775-777.
Dervan, A.G. and Roberts, B.L. 2003. The meningeal sheath of the regenerating spinal cord of the eel, Anguilla. *Anat Embryol (Berl).* **207**(2), pp.157-167.
Devesa, J., Alonso, A., López, N., García, J., Puell, C.I., Pablos, T. and Devesa, P. 2017. Growth Hormone (GH) and Rehabilitation Promoted Distal Innervation in a Child Affected by Caudal Regression Syndrome. *International journal of molecular sciences.* **18**(1), p230.
Dhir, A. and Rogawski, M.A. 2012. Role of neurosteroids in the anticonvulsant activity of midazolam. *Br J Pharmacol.* **165**(8), pp.2684-2691.
Dickmeis, T. and Foulkes, N.S. 2011. Glucocorticoids and circadian clock control of cell proliferation: at the interface between three dynamic systems. *Mol Cell Endocrinol.* **331**(1), pp.11-22.
Diermeier-Daucher, S., Clarke, S.T., Hill, D., Vollmann-Zwerenz, A., Bradford, J.A. and Brockhoff, G. 2009. Cell type specific applicability of 5-ethynyl-2'-deoxyuridine (EdU) for dynamic proliferation assessment in flow cytometry. *Cytometry A.* **75**(6), pp.535-546.
do Rego, J.L., Vaudry, D. and Vaudry, H. 2015. The Non-Benzodiazepine Anxiolytic Drug Etifoxine Causes a Rapid, Receptor-Independent Stimulation of Neurosteroid Biosynthesis. *PLOS ONE.* **10**(3), pe0120473.
Doetsch, F. and Alvarez-Buylla, A. 1996. Network of tangential pathways for neuronal migration in adult mammalian brain. *Proc Natl Acad Sci U S A.* **93**(25), pp.14895-14900.
Doetsch, F., Caille, I., Lim, D.A., Garcia-Verdugo, J.M. and Alvarez-Buylla, A. 1999a. Subventricular zone astrocytes are neural stem cells in the adult mammalian brain. *Cell.* **97**(6), pp.703-716.
Doetsch, F., Garcia-Verdugo, J.M. and Alvarez-Buylla, A. 1997. Cellular composition and three-dimensional organization of the subventricular germinal zone in the adult mammalian brain. *J Neurosci.* **17**(13), pp.5046-5061.
Doetsch, F., García-Verdugo, J.M. and Alvarez-Buylla, A. 1999b. Regeneration of a germinal layer in the adult mammalian brain. *Proceedings of the National Academy of Sciences of the United States of America.* **96**(20), pp.11619-11624.
Donat, C.K., Gaber, K., Meixensberger, J., Brust, P., Pinborg, L.H., Hansen, H.H. and Mikkelsen, J.D. 2016. Changes in Binding of [(123)I]CLINDE, a High-Affinity

Translocator Protein 18 kDa (TSPO) Selective Radioligand in a Rat Model of Traumatic Brain Injury. *Neuromolecular Med.* **18**(2), pp.158-169.
Dou, Y.L., Lin, J.P., Liu, F.E., Wang, L.Y., Shu, H.H., Jiang, N., Xie, Y. and Duan, Q. 2014. Midazolam inhibits the proliferation of human head and neck squamous carcinoma cells by downregulating p300 expression. *Tumour Biol.* **35**(8), pp.7499-7504.
Drew, G.M., Siddall, P.J. and Duggan, A.W. 2004. Mechanical allodynia following contusion injury of the rat spinal cord is associated with loss of GABAergic inhibition in the dorsal horn. *Pain.* **109**(3), pp.379-388.
Dromard, C., Guillon, H., Rigau, V., Ripoll, C., Sabourin, J.C., Perrin, F.E., Scamps, F., Bozza, S., Sabatier, P., Lonjon, N., Duffau, H., Vachiery-Lahaye, F., Prieto, M., Tran Van Ba, C., Deleyrolle, L., Boularan, A., Langley, K., Gaviria, M., Privat, A., Hugnot, J.P. and Bauchet, L. 2008. Adult human spinal cord harbors neural precursor cells that generate neurons and glial cells *in vitro*. *J Neurosci Res.* **86**(9), pp.1916-1926.
Duerden, E.G., Guo, T., Dodbiba, L., Chakravarty, M.M., Chau, V., Poskitt, K.J., Synnes, A., Grunau, R.E. and Miller, S.P. 2016. Midazolam dose correlates with abnormal hippocampal growth and neurodevelopmental outcome in preterm infants. *Ann Neurol.* **79**(4), pp.548-559.
Dumitru, I., Neitz, A., Alfonso, J. and Monyer, H. 2017. Diazepam Binding Inhibitor Promotes Stem Cell Expansion Controlling Environment-Dependent Neurogenesis. *Neuron.* **94**(1), pp.125-137.e125.
Duncan, I.D., Marik, R.L., Broman, A.T. and Heidari, M. 2017. Thin myelin sheaths as the hallmark of remyelination persist over time and preserve axon function. *Proceedings of the National Academy of Sciences.* **114**(45), pE9685.
E Marzan, D., L West, B. and L Salzer, J. 2018. *Microglia are necessary for toxin-mediated demyelination and activation of microglia is sufficient to induce demyelination.*
Edelmann, L., Hanson, P.I., Chapman, E.R. and Jahn, R. 1995. Synaptobrevin binding to synaptophysin: a potential mechanism for controlling the exocytotic fusion machine. *Embo j.* **14**(2), pp.224-231.
Edwards, I.J., Singh, M., Morris, S., Osborne, L., Le Ruez, T., Fuad, M., Deuchars, S.A. and Deuchars, J. 2013. A simple method to fluorescently label pericytes in the CNS and skeletal muscle. *Microvasc Res.* **89**, pp.164-168.
Egger, B., Gold, K.S. and Brand, A.H. 2010. Notch regulates the switch from symmetric to asymmetric neural stem cell division in the Drosophila optic lobe. *Development.* **137**(18), pp.2981-2987.
Eriksson, P.S., Perfilieva, E., Bjork-Eriksson, T., Alborn, A.M., Nordborg, C., Peterson, D.A. and Gage, F.H. 1998. Neurogenesis in the adult human hippocampus. *Nat Med.* **4**(11), pp.1313-1317.
Ernst, M., Brauchart, D., Boresch, S. and Sieghart, W. 2003. Comparative modeling of GABA(A) receptors: limits, insights, future developments. *Neuroscience.* **119**(4), pp.933-943.
Essrich, C., Lorez, M., Benson, J.A., Fritschy, J.M. and Luscher, B. 1998. Postsynaptic clustering of major GABAA receptor subtypes requires the gamma 2 subunit and gephyrin. *Nat Neurosci.* **1**(7), pp.563-571.
Etlin, A., Braz, J.M., Kuhn, J.A., Wang, X., Hamel, K.A., Llewellyn-Smith, I.J. and Basbaum, A.I. 2016. Functional Synaptic Integration of Forebrain GABAergic Precursors into the Adult Spinal Cord. *J Neurosci.* **36**(46), pp.11634-11645.

Fahrenkrug, J., Schaffalitzky de Muckadell, O.B. and Fahrenkrug, A. 1977. Vasoactive intestinal polypeptide (VIP) in human cerebrospinal fluid. *Brain Res.* **124**(3), pp.581-584.
Farrant, M. and Nusser, Z. 2005. Variations on an inhibitory theme: phasic and tonic activation of GABA(A) receptors. *Nat Rev Neurosci.* **6**(3), pp.215-229.
Faulkner, J.R., Herrmann, J.E., Woo, M.J., Tansey, K.E., Doan, N.B. and Sofroniew, M.V. 2004. Reactive astrocytes protect tissue and preserve function after spinal cord injury. *J Neurosci.* **24**(9), pp.2143-2155.
Fernandez-Zafra, T., Codeluppi, S. and Uhlen, P. 2017. An ex vivo spinal cord injury model to study ependymal cells in adult mouse tissue. *Exp Cell Res.* **357**(2), pp.236-242.
Fernando, R.N., Eleuteri, B., Abdelhady, S., Nussenzweig, A., Andäng, M. and Ernfors, P. 2011. Cell cycle restriction by histone H2AX limits proliferation of adult neural stem cells. *Proceedings of the National Academy of Sciences.* **108**(14), p5837.
Ferrarese, C., Alho, H., Guidotti, A. and Costa, E. 1987a. Co-localization and co-release of GABA and putative allosteric modulators of GABA receptor. *Neuropharmacology.* **26**(7b), pp.1011-1018.
Ferrarese, C., Appollonio, I., Bianchi, G., Frigo, M., Marzorati, C., Pecora, N., Perego, M., Pierpaoli, C. and Frattola, L. 1993. Benzodiazepine receptors and diazepam binding inhibitor: a possible link between stress, anxiety and the immune system. *Psychoneuroendocrinology.* **18**(1), pp.3-22.
Ferrarese, C., Appollonio, I., Frigo, M., Gaini, S.M., Piolti, R. and Frattola, L. 1989. Benzodiazepine receptors and diazepam-binding inhibitor in human cerebral tumors. *Ann Neurol.* **26**(4), pp.564-568.
Ferrarese, C., Vaccarino, F., Alho, H., Mellstrom, B., Costa, E. and Guidotti, A. 1987b. Subcellular location and neuronal release of diazepam binding inhibitor. *J Neurochem.* **48**(4), pp.1093-1102.
Ferrero, P., Costa, E., Conti-Tronconi, B. and Guidotti, A. 1986a. A diazepam binding inhibitor (DBI)-like neuropeptide is detected in human brain. *Brain Res.* **399**(1), pp.136-142.
Ferrero, P., Guidotti, A., Conti-Tronconi, B. and Costa, E. 1984. A brain octadecaneuropeptide generated by tryptic digestion of DBI (diazepam binding inhibitor) functions as a proconflict ligand of benzodiazepine recognition sites. *Neuropharmacology.* **23**(11), pp.1359-1362.
Ferrero, P., Santi, M.R., Conti-Tronconi, B., Costa, E. and Guidotti, A. 1986b. Study of an octadecaneuropeptide derived from diazepam binding inhibitor (DBI): biological activity and presence in rat brain. *Proc Natl Acad Sci U S A.* **83**(3), pp.827-831.
Figley, S.A., Khosravi, R., Legasto, J.M., Tseng, Y.-F. and Fehlings, M.G. 2014. Characterization of vascular disruption and blood-spinal cord barrier permeability following traumatic spinal cord injury. *Journal of neurotrauma.* **31**(6), pp.541-552.
File, S.E. and Pellow, S. 1985. The anxiogenic action of RO 5-4864 in the social interaction test: effect of chlordiazepoxide, RO 15-1788 and CGS 8216. *Naunyn Schmiedebergs Arch Pharmacol.* **328**(3), pp.225-228.
Fonken, L.K., Aubrecht, T.G., Melendez-Fernandez, O.H., Weil, Z.M. and Nelson, R.J. 2013. Dim light at night disrupts molecular circadian rhythms and increases body weight. *J Biol Rhythms.* **28**(4), pp.262-271.
Foret, A., Quertainmont, R., Botman, O., Bouhy, D., Amabili, P., Brook, G., Schoenen, J. and Franzen, R. 2010. Stem cells in the adult rat spinal cord: plasticity

after injury and treadmill training exercise. *Journal of Neurochemistry.* **112**(3), pp.762-772.
Franklin, R.J. and Goldman, S.A. 2015. Glia Disease and Repair-Remyelination. *Cold Spring Harb Perspect Biol.* **7**(7), pa020594.
Frisen, J., Johansson, C.B., Torok, C., Risling, M. and Lendahl, U. 1995. Rapid, widespread, and longlasting induction of nestin contributes to the generation of glial scar tissue after CNS injury. *J Cell Biol.* **131**(2), pp.453-464.
Funfschilling, U., Supplie, L.M., Mahad, D., Boretius, S., Saab, A.S., Edgar, J., Brinkmann, B.G., Kassmann, C.M., Tzvetanova, I.D., Mobius, W., Diaz, F., Meijer, D., Suter, U., Hamprecht, B., Sereda, M.W., Moraes, C.T., Frahm, J., Goebbels, S. and Nave, K.A. 2012. Glycolytic oligodendrocytes maintain myelin and long-term axonal integrity. *Nature.* **485**(7399), pp.517-521.
Gandolfo, P., Louiset, E., Patte, C., Leprince, J., Masmoudi, O., Malagon, M., Gracia-Navarro, F., Vaudry, H. and Tonon, M.C. 2001. The triakontatetraneuropeptide TTN increases [CA2+]i in rat astrocytes through activation of peripheral-type benzodiazepine receptors. *Glia.* **35**(2), pp.90-100.
Gandolfo, P., Patte, C., Leprince, J., Rego, J.L., Mensah-Nyagan, A.G., Vaudry, H. and Tonon, M.C. 2000. The triakontatetraneuropeptide (TTN) stimulates thymidine incorporation in rat astrocytes through peripheral-type benzodiazepine receptors. *J Neurochem.* **75**(2), pp.701-707.
Garcia-Ovejero, D., Arevalo-Martin, A., Paniagua-Torija, B., Florensa-Vila, J., Ferrer, I., Grassner, L. and Molina-Holgado, E. 2015. The ependymal region of the adult human spinal cord differs from other species and shows ependymoma-like features. *Brain.* **138**(Pt 6), pp.1583-1597.
Gavish, M., Bachman, I., Shoukrun, R., Katz, Y., Veenman, L., Weisinger, G. and Weizman, A. 1999. Enigma of the peripheral benzodiazepine receptor. *Pharmacol Rev.* **51**(4), pp.629-650.
Gavish, M., Katz, Y., Bar-Ami, S. and Weizman, R. 1992. Biochemical, physiological, and pathological aspects of the peripheral benzodiazepine receptor. *J Neurochem.* **58**(5), pp.1589-1601.
Ge, S., Pradhan, D.A., Ming, G.L. and Song, H. 2007. GABA sets the tempo for activity-dependent adult neurogenesis. *Trends Neurosci.* **30**(1), pp.1-8.
George, M.S., Guidotti, A., Rubinow, D., Pan, B., Mikalauskas, K. and Post, R.M. 1994. CSF neuroactive steroids in affective disorders: pregnenolone, progesterone, and DBI. *Biol Psychiatry.* **35**(10), pp.775-780.
Ghasemlou, N., Jeong, S.Y., Lacroix, S. and David, S. 2007. T cells contribute to lysophosphatidylcholine-induced macrophage activation and demyelination in the CNS. *Glia.* **55**(3), pp.294-302.
Ghouili, I., Bahdoudi, S., Morin, F., Amri, F., Hamdi, Y., Coly, P.M., Walet-Balieu, M.L., Leprince, J., Zekri, S., Vaudry, H., Vaudry, D., Castel, H., Amri, M., Tonon, M.C. and Masmoudi-Kouki, O. 2018. Endogenous Expression of ODN-Related Peptides in Astrocytes Contributes to Cell Protection Against Oxidative Stress: Astrocyte-Neuron Crosstalk Relevance for Neuronal Survival. *Mol Neurobiol.* **55**(6), pp.4596-4611.
Ghoumari, A.M., Baulieu, E.E. and Schumacher, M. 2005. Progesterone increases oligodendroglial cell proliferation in rat cerebellar slice cultures. *Neuroscience.* **135**(1), pp.47-58.
Ghoumari, A.M., Ibanez, C., El-Etr, M., Leclerc, P., Eychenne, B., O'Malley, B.W., Baulieu, E.E. and Schumacher, M. 2003. Progesterone and its metabolites increase

myelin basic protein expression in organotypic slice cultures of rat cerebellum. *J Neurochem.* **86**(4), pp.848-859.
Giannaccini, G., Betti, L., Palego, L., Pirone, A., Schmid, L., Lanza, M., Fabbrini, L., Pelosini, C., Maffei, M., Santini, F., Pinchera, A. and Lucacchini, A. 2011. Serotonin transporter (SERT) and translocator protein (TSPO) expression in the obese ob/ob mouse. *BMC neuroscience.* **12**, pp.18-18.
Gibson, E.M., Purger, D., Mount, C.W., Goldstein, A.K., Lin, G.L., Wood, L.S., Inema, I., Miller, S.E., Bieri, G., Zuchero, J.B., Barres, B.A., Woo, P.J., Vogel, H. and Monje, M. 2014. Neuronal activity promotes oligodendrogenesis and adaptive myelination in the mammalian brain. *Science.* **344**(6183), p1252304.
Gibson, E.M., Wang, C., Tjho, S., Khattar, N. and Kriegsfeld, L.J. 2010. Experimental 'jet lag' inhibits adult neurogenesis and produces long-term cognitive deficits in female hamsters. *PloS one.* **5**(12), pp.e15267-e15267.
Girard, C., Liu, S., Cadepond, F., Adams, D., Lacroix, C., Verleye, M., Gillardin, J.-M., Baulieu, E.-E., Schumacher, M. and Schweizer-Groyer, G. 2008. Etifoxine improves peripheral nerve regeneration and functional recovery. *Proceedings of the National Academy of Sciences of the United States of America.* **105**(51), pp.20505-20510.
Giri, P.K., Lu, Y., Lei, S., Li, W., Zheng, J., Lu, H., Chen, X., Liu, Y. and Zhang, P. 2018. Pretreatment with minocycline improves neurogenesis and behavior performance after midazolam exposure in neonatal rats. *Neuroreport.* **29**(3), pp.153-159.
Gledhill, R.F., Harrison, B.M. and McDonald, W.I. 1973. Demyelination and remyelination after acute spinal cord compression. *Exp Neurol.* **38**(3), pp.472-487.
Glowa, J.R., Crawley, J., Suzdak, P.D. and Paul, S.M. 1988. Ethanol and the GABA receptor complex: studies with the partial inverse benzodiazepine receptor agonist Ro 15-4513. *Pharmacol Biochem Behav.* **31**(3), pp.767-772.
Gnocchi, D., Pedrelli, M., Hurt-Camejo, E. and Parini, P. 2015. Lipids around the Clock: Focus on Circadian Rhythms and Lipid Metabolism. *Biology.* **4**(1), pp.104-132.
Gobbel, G.T., Bellinzona, M., Vogt, A.R., Gupta, N., Fike, J.R. and Chan, P.H. 1998. Response of postmitotic neurons to X-irradiation: implications for the role of DNA damage in neuronal apoptosis. *J Neurosci.* **18**(1), pp.147-155.
Gold, S.M., Sasidhar, M.V., Morales, L.B., Du, S., Sicotte, N.L., Tiwari-Woodruff, S.K. and Voskuhl, R.R. 2009. Estrogen treatment decreases matrix metalloproteinase (MMP)-9 in autoimmune demyelinating disease through estrogen receptor alpha (ERalpha). *Laboratory investigation; a journal of technical methods and pathology.* **89**(10), pp.1076-1083.
Goldschmidt, T., Antel, J., Konig, F.B., Bruck, W. and Kuhlmann, T. 2009. Remyelination capacity of the MS brain decreases with disease chronicity. *Neurology.* **72**(22), pp.1914-1921.
Goren, E.N., Reeves, D.C. and Akabas, M.H. 2004. Loose protein packing around the extracellular half of the GABA(A) receptor beta1 subunit M2 channel-lining segment. *J Biol Chem.* **279**(12), pp.11198-11205.
Goritz, C. and Frisen, J. 2012. Neural stem cells and neurogenesis in the adult. *Cell Stem Cell.* **10**(6), pp.657-659.
Gotts, J., Atkinson, L., Yanagawa, Y., Deuchars, J. and Deuchars, S.A. 2016. Co-expression of GAD67 and choline acetyltransferase in neurons in the mouse spinal cord: A focus on lamina X. *Brain research.* **1646**, pp.570-579.

Graham, V., Khudyakov, J., Ellis, P. and Pevny, L. 2003. SOX2 functions to maintain neural progenitor identity. *Neuron.* **39**(5), pp.749-765.
Gram, L., Larsson, O.M., Johnsen, A.H. and Schousboe, A. 1988. Effects of valproate, vigabatrin and aminooxyacetic acid on release of endogenous and exogenous GABA from cultured neurons. *Epilepsy Res.* **2**(2), pp.87-95.
Grossman, S.D., Rosenberg, L.J. and Wrathall, J.R. 2001. Temporal-spatial pattern of acute neuronal and glial loss after spinal cord contusion. *Exp Neurol.* **168**(2), pp.273-282.
Guarneri, P., Berkovich, A., Guidotti, A. and Costa, E. 1990. A study of diazepam binding inhibitor (DBI) processing products in human cerebrospinal fluid and in postmortem human brain. *Neuropharmacology.* **29**(5), pp.419-428.
Guidotti, A., Forchetti, C.M., Corda, M.G., Konkel, D., Bennett, C.D. and Costa, E. 1983. Isolation, characterization, and purification to homogeneity of an endogenous polypeptide with agonistic action on benzodiazepine receptors. *Proc Natl Acad Sci U S A.* **80**(11), pp.3531-3535.
Guillebaud, F., Girardet, C., Abysique, A., Gaigé, S., Barbouche, R., Verneuil, J., Jean, A., Leprince, J., Tonon, M.-C., Dallaporta, M., Lebrun, B. and Troadec, J.-D. 2017. Glial Endozepines Inhibit Feeding-Related Autonomic Functions by Acting at the Brainstem Level. *Frontiers in neuroscience.* **11**, pp.308-308.
Gunn, B.G., Cunningham, L., Mitchell, S.G., Swinny, J.D., Lambert, J.J. and Belelli, D. 2015. GABAA receptor-acting neurosteroids: A role in the development and regulation of the stress response. *Frontiers in Neuroendocrinology.* **36**, pp.28-48.
Gunther, U., Benson, J., Benke, D., Fritschy, J.M., Reyes, G., Knoflach, F., Crestani, F., Aguzzi, A., Arigoni, M., Lang, Y., Bluethmann, H., Mohler, H. and Luscher, B. 1995. Benzodiazepine-insensitive mice generated by targeted disruption of the gamma 2 subunit gene of gamma-aminobutyric acid type A receptors. *Proc Natl Acad Sci U S A.* **92**(17), pp.7749-7753.
Guo, W., Patzlaff, N.E., Jobe, E.M. and Zhao, X. 2012. Isolation of multipotent neural stem or progenitor cells from both the dentate gyrus and subventricular zone of a single adult mouse. *Nature Protocols.* **7**, p2005.
Gwak, Y.S. and Hulsebosch, C.E. 2011. GABA and central neuropathic pain following spinal cord injury. *Neuropharmacology.* **60**(5), pp.799-808.
Gwak, Y.S., Tan, H.Y., Nam, T.S., Paik, K.S., Hulsebosch, C.E. and Leem, J.W. 2006. Activation of spinal GABA receptors attenuates chronic central neuropathic pain after spinal cord injury. *J Neurotrauma.* **23**(7), pp.1111-1124.
Hadingham, K.L., Wafford, K.A., Thompson, S.A., Palmer, K.J. and Whiting, P.J. 1995. Expression and pharmacology of human GABAA receptors containing gamma 3 subunits. *Eur J Pharmacol.* **291**(3), pp.301-309.
Hall, S.M. 1972. The effect of injections of lysophosphatidyl choline into white matter of the adult mouse spinal cord. *J Cell Sci.* **10**(2), pp.535-546.
Hamaguchi, M., Muramatsu, R., Matoba, K., Maedera, N. and Yamashita, T. 2017. Lysophosphatidylcholine-induced demyelination model of mouse.
Hamdi, Y., Kaddour, H., Vaudry, D., Leprince, J., Zarrouk, A., Hammami, M., Vaudry, H., Tonon, M.C., Amri, M. and Masmoudi-Kouki, O. 2015. Octadecaneuropeptide ODN prevents hydrogen peroxide-induced oxidative damage of biomolecules in cultured rat astrocytes. *Peptides.* **71**, pp.56-65.
Hamilton, L.K., Truong, M.K., Bednarczyk, M.R., Aumont, A. and Fernandes, K.J. 2009. Cellular organization of the central canal ependymal zone, a niche of latent

neural stem cells in the adult mammalian spinal cord. *Neuroscience.* **164**(3), pp.1044-1056.
Hamilton, N.B., Clarke, L.E., Arancibia-Carcamo, I.L., Kougioumtzidou, E., Matthey, M., Káradóttir, R., Whiteley, L., Bergersen, L.H., Richardson, W.D. and Attwell, D. 2017. Endogenous GABA controls oligodendrocyte lineage cell number, myelination, and CNS internode length. *Glia.* **65**(2), pp.309-321.
Hamon, A., Morel, A., Hue, B., Verleye, M. and Gillardin, J.M. 2003. The modulatory effects of the anxiolytic etifoxine on GABA(A) receptors are mediated by the beta subunit. *Neuropharmacology.* **45**(3), pp.293-303.
Hanson, S.M. and Czajkowski, C. 2008. Structural mechanisms underlying benzodiazepine modulation of the GABA(A) receptor. *The Journal of neuroscience : the official journal of the Society for Neuroscience.* **28**(13), pp.3490-3499.
Hardy, R.J. 1998. Molecular defects in the dysmyelinating mutant quaking. *J Neurosci Res.* **51**(4), pp.417-422.
Harlow, D.E., Honce, J.M. and Miravalle, A.A. 2015. Remyelination Therapy in Multiple Sclerosis. *Frontiers in neurology.* **6**, pp.257-257.
Harrison, B.M. and McDonald, W.I. 1977. Remyelination after transient experimental compression of the spinal cord. *Annals of Neurology.* **1**(6), pp.542-551.
Harvey, L.A. 2016. Physiotherapy rehabilitation for people with spinal cord injuries. *J Physiother.* **62**(1), pp.4-11.
Hawryluk, G.W., Rowland, J., Kwon, B.K. and Fehlings, M.G. 2008. Protection and repair of the injured spinal cord: a review of completed, ongoing, and planned clinical trials for acute spinal cord injury. *Neurosurg Focus.* **25**(5), pE14.
Hernstadt, H., Wang, S., Lim, G. and Mao, J. 2009. Spinal translocator protein (TSPO) modulates pain behavior in rats with CFA-induced monoarthritis. *Brain Res.* **1286**, pp.42-52.
Herranz, E., Gianni, C., Louapre, C., Treaba, C.A., Govindarajan, S.T., Ouellette, R., Loggia, M.L., Sloane, J.A., Madigan, N., Izquierdo-Garcia, D., Ward, N., Mangeat, G., Granberg, T., Klawiter, E.C., Catana, C., Hooker, J.M., Taylor, N., Ionete, C., Kinkel, R.P. and Mainero, C. 2016. Neuroinflammatory component of gray matter pathology in multiple sclerosis. *Ann Neurol.* **80**(5), pp.776-790.
Herrmann, J.E., Imura, T., Song, B., Qi, J., Ao, Y., Nguyen, T.K., Korsak, R.A., Takeda, K., Akira, S. and Sofroniew, M.V. 2008. STAT3 is a critical regulator of astrogliosis and scar formation after spinal cord injury. *J Neurosci.* **28**(28), pp.7231-7243.
Hess, L., Votava, M., Sliva, J., Malek, J. and Kurzova, A. 2013. Sedative and anxiolytic properties of flumazenil in rats and rabbits: 9AP4-8. **30**, pp.150-150.
Hevers, W. and Luddens, H. 1998. The diversity of GABAA receptors. Pharmacological and electrophysiological properties of GABAA channel subtypes. *Mol Neurobiol.* **18**(1), pp.35-86.
Hill, R.A., Li, A.M. and Grutzendler, J. 2018. Lifelong cortical myelin plasticity and age-related degeneration in the live mammalian brain. *Nat Neurosci.* **21**(5), pp.683-695.
Hofstetter, C.P., Holmstrom, N.A., Lilja, J.A., Schweinhardt, P., Hao, J., Spenger, C., Wiesenfeld-Hallin, Z., Kurpad, S.N., Frisen, J. and Olson, L. 2005. Allodynia limits the usefulness of intraspinal neural stem cell grafts; directed differentiation improves outcome. *Nat Neurosci.* **8**(3), pp.346-353.

Horner, P.J., Power, A.E., Kempermann, G., Kuhn, H.G., Palmer, T.D., Winkler, J., Thal, L.J. and Gage, F.H. 2000. Proliferation and differentiation of progenitor cells throughout the intact adult rat spinal cord. *J Neurosci.* **20**(6), pp.2218-2228.
Hou, S., Saltos, T.M., Iredia, I.W. and Tom, V.J. 2018. Surgical techniques influence local environment of injured spinal cord and cause various grafted cell survival and integration. *J Neurosci Methods.* **293**, pp.144-150.
Huang, A.L., Chen, X., Hoon, M.A., Chandrashekar, J., Guo, W., Tränkner, D., Ryba, N.J.P. and Zuker, C.S. 2006. The cells and logic for mammalian sour taste detection. *Nature.* **442**, p934.
Huang, J., Feng, F., Tamamaki, N., Yanagawa, Y., Obata, K., Li, Y.Q. and Wu, S.X. 2006. Prenatal and Postnatal Development of GABAergic Neurons in the Spinal Cord Revealed by Green Fluorescence Protein Expression in the GAD67-GFP Knock-In Mouse. *Neuroembryology and Aging.* **4**(3), pp.147-154.
Hughes, E.G., Orthmann-Murphy, J.L., Langseth, A.J. and Bergles, D.E. 2018. Myelin remodeling through experience-dependent oligodendrogenesis in the adult somatosensory cortex. *Nat Neurosci.* **21**(5), pp.696-706.
Hugnot, J.P. and Franzen, R. 2011. The spinal cord ependymal region: a stem cell niche in the caudal central nervous system. *Front Biosci (Landmark Ed).* **16**, pp.1044-1059.
Iggena, D., Winter, Y. and Steiner, B. 2017. Melatonin restores hippocampal neural precursor cell proliferation and prevents cognitive deficits induced by jet lag simulation in adult mice. *J Pineal Res.* **62**(4).
Irvine, K.A. and Blakemore, W.F. 2008. Remyelination protects axons from demyelination-associated axon degeneration. *Brain.* **131**(Pt 6), pp.1464-1477.
Iwanami, A., Kaneko, S., Nakamura, M., Kanemura, Y., Mori, H., Kobayashi, S., Yamasaki, M., Momoshima, S., Ishii, H., Ando, K., Tanioka, Y., Tamaoki, N., Nomura, T., Toyama, Y. and Okano, H. 2005. Transplantation of human neural stem cells for spinal cord injury in primates. *J Neurosci Res.* **80**(2), pp.182-190.
Jansson, L.C. and Akerman, K.E. 2014. The role of glutamate and its receptors in the proliferation, migration, differentiation and survival of neural progenitor cells. *J Neural Transm (Vienna).* **121**(8), pp.819-836.
Jayakumar, A.R., Panickar, K.S. and Norenberg, M.D. 2002. Effects on free radical generation by ligands of the peripheral benzodiazepine receptor in cultured neural cells. *J Neurochem.* **83**(5), pp.1226-1234.
Jeffery, N.D. and Blakemore, W.F. 1995. Remyelination of mouse spinal cord axons demyelinated by local injection of lysolecithin. *J Neurocytol.* **24**(10), pp.775-781.
Jeon, S.G., Bahn, J.H., Jang, J.S., Park, J., Kwon, O.S., Cho, S.W. and Choi, S.Y. 2000. Human brain GABA transaminase tissue distribution and molecular expression. *Eur J Biochem.* **267**(17), pp.5601-5607.
Jiao, J., Wang, Y., Sun, X. and Jiang, X. 2017. Insights into the Roles of Midazolam in Cancer Therapy. *Evid Based Complement Alternat Med.* **2017**, p3826506.
Johansson, C.B., Momma, S., Clarke, D.L., Risling, M., Lendahl, U. and Frisen, J. 1999. Identification of a neural stem cell in the adult mammalian central nervous system. *Cell.* **96**(1), pp.25-34.
Jones, L.L., Margolis, R.U. and Tuszynski, M.H. 2003. The chondroitin sulfate proteoglycans neurocan, brevican, phosphacan, and versican are differentially regulated following spinal cord injury. *Exp Neurol.* **182**(2), pp.399-411.
Jung, M.J., Lippert, B., Metcalf, B.W., Bohlen, P. and Schechter, P.J. 1977. gamma-Vinyl GABA (4-amino-hex-5-enoic acid), a new selective irreversible inhibitor of

GABA-T: effects on brain GABA metabolism in mice. *J Neurochem.* **29**(5), pp.797-802.
Kaduri, A.J., Magoul, R., Lescaudron, L., Campistron, G. and Calas, A. 1987. Immunocytochemical approach of GABAergic innervation of the mouse spinal cord using antibodies to GABA. *J Hirnforsch.* **28**(3), pp.349-355.
Kang, E., Berg, D.A., Furmanski, O., Jackson, W.M., Ryu, Y.K., Gray, C.D. and Mintz, C.D. 2017. Neurogenesis and developmental anesthetic neurotoxicity. *Neurotoxicology and teratology.* **60**, pp.33-39.
Kao, J., Rosenstein, B.S., Peters, S., Milano, M.T. and Kron, S.J. 2005. Cellular response to DNA damage. *Ann N Y Acad Sci.* **1066**, pp.243-258.
Karchewski, L.A., Bloechlinger, S. and Woolf, C.J. 2004. Axonal injury-dependent induction of the peripheral benzodiazepine receptor in small-diameter adult rat primary sensory neurons. *Eur J Neurosci.* **20**(3), pp.671-683.
Katsura, M., Mohri, Y., Shuto, K., Tsujimura, A., Ukai, M. and Ohkuma, S. 2002. Psychological stress, but not physical stress, causes increase in diazepam binding inhibitor (DBI) mRNA expression in mouse brains. *Brain Res Mol Brain Res.* **104**(1), pp.103-109.
Kelly, M.D., Smith, A., Banks, G., Wingrove, P., Whiting, P.W., Atack, J., Seabrook, G.R. and Maubach, K.A. 2002. Role of the histidine residue at position 105 in the human alpha 5 containing GABA(A) receptor on the affinity and efficacy of benzodiazepine site ligands. *Br J Pharmacol.* **135**(1), pp.248-256.
Kempermann, G., Fabel, K., Ehninger, D., Babu, H., Leal-Galicia, P., Garthe, A. and Wolf, S.A. 2010. Why and how physical activity promotes experience-induced brain plasticity. *Frontiers in neuroscience.* **4**, pp.189-189.
Kempermann, G. and Gage, F.H. 1999. Experience-dependent regulation of adult hippocampal neurogenesis: effects of long-term stimulation and stimulus withdrawal. *Hippocampus.* **9**(3), pp.321-332.
Kenakin, T. 2001. Inverse, protean, and ligand-selective agonism: matters of receptor conformation. *Faseb j.* **15**(3), pp.598-611.
Keough, M.B., Jensen, S.K. and Yong, V.W. 2015. Experimental demyelination and remyelination of murine spinal cord by focal injection of lysolecithin. *J Vis Exp.* (97).
Khilnani, G. and Khilnani, A.K. 2011. Inverse agonism and its therapeutic significance. *Indian J Pharmacol.* **43**(5), pp.492-501.
Kim, K.K., Adelstein, R.S. and Kawamoto, S. 2009. Identification of neuronal nuclei (NeuN) as Fox-3, a new member of the Fox-1 gene family of splicing factors. *J Biol Chem.* **284**(45), pp.31052-31061.
Ko, C.H. and Takahashi, J.S. 2006. Molecular components of the mammalian circadian clock. *Hum Mol Genet.* **15 Spec No 2**, pp.R271-277.
Koenig, H.L., Schumacher, M., Ferzaz, B., Thi, A.N., Ressouches, A., Guennoun, R., Jung-Testas, I., Robel, P., Akwa, Y. and Baulieu, E.E. 1995. Progesterone synthesis and myelin formation by Schwann cells. *Science.* **268**(5216), p1500.
Kohlmeier, F., Maya-Mendoza, A. and Jackson, D.A. 2013. EdU induces DNA damage response and cell death in mESC in culture. *Chromosome research : an international journal on the molecular, supramolecular and evolutionary aspects of chromosome biology.* **21**(1), pp.87-100.
Kotter, M.R., Setzu, A., Sim, F.J., Van Rooijen, N. and Franklin, R.J.M. 2001. Macrophage depletion impairs oligodendrocyte remyelination following lysolecithin-induced demyelination. *Glia.* **35**(3), pp.204-212.

Kriegstein, A. and Alvarez-Buylla, A. 2009. The glial nature of embryonic and adult neural stem cells. *Annual review of neuroscience.* **32**, pp.149-184.
Krityakiarana, W., Espinosa-Jeffrey, A., Ghiani, C.A., Zhao, P.M., Topaldjikian, N., Gomez-Pinilla, F., Yamaguchi, M., Kotchabhakdi, N. and de Vellis, J. 2010. Voluntary exercise increases oligodendrogenesis in spinal cord. *Int J Neurosci.* **120**(4), pp.280-290.
Kruse, H.J. and Kuch, H. 1985. Etifoxine: evaluation of its anticonvulsant profile in mice in comparison with sodium valproate, phenytoin and clobazam. *Arzneimittelforschung.* **35**(1), pp.133-135.
Kucken, A.M., Teissere, J.A., Seffinga-Clark, J., Wagner, D.A. and Czajkowski, C. 2003. Structural requirements for imidazobenzodiazepine binding to GABA(A) receptors. *Mol Pharmacol.* **63**(2), pp.289-296.
Kuhn, H.G., Dickinson-Anson, H. and Gage, F.H. 1996. Neurogenesis in the dentate gyrus of the adult rat: age-related decrease of neuronal progenitor proliferation. *The Journal of Neuroscience.* **16**(6), p2027.
Kulbatski, I., Mothe, A.J., Keating, A., Hakamata, Y., Kobayashi, E. and Tator, C.H. 2007. Oligodendrocytes and radial glia derived from adult rat spinal cord progenitors: morphological and immunocytochemical characterization. *J Histochem Cytochem.* **55**(3), pp.209-222.
Lacor, P., Gandolfo, P., Tonon, M.C., Brault, E., Dalibert, I., Schumacher, M., Benavides, J. and Ferzaz, B. 1999. Regulation of the expression of peripheral benzodiazepine receptors and their endogenous ligands during rat sciatic nerve degeneration and regeneration: a role for PBR in neurosteroidogenesis. *Brain Res.* **815**(1), pp.70-80.
Lacroix, S., Hamilton, L.K., Vaugeois, A., Beaudoin, S., Breault-Dugas, C., Pineau, I., Levesque, S.A., Gregoire, C.A. and Fernandes, K.J. 2014. Central canal ependymal cells proliferate extensively in response to traumatic spinal cord injury but not demyelinating lesions. *PLoS One.* **9**(1), pe85916.
Lambert, J.J., Cooper, M.A., Simmons, R.D.J., Weir, C.J. and Belelli, D. 2009. Neurosteroids: Endogenous allosteric modulators of GABAA receptors. *Psychoneuroendocrinology.* **34**, pp.S48-S58.
Lanfray, D., Arthaud, S., Ouellet, J., Compère, V., Do Rego, J.-L., Leprince, J., Lefranc, B., Castel, H., Bouchard, C., Monge-Roffarello, B., Richard, D., Pelletier, G., Vaudry, H., Tonon, M.-C. and Morin, F. 2013. Gliotransmission and brain glucose sensing: critical role of endozepines. *Diabetes.* **62**(3), pp.801-810.
Lau, L.W., Keough, M.B., Haylock-Jacobs, S., Cua, R., Doring, A., Sloka, S., Stirling, D.P., Rivest, S. and Yong, V.W. 2012. Chondroitin sulfate proteoglycans in demyelinated lesions impair remyelination. *Ann Neurol.* **72**(3), pp.419-432.
Lavoie, A.M. and Twyman, R.E. 1996. Direct evidence for diazepam modulation of GABAA receptor microscopic affinity. *Neuropharmacology.* **35**(9-10), pp.1383-1392.
Le Fur, G., Vaucher, N., Perrier, M.L., Flamier, A., Benavides, J., Renault, C., Dubroeucq, M.C., Gueremy, C. and Uzan, A. 1983. Differentiation between two ligands for peripheral benzodiazepine binding sites, [3H]RO5-4864 and [3H]PK 11195, by thermodynamic studies. *Life Sci.* **33**(5), pp.449-457.
Leach, J.P., Sills, G.J., Majid, A., Butler, E., Carswell, A., Thompson, G.G. and Brodie, M.J. 1996. Effects of tiagabine and vigabatrin on GABA uptake into primary cultures of rat cortical astrocytes. *Seizure.* **5**(3), pp.229-234.
Leadon, S.A. 1996. Repair of DNA Damage Produced by Ionizing Radiation: A Minireview. *Semin Radiat Oncol.* **6**(4), pp.295-305.

Lee-Kubli, C.A. and Lu, P. 2015. Induced pluripotent stem cell-derived neural stem cell therapies for spinal cord injury. *Neural Regen Res.* **10**(1), pp.10-16.
Lee, A.S., Tang, C., Rao, M.S., Weissman, I.L. and Wu, J.C. 2013. Tumorigenicity as a clinical hurdle for pluripotent stem cell therapies. *Nature medicine.* **19**(8), pp.998-1004.
Lee, C. and Rodgers, R.J. 1991. Effects of benzodiazepine receptor antagonist, flumazenil, on antinociceptive and behavioural responses to the elevated plus-maze in mice. *Neuropharmacology.* **30**(12a), pp.1263-1267.
Lee, K. and Ko, H.W. 2018. Repeated restraint stress promotes hippocampal neuronal cell ciliogenesis and proliferation in mice. *Laboratory animal research.* **34**(4), pp.203-210.
Lee, Y.-H. and Stallcup, M.R. 2011. Roles of protein arginine methylation in DNA damage signaling pathways is CARM1 a life-or-death decision point? *Cell cycle (Georgetown, Tex.).* **10**(9), pp.1343-1344.
Lee, Y., Morrison, B.M., Li, Y., Lengacher, S., Farah, M.H., Hoffman, P.N., Liu, Y., Tsingalia, A., Jin, L., Zhang, P.W., Pellerin, L., Magistretti, P.J. and Rothstein, J.D. 2012. Oligodendroglia metabolically support axons and contribute to neurodegeneration. *Nature.* **487**(7408), pp.443-448.
Leonhardt, H. 1976. [The cerebrospinal fluid contact processes in the central canal of the spinal cord. A scanning and transmission electron microscopic study of the rabbit]. *Z Mikrosk Anat Forsch.* **90**(1), pp.1-15.
Li, G.D., Chiara, D.C., Sawyer, G.W., Husain, S.S., Olsen, R.W. and Cohen, J.B. 2006. Identification of a GABAA receptor anesthetic binding site at subunit interfaces by photolabeling with an etomidate analog. *J Neurosci.* **26**(45), pp.11599-11605.
Li, J. and Lepski, G. 2013. Cell transplantation for spinal cord injury: a systematic review. *BioMed research international.* **2013**, pp.786475-786475.
Li, L., Story, M. and Legerski, R.J. 2001. Cellular responses to ionizing radiation damage. *International Journal of Radiation Oncology • Biology • Physics.* **49**(4), pp.1157-1162.
Li, X.-m., Meng, J., Li, L.t., Guo, T., Yang, L.-k., Shi, Q.-x., Li, X.-b., Chen, Y., Yang, Q. and Zhao, J.-n. 2017. Effect of ZBD-2 on chronic pain, depressive-like behaviors, and recovery of motor function following spinal cord injury in mice. *Behavioural Brain Research.* **322**, pp.92-99.
Li, X., Floriddia, E.M., Toskas, K., Fernandes, K.J.L., Guerout, N. and Barnabe-Heider, F. 2016. Regenerative Potential of Ependymal Cells for Spinal Cord Injuries Over Time. *EBioMedicine.* **13**, pp.55-65.
Liere, P., Pianos, A., Oudinet, J.P., Schumacher, M. and Akwa, Y. 2017. Differential effects of the 18-kDa translocator protein (TSPO) ligand etifoxine on steroidogenesis in rat brain, plasma and steroidogenic glands: Pharmacodynamic studies. *Psychoneuroendocrinology.* **83**, pp.122-134.
Lihrmann, I., Plaquevent, J.C., Tostivint, H., Raijmakers, R., Tonon, M.C., Conlon, J.M. and Vaudry, H. 1994. Frog diazepam-binding inhibitor: peptide sequence, cDNA cloning, and expression in the brain. *Proceedings of the National Academy of Sciences of the United States of America.* **91**(15), pp.6899-6903.
Lim, D.A. and Alvarez-Buylla, A. 2016. The Adult Ventricular-Subventricular Zone (V-SVZ) and Olfactory Bulb (OB) Neurogenesis. *Cold Spring Harb Perspect Biol.* **8**(5).
Lim, D.A., Tramontin, A.D., Trevejo, J.M., Herrera, D.G., Garcia-Verdugo, J.M. and Alvarez-Buylla, A. 2000. Noggin antagonizes BMP signaling to create a niche for adult neurogenesis. *Neuron.* **28**(3), pp.713-726.

Lin, S.C. and Bergles, D.E. 2004. Synaptic signaling between GABAergic interneurons and oligodendrocyte precursor cells in the hippocampus. *Nat Neurosci.* **7**(1), pp.24-32.
Lister, R.G. and Nutt, D.J. 1988. Interactions of the imidazodiazepine Ro 15-4513 with chemical convulsants. *Br J Pharmacol.* **93**(1), pp.210-214.
Liu, G.J., Middleton, R.J., Hatty, C.R., Kam, W.W., Chan, R., Pham, T., Harrison-Brown, M., Dodson, E., Veale, K. and Banati, R.B. 2014. The 18 kDa translocator protein, microglia and neuroinflammation. *Brain Pathol.* **24**(6), pp.631-653.
Liu, X., Wang, Q., Haydar, T.F. and Bordey, A. 2005. Nonsynaptic GABA signaling in postnatal subventricular zone controls GFAP-expressing progenitor proliferation. *Nature neuroscience.* **8**(9), pp.1179-1187.
Llewellyn-Smith, I.J., Basbaum, A.I. and Braz, J.M. 2018. Long-term, dynamic synaptic reorganization after GABAergic precursor cell transplantation into adult mouse spinal cord. *J Comp Neurol.* **526**(3), pp.480-495.
Lois, C. and Alvarez-Buylla, A. 1993. Proliferating subventricular zone cells in the adult mammalian forebrain can differentiate into neurons and glia. *Proc Natl Acad Sci U S A.* **90**(5), pp.2074-2077.
Lois, C. and Alvarez-Buylla, A. 1994. Long-distance neuronal migration in the adult mammalian brain. *Science.* **264**(5162), pp.1145-1148.
Loomis, W.F., Behrens, M.M., Williams, M.E. and Anjard, C. 2010. Pregnenolone sulfate and cortisol induce secretion of acyl-CoA-binding protein and its conversion into endozepines from astrocytes. *J Biol Chem.* **285**(28), pp.21359-21365.
Löscher, W., Hönack, D. and Gramer, M. 1989. Use of Inhibitors of γ-Aminobutyric Acid (GABA) Transaminase for the Estimation of GABA Turnover in Various Brain Regions of Rats: A Reevaluation of Aminooxyacetic Acid. *Journal of Neurochemistry.* **53**(6), pp.1737-1750.
Lowndes, N.F. and Murguia, J.R. 2000. Sensing and responding to DNA damage. *Curr Opin Genet Dev.* **10**(1), pp.17-25.
Lu, P., Woodruff, G., Wang, Y., Graham, L., Hunt, M., Wu, D., Boehle, E., Ahmad, R., Poplawski, G., Brock, J., Goldstein, L.S. and Tuszynski, M.H. 2014. Long-distance axonal growth from human induced pluripotent stem cells after spinal cord injury. *Neuron.* **83**(4), pp.789-796.
Lytle, J.M. and Wrathall, J.R. 2007. Glial cell loss, proliferation and replacement in the contused murine spinal cord. *Eur J Neurosci.* **25**(6), pp.1711-1724.
Ma, W., Li, B.S., Zhang, L. and Pant, H.C. 2004. Signaling cascades implicated in muscarinic regulation of proliferation of neural stem and progenitor cells. *Drug News Perspect.* **17**(4), pp.258-266.
Maaser, K., Höpfner, M., Jansen, A., Weisinger, G., Gavish, M., Kozikowski, A.P., Weizman, A., Carayon, P., Riecken, E.O., Zeitz, M. and Scherübl, H. 2001. Specific ligands of the peripheral benzodiazepine receptor induce apoptosis and cell cycle arrest in human colorectal cancer cells. *British journal of cancer.* **85**(11), pp.1771-1780.
Mackay-Sim, A. and St John, J.A. 2011. Olfactory ensheathing cells from the nose: clinical application in human spinal cord injuries. *Exp Neurol.* **229**(1), pp.174-180.
Mackowiak, B., Li, L., Welch, M.A., Li, D., Jones, J.W., Heyward, S., Kane, M.A., Swaan, P.W. and Wang, H. 2017. Molecular Basis of Metabolism-Mediated Conversion of PK11195 from an Antagonist to an Agonist of the Constitutive Androstane Receptor. *Mol Pharmacol.* **92**(1), pp.75-87.

Magoul, R., Onteniente, B., Geffard, M. and Calas, A. 1987. Anatomical distribution and ultrastructural organization of the GABAergic system in the rat spinal cord. An immunocytochemical study using anti-GABA antibodies. *Neuroscience.* **20**(3), pp.1001-1009.
Mak, N.K., Szeto, Y.Y., Fung, M.C., Leung, K.N. and Kwan, S.K. 1997. Effects of midazolam on the differentiation of murine myeloid leukemia cells. *Chemotherapy.* **43**(4), pp.272-281.
Malagon, M., Vaudry, H., Van Strien, F., Pelletier, G., Gracia-Navarro, F. and Tonon, M.C. 1993. Ontogeny of diazepam-binding inhibitor-related peptides (endozepines) in the rat brain. *Neuroscience.* **57**(3), pp.777-786.
Malik, A., Kondratov, R.V., Jamasbi, R.J. and Geusz, M.E. 2015. Circadian Clock Genes Are Essential for Normal Adult Neurogenesis, Differentiation, and Fate Determination. *PloS one.* **10**(10), pp.e0139655-e0139655.
Marichal, N., Fabbiani, G., Trujillo-Cenoz, O. and Russo, R.E. 2016. Purinergic signalling in a latent stem cell niche of the rat spinal cord. *Purinergic Signal.* **12**(2), pp.331-341.
Marichal, N., García, G., Radmilovich, M., Trujillo-Cenóz, O. and Russo, R.E. 2009. Enigmatic central canal contacting cells: immature neurons in "standby mode"? *The Journal of neuroscience : the official journal of the Society for Neuroscience.* **29**(32), pp.10010-10024.
Martens, D.J., Seaberg, R.M. and van der Kooy, D. 2002. *In vivo* infusions of exogenous growth factors into the fourth ventricle of the adult mouse brain increase the proliferation of neural progenitors around the fourth ventricle and the central canal of the spinal cord. *Eur J Neurosci.* **16**(6), pp.1045-1057.
Martens, F., Koppel, C., Ibe, K., Wagemann, A. and Tenczer, J. 1990. Clinical experience with the benzodiazepine antagonist flumazenil in suspected benzodiazepine or ethanol poisoning. *J Toxicol Clin Toxicol.* **28**(3), pp.341-356.
Massirer, K.B., Carromeu, C., Griesi-Oliveira, K. and Muotri, A.R. 2011. Maintenance and differentiation of neural stem cells. *Wiley Interdiscip Rev Syst Biol Med.* **3**(1), pp.107-114.
Matoba, K., Muramatsu, R. and Yamashita, T. 2017. Leptin sustains spontaneous remyelination in the adult central nervous system. *Scientific Reports.* **7**, p40397.
Matsumura, S., Takagi, K., Okuda-Ashitaka, E., Lu, J., Naritsuka, H., Yamaguchi, M. and Ito, S. 2010. Characterization of nestin expression in the spinal cord of GFP transgenic mice after peripheral nerve injury. *Neuroscience.* **170**(3), pp.942-953.
Mazzone, G.L., Mladinic, M. and Nistri, A. 2013. Excitotoxic cell death induces delayed proliferation of endogenous neuroprogenitor cells in organotypic slice cultures of the rat spinal cord. *Cell Death Dis.* **4**, pe902.
McDonough, A., Hoang, A.N., Monterrubio, A.M., Greenhalgh, S. and Martinez-Cerdeno, V. 2013. Compression injury in the mouse spinal cord elicits a specific proliferative response and distinct cell fate acquisition along rostro-caudal and dorso-ventral axes. *Neuroscience.* **254**, pp.1-17.
McDonough, A. and Martínez-Cerdeño, V. 2012. Endogenous proliferation after spinal cord injury in animal models. *Stem cells international.* **2012**, pp.387513-387513.
McEnery, M.W., Snowman, A.M., Trifiletti, R.R. and Snyder, S.H. 1992. Isolation of the mitochondrial benzodiazepine receptor: association with the voltage-dependent anion channel and the adenine nucleotide carrier. *Proc Natl Acad Sci U S A.* **89**(8), pp.3170-3174.

McKeon, R.J., Schreiber, R.C., Rudge, J.S. and Silver, J. 1991. Reduction of neurite outgrowth in a model of glial scarring following CNS injury is correlated with the expression of inhibitory molecules on reactive astrocytes. *J Neurosci.* **11**(11), pp.3398-3411.
McKernan, R.M. and Whiting, P.J. 1996. Which GABAA-receptor subtypes really occur in the brain? *Trends Neurosci.* **19**(4), pp.139-143.
McLaughlin, B.J., Barber, R., Saito, K., Roberts, E. and Wu, J.Y. 1975. Immunocytochemical localization of glutamate decarboxylase in rat spinal cord. *J Comp Neurol.* **164**(3), pp.305-321.
Meisner, J.G., Marsh, A.D. and Marsh, D.R. 2010. Loss of GABAergic interneurons in laminae I-III of the spinal cord dorsal horn contributes to reduced GABAergic tone and neuropathic pain after spinal cord injury. *J Neurotrauma.* **27**(4), pp.729-737.
Meletis, K., Barnabe-Heider, F., Carlen, M., Evergren, E., Tomilin, N., Shupliakov, O. and Frisen, J. 2008. Spinal cord injury reveals multilineage differentiation of ependymal cells. *PLoS Biol.* **6**(7), pe182.
Mellon, S.H. and Deschepper, C.F. 1993. Neurosteroid biosynthesis: genes for adrenal steroidogenic enzymes are expressed in the brain. *Brain Res.* **629**(2), pp.283-292.
Menachem, E.B., Persson, L.I., Schechter, P.J., Haegele, K.D., Huebert, N., Hardenberg, J., Dahlgren, L. and Mumford, J.P. 1988. Effects of single doses of vigabatrin on CSF concentrations of GABA, homocarnosine, homovanillic acid and 5-hydroxyindoleacetic acid in patients with complex partial epilepsy. *Epilepsy Res.* **2**(2), pp.96-101.
Mendonça-Torres, M.C. and Roberts, S.S. 2013. The translocator protein (TSPO) ligand PK11195 induces apoptosis and cell cycle arrest and sensitizes to chemotherapy treatment in pre- and post-relapse neuroblastoma cell lines. *Cancer biology & therapy.* **14**(4), pp.319-326.
Menet, V., Prieto, M., Privat, A. and Gimenez y Ribotta, M. 2003. Axonal plasticity and functional recovery after spinal cord injury in mice deficient in both glial fibrillary acidic protein and vimentin genes. *Proc Natl Acad Sci U S A.* **100**(15), pp.8999-9004.
Mereu, G., Passino, N., Carcangiu, P., Boi, V. and Gessa, G.L. 1987. Electrophysiological evidence that Ro 15-4513 is a benzodiazepine receptor inverse agonist. *Eur J Pharmacol.* **135**(3), pp.453-454.
Mesa, F.L., Osuna, A., Aneiros, J., Gonzalez-Jaranay, M., Bravo, J., Junco, P., Del Moral, R.G. and O'Valle, F. 2003. Antibiotic treatment of incipient drug-induced gingival overgrowth in adult renal transplant patients. *J Periodontal Res.* **38**(2), pp.141-146.
Miettinen, H., Kononen, J., Haapasalo, H., Helen, P., Sallinen, P., Harjuntausta, T., Helin, H. and Alho, H. 1995. Expression of peripheral-type benzodiazepine receptor and diazepam binding inhibitor in human astrocytomas: relationship to cell proliferation. *Cancer Res.* **55**(12), pp.2691-2695.
Mignone, J.L., Kukekov, V., Chiang, A.S., Steindler, D. and Enikolopov, G. 2004. Neural stem and progenitor cells in nestin-GFP transgenic mice. *J Comp Neurol.* **469**(3), pp.311-324.
Milhorat, T.H., Kotzen, R.M. and Anzil, A.P. 1994. Stenosis of central canal of spinal cord in man: incidence and pathological findings in 232 autopsy cases. *J Neurosurg.* **80**(4), pp.716-722.

Mills, C.D., Bitler, J.L. and Woolf, C.J. 2005. Role of the peripheral benzodiazepine receptor in sensory neuron regeneration. *Mol Cell Neurosci.* **30**(2), pp.228-237.
Mims, C.A. 1960. Intracerebral injections and the growth of viruses in the mouse brain. *British journal of experimental pathology.* **41**(1), pp.52-59.
Miron, V.E., Boyd, A., Zhao, J.-W., Yuen, T.J., Ruckh, J.M., Shadrach, J.L., van Wijngaarden, P., Wagers, A.J., Williams, A., Franklin, R.J.M. and Ffrench-Constant, C. 2013. M2 microglia and macrophages drive oligodendrocyte differentiation during CNS remyelination. *Nature neuroscience.* **16**(9), pp.1211-1218.
Mirzadeh, Z., Merkle, F.T., Soriano-Navarro, M., Garcia-Verdugo, J.M. and Alvarez-Buylla, A. 2008. Neural stem cells confer unique pinwheel architecture to the ventricular surface in neurogenic regions of the adult brain. *Cell Stem Cell.* **3**(3), pp.265-278.
Moreno-Manzano, V., Rodriguez-Jimenez, F.J., Garcia-Rosello, M., Lainez, S., Erceg, S., Calvo, M.T., Ronaghi, M., Lloret, M., Planells-Cases, R., Sanchez-Puelles, J.M. and Stojkovic, M. 2009. Activated spinal cord ependymal stem cells rescue neurological function. *Stem Cells.* **27**(3), pp.733-743.
Morizur, L., Chicheportiche, A., Gauthier, L.R., Daynac, M., Boussin, F.D. and Mouthon, M.-A. 2018. Distinct Molecular Signatures of Quiescent and Activated Adult Neural Stem Cells Reveal Specific Interactions with Their Microenvironment. *Stem cell reports.* **11**(2), pp.565-577.
Morshead, C.M., Reynolds, B.A., Craig, C.G., McBurney, M.W., Staines, W.A., Morassutti, D., Weiss, S. and van der Kooy, D. 1994. Neural stem cells in the adult mammalian forebrain: a relatively quiescent subpopulation of subependymal cells. *Neuron.* **13**(5), pp.1071-1082.
Mothe, A.J. and Tator, C.H. 2005. Proliferation, migration, and differentiation of endogenous ependymal region stem/progenitor cells following minimal spinal cord injury in the adult rat. *Neuroscience.* **131**(1), pp.177-187.
Mothe, A.J., Zahir, T., Santaguida, C., Cook, D. and Tator, C.H. 2011. Neural stem/progenitor cells from the adult human spinal cord are multipotent and self-renewing and differentiate after transplantation. *PLoS One.* **6**(11), pe27079.
Mukhin, A.G., Papadopoulos, V., Costa, E. and Krueger, K.E. 1989. Mitochondrial benzodiazepine receptors regulate steroid biosynthesis. *Proc Natl Acad Sci U S A.* **86**(24), pp.9813-9816.
Mumford, J.P. and Dam, M. 1989. Meta-analysis of European placebo controlled studies of vigabatrin in drug resistant epilepsy. *Br J Clin Pharmacol.* **27 Suppl 1**, pp.101s-107s.
Murdoch, B. and Roskams, A.J. 2008. A novel embryonic nestin-expressing radial glia-like progenitor gives rise to zonally restricted olfactory and vomeronasal neurons. *J Neurosci.* **28**(16), pp.4271-4282.
Nakamura, M. and Okano, H. 2013. Cell transplantation therapies for spinal cord injury focusing on induced pluripotent stem cells. *Cell research.* **23**(1), pp.70-80.
Namiki, J. and Tator, C.H. 1999. Cell proliferation and nestin expression in the ependyma of the adult rat spinal cord after injury. *J Neuropathol Exp Neurol.* **58**(5), pp.489-498.
Nazar, M., Jessa, M. and Plaznik, A. 1997. Benzodiazepine-GABAA receptor complex ligands in two models of anxiety. *J Neural Transm (Vienna).* **104**(6-7), pp.733-746.
Neman, J., Termini, J., Wilczynski, S., Vaidehi, N., Choy, C., Kowolik, C.M., Li, H., Hambrecht, A.C., Roberts, E. and Jandial, R. 2014. Human breast cancer

metastases to the brain display GABAergic properties in the neural niche. *Proc Natl Acad Sci U S A.* **111**(3), pp.984-989.
Nguyen, L., Malgrange, B., Breuskin, I., Bettendorff, L., Moonen, G., Belachew, S. and Rigo, J.M. 2003. Autocrine/paracrine activation of the GABA(A) receptor inhibits the proliferation of neurogenic polysialylated neural cell adhesion molecule-positive (PSA-NCAM+) precursor cells from postnatal striatum. *J Neurosci.* **23**(8), pp.3278-3294.
Nochi, R., Kaneko, J., Okada, N., Terazono, Y., Matani, A. and Hisatsune, T. 2013. Diazepam treatment blocks the elevation of hippocampal activity and the accelerated proliferation of hippocampal neural stem cells after focal cerebral ischemia in mice. *J Neurosci Res.* **91**(11), pp.1429-1439.
Noorbakhsh, F., Baker, G.B. and Power, C. 2014. Allopregnanolone and neuroinflammation: a focus on multiple sclerosis. *Frontiers in cellular neuroscience.* **8**, pp.134-134.
Norbury, C.J. and Zhivotovsky, B. 2004. DNA damage-induced apoptosis. *Oncogene.* **23**, p2797.
Nori, S., Okada, Y., Yasuda, A., Tsuji, O., Takahashi, Y., Kobayashi, Y., Fujiyoshi, K., Koike, M., Uchiyama, Y., Ikeda, E., Toyama, Y., Yamanaka, S., Nakamura, M. and Okano, H. 2011. Grafted human-induced pluripotent stem-cell-derived neurospheres promote motor functional recovery after spinal cord injury in mice. *Proceedings of the National Academy of Sciences of the United States of America.* **108**(40), pp.16825-16830.
Notter, T., Coughlin, J.M., Sawa, A. and Meyer, U. 2018. Reconceptualization of translocator protein as a biomarker of neuroinflammation in psychiatry. *Mol Psychiatry.* **23**(1), pp.36-47.
Nutt, D.J., Besson, M., Wilson, S.J., Dawson, G.R. and Lingford-Hughes, A.R. 2007. Blockade of alcohol's amnestic activity in humans by an alpha5 subtype benzodiazepine receptor inverse agonist. *Neuropharmacology.* **53**(7), pp.810-820.
Nutt, D.J. and Lister, R.G. 1987. The effect of the imidazodiazepine Ro 15-4513 on the anticonvulsant effects of diazepam, sodium pentobarbital and ethanol. *Brain Res.* **413**(1), pp.193-196.
Ogawa, Y., Sawamoto, K., Miyata, T., Miyao, S., Watanabe, M., Nakamura, M., Bregman, B.S., Koike, M., Uchiyama, Y., Toyama, Y. and Okano, H. 2002. Transplantation of *in vitro*-expanded fetal neural progenitor cells results in neurogenesis and functional recovery after spinal cord contusion injury in adult rats. *J Neurosci Res.* **69**(6), pp.925-933.
Ogris, W., Pöltl, A., Hauer, B., Ernst, M., Oberto, A., Wulff, P., Höger, H., Wisden, W. and Sieghart, W. 2004. *Affinity of various benzodiazepine site ligands in mice with a point mutation in the GABAA receptor γ2 subunit.*
Okada, S., Ishii, K., Yamane, J., Iwanami, A., Ikegami, T., Katoh, H., Iwamoto, Y., Nakamura, M., Miyoshi, H., Okano, H.J., Contag, C.H., Toyama, Y. and Okano, H. 2005. *In vivo* imaging of engrafted neural stem cells: its application in evaluating the optimal timing of transplantation for spinal cord injury. *Faseb j.* **19**(13), pp.1839-1841.
Okada, S., Nakamura, M., Katoh, H., Miyao, T., Shimazaki, T., Ishii, K., Yamane, J., Yoshimura, A., Iwamoto, Y., Toyama, Y. and Okano, H. 2006. Conditional ablation of Stat3 or Socs3 discloses a dual role for reactive astrocytes after spinal cord injury. *Nat Med.* **12**(7), pp.829-834.

Okada, Y., Matsumoto, A., Shimazaki, T., Enoki, R., Koizumi, A., Ishii, S., Itoyama, Y., Sobue, G. and Okano, H. 2008. Spatiotemporal recapitulation of central nervous system development by murine embryonic stem cell-derived neural stem/progenitor cells. *Stem Cells.* **26**(12), pp.3086-3098.
Oke, O., Suárez-Quian, C., Riond, J., Ferrara, P. and Papadopoulos, V. 1992. *Cell surface localization of peripheral-type benzodiazepine receptor (PBR) in adrenal cortex.*
Oliva, A.A., Jr., Jiang, M., Lam, T., Smith, K.L. and Swann, J.W. 2000. Novel hippocampal interneuronal subtypes identified using transgenic mice that express green fluorescent protein in GABAergic interneurons. *J Neurosci.* **20**(9), pp.3354-3368.
Olsen, R.W. 2018. GABAA receptor: Positive and negative allosteric modulators. *Neuropharmacology.* **136**(Pt A), pp.10-22.
Olsen, R.W., Hanchar, H.J., Meera, P. and Wallner, M. 2007. GABAA receptor subtypes: the "one glass of wine" receptors. *Alcohol.* **41**(3), pp.201-209.
Olsen, R.W. and Sieghart, W. 2008. International Union of Pharmacology. LXX. Subtypes of gamma-aminobutyric acid(A) receptors: classification on the basis of subunit composition, pharmacology, and function. Update. *Pharmacol Rev.* **60**(3), pp.243-260.
Ortega, F., Gascon, S., Masserdotti, G., Deshpande, A., Simon, C., Fischer, J., Dimou, L., Chichung Lie, D., Schroeder, T. and Berninger, B. 2013. Oligodendrogliogenic and neurogenic adult subependymal zone neural stem cells constitute distinct lineages and exhibit differential responsiveness to Wnt signalling. *Nat Cell Biol.* **15**(6), pp.602-613.
Osorio-Querejeta, I., Saenz-Cuesta, M., Munoz-Culla, M. and Otaegui, D. 2017. Models for Studying Myelination, Demyelination and Remyelination. *Neuromolecular Med.* **19**(2-3), pp.181-192.
Otis, T.S., Staley, K.J. and Mody, I. 1991. Perpetual inhibitory activity in mammalian brain slices generated by spontaneous GABA release. *Brain Res.* **545**(1-2), pp.142-150.
Paez-Gonzalez, P., Asrican, B., Rodriguez, E. and Kuo, C.T. 2014. Identification of distinct ChAT(+) neurons and activity-dependent control of postnatal SVZ neurogenesis. *Nat Neurosci.* **17**(7), pp.934-942.
Panayiotou, E. and Malas, S. 2013. Adult spinal cord ependymal layer: a promising pool of quiescent stem cells to treat spinal cord injury. *Frontiers in physiology.* **4**, pp.340-340.
Pandamooz, S., Salehi, M.S., Zibaii, M.I., Safari, A., Nabiuni, M., Ahmadiani, A. and Dargahi, L. 2019. Modeling traumatic injury in organotypic spinal cord slice culture obtained from adult rat. *Tissue and Cell.* **56**, pp.90-97.
Paniagua-Torija, B., Arevalo-Martin, A., Ferrer, I., Molina-Holgado, E. and Garcia-Ovejero, D. 2015. CB1 cannabinoid receptor enrichment in the ependymal region of the adult human spinal cord. *Scientific Reports.* **5**, p17745.
Paniagua-Torija, B., Norenberg, M., Arevalo-Martin, A., Carballosa-Gautam, M.M., Campos-Martin, Y., Molina-Holgado, E. and Garcia-Ovejero, D. 2018. Cells in the adult human spinal cord ependymal region do not proliferate after injury. *The Journal of Pathology.* **246**(4), pp.415-421.
Panner, A. and Wurster, R.D. 2006. T-type calcium channels and tumor proliferation. *Cell Calcium.* **40**(2), pp.253-259.

Papadopoulos, V. 1993. Peripheral-type benzodiazepine/diazepam binding inhibitor receptor: biological role in steroidogenic cell function. *Endocr Rev.* **14**(2), pp.222-240.
Papadopoulos, V., Amri, H., Boujrad, N., Cascio, C., Culty, M., Garnier, M., Hardwick, M., Li, H., Vidic, B., Brown, A.S., Reversa, J.L., Bernassau, J.M. and Drieu, K. 1997. Peripheral benzodiazepine receptor in cholesterol transport and steroidogenesis. *Steroids.* **62**(1), pp.21-28.
Papadopoulos, V., Baraldi, M., Guilarte, T.R., Knudsen, T.B., Lacapere, J.J., Lindemann, P., Norenberg, M.D., Nutt, D., Weizman, A., Zhang, M.R. and Gavish, M. 2006. Translocator protein (18kDa): new nomenclature for the peripheral-type benzodiazepine receptor based on its structure and molecular function. *Trends Pharmacol Sci.* **27**(8), pp.402-409.
Papadopoulos, V., Berkovich, A., Krueger, K.E., Costa, E. and Guidotti, A. 1991. Diazepam binding inhibitor and its processing products stimulate mitochondrial steroid biosynthesis via an interaction with mitochondrial benzodiazepine receptors. *Endocrinology.* **129**(3), pp.1481-1488.
Papadopoulos, V., Fan, J. and Zirkin, B. 2018. Translocator protein (18 kDa): an update on its function in steroidogenesis. *J Neuroendocrinol.* **30**(2).
Papadopoulos, V. and Lecanu, L. 2009. Translocator protein (18 kDa) TSPO: an emerging therapeutic target in neurotrauma. *Exp Neurol.* **219**(1), pp.53-57.
Papadopoulos, V., Mukhin, A.G., Costa, E. and Krueger, K.E. 1990. The peripheral-type benzodiazepine receptor is functionally linked to Leydig cell steroidogenesis. *J Biol Chem.* **265**(7), pp.3772-3779.
Park, E., Velumian, A.A. and Fehlings, M.G. 2004. The role of excitotoxicity in secondary mechanisms of spinal cord injury: a review with an emphasis on the implications for white matter degeneration. *J Neurotrauma.* **21**(6), pp.754-774.
Park, S.Y., Cho, N., Chang, I., Chung, J.H., Min, Y.K., Lee, M.K., Kim, K.W., Kim, S.J. and Lee, M.S. 2005. Effect of PK11195, a peripheral benzodiazepine receptor agonist, on insulinoma cell death and insulin secretion. *Apoptosis.* **10**(3), pp.537-544.
Patrikios, P., Stadelmann, C., Kutzelnigg, A., Rauschka, H., Schmidbauer, M., Laursen, H., Sorensen, P.S., Bruck, W., Lucchinetti, C. and Lassmann, H. 2006. Remyelination is extensive in a subset of multiple sclerosis patients. *Brain.* **129**(Pt 12), pp.3165-3172.
Patte, C., Gandolfo, P., Leprince, J., Thoumas, J.-L., Fontaine, M., Vaudry, H. and Tonon, M.-C. 1999. GABA inhibits endozepine release from cultured rat astrocytes. *Glia.* **25**(4), pp.404-411.
Pfenninger, C.V., Steinhoff, C., Hertwig, F. and Nuber, U.A. 2011. Prospectively isolated CD133/CD24-positive ependymal cells from the adult spinal cord and lateral ventricle wall differ in their long-term *in vitro* self-renewal and *in vivo* gene expression. *Glia.* **59**(1), pp.68-81.
Ping Yuan, J., Wei Wang, L., Qu, A., Mei Chen, J., Ming Xiang, Q., Chen, C., Sun, S.-R., Pang, D.-W., Liu, J. and Li, Y. 2015. *Quantum Dots-Based Quantitative and In Situ Multiple Imaging on Ki67 and Cytokeratin to Improve Ki67 Assessment in Breast Cancer.*
Plemel, J.R., Liu, W.Q. and Yong, V.W. 2017. Remyelination therapies: a new direction and challenge in multiple sclerosis. *Nat Rev Drug Discov.* **16**(9), pp.617-634.

Pratt, H., Zaaroor, M., Bleich, N. and Starr, A. 1991. Effects of myelin or cell body brainstem lesions on 3-channel Lissajous' trajectories of feline auditory brainstem evoked potentials. *Hear Res.* **53**(2), pp.237-252.
Qiu, Z.K., Li, M.S., He, J.L., Liu, X., Zhang, G.H., Lai, S., Ma, J.C., Zeng, J., Li, Y., Wu, H.W., Chen, Y., Shen, Y.G. and Chen, J.S. 2015. Translocator protein mediates the anxiolytic and antidepressant effects of midazolam. *Pharmacol Biochem Behav.* **139**(Pt A), pp.77-83.
Rabchevsky, A.G., Sullivan, P.G. and Scheff, S.W. 2007. Temporal-spatial dynamics in oligodendrocyte and glial progenitor cell numbers throughout ventrolateral white matter following contusion spinal cord injury. *Glia.* **55**(8), pp.831-843.
Rahimi, Y., Goulding, A., Shrestha, S., Mirpuri, S. and Deo, S.K. 2008. Mechanism of copper induced fluorescence quenching of red fluorescent protein, DsRed. *Biochemical and biophysical research communications.* **370**(1), pp.57-61.
Rakai, B.D., Chrusch, M.J., Spanswick, S.C., Dyck, R.H. and Antle, M.C. 2014. Survival of Adult Generated Hippocampal Neurons Is Altered in Circadian Arrhythmic Mice. *PLOS ONE.* **9**(6), pe99527.
Ramerstorfer, J., Furtmuller, R., Vogel, E., Huck, S. and Sieghart, W. 2010. The point mutation gamma 2F77I changes the potency and efficacy of benzodiazepine site ligands in different GABAA receptor subtypes. *Eur J Pharmacol.* **636**(1-3), pp.18-27.
Reali, C., Fernandez, A., Radmilovich, M., Trujillo-Cenoz, O. and Russo, R.E. 2011. GABAergic signalling in a neurogenic niche of the turtle spinal cord. *J Physiol.* **589**(Pt 23), pp.5633-5647.
Reimer, M.M., Sorensen, I., Kuscha, V., Frank, R.E., Liu, C., Becker, C.G. and Becker, T. 2008. Motor neuron regeneration in adult zebrafish. *J Neurosci.* **28**(34), pp.8510-8516.
Ren, Y., Ao, Y., O'Shea, T.M., Burda, J.E., Bernstein, A.M., Brumm, A.J., Muthusamy, N., Ghashghaei, H.T., Carmichael, S.T., Cheng, L. and Sofroniew, M.V. 2017. Ependymal cell contribution to scar formation after spinal cord injury is minimal, local and dependent on direct ependymal injury. *Sci Rep.* **7**, p41122.
Renault-Mihara, F., Mukaino, M., Shinozaki, M., Kumamaru, H., Kawase, S., Baudoux, M., Ishibashi, T., Kawabata, S., Nishiyama, Y., Sugai, K., Yasutake, K., Okada, S., Nakamura, M. and Okano, H. 2017. Regulation of RhoA by STAT3 coordinates glial scar formation. *J Cell Biol.* **216**(8), pp.2533-2550.
Rexed, B. 1952. The cytoarchitectonic organization of the spinal cord in the cat. *J Comp Neurol.* **96**(3), pp.414-495.
Rexed, B. 1954. A cytoarchitectonic atlas of the spinal cord in the cat. *J Comp Neurol.* **100**(2), pp.297-379.
Roberts, B.L., Maslam, S., Scholten, G. and Smit, W. 1995. Dopaminergic and GABAergic cerebrospinal fluid-contacting neurons along the central canal of the spinal cord of the eel and trout. *J Comp Neurol.* **354**(3), pp.423-437.
Roderick, H.L. and Cook, S.J. 2008. Ca2+ signalling checkpoints in cancer: remodelling Ca2+ for cancer cell proliferation and survival. *Nat Rev Cancer.* **8**(5), pp.361-375.
Roncaroli, F., Su, Z., Herholz, K., Gerhard, A. and Turkheimer, F.E. 2016. TSPO expression in brain tumours: is TSPO a target for brain tumour imaging? *Clinical and translational imaging.* **4**, pp.145-156.
Rone, M.B., Midzak, A.S., Issop, L., Rammouz, G., Jagannathan, S., Fan, J., Ye, X., Blonder, J., Veenstra, T. and Papadopoulos, V. 2012. Identification of a dynamic

mitochondrial protein complex driving cholesterol import, trafficking, and metabolism to steroid hormones. *Mol Endocrinol.* **26**(11), pp.1868-1882.
Rosenfeld, J.V., Bandopadhayay, P., Goldschlager, T. and Brown, D.J. 2008. The Ethics of the Treatment of Spinal Cord Injury: Stem Cell Transplants, Motor Neuroprosthetics, and Social Equity. *Top Spinal Cord Inj Rehabil.* **14**(1), pp.76-88.
Roth, G.I. and Yamamoto, W.S. 1968. The microcirculation of the area postrema in the rat. *J Comp Neurol.* **133**(3), pp.329-340.
Rupprecht, R. and Holsboer, F. 1999. Neuroactive steroids: mechanisms of action and neuropsychopharmacological perspectives. *Trends in Neurosciences.* **22**(9), pp.410-416.
Rüsch, D.M.D. and Forman, Stuart A.M.D.P.D. 2005. Classic Benzodiazepines Modulate the Open–Close Equilibrium in α1β2γ2Lγ-Aminobutyric Acid Type A Receptors. *Anesthesiology: The Journal of the American Society of Anesthesiologists.* **102**(4), pp.783-792.
Russart, K.L.G. and Nelson, R.J. 2018. Light at night as an environmental endocrine disruptor. *Physiol Behav.* **190**, pp.82-89.
Ryu, J.K., Choi, H.B. and McLarnon, J.G. 2005. Peripheral benzodiazepine receptor ligand PK11195 reduces microglial activation and neuronal death in quinolinic acid-injected rat striatum. *Neurobiol Dis.* **20**(2), pp.550-561.
Sabelstrom, H., Stenudd, M. and Frisen, J. 2014. Neural stem cells in the adult spinal cord. *Exp Neurol.* **260**, pp.44-49.
Sabelstrom, H., Stenudd, M., Reu, P., Dias, D.O., Elfineh, M., Zdunek, S., Damberg, P., Goritz, C. and Frisen, J. 2013. Resident neural stem cells restrict tissue damage and neuronal loss after spinal cord injury in mice. *Science.* **342**(6158), pp.637-640.
Saberi, H., Firouzi, M., Habibi, Z., Moshayedi, P., Aghayan, H.R., Arjmand, B., Hosseini, K., Razavi, H.E. and Yekaninejad, M.S. 2011. Safety of intramedullary Schwann cell transplantation for postrehabilitation spinal cord injuries: 2-year follow-up of 33 cases. *J Neurosurg Spine.* **15**(5), pp.515-525.
Sabourin, J.C., Ackema, K.B., Ohayon, D., Guichet, P.O., Perrin, F.E., Garces, A., Ripoll, C., Charite, J., Simonneau, L., Kettenmann, H., Zine, A., Privat, A., Valmier, J., Pattyn, A. and Hugnot, J.P. 2009. A mesenchymal-like ZEB1(+) niche harbors dorsal radial glial fibrillary acidic protein-positive stem cells in the spinal cord. *Stem Cells.* **27**(11), pp.2722-2733.
Sage, D.J. 1988. Reversal of sedation with flumazenil in regional anaesthesia: a review. *Eur J Anaesthesiol Suppl.* **2**, pp.201-207.
Sahel, A., Ortiz, F.C., Kerninon, C., Maldonado, P.P., Angulo, M.C. and Nait-Oumesmar, B. 2015. Alteration of synaptic connectivity of oligodendrocyte precursor cells following demyelination. *Front Cell Neurosci.* **9**, p77.
Saker, E., Henry, B.M., Tomaszewski, K.A., Loukas, M., Iwanaga, J., Oskouian, R.J. and Tubbs, R.S. 2016. The Human Central Canal of the Spinal Cord: A Comprehensive Review of its Anatomy, Embryology, Molecular Development, Variants, and Pathology. *Cureus.* **8**(12), pp.e927-e927.
Salat, K. and Kulig, K. 2011. *GABA transporters as targets for new drugs.*
Salic, A. and Mitchison, T.J. 2008. A chemical method for fast and sensitive detection of DNA synthesis *in vivo*. *Proc Natl Acad Sci U S A.* **105**(7), pp.2415-2420.
Salin, P.A. and Prince, D.A. 1996a. Electrophysiological mapping of GABAA receptor-mediated inhibition in adult rat somatosensory cortex. *J Neurophysiol.* **75**(4), pp.1589-1600.

Salin, P.A. and Prince, D.A. 1996b. Spontaneous GABAA receptor-mediated inhibitory currents in adult rat somatosensory cortex. *J Neurophysiol.* **75**(4), pp.1573-1588.
Sama, D.M. and Norris, C.M. 2013. Calcium dysregulation and neuroinflammation: discrete and integrated mechanisms for age-related synaptic dysfunction. *Ageing research reviews.* **12**(4), pp.982-995.
Santhakumar, V., Wallner, M. and Otis, T.S. 2007. Ethanol acts directly on extrasynaptic subtypes of GABAA receptors to increase tonic inhibition. *Alcohol (Fayetteville, N.Y.).* **41**(3), pp.211-221.
Santidrian, A.F., Cosialls, A.M., Coll-Mulet, L., Iglesias-Serret, D., de Frias, M., Gonzalez-Girones, D.M., Campas, C., Domingo, A., Pons, G. and Gil, J. 2007. The potential anticancer agent PK11195 induces apoptosis irrespective of p53 and ATM status in chronic lymphocytic leukemia cells. *Haematologica.* **92**(12), pp.1631-1638.
Sarhan, S., Seiler, N., Grove, J. and Bink, G. 1979. Rapid method for the assay of 4-aminobutyric acid (GABA), glutamic acid and aspartic acid in brain tissue and subcellular fractions. *J Chromatogr.* **162**(4), pp.561-572.
Scarf, A.M., Ittner, L.M. and Kassiou, M. 2009. The translocator protein (18 kDa): central nervous system disease and drug design. *J Med Chem.* **52**(3), pp.581-592.
Schlichter, R., Rybalchenko, V., Poisbeau, P., Verleye, M. and Gillardin, J. 2000. Modulation of GABAergic synaptic transmission by the non-benzodiazepine anxiolytic etifoxine. *Neuropharmacology.* **39**(9), pp.1523-1535.
Schousboe, A., Wu, J.Y. and Roberts, E. 1973. Purification and characterization of the 4-aminobutyrate-2-ketoglutarate transaminase from mouse brain. *Biochemistry.* **12**(15), pp.2868-2873.
Schumacher, M., Hussain, R., Gago, N., Oudinet, J.-P., Mattern, C. and Ghoumari, A.M. 2012. Progesterone synthesis in the nervous system: implications for myelination and myelin repair. *Frontiers in neuroscience.* **6**, pp.10-10.
Schweizer, C., Balsiger, S., Bluethmann, H., Mansuy, I.M., Fritschy, J.M., Mohler, H. and Luscher, B. 2003. The gamma 2 subunit of GABA(A) receptors is required for maintenance of receptors at mature synapses. *Mol Cell Neurosci.* **24**(2), pp.442-450.
Seki, T. and Arai, Y. 1993. Highly polysialylated neural cell adhesion molecule (NCAM-H) is expressed by newly generated granule cells in the dentate gyrus of the adult rat. *Journal of Neuroscience.* **13**(6), pp.2351-2358.
Seo, D.O., Funderburk, S.C., Bhatti, D.L., Motard, L.E., Newbold, D., Girven, K.S., McCall, J.G., Krashes, M., Sparta, D.R. and Bruchas, M.R. 2016. A GABAergic Projection from the Centromedial Nuclei of the Amygdala to Ventromedial Prefrontal Cortex Modulates Reward Behavior. *J Neurosci.* **36**(42), pp.10831-10842.
Serfozo, P. and Cash, D.J. 1992. Effect of a benzodiazepine (chlordiazepoxide) on a GABAA receptor from rat brain. Requirement of only one bound GABA molecule for channel opening. *FEBS Lett.* **310**(1), pp.55-59.
Seri, B., Garcia-Verdugo, J.M., McEwen, B.S. and Alvarez-Buylla, A. 2001. Astrocytes give rise to new neurons in the adult mammalian hippocampus. *J Neurosci.* **21**(18), pp.7153-7160.
Shah, P.T., Stratton, J.A., Stykel, M.G., Abbasi, S., Sharma, S., Mayr, K.A., Koblinger, K., Whelan, P.J. and Biernaskie, J. 2018. Single-Cell Transcriptomics and Fate Mapping of Ependymal Cells Reveals an Absence of Neural Stem Cell Function. *Cell.* **173**(4), pp.1045-1057.e1049.

Sharpless, N.S., Thal, L.J., Perlow, M.J., Tabaddor, K., Waltz, J.M., Shapiro, K.N., Amin, I.M., Engel, J., Jr. and Crandall, P.H. 1984. Vasoactive intestinal peptide in cerebrospinal fluid. *Peptides.* **5**(2), pp.429-433.
Shields, S.A., Gilson, J.M., Blakemore, W.F. and Franklin, R.J. 1999. Remyelination occurs as extensively but more slowly in old rats compared to young rats following gliotoxin-induced CNS demyelination. *Glia.* **28**(1), pp.77-83.
Shihabuddin, L.S., Horner, P.J., Ray, J. and Gage, F.H. 2000. Adult spinal cord stem cells generate neurons after transplantation in the adult dentate gyrus. *J Neurosci.* **20**(23), pp.8727-8735.
Sieghart, W. 2015. Chapter Three - Allosteric Modulation of GABAA Receptors via Multiple Drug-Binding Sites. In: Rudolph, U. ed. *Advances in Pharmacology.* Academic Press, pp.53-96.
Sieghart, W. and Sperk, G. 2002. Subunit composition, distribution and function of GABA(A) receptor subtypes. *Curr Top Med Chem.* **2**(8), pp.795-816.
Sigel, E. 2002. Mapping of the benzodiazepine recognition site on GABA(A) receptors. *Curr Top Med Chem.* **2**(8), pp.833-839.
Sigel, E. and Buhr, A. 1997. The benzodiazepine binding site of GABAA receptors. *Trends Pharmacol Sci.* **18**(11), pp.425-429.
Sigel, E. and P. Luscher, B. 2011. A Closer Look at the High Affinity Benzodiazepine Binding Site on GABAA Receptors. *Current Topics in Medicinal Chemistry.* **11**(2), pp.241-246.
Sigel, E. and Steinmann, M.E. 2012. Structure, function, and modulation of GABA(A) receptors. *J Biol Chem.* **287**(48), pp.40224-40231.
Silva, N.A., Sousa, N., Reis, R.L. and Salgado, A.J. 2014. From basics to clinical: a comprehensive review on spinal cord injury. *Prog Neurobiol.* **114**, pp.25-57.
Sivilotti, M.L. 2016. Flumazenil, naloxone and the 'coma cocktail'. *Br J Clin Pharmacol.* **81**(3), pp.428-436.
Slobodyansky, E., Guidotti, A., Wambebe, C., Berkovich, A. and Costa, E. 1989. Isolation and characterization of a rat brain triakontatetraneuropeptide, a posttranslational product of diazepam binding inhibitor: specific action at the Ro 5-4864 recognition site. *J Neurochem.* **53**(4), pp.1276-1284.
Smart, I. and Leblond, C.P. 1961. Evidence for division and transformations of neuroglia cells in the mouse brain, as derived from radioautography after injection of thymidine-H3. *Journal of Comparative Neurology.* **116**(3), pp.349-367.
Smith, G.B. and Olsen, R.W. 1995. Functional domains of GABAA receptors. *Trends Pharmacol Sci.* **16**(5), pp.162-168.
Smith, K.J., Blakemore, W.F. and McDonald, W.I. 1979. Central remyelination restores secure conduction. *Nature.* **280**(5721), pp.395-396.
So, E.C., Chang, Y.-T., Hsing, C.-H., Poon, P.W.-F., Leu, S.-F. and Huang, B.-M. 2010. The effect of midazolam on mouse Leydig cell steroidogenesis and apoptosis. *Toxicology Letters.* **192**(2), pp.169-178.
Sobecki, M., Mrouj, K., Colinge, J., Gerbe, F., Jay, P., Krasinska, L., Dulic, V. and Fisher, D. 2017. Cell-Cycle Regulation Accounts for Variability in Ki-67 Expression Levels. *Cancer Res.* **77**(10), pp.2722-2734.
Sofroniew, M.V. 2015. Astrocyte barriers to neurotoxic inflammation. *Nat Rev Neurosci.* **16**(5), pp.249-263.
Soldan, S.S., Alvarez Retuerto, A.I., Sicotte, N.L. and Voskuhl, R.R. 2003. Immune modulation in multiple sclerosis patients treated with the pregnancy hormone estriol. *J Immunol.* **171**(11), pp.6267-6274.

Song, J., Sun, J., Moss, J., Wen, Z., Sun, G.J., Hsu, D., Zhong, C., Davoudi, H., Christian, K.M., Toni, N., Ming, G.-L. and Song, H. 2013. Parvalbumin interneurons mediate neuronal circuitry-neurogenesis coupling in the adult hippocampus. *Nature neuroscience.* **16**(12), pp.1728-1730.
Song, J., Zhong, C., Bonaguidi, M.A., Sun, G.J., Hsu, D., Gu, Y., Meletis, K., Huang, Z.J., Ge, S., Enikolopov, G., Deisseroth, K., Luscher, B., Christian, K.M., Ming, G.L. and Song, H. 2012. Neuronal circuitry mechanism regulating adult quiescent neural stem-cell fate decision. *Nature.* **489**(7414), pp.150-154.
Soudijn, W. and van Wijngaarden, I. 2000. The GABA transporter and its inhibitors. *Curr Med Chem.* **7**(10), pp.1063-1079.
Spalding, K.L., Bergmann, O., Alkass, K., Bernard, S., Salehpour, M., Huttner, H.B., Bostrom, E., Westerlund, I., Vial, C., Buchholz, B.A., Possnert, G., Mash, D.C., Druid, H. and Frisen, J. 2013. Dynamics of hippocampal neurogenesis in adult humans. *Cell.* **153**(6), pp.1219-1227.
Spassky, N., Merkle, F.T., Flames, N., Tramontin, A.D., Garcia-Verdugo, J.M. and Alvarez-Buylla, A. 2005. Adult ependymal cells are postmitotic and are derived from radial glial cells during embryogenesis. *J Neurosci.* **25**(1), pp.10-18.
Spitzer, N.C. 2010. How GABA generates depolarization. *The Journal of physiology.* **588**(Pt 5), pp.757-758.
Squires, R.F. and Braestrup, C. 1977. Benzodiazepine receptors in rat brain. *Nature.* **266**(5604), pp.732-734.
Stammers, A.T., Liu, J. and Kwon, B.K. 2012. Expression of inflammatory cytokines following acute spinal cord injury in a rodent model. *J Neurosci Res.* **90**(4), pp.782-790.
Stephenson, D.T., Schober, D.A., Smalstig, E.B., Mincy, R.E., Gehlert, D.R. and Clemens, J.A. 1995. Peripheral benzodiazepine receptors are colocalized with activated microglia following transient global forebrain ischemia in the rat. *J Neurosci.* **15**(7 Pt 2), pp.5263-5274.
Stevens, M.F., Werdehausen, R., Gaza, N., Hermanns, H., Kremer, D., Bauer, I., Kury, P., Hollmann, M.W. and Braun, S. 2011. Midazolam activates the intrinsic pathway of apoptosis independent of benzodiazepine and death receptor signaling. *Reg Anesth Pain Med.* **36**(4), pp.343-349.
Stoeckel, M.E., Uhl-Bronner, S., Hugel, S., Veinante, P., Klein, M.J., Mutterer, J., Freund-Mercier, M.J. and Schlichter, R. 2003. Cerebrospinal fluid-contacting neurons in the rat spinal cord, a gamma-aminobutyric acidergic system expressing the P2X2 subunit of purinergic receptors, PSA-NCAM, and GAP-43 immunoreactivities: light and electron microscopic study. *J Comp Neurol.* **457**(2), pp.159-174.
Stys, P.K. and Lopachin, R.M. 1998. Mechanisms of calcium and sodium fluxes in anoxic myelinated central nervous system axons. *Neuroscience.* **82**(1), pp.21-32.
Sudakov, S.K., Medvedeva, O.F., Rusakova, I.V., Terebilina, N.N. and Goldberg, S.R. 2001. Differences in genetic predisposition to high anxiety in two inbred rat strains: role of substance P, diazepam binding inhibitor fragment and neuropeptide Y. *Psychopharmacology (Berl).* **154**(4), pp.327-335.
Suhonen, J.O., Peterson, D.A., Ray, J. and Gage, F.H. 1996. Differentiation of adult hippocampus-derived progenitors into olfactory neurons *in vivo*. *Nature.* **383**(6601), pp.624-627.
Sun, G.J., Sailor, K.A., Mahmood, Q.A., Chavali, N., Christian, K.M., Song, H. and Ming, G.L. 2013. Seamless reconstruction of intact adult-born neurons by serial end-

block imaging reveals complex axonal guidance and development in the adult hippocampus. *J Neurosci.* **33**(28), pp.11400-11411.
Sun, L.O., Mulinyawe, S.B., Collins, H.Y., Ibrahim, A., Li, Q., Simon, D.J., Tessier-Lavigne, M. and Barres, B.A. 2018. Spatiotemporal Control of CNS Myelination by Oligodendrocyte Programmed Cell Death through the TFEB-PUMA Axis. *Cell.* **175**(7), pp.1811-1826.e1821.
Sun, W., Kim, H. and Moon, Y. 2010. Control of neuronal migration through rostral migratory stream in mice. *Anatomy & Cell Biology.* **43**(4), pp.269-279.
Sutter, A.P., Maaser, K., Barthel, B. and Scherübl, H. 2003. Ligands of the peripheral benzodiazepine receptor induce apoptosis and cell cycle arrest in oesophageal cancer cells: involvement of the p38MAPK signalling pathway. *British journal of cancer.* **89**(3), pp.564-572.
Suzdak, P.D., Glowa, J.R., Crawley, J.N., Schwartz, R.D., Skolnick, P. and Paul, S.M. 1986. A selective imidazobenzodiazepine antagonist of ethanol in the rat. *Science.* **234**(4781), pp.1243-1247.
Syapin, P.J., Jones, B.L., Kobayashi, L.S., Finn, D.A. and Alkana, R.L. 1990. Interactions between benzodiazepine antagonists, inverse agonists, and acute behavioral effects of ethanol in mice. *Brain Res Bull.* **24**(5), pp.705-709.
Takahashi, K., Tanabe, K., Ohnuki, M., Narita, M., Ichisaka, T., Tomoda, K. and Yamanaka, S. 2007. Induction of pluripotent stem cells from adult human fibroblasts by defined factors. *Cell.* **131**(5), pp.861-872.
Tallman, J.F. and Gallager, D.W. 1985. The GABA-ergic system: a locus of benzodiazepine action. *Annu Rev Neurosci.* **8**, pp.21-44.
Tamamaki, N., Yanagawa, Y., Tomioka, R., Miyazaki, J., Obata, K. and Kaneko, T. 2003. Green fluorescent protein expression and colocalization with calretinin, parvalbumin, and somatostatin in the GAD67-GFP knock-in mouse. *J Comp Neurol.* **467**(1), pp.60-79.
Tan, K.R., Rudolph, U. and Lüscher, C. 2011. Hooked on benzodiazepines: GABAA receptor subtypes and addiction. *Trends in neurosciences.* **34**(4), pp.188-197.
Tang, X., Davies, J.E. and Davies, S.J. 2003. Changes in distribution, cell associations, and protein expression levels of NG2, neurocan, phosphacan, brevican, versican V2, and tenascin-C during acute to chronic maturation of spinal cord scar tissue. *J Neurosci Res.* **71**(3), pp.427-444.
Tator, C.H. and Koyanagi, I. 1997. Vascular mechanisms in the pathophysiology of human spinal cord injury. *J Neurosurg.* **86**(3), pp.483-492.
Thompson, S.A., Whiting, P.J. and Wafford, K.A. 1996. Barbiturate interactions at the human GABAA receptor: dependence on receptor subunit combination. *Br J Pharmacol.* **117**(3), pp.521-527.
Thygesen, M.M., Lauridsen, H., Pedersen, M. and Rasmussen, M.M. 2016. The regenerative potential of the axolotl spinal cord: A blunt spinal cord injury model. *The FASEB Journal.* **30**(1_supplement), pp.564.565-564.565.
Ticku, M.K., Ban, M. and Olsen, R.W. 1978. Binding of [3H]alpha-dihydropicrotoxinin, a gamma-aminobutyric acid synaptic antagonist, to rat brain membranes. *Mol Pharmacol.* **14**(3), pp.391-402.
Toborek, M., Malecki, A., Garrido, R., Mattson, M.P., Hennig, B. and Young, B. 1999. Arachidonic acid-induced oxidative injury to cultured spinal cord neurons. *J Neurochem.* **73**(2), pp.684-692.
Tokuda, K., O'Dell, K.A., Izumi, Y. and Zorumski, C.F. 2010. Midazolam inhibits hippocampal long-term potentiation and learning through dual central and peripheral

benzodiazepine receptor activation and neurosteroidogenesis. *J Neurosci.* **30**(50), pp.16788-16795.
Tokuda, K., O'Dell, K.A., Izumi, Y. and Zorumski, C.F. 2010. Midazolam inhibits hippocampal long-term potentiation and learning through dual central and peripheral benzodiazepine receptor activation and neurosteroidogenesis. *The Journal of neuroscience : the official journal of the Society for Neuroscience.* **30**(50), pp.16788-16795.
Tomita, K., Nakanishi, S., Guillemot, F. and Kageyama, R. 1996. Mash1 promotes neuronal differentiation in the retina. *Genes Cells.* **1**(8), pp.765-774.
Tong, X.P., Li, X.Y., Zhou, B., Shen, W., Zhang, Z.J., Xu, T.L. and Duan, S. 2009. Ca(2+) signaling evoked by activation of Na(+) channels and Na(+)/Ca(2+) exchangers is required for GABA-induced NG2 cell migration. *J Cell Biol.* **186**(1), pp.113-128.
Tong, Y., Toranzo, D. and Pelletier, G. 1991. Localization of diazepam-binding inhibitor (DBI) mRNA in the rat brain by high resolution in situ hybridization. *Neuropeptides.* **20**(1), pp.33-40.
Tonon, M.C., Desy, L., Nicolas, P., Vaudry, H. and Pelletier, G. 1990. Immunocytochemical localization of the endogenous benzodiazepine ligand octadecaneuropeptide (ODN) in the rat brain. *Neuropeptides.* **15**(1), pp.17-24.
Tozuka, Y., Fukuda, S., Namba, T., Seki, T. and Hisatsune, T. 2005. GABAergic excitation promotes neuronal differentiation in adult hippocampal progenitor cells. *Neuron.* **47**(6), pp.803-815.
Trujillo, C.A., Schwindt, T.T., Martins, A.H., Alves, J.M., Mello, L.E. and Ulrich, H. 2009. Novel perspectives of neural stem cell differentiation: from neurotransmitters to therapeutics. *Cytometry A.* **75**(1), pp.38-53.
Uchida, I., Li, L. and Yang, J. 1997. The role of the GABA(A) receptor alpha1 subunit N-terminal extracellular domain in propofol potentiation of chloride current. *Neuropharmacology.* **36**(11-12), pp.1611-1621.
Ugale, R.R., Sharma, A.N., Kokare, D.M., Hirani, K., Subhedar, N.K. and Chopde, C.T. 2007. Neurosteroid allopregnanolone mediates anxiolytic effect of etifoxine in rats. *Brain Res.* **1184**, pp.193-201.
Uhlirova, L., Sustkova-Fiserova, M. and Krsiak, M. 2004. Behavioral effects of flumazenil in the social conflict test in mice. *Psychopharmacology (Berl).* **171**(3), pp.259-269.
Urban, N., van den Berg, D.L., Forget, A., Andersen, J., Demmers, J.A., Hunt, C., Ayrault, O. and Guillemot, F. 2016. Return to quiescence of mouse neural stem cells by degradation of a proactivation protein. *Science.* **353**(6296), pp.292-295.
van Praag, H., Kempermann, G. and Gage, F.H. 2000. Neural consequences of environmental enrichment. *Nat Rev Neurosci.* **1**(3), pp.191-198.
van Praag, H., Shubert, T., Zhao, C. and Gage, F.H. 2005. Exercise enhances learning and hippocampal neurogenesis in aged mice. *J Neurosci.* **25**(38), pp.8680-8685.
Varga, B., Marko, K., Hadinger, N., Jelitai, M., Demeter, K., Tihanyi, K., Vas, A. and Madarasz, E. 2009. Translocator protein (TSPO 18kDa) is expressed by neural stem and neuronal precursor cells. *Neurosci Lett.* **462**(3), pp.257-262.
Varju, P., Katarova, Z., Madarasz, E. and Szabo, G. 2001. GABA signalling during development: new data and old questions. *Cell Tissue Res.* **305**(2), pp.239-246.

Veenman, L. and Gavish, M. 2012. The role of 18 kDa mitochondrial translocator protein (TSPO) in programmed cell death, and effects of steroids on TSPO expression. *Curr Mol Med.* **12**(4), pp.398-412.
Veenman, L., Papadopoulos, V. and Gavish, M. 2007. Channel-like functions of the 18-kDa translocator protein (TSPO): regulation of apoptosis and steroidogenesis as part of the host-defense response. *Curr Pharm Des.* **13**(23), pp.2385-2405.
Veiga, S., Azcoitia, I. and Garcia-Segura, L.M. 2005. Ro5-4864, a peripheral benzodiazepine receptor ligand, reduces reactive gliosis and protects hippocampal hilar neurons from kainic acid excitotoxicity. *J Neurosci Res.* **80**(1), pp.129-137.
Veiga, S., Carrero, P., Pernia, O., Azcoitia, I. and Garcia-Segura, L.M. 2007. Translocator protein 18 kDa is involved in the regulation of reactive gliosis. *Glia.* **55**(14), pp.1426-1436.
Verleye, M., Akwa, Y., Liere, P., Ladurelle, N., Pianos, A., Eychenne, B., Schumacher, M. and Gillardin, J.-M. 2005. The anxiolytic etifoxine activates the peripheral benzodiazepine receptor and increases the neurosteroid levels in rat brain. *Pharmacology Biochemistry and Behavior.* **82**(4), pp.712-720.
Verleye, M., Akwa, Y., Liere, P., Ladurelle, N., Pianos, A., Eychenne, B., Schumacher, M. and Gillardin, J.M. 2005. The anxiolytic etifoxine activates the peripheral benzodiazepine receptor and increases the neurosteroid levels in rat brain. *Pharmacol Biochem Behav.* **82**(4), pp.712-720.
Verleye, M., Pansart, Y. and Gillardin, J. 2002. Effects of etifoxine on ligand binding to GABA(A) receptors in rodents. *Neurosci Res.* **44**(2), pp.167-172.
Verleye, M., Schlichter, R., Neliat, G., Pansart, Y. and Gillardin, J.M. 2001. Functional modulation of gamma-aminobutyric acidA receptors by etifoxine and allopregnanolone in rodents. *Neuroscience Letters.* **301**(3), pp.191-194.
Vidnyánszky, Z., Görcs, T.J. and Hámori, J. 1994. Diazepam binding inhibitor fragment 33–50 (octadecaneuropeptide) immunoreactivity in the cerebellar cortex is restricted to glial cells. *Glia.* **10**(2), pp.132-141.
Vigh, B., Vigh-Teichmann, I. and Aros, B. 1977. Special dendritic and axonal endings formed by the cerebrospinal fluid contacting neurons of the spinal cord. *Cell and Tissue Research.* **183**(4), pp.541-552.
Vigh, B., Vigh-Teichmann, I., Manzano e Silva, M.J. and van den Pol, A.N. 1983a. Cerebrospinal fluid-contacting neurons of the central canal and terminal ventricle in various vertebrates. *Cell Tissue Res.* **231**(3), pp.615-621.
Vigh, B., Vigh-Teichmann, I., Manzano e Silva, M.J. and van den Pol, A.N. 1983b. Cerebrospinal fluid-contacting neurons of the central canal and terminal ventricle in various vertebrates. *Cell and Tissue Research.* **231**(3), pp.615-621.
Vodicka, M.A. 2001. Determinants for Lentiviral Infection of Non-Dividing Cells. *Somatic Cell and Molecular Genetics.* **26**(1), pp.35-49.
Votey, S.R., Bosse, G.M., Bayer, M.J. and Hoffman, J.R. 1991. Flumazenil: A new benzodiazepine antagonist. *Annals of Emergency Medicine.* **20**(2), pp.181-188.
Wagner, D.A. and Czajkowski, C. 2001. Structure and Dynamics of the GABA Binding Pocket: A Narrowing Cleft that Constricts during Activation. *The Journal of Neuroscience.* **21**(1), p67.
Wang, D.D. and Kriegstein, A.R. 2009. Defining the role of GABA in cortical development. *J Physiol.* **587**(Pt 9), pp.1873-1879.
Wang, D.D., Krueger, D.D. and Bordey, A. 2003. GABA depolarizes neuronal progenitors of the postnatal subventricular zone via GABAA receptor activation. *J Physiol.* **550**(Pt 3), pp.785-800.

Wang, H., Zhai, K., Xue, Y., Yang, J., Yang, Q., Fu, Y., Hu, Y., Liu, F., Wang, W., Cui, L., Chen, H., Zhang, J. and He, W. 2016. Global Deletion of TSPO Does Not Affect the Viability and Gene Expression Profile. *PLoS One.* **11**(12), pe0167307.
Wang, H.J., Fan, J. and Papadopoulos, V. 2012. Translocator protein (Tspo) gene promoter-driven green fluorescent protein synthesis in transgenic mice: an *in vivo* model to study Tspo transcription. *Cell Tissue Res.* **350**(2), pp.261-275.
Wang, J.M., Singh, C., Liu, L., Irwin, R.W., Chen, S., Chung, E.J., Thompson, R.F. and Brinton, R.D. 2010. Allopregnanolone reverses neurogenic and cognitive deficits in mouse model of Alzheimer's disease. *Proc Natl Acad Sci U S A.* **107**(14), pp.6498-6503.
Wang, L., Spary, E., Deuchars, J. and Deuchars, S.A. 2008. Tonic GABAergic inhibition of sympathetic preganglionic neurons: a novel substrate for sympathetic control. *J Neurosci.* **28**(47), pp.12445-12452.
Wang, M. 2011. Neurosteroids and GABA-A Receptor Function. *Frontiers in endocrinology.* **2**, pp.44-44.
Wang, M., Wang, X., Zhao, L., Ma, W., Rodriguez, I.R., Fariss, R.N. and Wong, W.T. 2014. Macroglia-microglia interactions via TSPO signaling regulates microglial activation in the mouse retina. *J Neurosci.* **34**(10), pp.3793-3806.
Wanner, I.B., Anderson, M.A., Song, B., Levine, J., Fernandez, A., Gray-Thompson, Z., Ao, Y. and Sofroniew, M.V. 2013. Glial scar borders are formed by newly proliferated, elongated astrocytes that interact to corral inflammatory and fibrotic cells via STAT3-dependent mechanisms after spinal cord injury. *J Neurosci.* **33**(31), pp.12870-12886.
Weiss, S., Dunne, C., Hewson, J., Wohl, C., Wheatley, M., Peterson, A.C. and Reynolds, B.A. 1996. Multipotent CNS stem cells are present in the adult mammalian spinal cord and ventricular neuroaxis. *J Neurosci.* **16**(23), pp.7599-7609.
Williams, G.L., Pollay, M., Seale, T., Hisey, B. and Roberts, P.A. 1990. Benzodiazepine receptors and cerebrospinal fluid formation. *J Neurosurg.* **72**(5), pp.759-762.
Wimberley, C., Lavisse, S., Brulon, V., Peyronneau, M.A., Leroy, C., Bodini, B., Remy, P., Stankoff, B., Buvat, I. and Bottlaender, M. 2018. Impact of Endothelial 18-kDa Translocator Protein on the Quantification of (18)F-DPA-714. *J Nucl Med.* **59**(2), pp.307-314.
Wingrove, P.B., Thompson, S.A., Wafford, K.A. and Whiting, P.J. 1997. Key amino acids in the gamma subunit of the gamma-aminobutyric acidA receptor that determine ligand binding and modulation at the benzodiazepine site. *Mol Pharmacol.* **52**(5), pp.874-881.
Wirth, E.D., 3rd, Reier, P.J., Fessler, R.G., Thompson, F.J., Uthman, B., Behrman, A., Beard, J., Vierck, C.J. and Anderson, D.K. 2001. Feasibility and safety of neural tissue transplantation in patients with syringomyelia. *J Neurotrauma.* **18**(9), pp.911-929.
Wisden, W. and Stephens, D.N. 1999. Towards better benzodiazepines. *Nature.* **401**(6755), pp.751-752.
Wojtowicz, J.M. and Kee, N. 2006. BrdU assay for neurogenesis in rodents. *Nat Protoc.* **1**(3), pp.1399-1405.
Wolf, L., Bauer, A., Melchner, D., Hallof-Buestrich, H., Stoertebecker, P., Haen, E., Kreutz, M., Sarubin, N., Milenkovic, V.M., Wetzel, C.H., Rupprecht, R. and Nothdurfter, C. 2015. Enhancing neurosteroid synthesis--relationship to the

pharmacology of translocator protein (18 kDa) (TSPO) ligands and benzodiazepines. *Pharmacopsychiatry.* **48**(2), pp.72-77.
Woodruff, R.H. and Franklin, R.J. 1999. Demyelination and remyelination of the caudal cerebellar peduncle of adult rats following stereotaxic injections of lysolecithin, ethidium bromide, and complement/anti-galactocerebroside: a comparative study. *Glia.* **25**(3), pp.216-228.
Wu, H.Y., Dawson, M.R., Reynolds, R. and Hardy, R.J. 2001. Expression of QKI proteins and MAP1B identifies actively myelinating oligodendrocytes in adult rat brain. *Mol Cell Neurosci.* **17**(2), pp.292-302.
Xiao, H.S., Huang, Q.H., Zhang, F.X., Bao, L., Lu, Y.J., Guo, C., Yang, L., Huang, W.J., Fu, G., Xu, S.H., Cheng, X.P., Yan, Q., Zhu, Z.D., Zhang, X., Chen, Z., Han, Z.G. and Zhang, X. 2002. Identification of gene expression profile of dorsal root ganglion in the rat peripheral axotomy model of neuropathic pain. *Proc Natl Acad Sci U S A.* **99**(12), pp.8360-8365.
Xu, J., Mathena, R., Singh, S., Kim, J., J. Long, J., Li, Q., Junn, S., Blaize, E. and David Mintz, C. 2019. *Early Developmental Exposure to Repetitive Long Duration of Midazolam Sedation Causes Behavioral and Synaptic Alterations in a Rodent Model of Neurodevelopment.*
Xu, M. and Akabas, M.H. 1996. Identification of channel-lining residues in the M2 membrane-spanning segment of the GABA(A) receptor alpha1 subunit. *J Gen Physiol.* **107**(2), pp.195-205.
Xu, R., Wu, C., Tao, Y., Yi, J., Yang, Y., Zhang, X. and Liu, R. 2008. Nestin-positive cells in the spinal cord: a potential source of neural stem cells. *International Journal of Developmental Neuroscience.* **26**(7), pp.813-820.
Yagita, K., Horie, K., Koinuma, S., Nakamura, W., Yamanaka, I., Urasaki, A., Shigeyoshi, Y., Kawakami, K., Shimada, S., Takeda, J. and Uchiyama, Y. 2010. Development of the circadian oscillator during differentiation of mouse embryonic stem cells *in vitro*. *Proc Natl Acad Sci U S A.* **107**(8), pp.3846-3851.
Yamaguchi, M., Saito, H., Suzuki, M. and Mori, K. 2000. Visualization of neurogenesis in the central nervous system using nestin promoter-GFP transgenic mice. *Neuroreport.* **11**(9), pp.1991-1996.
Yamamoto, S., Nagao, M., Sugimori, M., Kosako, H., Nakatomi, H., Yamamoto, N., Takebayashi, H., Nabeshima, Y., Kitamura, T., Weinmaster, G., Nakamura, K. and Nakafuku, M. 2001a. Transcription factor expression and Notch-dependent regulation of neural progenitors in the adult rat spinal cord. *J Neurosci.* **21**(24), pp.9814-9823.
Yamamoto, S., Yamamoto, N., Kitamura, T., Nakamura, K. and Nakafuku, M. 2001b. Proliferation of parenchymal neural progenitors in response to injury in the adult rat spinal cord. *Exp Neurol.* **172**(1), pp.115-127.
Yanase, H., Shimizu, H., Kanda, T., Fujii, H. and Iwanaga, T. 2001. Cellular localization of the diazepam binding inhibitor (DBI) in the gastrointestinal tract of mice and its coexistence with the fatty acid binding protein (FABP). *Arch Histol Cytol.* **64**(4), pp.449-460.
Yanase, H., Shimizu, H., Yamada, K. and Iwanaga, T. 2002. Cellular localization of the diazepam binding inhibitor in glial cells with special reference to its coexistence with brain-type fatty acid binding protein. *Arch Histol Cytol.* **65**(1), pp.27-36.
Yang, J. and Shen, J. 2009. Elevated endogenous GABA concentration attenuates glutamate-glutamine cycling between neurons and astroglia. *Journal of neural transmission (Vienna, Austria : 1996).* **116**(3), pp.291-300.

Yankam Njiwa, J., Bouvard, S., Catenoix, H., Mauguiere, F., Ryvlin, P. and Hammers, A. 2013. Periventricular [(11)C]flumazenil binding for predicting postoperative outcome in individual patients with temporal lobe epilepsy and hippocampal sclerosis. *Neuroimage Clin.* **3**, pp.242-248.
Yasin, N., Veenman, L., Singh, S., Azrad, M., Bode, J., Vainshtein, A., Caballero, B., Marek, I. and Gavish, M. 2017. Classical and Novel TSPO Ligands for the Mitochondrial TSPO Can Modulate Nuclear Gene Expression: Implications for Mitochondrial Retrograde Signaling. *International journal of molecular sciences.* **18**(4), p786.
Yates, M.A., Li, Y., Chlebeck, P., Proctor, T., Vandenbark, A.A. and Offner, H. 2010. Progesterone treatment reduces disease severity and increases IL-10 in experimental autoimmune encephalomyelitis. *J Neuroimmunol.* **220**(1-2), pp.136-139.
Yiu, G. and He, Z. 2006. Glial inhibition of CNS axon regeneration. *Nat Rev Neurosci.* **7**(8), pp.617-627.
Ymer, S., Draguhn, A., Wisden, W., Werner, P., Keinanen, K., Schofield, P.R., Sprengel, R., Pritchett, D.B. and Seeburg, P.H. 1990. Structural and functional characterization of the gamma 1 subunit of GABAA/benzodiazepine receptors. *Embo j.* **9**(10), pp.3261-3267.
Yoo, S. and Wrathall, J.R. 2007. Mixed primary culture and clonal analysis provide evidence that NG2 proteoglycan-expressing cells after spinal cord injury are glial progenitors. *Dev Neurobiol.* **67**(7), pp.860-874.
Young, K.M., Psachoulia, K., Tripathi, R.B., Dunn, S.J., Cossell, L., Attwell, D., Tohyama, K. and Richardson, W.D. 2013. Oligodendrocyte dynamics in the healthy adult CNS: evidence for myelin remodeling. *Neuron.* **77**(5), pp.873-885.
Young, S.Z. and Bordey, A. 2009. GABA's control of stem and cancer cell proliferation in adult neural and peripheral niches. *Physiology (Bethesda, Md.).* **24**, pp.171-185.
Young, S.Z., Platel, J.-C., Nielsen, J.V., Jensen, N.A. and Bordey, A. 2010. GABA(A) Increases Calcium in Subventricular Zone Astrocyte-Like Cells Through L- and T-Type Voltage-Gated Calcium Channels. *Frontiers in cellular neuroscience.* **4**, pp.8-8.
Yun, J., Koike, H., Ibi, D., Toth, E., Mizoguchi, H., Nitta, A., Yoneyama, M., Ogita, K., Yoneda, Y., Nabeshima, T., Nagai, T. and Yamada, K. 2010. Chronic restraint stress impairs neurogenesis and hippocampus-dependent fear memory in mice: possible involvement of a brain-specific transcription factor Npas4. *J Neurochem.* **114**(6), pp.1840-1851.
Zagorchev, P., Yu Kokova, V., Apostolova, E. and P Peychev, L. 2018. *Possible role of 18-kDa translocator protein (TSPO) in etifoxine-induced reduction of direct twitch responses in isolated rat nerve-skeletal muscle preparations.*
Zariwala, H.A., Borghuis, B.G., Hoogland, T.M., Madisen, L., Tian, L., De Zeeuw, C.I., Zeng, H., Looger, L.L., Svoboda, K. and Chen, T.W. 2012. A Cre-dependent GCaMP3 reporter mouse for neuronal imaging *in vivo*. *J Neurosci.* **32**(9), pp.3131-3141.
Zeng, C., Pan, F., Jones, L.A., Lim, M.M., Griffin, E.A., Sheline, Y.I., Mintun, M.A., Holtzman, D.M. and Mach, R.H. 2010. Evaluation of 5-ethynyl-2′-deoxyuridine staining as a sensitive and reliable method for studying cell proliferation in the adult nervous system. *Brain research.* **1319C**, pp.21-32.
Zhang, A.L., Hao, J.X., Seiger, Å., Xu, X.J., Wiesenfeld-Hallin, Z., Grant, G. and Aldskogius, H. 1994. Decreased GABA immunoreactivity in spinal cord dorsal horn

neurons after transient spinal cord ischemia in the rat. *Brain Research.* **656**(1), pp.187-190.
Zhang, B., McDaniel, S.S., Rensing, N.R. and Wong, M. 2013. Vigabatrin Inhibits Seizures and mTOR Pathway Activation in a Mouse Model of Tuberous Sclerosis Complex. *PLOS ONE.* **8**(2), pe57445.
Zhang, G., Vidal Pizarro, I., Swain, G.P., Kang, S.H. and Selzer, M.E. 2014. Neurogenesis in the lamprey central nervous system following spinal cord transection. *The Journal of comparative neurology.* **522**(6), pp.1316-1332.
Zhang, J. and Jiao, J. 2015. Molecular Biomarkers for Embryonic and Adult Neural Stem Cell and Neurogenesis. *Biomed Res Int.* **2015**, p727542.
Zhang, R., Lahens, N.F., Ballance, H.I., Hughes, M.E. and Hogenesch, J.B. 2014. A circadian gene expression atlas in mammals: implications for biology and medicine. *Proc Natl Acad Sci U S A.* **111**(45), pp.16219-16224.
Zhao, H., Halicka, H.D., Li, J., Biela, E., Berniak, K., Dobrucki, J. and Darzynkiewicz, Z. 2013. DNA damage signaling, impairment of cell cycle progression, and apoptosis triggered by 5-ethynyl-2'-deoxyuridine incorporated into DNA. *Cytometry A.* **83**(11), pp.979-988.
Zhao, L., Ku, L., Chen, Y., Xia, M., LoPresti, P. and Feng, Y. 2006. QKI binds MAP1B mRNA and enhances MAP1B expression during oligodendrocyte development. *Mol Biol Cell.* **17**(10), pp.4179-4186.
Zhao, S., Zhu, Y., Xue, R., Li, Y., Lu, H. and Mi, W. 2012. Effect of midazolam on the proliferation of neural stem cells isolated from rat hippocampus. *Neural Regeneration Research.* **7**(19), pp.1475-1482.
Zonouzi, M., Scafidi, J., Li, P., McEllin, B., Edwards, J., Dupree, J.L., Harvey, L., Sun, D., Hubner, C.A., Cull-Candy, S.G., Farrant, M. and Gallo, V. 2015. GABAergic regulation of cerebellar NG2 cell development is altered in perinatal white matter injury. *Nat Neurosci.* **18**(5), pp.674-682.